U.S. DEPARTMENT OF COMMERCE
National Technical Information Service
PB-284 041

Measurement of High-Temperature, High-Pressure Processes

Acurex Corp, Mountain View, Calif Aerotherm Div

Prepared for

Industrial Environmental Research Lab, Research Triangle Park, N C

Jan 78

EPA U.S. Environmental Protection Agency
Office of Research and Development

Industrial Environmental Research
Laboratory
Research Triangle Park, North Carolina 27711

EPA-600/7-78-011
January 1978

PB 284 041

MEASUREMENT OF HIGH-TEMPERATURE, HIGH-PRESSURE PROCESSES:

Annual Report

Interagency
Energy-Environment
Research and Development
Program Report

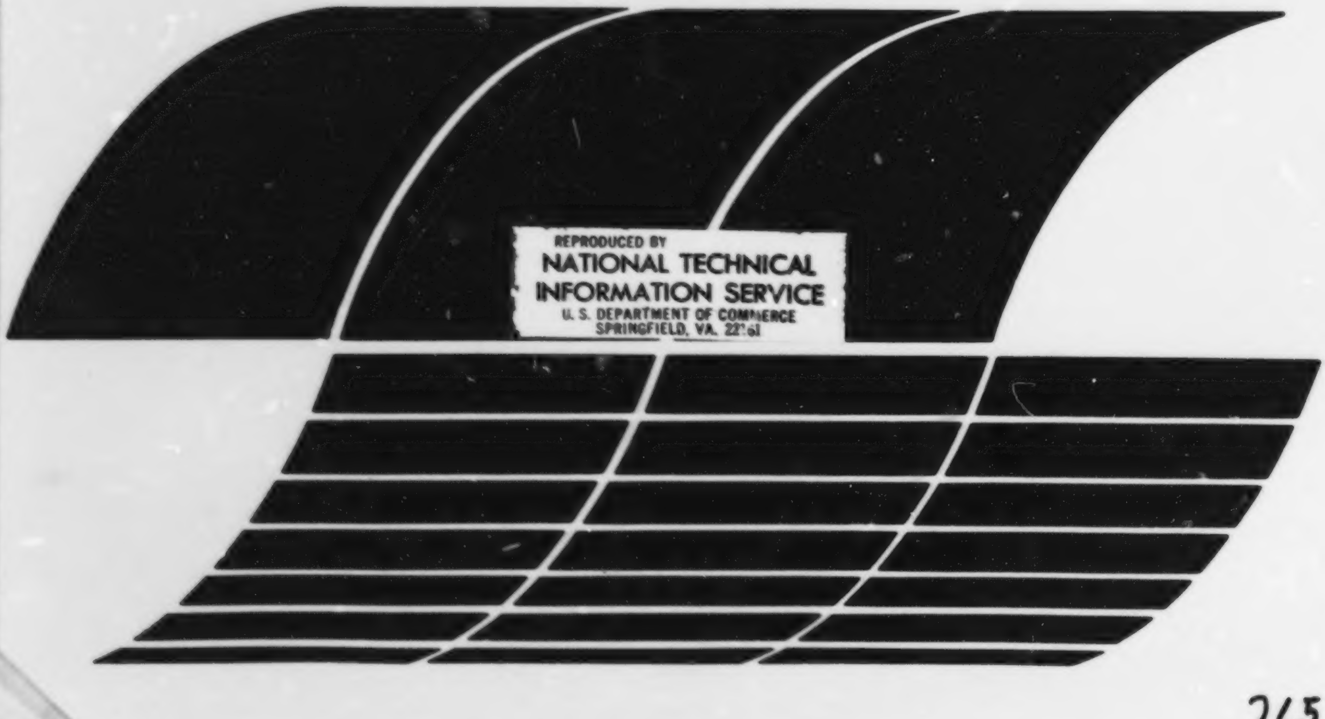

REPRODUCED BY
NATIONAL TECHNICAL
INFORMATION SERVICE
U. S. DEPARTMENT OF COMMERCE
SPRINGFIELD, VA. 22161

265

RESEARCH REPORTING SERIES

Research reports of the Office of Research and Development, U.S. Environmental Protection Agency, have been grouped into nine series. These nine broad categories were established to facilitate further development and application of environmental technology. Elimination of traditional grouping was consciously planned to foster technology transfer and a maximum interface in related fields. The nine series are:

1. Environmental Health Effects Research
2. Environmental Protection Technology
3. Ecological Research
4. Environmental Monitoring
5. Socioeconomic Environmental Studies
6. Scientific and Technical Assessment Reports (STAR)
7. Interagency Energy-Environment Research and Development
8. "Special" Reports
9. Miscellaneous Reports

This report has been assigned to the INTERAGENCY ENERGY-ENVIRONMENT RESEARCH AND DEVELOPMENT series. Reports in this series result from the effort funded under the 17-agency Federal Energy/Environment Research and Development Program. These studies relate to EPA's mission to protect the public health and welfare from adverse effects of pollutants associated with energy systems. The goal of the Program is to assure the rapid development of domestic energy supplies in an environmentally-compatible manner by providing the necessary environmental data and control technology. Investigations include analyses of the transport of energy-related pollutants and their health and ecological effects; assessments of, and development of, control technologies for energy systems; and integrated assessments of a wide range of energy-related environmental issues.

EPA REVIEW NOTICE

This report has been reviewed by the participating Federal Agencies, and approved for publication. Approval does not signify that the contents necessarily reflect the views and policies of the Government, nor does mention of trade names or commercial products constitute endorsement or recommendation for use.

This document is available to the public through the National Technical Information Service, Springfield, Virginia 22161.

TECHNICAL REPORT DATA
(Please read Instructions on the reverse before completing)

1. REPORT NO.
EPA-600/7-78-011

2.

3. RECIPIENT'S ACCESSION NO.
PB284041

4. TITLE AND SUBTITLE
Measurement of High-temperature, High-pressure Processes: Annual Report

5. REPORT DATE
January 1978

6. PERFORMING ORGANIZATION CODE

7. AUTHOR(S)
Larry Cooper

8. PERFORMING ORGANIZATION REPORT NO.

9. PERFORMING ORGANIZATION NAME AND ADDRESS
Aerotherm Division/Acurex Corporation
485 Clyde Avenue
Mountain View, California 94042

10. PROGRAM ELEMENT NO.
EHE623 and 624

11. CONTRACT/GRANT NO.
68-02-2153

12. SPONSORING AGENCY NAME AND ADDRESS
EPA, Office of Research and Development
Industrial Environmental Research Laboratory
Research Triangle Park, NC 27711

13. TYPE OF REPORT AND PERIOD COVERED
Annual; 4/76-7/77

14. SPONSORING AGENCY CODE
EPA/600/13

15. SUPPLEMENTARY NOTES IERL-RTP project officer is William B. Kuykendal, Mail Drop 62, 919/541-2557.

16. ABSTRACT The report reviews the first year's efforts under a planned 3-year program to develop measurement techniques for high-temperature, high-pressure (HTP) processes. Several related topics are discussed in detail, including: (1) the design, development, and successful demonstration of a system for sampling particulate from a pressurized fluidized-bed combustor operating at 740 C and 9 atmospheres; (2) a review of existing measurement methods to determine the best available techniques for measuring gas flow velocities, pressures, and temperatures in HTP process streams; (3) a review of various HTP coal conversion processes and recommendations for material selection for sampling them; and (4) recommendations for sampling tars in a coal gasification process.

17. KEY WORDS AND DOCUMENT ANALYSIS

a. DESCRIPTORS		b. IDENTIFIERS/OPEN ENDED TERMS	c. COSATI Field/Group	
Pollution	Fluidized-bed	Pollution Control	13B	
Measurement	Processing	Stationary Sources	14B	07A
Sampling	Gas Flow	Particulate		20D
Industrial Processes	Velocity		13H	
High Temperature Tests	Pressure			
High Pressure Tests	Temperature			
Coal Gasification	Dust, Tars		11G 07C	

18. DISTRIBUTION STATEMENT
Unlimited

19. SECURITY CLASS *(This Report)*
Unclassified

20. SECURITY CLASS *(This page)*
Unclassified

21. NO. OF PAGES
265

22. PRICE
PCA12 MFA01

EPA Form 2220-1 (9-73)

EPA-600/7-78-011
January 1978

MEASUREMENT OF HIGH-TEMPERATURE, HIGH-PRESSURE PROCESSES:

Annual Report

by

Larry Cooper

Aerotherm Division/Acurex Corporation
485 Clyde Avenue
Mountain View, California 94042

Contract No. 68-02-2153
Program Element No. EHE623 and 624

EPA Project Officer: William B. Kuykendal

Industrial Environmental Research Laboratory
Office of Energy, Minerals, and Industry
Research Triangle Park, N.C. 27711

Prepared for

U.S. ENVIRONMENTAL PROTECTION AGENCY
Office of Research and Development
Washington, D.C. 20460

TABLE OF CONTENTS

EXECUTIVE SUMMARY 1

APPENDICES . . . .

A. Measurement of Velocity, Pressure and Temperature in HTHP Process Streams, V. Kulkarni and L. Cooper, Aerotherm Report TN-76-34 A-i

B. Material Selection for Sampling in Coal Conversion Systems, J. Hull, Aerotherm Report TM-77-180 B-i

C. Tar Sampling in Coal Gasification Processes, W. Krill, Aerotherm Report TM-77-173 C-i

D. Field Testing of a Sampling System for High-Temperature/High-Pressure Processes, W. Masters, Aerotherm Report TM-77-177 D-i

E. IERL-CRB Sampling Manual for Level 1 Environment Assessment, W. Krill, Aerotherm Report TM-77-160 E-i

F. A Progress Review of Source Assessment of Sampling System Programs, D. Blake, Aerotherm Report TM-77-176 F-i

G. Conversion to International System of Units G-1

EXECUTIVE SUMMARY

Aerotherm Division of Acurex Corporation is conducting a program for Measurements of High-Temperature/High-Pressure (HTHP) Processes for the Process Measurements Branch of IERL under a 3-year term level-of-effort contract. The planned level-of-effort is 4 man-years per year. This report summarizes the activities of the first year of the program.

Under this contract, Aerotherm is evaluating and developing methods for measuring process streams for particulates and harmful gaseous components. These measurements assess the effluent cleanup requirements and indicate techniques which minimize the generation of toxic substances that require subsequent cleanup.

The tasks accomplished under this program were organized under three categories:

- State-of-the-art review
- Research and development
- Support services

Reports have been prepared under each task summarizing the work performed during the past year. Abstracts of these reports are given below; the complete reports are included in the Appendix.

STATE-OF-THE-ART REVIEW

Measurement of Velocity, Pressure and Temperature in HTHP Process Streams, V. Kulkarni and L. Cooper, Aerotherm Report TN-76-34

To determine particulate and gaseous concentrations in high-temperature, high-pressure process streams, gas flow velocities, pressures, and temperatures must be accurately measured. Various methods have been reviewed to determine which methods of measurement are most suitable.

The pitot static probe accurately measures static and dynamic pressures, and with the gas density can be used to determine velocity. The probe has shortcomings (e.g., plugging by dust), although these may be overcome by using purging techniques. The "S" type pitot static probe is perhaps the best solution for the near future. This probe resists plugging much longer than ordinary probes. However, to use this probe, a calibration factor dependent on the Reynolds number may be required to accurately determine velocity.

Other devices are also available for measuring velocity. These devices include flare gas probes, drag meters, and fluidic sensors. In addition, the application of other types of equipment such as orifice and venturi meters, as well as laser velocimeters is still being evaluated.

For measuring temperature, thermocouples are still the simplest and most convenient devices available. The shielded thermocouple is likely to give the best results in the immediate future. Other methods, such as radiation pyrometers, molecular beam, and velocity of sound techniques still have major drawbacks. More study including tests in HTHP environments would be required to determine whether another method should replace the thermocouple.

Material Selection for Sampling in Coal Conversion Systems, J. Hull, Aerotherm Report TM-77-180

To investigate prospective materials for coal conversion system sampling, Aerotherm made an extensive literature search and direct contacts with persons active in material research. Aerotherm had access to the latest information and data in this area, since one of our staff (the author of this report) is a member of the Metal Properties Council and its Subcommittee on Materials for the Gasification of Coal.

Sufficient laboratory and pilot plant data has been obtained to help designers select materials that will survive for several hundred hours in the environment found in coal conversion systems. For example, at 1800°F, adding at least 25-percent chromium establishes corrosion resistance in gasifiers for 1000 hours. And while there are no safe alloys for extended use in high sulfur gas above 1600°F, both Alloy 310 and Kanthal are acceptable below 1600°F.

When selecting materials, the local environment surrounding each probe is important, since temperature, pressure, gas composition, and flyash characteristics often vary with probe location. In addition, surface finish and other fabrication parameters such as heat treatment are also important to material survival.

Tar Sampling in Coal Gasification Processes, W. Krill, Aerotherm Report TM-77-173

Tars are a byproduct of many coal gasifiers. With decreases in temperature, tars condense on surfaces often restricting the flow. Since tars are chemically stable, it is hard to remove them from equipment. In addition, some tars are highly carcinogenic and should not be released to the environment. All of these factors make it difficult to extract particulate and gaseous samples in the presense of tar.

A comprehensive study was made to determine the best way to sample under these conditions. Brian Macnick, a UCB researcher under ERDA contract, "Physical Characteristics of Tars," was used as a consultant in this study. The gasifier facilities at Grand Forks Energy Research Center, Riley-Stoker, Blue Diamond Co., and Morgantown Energy Research Center were contacted to relate their specific experience with tars.

While tars have widely varying condensation temperatures, they tend to remain in the vapor state at temperatures above 1600°F. Thus, particulate can be separated out if the temperature is high enough. In addition, higher process pressures will result in fewer (if any) species condensing at a given temperature. Of all the equipment used for tar extraction (filters, cyclones, condensers, scrubbers, and electrostatic precipitators), the electrostatic precipitator (ESP) is judged best. The electrostatic precipitator collects tar particles of all sizes, while other collection methods cannot collect the smaller particles. Also, the ESP handles a large collected mass better than other methods.

To demonstrate the applicability of the electrostatic precipitator, Aerotherm derived a conceptual design for a compact two-stage collector (6 inches in length, 7 inches in diameter), based on a Southern Research Institute concept. The collector has been calculated to be 100 percent efficient for all particles above 1 micron, 99.6 percent efficient at 1 micron, and 99.2 percent efficient at 0.3 micron (tar particles can be as small as 0.1 micron).

Collecting solid particulate at stream temperatures avoids additional condensation of tars. Therefore, a possible sampling scheme for a gasification process begins by collecting solid particles at stream temperatures with a particulate cyclone, followed by an appropriate reduction in temperature and pressure using a condenser and then tar collection in an electrostatic precipitator.

RESEARCH AND DEVELOPMENT

Field Testing of a Sampling System for High-Temperature/High-Pressure Processes, W. Masters, Aerotherm Report TM-77-177

The Aerotherm HTHP sampling system for measuring particulate concentration and trace element content has recently been successfully demonstrated in field tests at the Exxon Pressurized Fluidized Bed Combustor (PFBC) Miniplant in Linden, N.J. The probe is of a hydraulically operated, telescoping design for operation in a severe, high-pressure FBC environment.

The versatility of the probe was demonstrated by the fact that the three sampling tests at Exxon used two types of particulate collectors: the first test used a glass fiber thimble filter with large total mass capacity, and the last two tests used a cascade impactor with seven stages for particulate sizing. Sample data obtained from the 1360°F, 9-atmosphere gas stream demonstrated that the system can operate in an extreme PFBC environment. The only problem encountered was a malfunctioning impactor heater. This heater was replaced in preparation for subsequent tests to be performed at Exxon.

The ability of the system to measure particulate loadings and size distributions were fully demonstrated in these tests. Particulate size distributions were obtained from the impactor runs, and most particulates were between 1 to 10 micrometers. The chemical composition of collected particulate was also analyzed using a dispersive X-ray fluorescence analyzer. The results of these tests and the subsequent tests will be fully detailed in a separate test report to be issued under EPA cover.

SUPPORT SERVICES

IERL-CRB Sampling Manual for Level 1 Environmental Assessment, W. Krill, Aerotherm Report TM-77-160

The IERL Combustion Research Branch plans to conduct a Level 1 environmental assessment at their combustion facilities at Research Triangle Park, North Carolina. Drawings were prepared by Aerotherm showing facility modifications which would allow a special sampling probe ("coke oven" probe) to be used. These drawings will be used by IERL-CRB to modify hardware at their facility. This manual includes instructions on test planning, preparation of sampling systems, obtaining samples, recovery of samples from sampling equipment, and data reduction.

A Progress Review of Source Assessment of Sampling System Programs, D. Blake, Aerotherm Report TM-77-176

Several tasks for using and improving the Source Assessment Sampling System (SASS) were undertaken in the past year. In one task, Aerotherm supported two SASS test observations. The first observation, at an experimental coal-fired boiler at K.V.B., Inc., established the need for several minor modifications. In the second, Radian Corporation used the SASS at the Comanche Power Plant of the Colorado Public Service Co. This test, at an increased flowrate, established the need to incorporate two vacuum pumps instead of one.

In another task, the performance of the three SASS cylcones was experimentally evaluated at SoRI using "real" solid particles at 205°C. Since the dye solution particles used at SoRI were not adequate for this temperature, a different method of cyclone calibration was devised. In this method, a test dust of known properties is used to generate a dust cloud which is fed into the cyclone. The efficiency of the cyclone is measured from the quantity and size distribution of dust collected in the cup and passed by the cyclone to the filter.

Well-characterized silica dust was used in the first experiments, and size distributions were measured using the X-ray sedograph at EPA/RTP. Inconsistent results from these tests showed that the test dust degraded. The easiest way to correct for this was to find a test dust that would not erode. A spherical aluminum powder material was chosen to solve this problem, while making the data analysis easier because of the simple shape. The possible problem introduced by the low melting point of aluminum (which could cause particles to stick to walls) can be solved by lengthening the heater to reduce wall temperatures.

A second series of tests has shown reasonable results, but no size distribution analysis (needed to calculate cyclone efficiency curves) has been performed yet.

Appendix A

Acurex Corporation/Aerotherm Division

October 1976

Aerotherm Project 7237

MEASUREMENT OF VELOCITY, PRESSURE AND TEMPERATURE IN HTHP PROCESS STREAMS

V. Kulkarni
L. Cooper

AEROTHERM REPORT TN-76-34

Prepared for

Industrial Environmental Research Laboratory
Environmental Protection Agency
Research Triangle Park
North Carolina 27711

Contract 68-02-2153

TABLE OF CONTENTS

Section Page

1 INTRODUCTION A-1

2 GENERAL CONSIDERATIONS A-2

2.1 Operating Environment A-2
2.2 Accuracy A-3
2.3 Operating Characteristics A-6

3 VELOCITY AND PRESSURE MEASUREMENT A-11

3.1 General Considerations A-12

3.1.1 Compressibility of Gas A-12
3.1.2 Reynolds Number A-13
3.1.3 Turbulence A-15
3.1.4 Solid Particles in Suspension A-15
3.1.5 Orientation of Probe and Flow Angularity Measurement A-16

3.2 Instruments for Velocity Measurement A-16

3.2.1 Pitot/Static Probe A-19
3.2.2 Disc/Static Heads A-21
3.2.3 "S" Type Pitot Tube A-21
3.2.4 Other Special Probe Designs for Measurements in Dust Laden Gases A-21
3.2.5 Flare Gas Probe A-24
3.2.6 Drag Meter A-28
3.2.7 Fluidic Sensors A-30
3.2.8 Acoustic Velocimeter A-30
3.2.9 Orifice and Venturi Meters A-30
3.2.10 Laser Velocimeter A-32

4 TEMPERATURE MEASUREMENT A-34

4.1 Temperature Measurement in Gas Flow A-34
4.2 Temperature Measurements with Thermocouples A-35

4.2.1 Convection A-35
4.2.2 Radiation A-36
4.2.3 Conduction A-38

4.3 Other Temperature Measurement Devices A-38

4.3.1 Radiation Pyrometers A-38
4.3.2 Molecular Beam A-39
4.3.3 Velocity of Sound Method A-39

5 CONCLUSIONS A-40

APPENDIX A — BIBLIOGRAPHY A-41

APPENDIX B — COAL COMBUSTION PRODUCT ANALYSIS A-43

LIST OF ILLUSTRATIONS

Figure		Page
2-1	Examples of Anisokinetic Sampling	A-5
2-2	Effect of Anisokinetic Sampling on the Measurement of Concentration	A-7
2-3	Circular Cylinder in a Steady, Uniform Flow Field	A-9
2-4	Velocity Disturbance with Distance, $\theta = 90°$	A-10
3-1	Correction Factor k for Low Reynolds Numbers for a Prandtl Pitot Tube	A-14
3-2	Influence of Pitot/Static Probe Orientation on Measured Pressure	A-17
3-3	Flow Angularity Determination Using a Cone Flow Probe	A-18
3-4	Typical Pitot/Static Probe	A-20
3-5	Disk/Static Head	A-22
3-6	"S" Type Pitot	A-23
3-7	Special Probes for Measurement in Dust Laden Gases	A-25
3-8	Purge Flow Pressure Sensors	A-26
3-9	Flare Gas Probe	A-27
3-10	Drag Meter	A-29
3-11	Fluidic Sensor	A-31
3-12	Schematic of the Interference Between Two Traveling Collimated Coherent Beams of Light of Wavelength λ Passing Through Each Other at an Angle θ	A-33
4-1	Relation Between Reynolds and Nusselt Numbers for Flow Over a Thermocouple	A-37
B-1	Equilibrium Combustion Products from Typical Eastern Coal	A-44
B-2	Ratio of Specific Heats of Combustion Products from Typical Eastern Coal	A-46
B-3	Molecular Weight of Combustion Products from Typical Eastern Coal	A-47

SECTION 1

INTRODUCTION

Accurate determination of gas flow velocities, pressures, and temperatures is essential for measuring particulate and gaseous concentrations in high temperature, high pressure process streams. Temperature measurement is required in velocity determination and along with pressure measurement serves to characterize the gas flow being sampled. In this memorandum, the various aspects and methods of velocity, pressure, and temperature measurements in a high temperature, high pressure, dust laden environment are examined. This study has been limited to a survey of the various methods available. The reader is referred to the bibliography (Appendix A) for further depth on the subject matter.

Some general considerations for the required measurements are presented in Section 2. Velocity, pressure, and temperature measurement techniques are examined in Sections 3 and 4. Finally, conclusions are given in Section 5.

SECTION 2

GENERAL CONSIDERATIONS

In this section several aspects of the velocity and temperature determination in a high temperature, high pressure environment are discussed. In Section 2.1, the problems arising from operating in a severe environment are presented. The need for accurate determination of velocity, pressure, and temperature is discussed in Section 2.2. Finally, the operating characteristics of the instrumentation are examined in Section 2.3.

2.1 OPERATING ENVIRONMENT

The operating environment for the high temperature, high pressure sampling systems of interest are assumed to be as follows:

- Maximum operating temperature = 2000°F*
- Maximum operating pressure = 1500 psia
- Maximum velocity = 300 ft/sec
- Particulate size range = 0.2 to 7 microns
- Particulate loading = up to 0.2 grains/scf
- Highly corrosive atmosphere due to the presence of H_2S, SO_3, chlorine and flourine compounds
- Highly erosive atmosphere due to high velocity particulate loading
- The typical pipe diameter where measurements will be made is assumed to be 4 to 10 inches.

In addition, the stream conditions may be somewhat nonuniform or unsteady in some instances as a result of large obstructions such as valves or bends in the flow. Under some operating conditions the possibility exists that the instrumentation can become coated with materials such as slag and tars. Tar condensation is most likely to occur at lower temepratures (800°F to 1200°F). Therefore, if the environment is particularly "dirty", some means of keeping the measuring ports clear must be provided.

---

*For the most part English units are shown which are customary to sampling technology. See Appendix B for appropriate conversion factors for metric units.

At the high temperatures (2000°F) and pressures (up to 100 atmospheres), is is important to maintain the structural integrity of the components since material strength is reduced at high temperatures and loads increase in proportion to the pressure. The environment is dust laden and highly corrosive and erosive. The presence of SO_3, flourine and chlorine compounds, alkali metal compounds, and water at high temperatures, combine to produce an environment which vigorously attacks most metals. The combination of high velocities (~300 ft/sec) and large dust loadings (~0.2 gr/scf) can cause significant erosion (mechanical removal of material from surface) over a relatively short period of time. The materials for the instrumentation should be chosen with these considerations in mind. High strength stainless steels, inconels, and hastalloys are among those metals which seem promising from the standpoint of survival. As mentioned previously, the ports in the instruments are liable to be blocked in the "dirty" environment. Larger ports could be used, however these perturb the the flow, significantly, and give less accurate results. Blockage by dust particles can be avoided by periodic purging of the ports with a compressed gas. In this case, care must be taken to protect the pressure transducers or manometers during blowing. After blowing, sufficient time must be allowed for the system to achieve equilibrium before a measurement is taken. Analytical methods* have been developed to predict the transient response characteristics of pressure instrumentation.

2.2 ACCURACY

The measurement of gas velocity, pressure, and temperature is required to set isokinetic sampling rates and determine the thermodynamic state of the gas. The instrumentation should have sufficient accuracy to provide valid and repeatable data. The measurements should be reasonably accurate over the whole operating range. It is preferrable to avoid individual calibration of each probe at several operating conditions. For example, standard pitot tubes and thermocouples are attractive because they are well characterized and there is no need for individual calibration.

To ensure collection of a representative sample of particles suspended in a moving gas stream, it is necessary that the flow pattern upstream of the sampling probe be unaffected by the presence of the probe. If the flowrate per unit area through the sampling probe is lower that the freestream flowrate per unit area, the streamlines ahead of the probe will diverge. This upstream influence is typical of low speed (subsonic) flows. On the other hand, if the suction flow through the sampling probe is set too high, the streamlines ahead of the probe will tend to converge. In either event, particles contained in the flow will not follow the streamlines due to their inertia and, consequently, sampling errors will occur. It has also been shown that errors in gas concentration measurements can result from deviations from the isokinetic condition.*

---

*Aerotherm has recently programmed a method for evaluation of pressure line response times.

These adverse effects can be avoided by setting the plane of the sampling orifice normal to the direction of the flow and adjusting the flowrate of the sampler so that velocity into the probe at the entrance plane is equal to that of the undisturbed stream. When this is done, sampling is said to be isokinetic, and a representative sample enters the probe. Therefore, there is need for accurate measurement of stream velocity in order to determine the proper suction rate through the sampling probe.

As mentioned previously, errors associated with anisokinetic sampling are due to particle inertia. If the sampling velocity is less than the stream velocity (Figure 2-1(a)). Some particles originally contained in the gas stream that pass around the probe are projected into the flow entering the probe, causing the concentration to be overestimated. The opposite effect occurs (Figure 2-1(b)), when the sampling velocity exceeds the stream velocity.

When the sampling is not isokinetic, that is, the sampling velocity, V_s, differs from the velocity, V_a, of the gas stream, the measured concentration of the particles, C_s, defined as the ratio of the weight of the particles to the volume of the gas drawn in, can be written as:

$$\frac{C_s}{C_a} = \alpha \frac{V_a}{V_s} + (1 - \alpha)$$

Where C_a is the actual concentration and α is a parameter depending on the particle character (shape, size, density), on the gas density and the pattern of the streamlines in the neighborhood of the probe. If the particles are very small, $\alpha \rightarrow 0$, and $C_s \rightarrow C_a$, regardless of the rate of suction, which amounts to saying that very small particles follow the streamlines and behave like gas molecules. On the other hand if the particles are very large, $\alpha \rightarrow 1$

$$\therefore \frac{C_s}{C_a} = \frac{V_a}{V_s}$$

Multiplying this equation by $\frac{SV_s}{SV_a}$, where S is the area of suction, gives:

---

*See Reference 6.

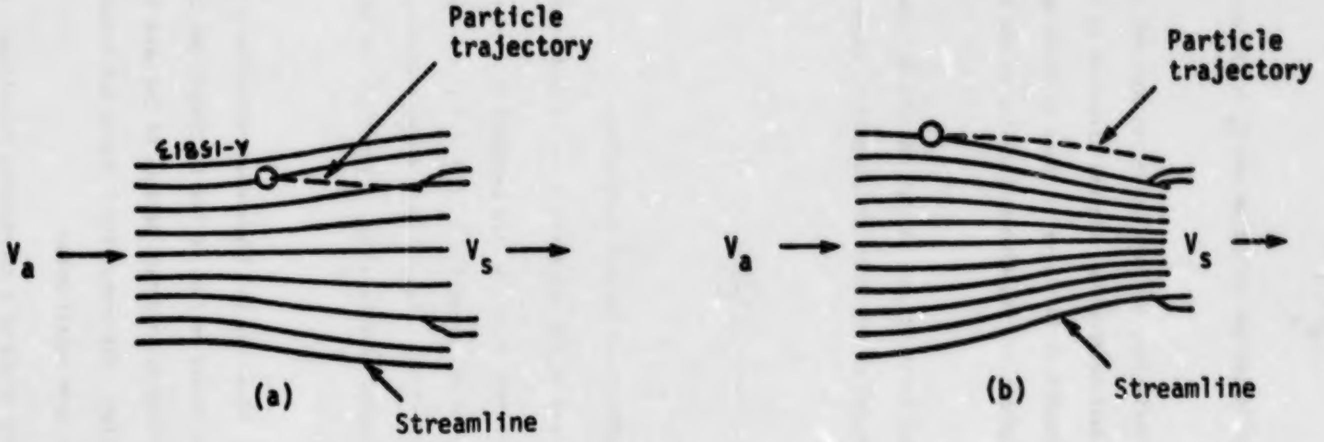
A-15813
Particle trajectory
V_a
V_s
Streamline
(a)
Particle trajectory
V_a
V_s
Streamline
(b)

Figure 2-1. Examples of anisokinetic sampling.

$$\frac{C_s S V_s}{C_a S V_a} = 1$$

$$\therefore \frac{M_s}{M_a} = 1$$

Where M_s is the mass of the particles collected per unit time and M_a is the actual mass of the particles in the stream.

Thus, in the case of very large particles, the mass collected does not depend upon the rate of suction because large particles do not deviate from the original direction of the flow due to their large inertia. The particulate concentration in this case is found by dividing this mass by the actual volume flowrate. Figure 2-2 shows the effect of anisokinetic sampling on the measurement of particulate concentration.

In the intermediate case, when the particles are neither too big nor too small, i.e., $0 < \alpha < 1$, either isokinetic sampling should be ensured or the value of α should be approximated. An expression for α is given by:

$$\alpha = 1 - \frac{e^{-L/\lambda}}{L/\lambda}$$

where: $\lambda = uV_s/g$

u = Velocity of free fall of particles in an undisturbed flow

L = Length of purturbation upstream of the probe (function of probe geometry)

In the present application, the maximum particle size expected is 7 microns. For C_s/C_a = 1.5 (i.e., 5 percent error in concentration measurement), V_a/V_s = 1.3 (i.e., 30 percent error in isokinetic sampling condition can be tolerated). Thus, given the required accuracy limit on concentration, the accuracy requirement on velocity, pressure, and temperature can be determined.

2.3 OPERATING CHARACTERISTICS

The instrumentation for velocity, pressure, and temperature measurement should be simple to use and easy to maintain. The response time should be low, so the instrument can quickly react to changing operating conditions. Traversing capability is important because of the need for obtaining data which is representative of the duct cross section. The probe itself should not disturb the flow field significantly. This problem is examined in more detail below:

In-situ probes disturb the velocity field of a surrounding flowstream. In HTHP applications the low subsonic (virtually incompressible) character of the flowstream permits these disturbances to

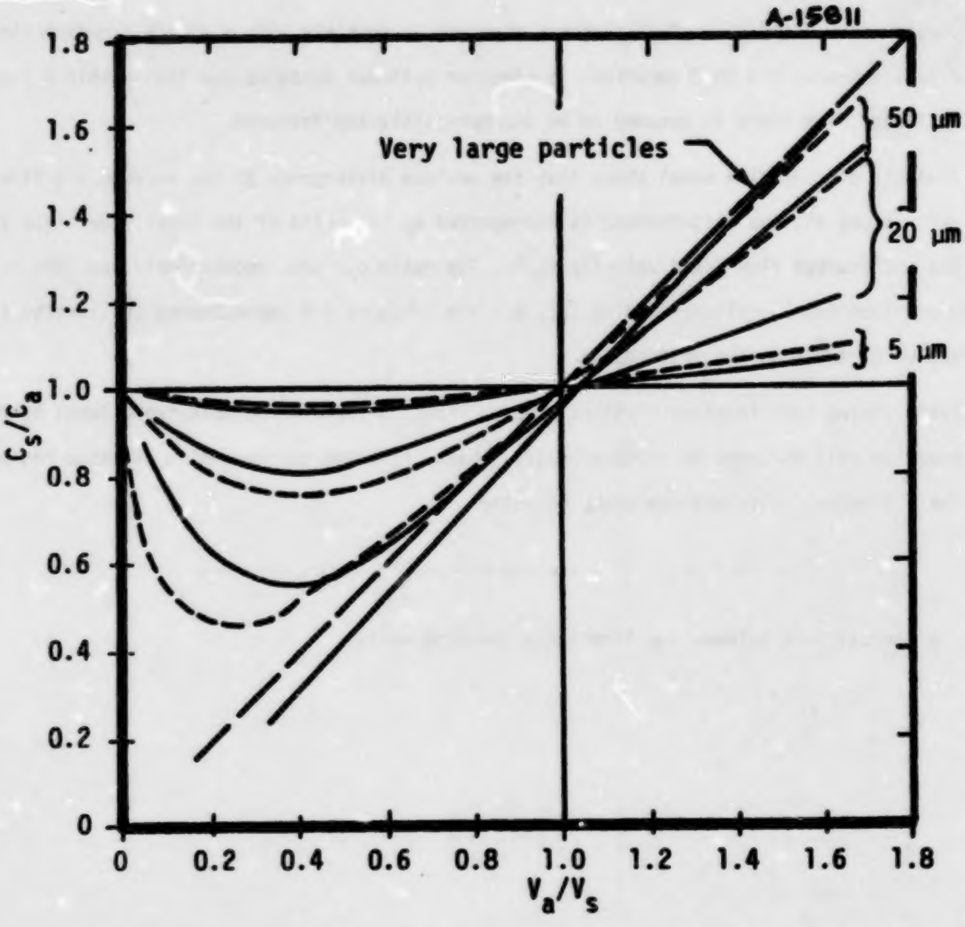

Figure 2-2. Effect of anisokinetic sampling on the measurement of concentration.

propagate for some distance in all directions from the probe. Disturbance strength depends upon the size of the probe; it also diminishes with increasing distance from the probe. Thus, it may be possible and practical in a given application to size the probe(s) so that interactions between the probe(s) and the flowstream bounding walls or other members are negligible.

Conservative estimation of disturbance strength is possible with a simple two-dimensional model. Figure 2-3 illustrates the configuration: a circular cylinder oriented parallel within a steady, uniform flow field. The fluid is assumed to be incompressible and inviscid.

Analysis of this flow model shows that the maximum disturgance to the surrounding flow occurs at $\theta = 90°$. Along AA, the disturbance, is represented by the ratio of the local flow field velocity (u) to the undisturbed flow field velocity (U_∞). The ratio $\Phi \equiv u/U_\infty$ depends only upon the ratio (R) of field position (r) to cylinder radius (a), $R \equiv r/a$. Figure 2-4 demonstrates the inverse square law effect of distance on the disturbance.

Probe sizing then involves distinct steps. First, determine the acceptable level of disturbance at the bounding wall in terms of velocity ratio. Next, find the corresponding distance ratio from Figure 2-4. Finally, calculate the probe diameter:

$$d = \frac{h}{r}$$

where h is the distance between the flowstream bounding walls.

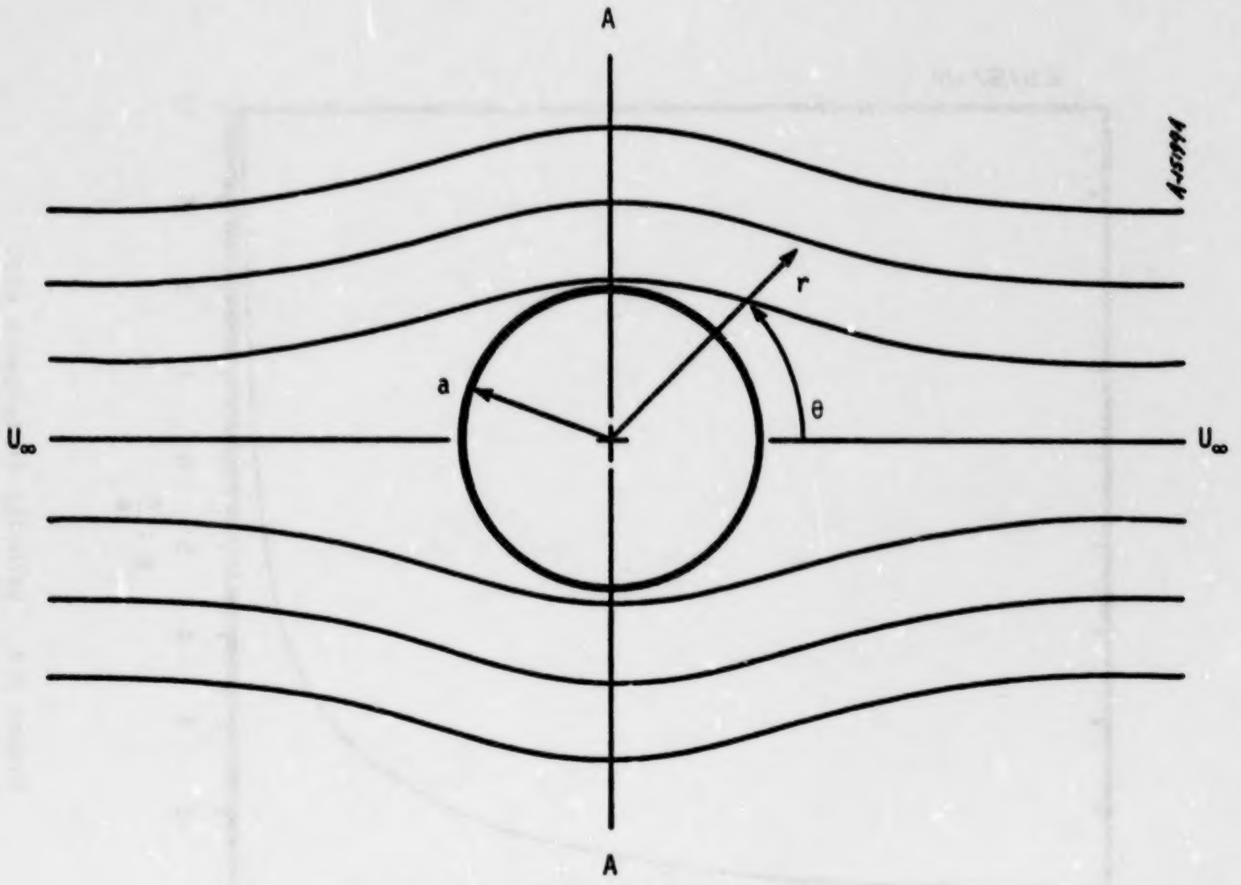
A
A
a
r
θ
U_∞
U_∞
A-15994

Figure 2-3. Circular cylinder in a steady, uniform flow field.

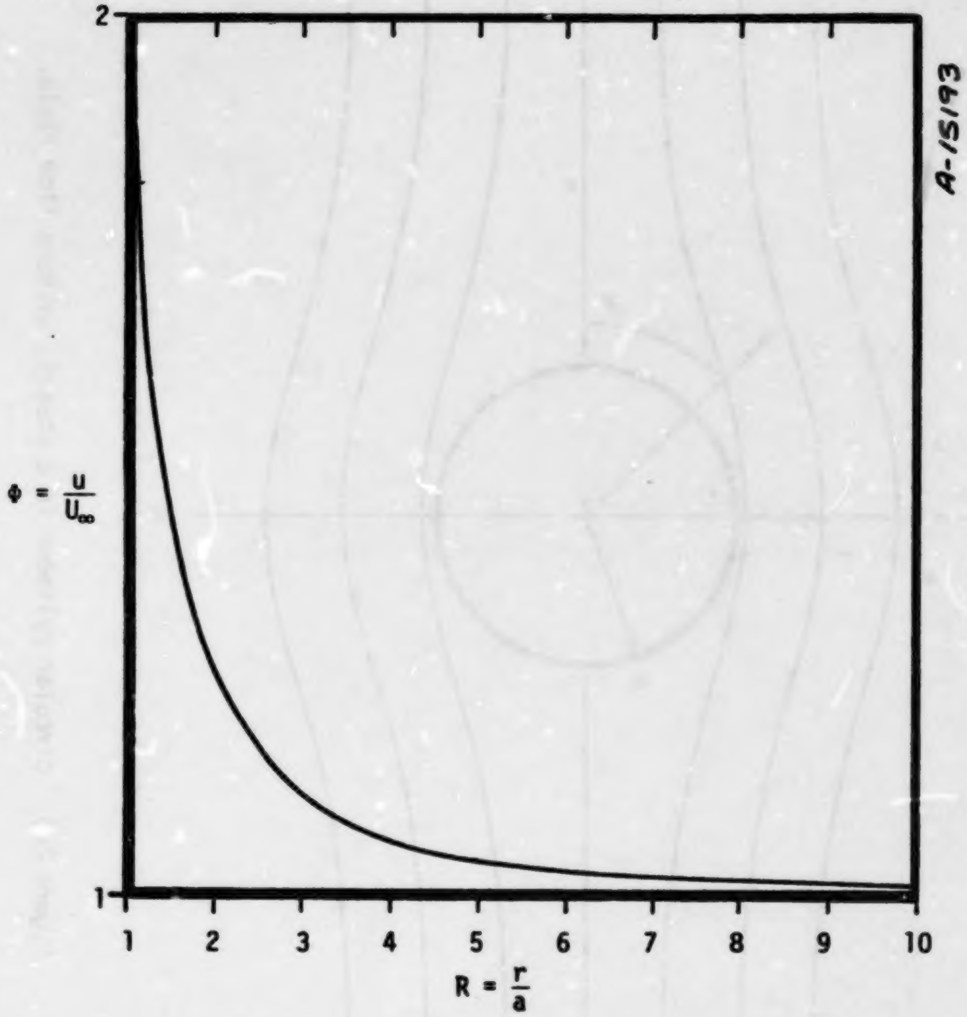

A-15193

Figure 2-4. Velocity disturbance with distance, θ = 90°.

SECTION 3

VELOCITY AND PRESSURE MEASUREMENT

Generally, the method used for the measurement of flow velocity in low speed flows is based on the Bernoulli equation for incompressible flow. The relation is given by:

$$p + \frac{\rho V^2}{2} = \text{constant}$$

This equation expresses conservation of energy along a streamline in a perfect fluid (inviscid and incompressible). The potential energy term (ρgz) has been omitted in this equation because for gaseous flows it is negligible compared to the other terms. Applying this relation at the stagnation point of the measuring probe,

$$p + \frac{\rho V^2}{2} = p_o$$

where: p_o = stagnation pressure

p = static pressure

V = freestream velocity

ρ = density of the fluid

Hence, the fluid velocity can be determined from the measurement of the differential pressure, $p_o - p$:

$$V = \sqrt{\frac{2(p_o - p)}{\rho}}$$

In most low speed flow situations temperature can be measured with sufficient accuracy by means of an ordinary thermocouple and the fluid density can be determined from the measured temperature and static pressure through the equation of state. If it is assumed that a lack of isokinetic sampling conditions can result in errors in gaseous concentration, then the determination of true gas density will depend upon a correct setting of the sampling rate. However, the above equation indicates that the density must be known apriori. Hence, the molecular weight, M, appearing in the equation of state* must be determined either iteratively from the measured quantities of each constituent and then adjusting the sampling rate, accordingly, or calculated by some means such as shown in Appendix B. Also in high temperature applications the temperature sensor must be able to survive the environment and, in addition, be free of errors produced by radiation effects. Several different instruments, using the simultaneous measurement of pressure differential and temperature measurement to obtain flow velocity are discussed in Section 3.2.

There are other methods of determining the flow velocity which do not require the measurement of differential pressure and static temperature. Some of these methods for example, include use of laser or sound beams. Others depend on determining the force exerted on a body of known drag characteristics. These methods are also discussed in Section 3.2.

3.1 GENERAL CONSIDERATIONS

In this section certain additional aspects of the problem of velocity measurement using pressure differential are discussed. First, we must consider under what conditions the flow may be treated as incompressible.

3.1.1 Compressibility of Gas

Bernoulli's equation for compressible flow is:

$$\frac{V^2}{2} + \frac{\gamma}{\gamma - 1}\,\frac{p}{\rho} = \text{constant}$$

Here, γ, is the ratio of specific heats** at constant pressure to that at constant volume. Applying the equation between the freestream and stagnation conditions,

$$\frac{V^2}{2} + \frac{\gamma}{\gamma - 1}\,\frac{p}{\rho} = \frac{\gamma}{\gamma - 1}\,\frac{p_o}{\rho_o}$$

Assuming ideal gas behavior, this equation can be expressed as,

$$p_o = p + \frac{\rho V^2}{2}\left(1 + \frac{M^2}{4} + \frac{2 - \gamma}{24} M^4 + \ldots\ldots\right)$$

where: M = Mach number $\equiv \frac{V}{a} = \frac{V}{\sqrt{\gamma R T}}$ (ideal gas)

---

* $\rho = \frac{PM}{RT}$

**See Appendix B

The Mach number expected (with maximum gas velocity = 300 ft/sec, and velocity of sound = 1100 ft/sec at room temperature)

$$M_{max}\Big|_{\text{room temperature}} = \frac{300}{1100} = 0.27$$

The error due to compressibility at M = 0.27 is less than 2 percent. At higher temperatures, the Mach number will be even less, since the speed of sound is proportional to $\sqrt{T}$. Therefore, compressibility effects are not important in the present application.

3.1.2 Reynolds Number

For low Reynolds numbers, viscous forces are no longer negligible in comparison to inertia forces and the Bernoulli equation is no longer strictly applicable. In this case the measured pressure differential can be corrected by dividing by a viscous correction factor, K. Figure 3-1 shows a theoretical calculation as well as experimental values for the factor, K, for a Prandtl type pitot/static tube. Several pitot/static tube designs exist; the so called Prandtl tube constituents one particular design (See Reference 13).

Low Reynolds numbers are obtained at low velocities and high temperatures. Consider air at 2000°F (maximum temperature for the application under consideration) and flowing at 10 ft/sec under 1 atmosphere pressure. Also assume a pitot tube diameter of 0.1 inch.

$$\rho = \frac{p}{RT} = \frac{14.7 \times 144}{53.3 \times 2460} = 0.016 \ \frac{\text{lbm}}{\text{ft}^3}$$

$$\mu = 338 \times 10^{-7} \ \frac{\text{lbm}}{\text{sec-ft}} \text{ at } \sim 2500°\text{R}$$

$$\therefore \ \text{Re} = \frac{0.016 \times 10 \times 0.1}{12 \times 338 \times 10^{-7}} = 39.4$$

This is about the lowest possible Reynolds number that can be expected since at lower temperatures and higher pressures the Reynolds number will increase. Deviations in the correction factor, K, from unity are not significant above this value of Reynolds number. If, however, Re drops below 20, the factor K rises rapidly and the correction factor needs to be considered. It is highly desirable to be operating above this critical Reynolds number at all times. It is, therefore, desirable to know the critical Reynolds number at which viscous effects need no longer be considered. It should be noted that for some other pressure probes the critical Reynolds number may be significantly higher and under a range of operation they need to be corrected for viscous effects.

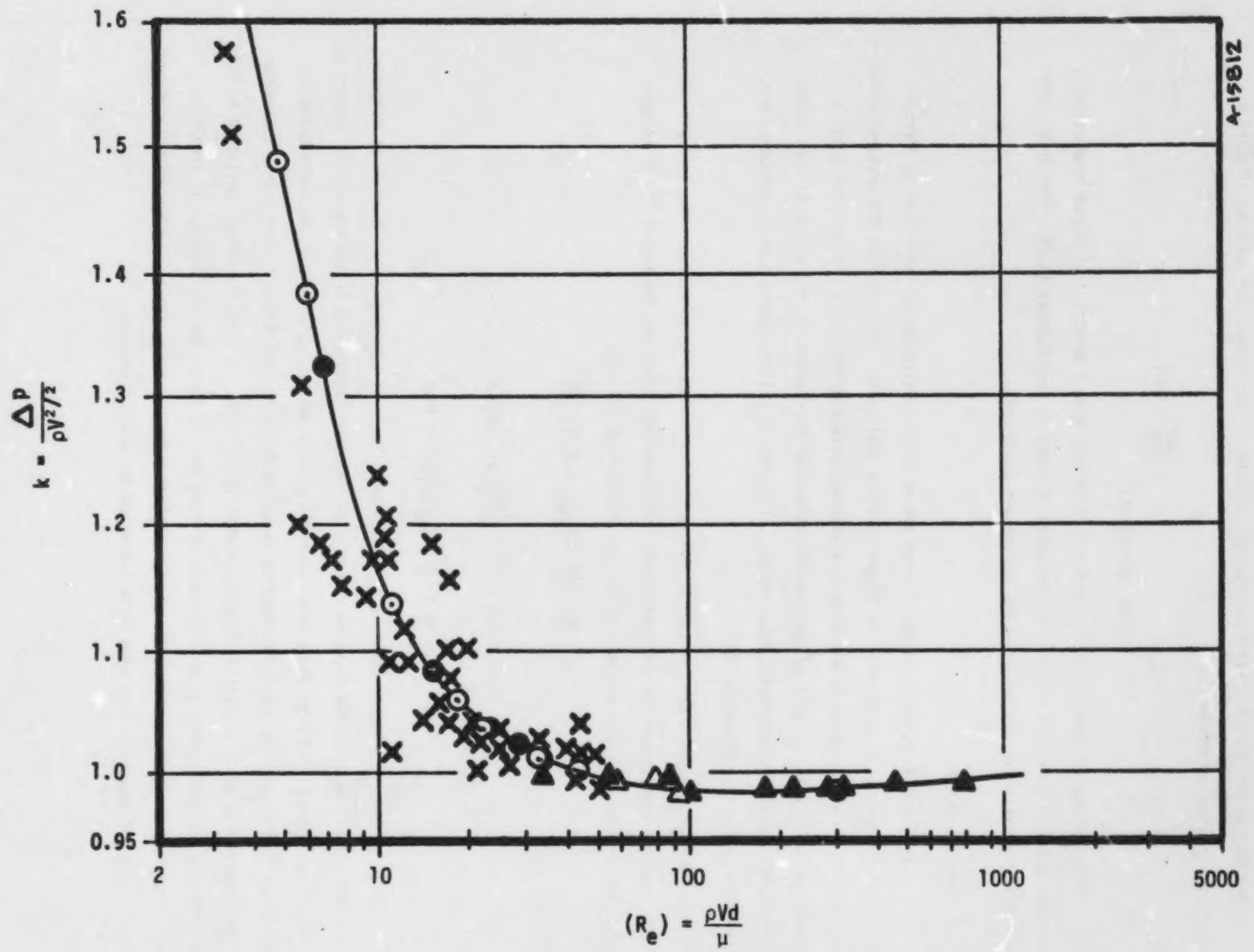

Figure 3-1. Correction factor k for low Reynolds numbers for a Prandtl pitot tube.

3.1.3 Turbulence

The differential pressure measurements are affected by turbulent velocity components. These turbulent components of velocity contribute to errors in the measurement of average static pressure levels. Corrections for the effects of turbulence are difficult to make since the intensity of turbulence is generally not known apriori and is difficult to measure. The effects of turbulence upon measured values are generally small (<1 percent) and can probably be neglected for the present application.

3.1.4 Solid Particles in Suspension

The solid particles suspended in the gas stream may affect the measurement of velocity by direct deposition on the probe thus blocking off the ports. As the pressure ports are blocked progressively by particle deposition, a drift in the reading will occur. Also, the deposited particles may combust under suitable conditions. Account also has to be taken of changes in the density of the fluid due to the presence of the particles. These can be considered as two phase flow effects.

The static pressure is generally measured where the flow is relatively undisturbed from its freestream condition. Under these circumstances the particles move at nearly the same velocity as the gas flow and follow the streamlines. Each particle, provided it is not too large, behaves as a fluid particle and the fluid density can be taken as the average density, i.e., total mass per unit volume;

$$\rho = \rho_{gas} + C$$

where C is the mass of particles per unit volume of gas under the measuring conditions. It is clear that under the conditions of concern this effect is negligible since at the lowest gas density of interest ($\rho = 0.016$ lb/ft^3 at 1 atm and T = 2000°F and for C = 0.2 gr/ft^3) the error in neglecting the last term is less than 0.2 percent.

The effect of the particles on the total pressure measurement is more complicated since the total pressure measurement is dependent upon the manner in which the particles are decelerated as they arrive at the stagnation point. Influencing factors are: the characteristics of the particles (dimensions, form, density, velocity, and concentration), of the gas (density, viscosity, and velocity) and of the probe (dimensions, form, etc.). Two extreme cases can arise in which the particles are sufficiently large so that they move independently of the streamlines, or alternatively they are sufficiently small so that they behave as particles of fluid.

In the case of large particles, there are two possibilities: (a) the particles will lose their kinetic energy by collision or friction against the probe in which case the fluid will not recover the energy and the density is to be taken as the density of the fluid itself and (b) the particles are decelerated by the fluid, in this case the change in kinetic energy of the particles results in an increase in the total pressure as given by the equation,

$$p_o = \rho_{gas}\frac{V^2}{2} + p + CV^2$$

that is,

$$p_o - p = \left(\frac{\rho_{gas} + 2C}{2}\right)V^2$$

The mixture is thus considered to have a density = $\rho_{gas} + 2C$.

When the particles are sufficiently small, they follow the streamlines and behave like elements of fluid. There is no exchange of energy between the particles and the fluid. Kinetic energy is transformed into potential energy according to the Bernoulli equation and the density is to be taken the average density, i.e., $\rho = \rho_{gas} + C$. However, in the present application, since C is less than 0.2 percent of the lowest gas density considered, the effect of particle concentration upon pressure measurement can be neglected.

3.1.5 Orientation of Probe and Flow Angularity Measurement

Errors can arise when the probe is inadvertently placed at an angle to the direction of flow. Figure 3-2 shows the typical errors that result when pressures are measured with a probe oriented at some angle, θ, to the direction of the flow. For flow in a pipe, it is adequate to align the probe along the centerline, hence, flow angularity is not considered a prime source of error in these applications.

Sometimes, it may be necessary to make a measurement in a region where the flow direction is not known. In such a case the direction of flow may be of interest. For this type of application a device known as a cone flow probe, which is intentionally sensitive to angle of attack, may be used. Figure 3-3 shows such a probe. In practice, the angle of attack may be deduced by two methods. First, by calibrating the static readings with angle of attack, or secondly, by moving the probe head, iteratively, until the static ports are nulled.

3.2 INSTRUMENTS FOR VELOCITY MEASUREMENT

In this section some of the instruments used for pressure and velocity measurement are described.

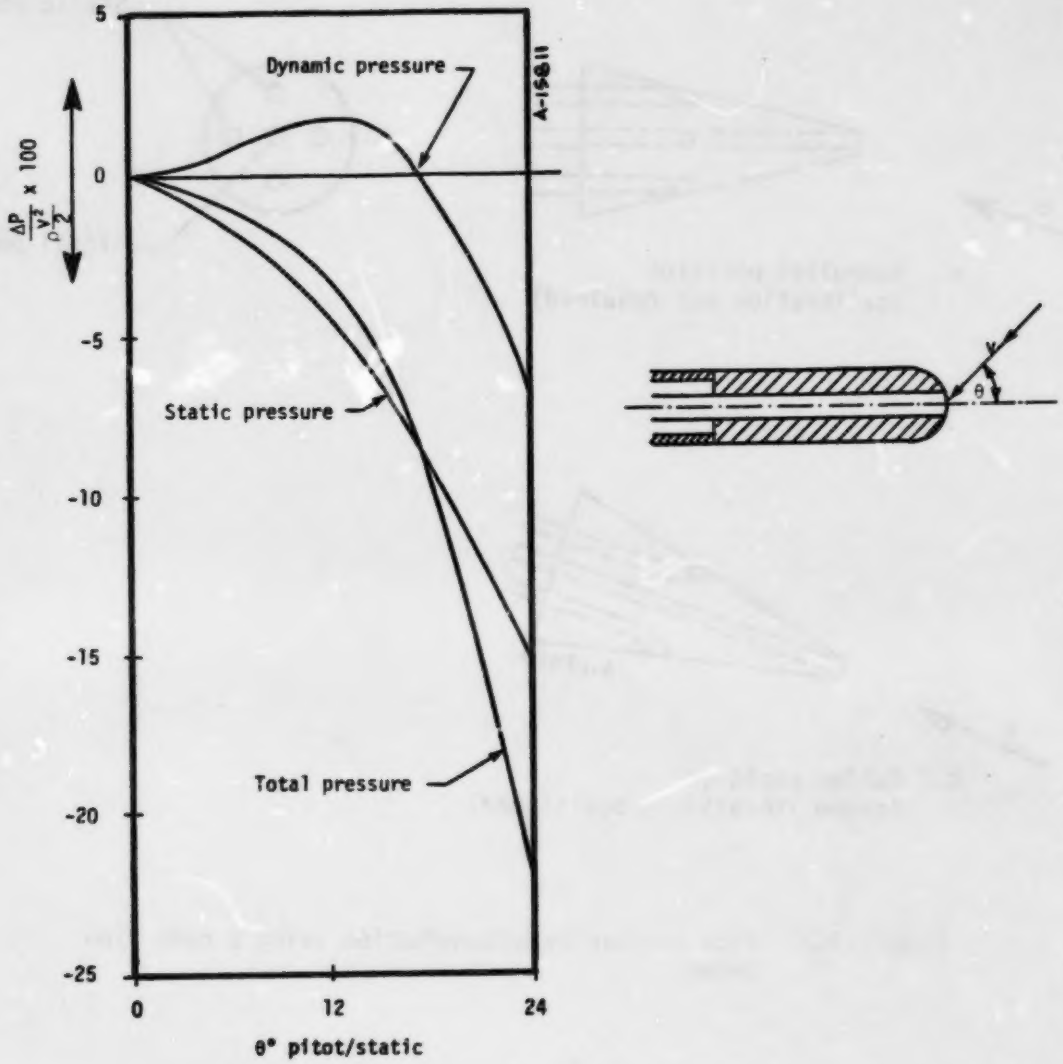

Figure 3-2. Influence of pitot/static probe orientation on measured pressure.

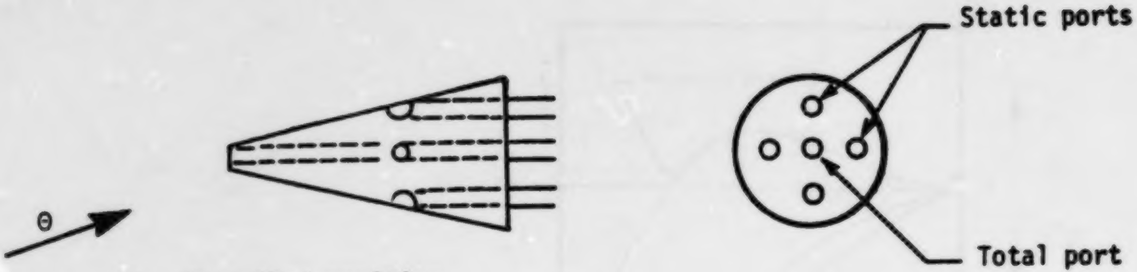
Static ports
Θ
Total port

a. Nonnulled position
(calibration map required)

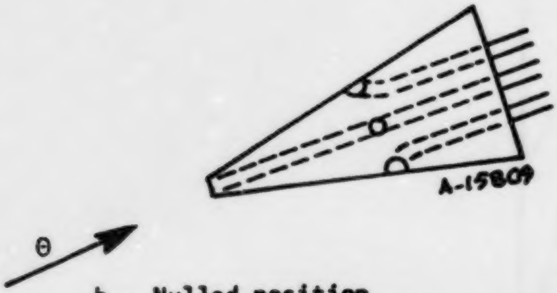

b. Nulled position
(probe iteratively positioned)

Figure 3-3. Flow angularity determination using a cone flow probe.

3.2.1 Pitot/Static Probe

Pitot/static probes can be used to obtain accurate velocity measurements. The typical probes shown in Figure 3-4 has an impact port at the head to measure stagnation pressure and one or more ports located on the side about 8 to 10 diameters downstream of the tip to measure static pressure. Usually the static ports are manifolded to provide an average value. For low Mach number flow (<0.3) the dynamic pressure is a direct measure of gas velocity and is simply the difference between stagnation and static pressures. As mentioned previously, to obtain the velocity from the dynamic pressure it is also necessary to know the gas density. This usually requires information about the gas composition, temperature, and pressure. Calculations of typical coal combustion products indicate that the gas constant, R, does not differ greatly from that of air (see Appendix B).

Advantages of the pitot tube are as follows:

- It is accurate
- Standard designs are available
- Calibration constants are well known
- Nominal flow field disturbance
- Relatively insensitive to flow angularity (especially with ellipsoidal nose design).

The disadvantages and possible remedies are:

- Small ports are likely to be clogged in dust laden environments – if feasible, back pressurization can be used to unclog the ports
- At low speeds, the pressure differential may be too small to measure with a standard manometer – sensitive differential pressure transducers can be used
- At high pressure levels manometers may be impractical – use differential pressure transducers
- The "L" shape may make it difficult to insert in small diameter pipe – use hook shape
- For high velocity streams at high temperature and pressure, aerodynamic loads may lead to structural problems – add reinforcement ribs (see Figure 3-4).

It seems likely that the shortcomings of the pitot/static probe can be overcome, and therefore, it is a viable candidate for pressure and velocity measurements.

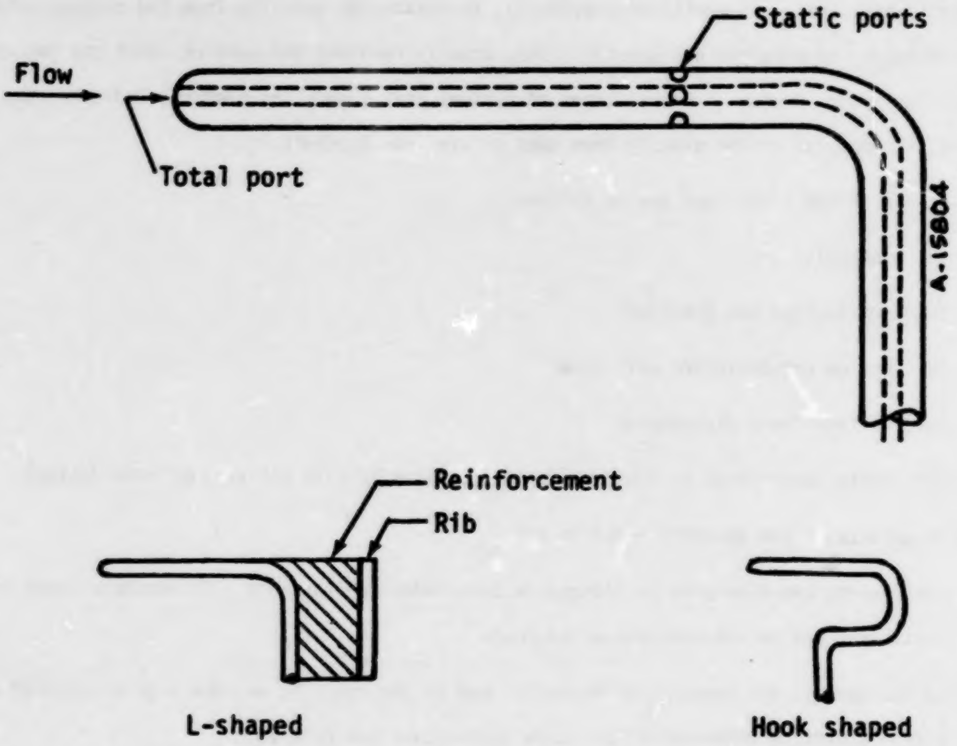
Static ports
Flow
Total port
A-15804
Reinforcement
Rib
L-shaped
Hook shaped

Figure 3-4. Typical pitot/static probe.

3.2.2 Disc/Static Heads

In dirty environments, the small holes in the static ports of the pitot tube are liable to be blocked. It is, therefore, desirable to provide larger port openings. Under such conditions, a disc/static head may be used with the usual form of pitot head as shown in Figure 3-5. Such a combination may disturb the flow field considerably more than the standard pitot/static tube. Another disadvantage is that the measurements are very sensitive to flow angularity that might be encountered near a pipe bend or near a sudden pipe expansion or contraction. For these reasons, the disc/static head is probably not appropriate for application to the present problem.

3.2.3 "S" Type Pitot Tube

The "S" type (stausscheibe) or reverse pitot tube (Figure 3-6) has gained popularity for dust laden environments. The large port openings can delay plugging by dust for a considerable time period. Also a suction effect on the downstream facing tube causes the pressure in the wake to be lower than the stream static pressure. As a consequence, measured pressure differences for "S" type tubes are greater in comparison to standard pitot devices thus increasing the sensitivity. However, it is usually desirable to know static pressure for other reasons such as determining stream density.

The large tube diameter, plus the fact that two lengths of tubing are coupled back-to-back, lead to more significant stream disturbances than the pitot/static probe. Hence, there is need for correct calibration of the "S" type probe. It has been observed that the calibration factor for the "S" type pitot tube depends on the overall probe configuration (i.e., sampling nozzle, thermocouple, etc.). Therefore, the "S" type pitot tube must be mounted on the complete probe assembly for proper calibration. The major disadvantage of the "S" probe is that the calibration factor may depend on Reynolds number, whereas, the pitot/static probe is relatively insensitive to viscous effects as mentioned previously. Therefore, the determination of Reynolds number becomes coupled to the measurement of velocity. Also the calibration is somewhat affected by the amount of turbulence present in the calibration stream compared to the test stream.

The "S" probe is also fairly sensitive to flow angularity. In spite of these negative aspects, the fact that the probe is much less susceptable to plugging than the pitot/static, makes it an attractive choice for use in highly particle laden streams. Its use, thereby, avoids the use of unproven, complex, purging systems.

3.2.4 Other Special Probe Designs for Measurements in Dust Laden Gases

Since an ordinary pitot tube can be easily blocked by particles, special probes may be used for the measurements of velocity. When the particles are small and their concentration is low, blockage

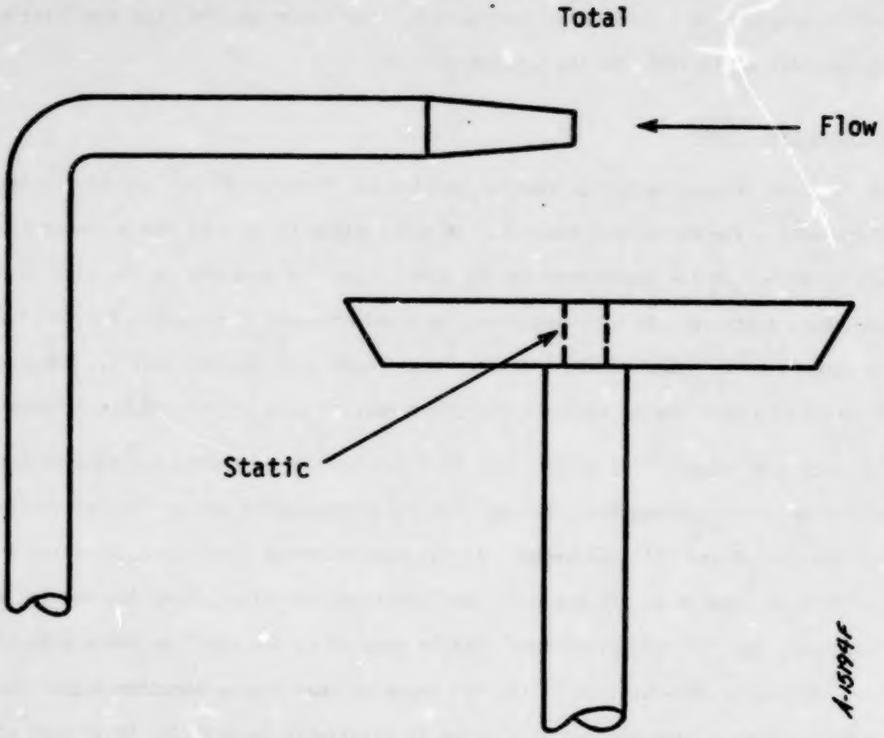
Total
Flow
Static
A-15194F

Figure 3-5. Disk/static head.

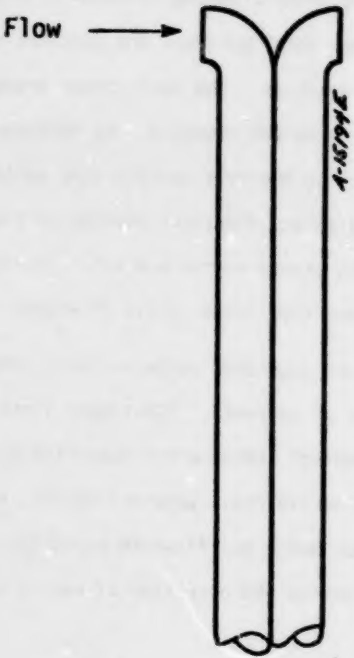
Flow
A-15794E

Figure 3-6. "S" type pitot.

of the total pressure port can be avoided by the method shown in Figure 3-7(a). A small tube facing downstream is fitted into a large cavity at the stagnation point. The static pressure is not actually measured, but a pseudo static (base) pressure is measured instead, by porting in an area protected from the particles by a flange. Since this is a nonstandard probe design, the configuration must be calibrated in a wind tunnel.

For large particles, the static pressure is measured with a cylindrical tube and instead of stagnation pressure, pressure in the wake of the tube is measured (Figure 3-7(b)). This probe design also has to be calibrated.

Another suggested means of preventing probe clogging is shown in Figure 3-8. Here, to avoid interference effects, the static pressure and total pressure are measured on separate heads. Purge gas is constantly pumped back through the port openings. The test stream pressure levels are not measured directly, but instead are deduced from the purge gas flowrate. By maintaining subsonic flow conditions in the purge flow, the local "back pressure" at the port opening acts as the control valve on the purge flow. By separately measuring the purge gas flowrates outside of the test stream with some device such as a venturi flowmeter, the test stream static and total pressure levels can be determined. By using a conical design similar to the cone flow probe, angle of attack could also be determined.

The design of a system such as the one suggested above would be strongly tied to the particular operating conditions and test configuration of interest. The supply lines and flow valves would have to be designed such that internal flow "choking" (point where mass flow per unit area is maximized) due to friction or area constriction would be avoided. Internal choking would obviate the fundamental basis of operation, in that the control over purge gas flowrate would shift from the port opening to the internal choke point. Therefore, the design and operation of such a system requires further research and development.

3.2.5 Flare Gas Probe

This probe is similar to an "S" type pitot probe with two openings at the probe tip as shown in Figure 3-9. These openings are connected by an internal tube. A portion of this tube is heated and a thermoelectric sensor measures temperature gradients along the wall of the tube, external to the flowstream. The sensor, in effect, acts as a flowmeter. Purge gas is injected into the tubing such that a pneumatic bridge is formed. At zero line velocity, the bridge is balanced and purge gas exhausts out of both tips equally. As flow across the tip occurs, a differential pressure is developed and the bridge is unbalanced. Purge gas still exhausts from both openings, but now they are slightly unequal. The thermoelectric sensors measure the shift in temperature gradients along the heated portion of the

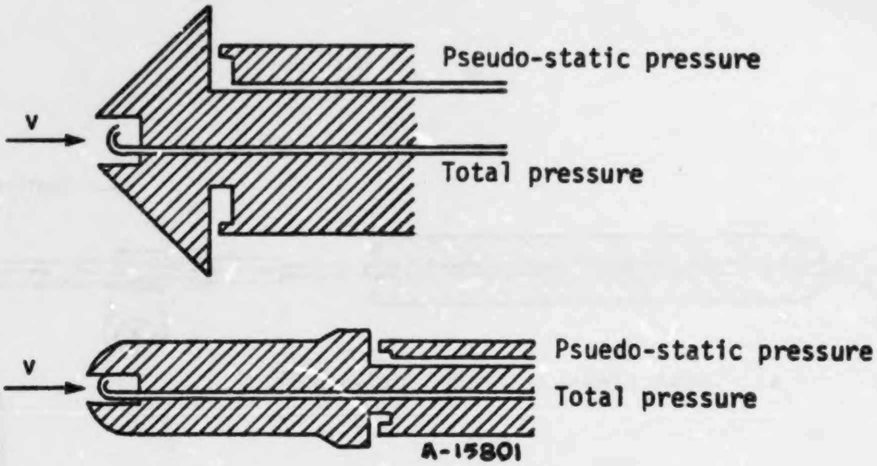
V
Pseudo-static pressure
Total pressure
V
Psuedo-static pressure
Total pressure
A-15801

a. Small particles

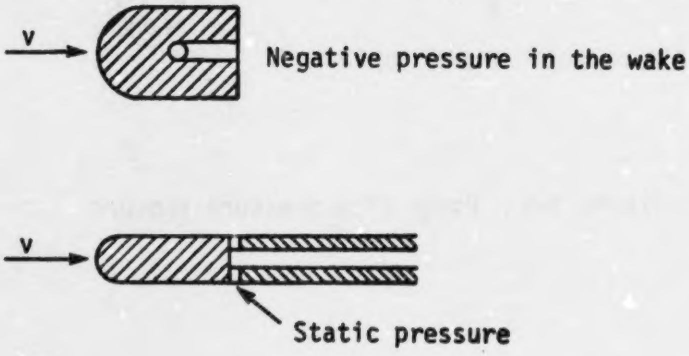
V
Negative pressure in the wake
V
Static pressure

b. Big particles

Figure 3-7. Special probes for measurement in dust laden gases.

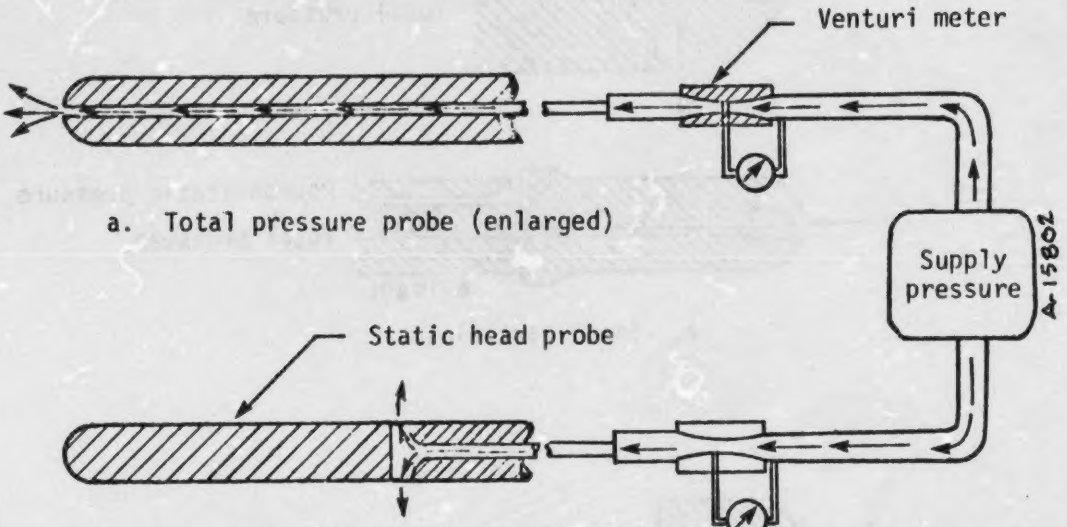
Venturi meter
Supply pressure
A-15802
Static head probe

a. Total pressure probe (enlarged)

b. Static pressure probe (enlarged)

Figure 3-8. Purge flow pressure sensors.

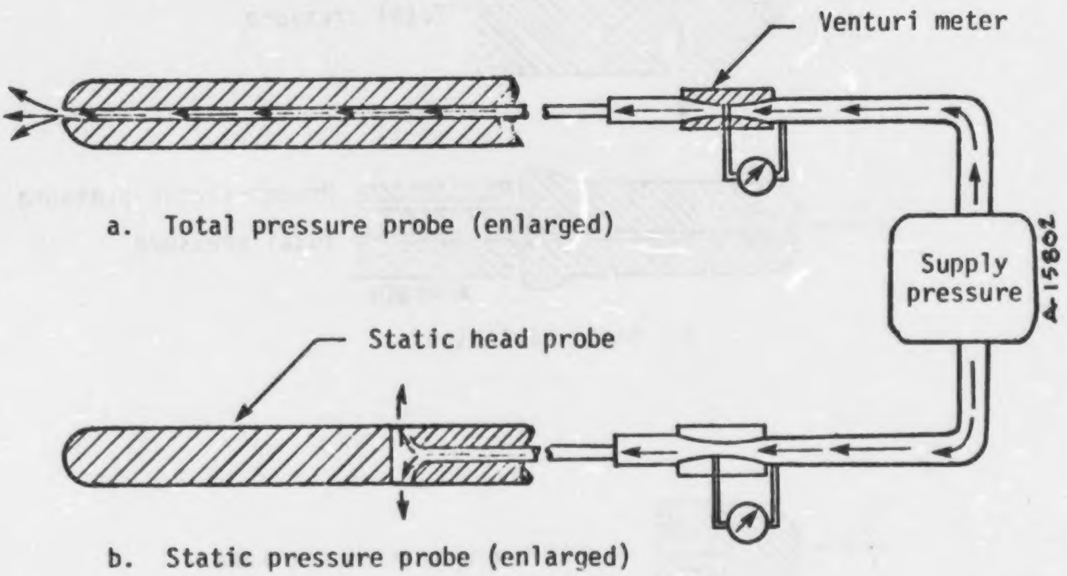
Venturi meter
a. Total pressure probe (enlarged)
Supply pressure
A-15802
Static head probe
b. Static pressure probe (enlarged)

Figure 3-8. Purge flow pressure sensors.

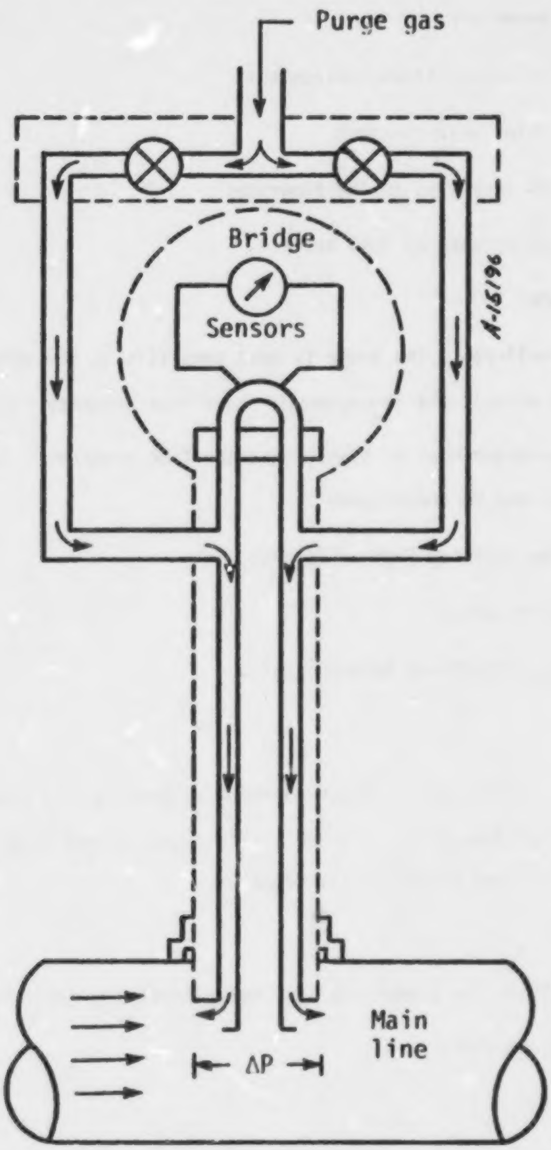
Purge gas
Bridge
Sensors
A-15196
Main line
ΔP

Figure 3-9. Flare gas probe.

tube which are directly related to the main gas flow. Because the purge gas is continuously exhausting into the flowing gas, corrosive of particulate laden gases are prevented from entering the probe.

Advantages of this probe are:

- It can be used in a dust laden environment
- Calibration is relatively constant
- The probe is most sensitive to low flowrates
- Good accuracy (±2 percent of full scale).

The disadvantages are:

- The output is nonlinear. The probe is most sensitive at low velocities. However, at high velocities (>20 m/sec), the measurements have less accuracy
- The purge gas pressure must be higher than the line pressure. In high pressure environments (~100 atm), this may be troublesome
- The probe must be isolated from vibrations
- Zero drift problems occur
- Initial setup and adjustment is complicated.

3.2.6 Drag Meter

The drag force on a target disc is measured and the velocity is calculated from knowledge of the meter drag coefficient (Figure 3-10). Bonded strain gages, in a bridge circuit outside the fluid stream, translate this force into an electrical signal.

Advantages are:

- Particulate loadings are acceptable (for heavy loading purge cleaning may be required)
- Good accuracy (±1 percent).

Disadvantages are:

- The probe is sensitive to flow angularity
- The stream density must be well known
- Heavy particulate loading could cause errors due to impacts.

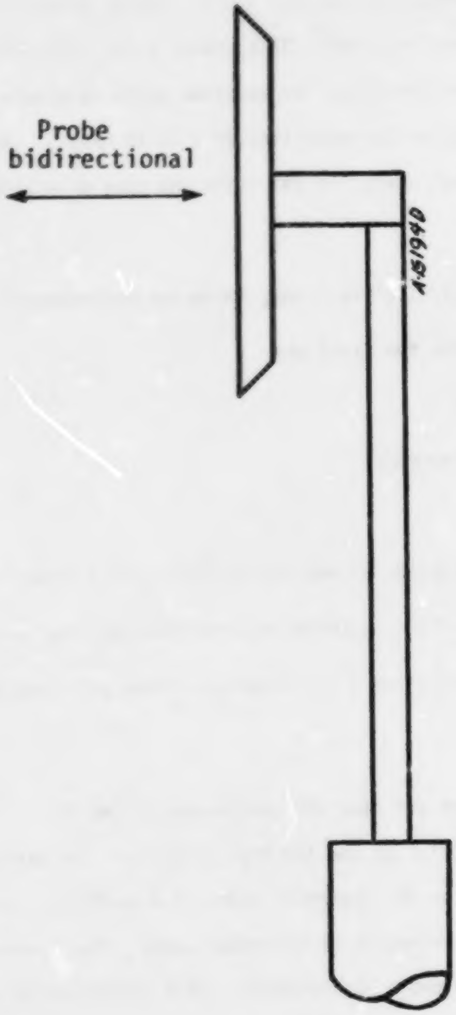
Probe bidirectional
A-51994D

Figure 3-10. Drag meter.

3.2.7 Fluidic Sensors

Two types of fluidic sensors are generally used: crossflow and co-flow. The crossflow sensor (Figure 3-11) employs a jet stream normal to the measured flow, two receiver ports and a device to measure the differential pressure across the receiver ports. Sensor operation depends upon the jet entraining and mixing with the surrounding fluid. This causes a jet deflection which is measured by the receiver port. The differential pressure across the receiver ports is a measure of flow velocity. The crossflow sensor is most accurate at low velocities (0.3 to 18 m/sec). At higher velocities (14 to 150 m/sec) co-flow sensors are used. Here the jet is in the same direction as the flow.

The advantages are:

- The probe can be used in particulate laden, corrosive environments
- Rugged construction suitable for field use
- Good accuracy (±3 percent)
- Good sensitivity at low flowrates.

The disadvantages are:

- Receiver ports may require purge to keep particulate matter from clogging ports
- Two sensors (cross- and co-flow) required to cover the required velocity range
- Calibration may be difficult since gas mixing may differ with test conditions.

3.2.8 Acoustic Velocimeter

Sound beams are transmitted both upstream and downstream of the flow. The speed of propagation is the vector sum of the local sound velocity and the flow velocity. The parameter measured is the time of transmission of a sound pulse or the change in phase of a continuous wave beam. The flow speed is determined without an explicit determination of the sound speed. One disadvantage is that heavy particulate loading can interfere with phase measurements. This technique is not yet commercially available for the type of applications discussed.

3.2.9 Orifice and Venturi Meters

With this method, a nozzle or orifice plate is inserted across the pipe . This restricts the area through which flow can pass and thus increases local velocity. A comparatively large drop in static pressure is experienced by the flow, which can be used as a measure of flow velocity. These devices are commonly used for measurement of process stream flowrates. They give average flow velocity rather than velocity at a point (which is essential for isokinetic sampling). However,

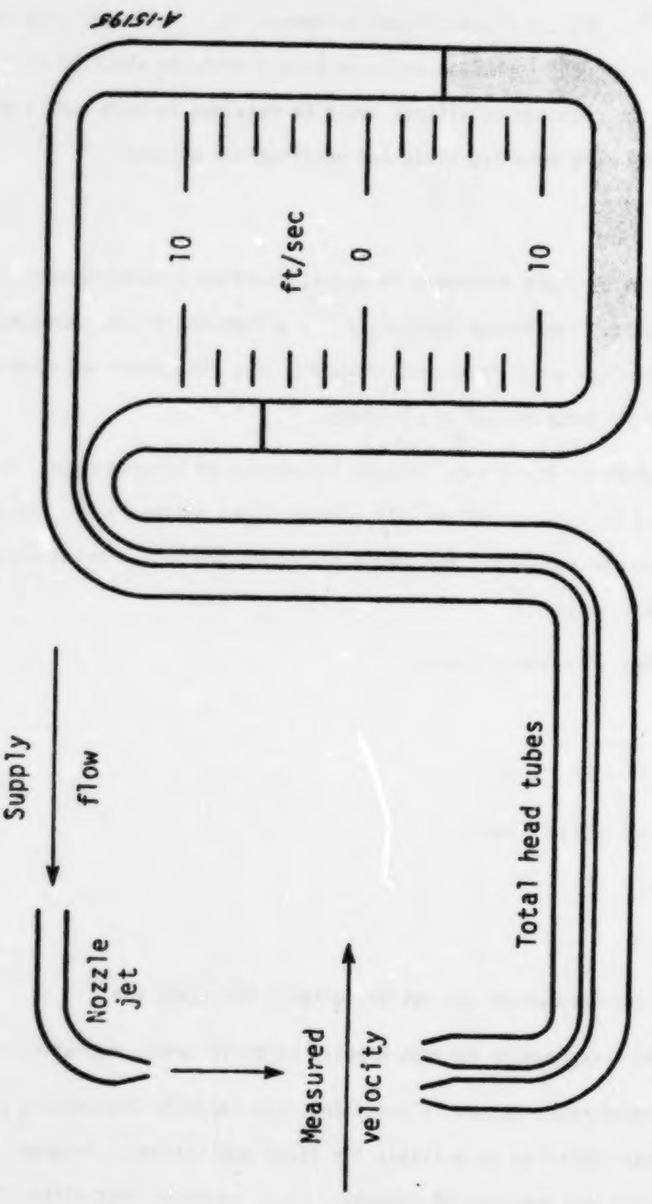
A-15195
Supply flow
Nozzle jet
Measured velocity
Total head tubes
10
ft/sec
0
10

Figure 3-11. Fluidic sensor.

if the stream is fully developed and well behaved, it may be possible to assume a fully developed turbulent velocity profile. Then knowing the total flowrate one could compute the local velocity.

In the present case, the lowest pipe Reynolds number would be about 1600 (1 atm, 10 fps, 4 in. dia., 2000°F). The entrance length required to establish fully developed flow would be given by L_e = 0.035D, or about 18 ft. At the highest Reynolds number, Re = 4.7×10^6 (100 atm, 300 fps, 4 in. dia., 2000°F) the corresponding turbulent entrance length would be about 10 ft. It is, therefore, conceivable that the required conditions could be obtained to make such a measurement. Such a technique would require more detailed study and verification by test.

3.2.10 Laser Velocimeter

When two coherent beams of light intersect in space, stationary three-dimensional interference fringe patterns are established. The fringe spacing, Δ, is a function of the wavelength, λ, of light and the angle, θ, at which the two beams intersect (Figure 3-12). The laser velocimeter utilizes the wave interference properties of two coherent light beams.

Particulate laden combustion gases pass through the region of interference. A particle moving through adjacent fringes of constant separation will scatter light periodically. This scattered light is collected by a photodetector which produces a pulsating electric current whose frequency is proportional to the particle's velocity.

The advantages of laser velocimeter are:

- High accuracy
- No perturbation of flow field
- No mechanical calibration errors.

The disadvantages are:

- High cost
- Elaborate setup required which may not be suitable for field use
- Problems of light transmission through heavily particle laden, radiating streams.

Although the laser velocimeter method is promising, considerable development problems must be overcome before it can be considered to be suitable for field application. Programs designed to test the feasibility of this method are underway at present. It is expected that within the next year or two the desirability of using this approach will be well defined.

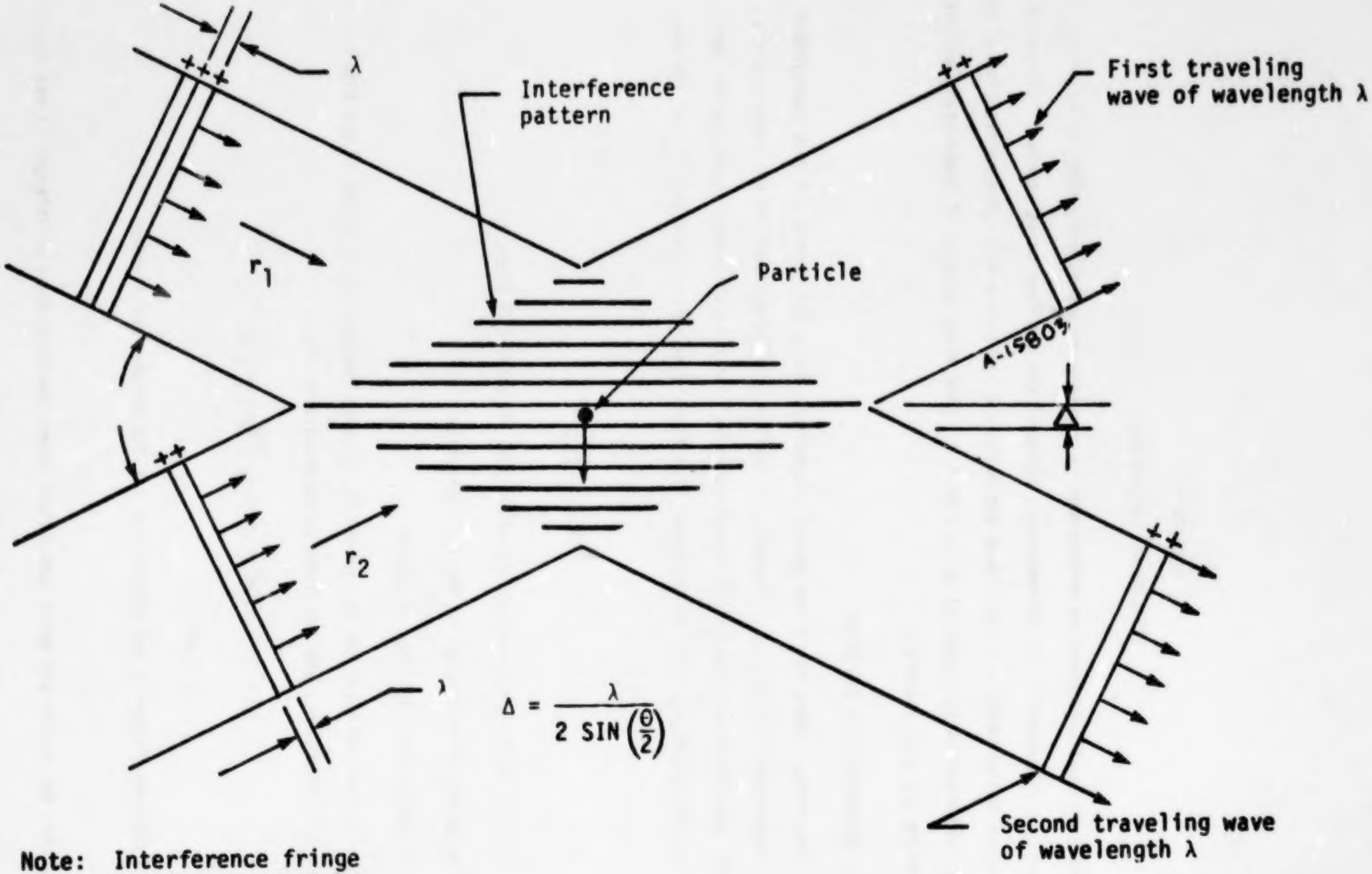
λ
Interference pattern
First traveling wave of wavelength λ
Particle
r_1
r_2
A-15803
Δ
λ
$\Delta = \frac{\lambda}{2 \sin\left(\frac{\theta}{2}\right)}$
Second traveling wave of wavelength λ

Note: Interference fringe spacing, Δ, must be greater than particle size.

Figure 3-12. Schematic of the interference between two traveling collimated coherent beams of light of wavelength λ passing through each other at an angle θ.

SECTION 4

TEMPERATURE MEASUREMENT

As mentioned previously, temperature measurement is required in the determination of velocity. It is also necessary to characterize the thermodynamic state of the gas flow being sampled. The various aspects of temperature measurement in a gas stream are discussed in Section 4.1. Determinization of gas temperature using thermocouples is discussed in Section 4.2. Some other methods of temperature measurement such as pyrometry are also described.

4.1 TEMPERATURE MEASUREMENT IN GAS FLOW

Ideally, a temperature measuring probe should stagnate a moving gas stream and give measurement of the stagnation temperature* of the gas. However, in reality, the temperature of the probe differs from the stagnation temperature as a result of energy exchange within the boundary layer, so the temperature measured by the probe, T_m, will be different from the stagnation temperature, T_o, of the gas by the amount

$$T_o - T_m = (1 - \alpha) \frac{V^2}{2JgC_p}$$

where: α is the recovery factor, with values for velocities up to Mach 3 given by,

$\alpha = 0.68$ for probe perpendicular to the flow direction

$\alpha = 0.86$ for probe along the flow direction

To establish the maximum error due to the use of recovery temperature in place of the total temperature, assume V = 300 ft/sec, and the probe perpendicular to flow

$$\therefore \Delta T = (1 - 0.68) \times \frac{300^2}{2 \times 778 \times 32.2 \times 0.24}$$

$$= 2.4°F$$

Thus, error due to recovery factor is not significant for the present application.

---

*The difference between the static and total temperature under the conditions of interest is negligible.

$$T_t - T_t = \frac{V^2}{2JgC_p} = \frac{300^2}{2 \times 778 \times 32.2 \times 0.24} = 7.5°F$$

The sensing probe and its surreoundings exchange heat by convection, radiation, and conduction. For radiant heat exchange, the probe will be "seeing" a temperature which is weighted towards the temperature of the wall. The wall temperature may be significantly less than the gas temperature; hence, there will be radiation heat loss from the probe to the walls. Also, the base of the probe may be at a lower temperature which will cause conduction heat loss. These losses have to be balanced by convective heat transfer from the gas to the probe and, hence, losses due to radiation and conduction will increase the temperature difference between the gas and the probe. To minimize this error, radiation and conduction losses should be minimized, while at the same time the convective heat transfer coefficient to the probe should be maximized.

4.2 TEMPERATURE MEASUREMENTS WITH THERMOCOUPLES

The simplest and most convenient temperature measurement device is a thermocouple. The thermocouple must be in thermal equilibrium with the surrounding media being measured. This presents several problems because the equilibrium temperature of the thermocouple junction inserted into a gaseous stream is the temperature resulting from:

1. Heat transfer by convection between the thermocouple and the gases across the boundary layer.
2. Heat transfer by radiation between the thermocouple, the gases, suspended particles, and the walls of the duct.
3. Heat conduction along thermocouple wires.

The true temperature of the gas can be determined by either minimizing the errors due to the above factors or applying corrections to the measured values. The equations governing the heat transfer between the thermocouple and its surroundings are briefly discussed below.

4.2.1 Convection

The convective heat transfer, Q_c, to the thermocouple is given by,

$$Q_c = h_c (T_o - T_t)$$

where: h_c = convective heat transfer coefficient

T_o = temperature of the gas

T_t = temperature of the thermocouple junction

The heat transfer coefficient, h_c, is generally calculated from the knowledge of the Nusselt, Prandtl, and Reynolds numbers. For combustion gases the Prandtl number is approximately 0.7 and the relations between the Nusselt number ($Nu = h_c d/k$) and the Reynolds number ($Re = \rho V d/\mu$) are as follows:

$Nu = 0.44\ Re^{0.5}$ for a thermocouple perpendicular to the flow

$Nu = 0.085\ Re^{0.674}$ for a thermocouple parallel to the flow

k = gas conductivity

Figure 4-1 shows the relationship between Nusselt and Reynolds numbers. It is apparent that in order to maximize convective heat transfer, the crossflow arrangement is preferable for $Re < 15{,}000$, whereas the parallel flow arrangement gives higher convective heat transfer for $Re > 15{,}000$.

Aspirating the gases at high velocity past the thermocouple, and decreasing the diameter of the thermocouple also increase the convective heat transfer coefficient according to:

$$h_c \propto V^n d^{-m}$$

where: $0.5 < n < 0.7$

$0.3 < m < 0.5$

Such a means of promoting convective heat transfer to the thermocouple will increase the accuracy of the device by bringing the temperature of the thermocouple closer to that of the gas stream.

4.2.2 Radiation

The radiant heat exchange, Q_R, between the thermocouple at temperature, T_T, and the surrounding walls which are at temperature, T, is given by,

$$Q_R = \varepsilon\sigma\ (T_T^4 - T^4)$$

where: ε = emissivity of the thermocouple

σ = Boltzmann constant

At high temperatures the radiative loss to the cool walls can be significant. Therefore, it is necessary to minimize this radiant heat exchange. One way to do this is to reduce the emissivity, ε. Polished metal surfaces have low emissivity at low temperature, but the emissivity increases rapidly with temperature. The emissivity also increases rapidly if the surface is altered by oxidation or deposition of foreign materials.

Radiation sheaths made of refractory materials such as Al_2O_3 possess, on the contrary, emissivities that decrease with increasing temperature. Also, they are much less subject to chemical attack by the gas mixture.

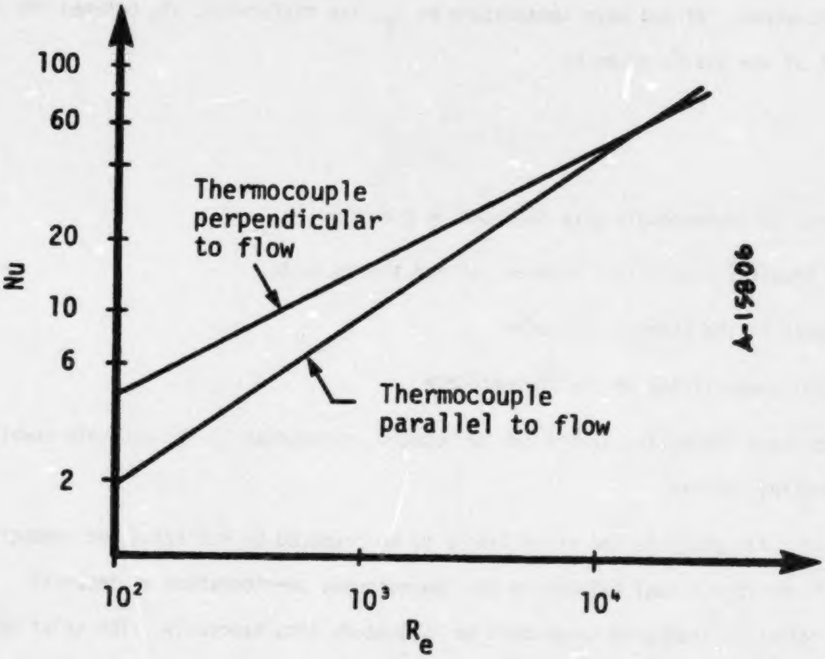

Figure 4-1. Relation between Reynolds and Nusselt numbers for flow over a thermocouple.

Another way to insure low radiant heat exchange is to create a local wall temperature, T, as close as possible to the thermocouple temperature, T_T. This can be achieved by surrounding the thermocouple by multiple radiation shields. In this configuration the emissivity of the probe and outside of the radiation shield should be as low as possible, whereas the emissivity of the inside of the shield should be as high as possible.

4.2.3 Conduction

Heat will be transferred from the tip of the thermocouple to its base by means of conduction along the junction wires. If the base temperature is T_B, the difference, ΔT, between the measured temperature and that of the gas is given by

$$\Delta T = \frac{T_T - T_B}{L\sqrt{4h/dk}}$$

where: L = length of thermocouple wire immersed in the flow

h = heat transfer coefficient between gas and thermocouple

d = diameter of the thermocouple wire

k = thermal conductivity of the thermocouple

It is likely that these conduction errors can be reduced, substantially, by adequate sheathing of the wires in an insulating material.

In order to fully evaluate the error likely to be produced by radiation and conduction effects, it is necessary to perform a heat balance on the thermocouple configuration of interest. The convective, conductive, and radiative transport terms must be evaluated, simultaneously. The solution is necessarily iterative owing to the transcendental nature of the equations.

4.3 OTHER TEMPERATURE MEASUREMENT DEVICES

4.3.1 Radiation Pyrometers

At high temperature, radiation pyrometers may be used for temperature measurement. There are two classes of pyrometers: (1) total radiation pyrometers which measure total thermal radiation emitted and (2) optical pyrometers which compare the brightness of the hot body with the brightness of a standard radiation source. The most obvious problem with pyrometry in the present application is the optical transparency of the gases. If the gas is transparent, the pyrometer will be seeing the walls and give a measurement which is weighted towards the wall temperature rather than the gas temperature. On the other hand, heavy particle loading will alter readings if the particles are not in thermal equilibrium with the gas. Other major drawbacks are a relatively high, lower temperature limit (~1500°F to 2000°F) and poor spatial resolution.

4.3.2 Molecular Beam

The temperature of the gas can be determined directly from measurement of molecular motion. The molecular beam sampling apparatus causes the gas to undergo a very rapid expansion to supersonic velocities. By intermittently chopping the molecular beam and measuring the time required for a chopped portion of the beam to arrive at a detector site, the velocity of the molecules can be determined. The velocity is a direct indication of the stagnation temperature of the gas. This technique has good accuracy and time response. However, the probe size is relatively large and is susceptible to blocking by particulate matter.

4.3.3 Velocity of Sound Method

Measurement of the velocity of sound can indcate the temperature of the gas if its thermodynamic properties are well known. Measurement of sound velocity results in determination of a value for $a = \sqrt{\gamma RT}$. This technique, however, has poor spatial resolution and requires a relatively large probe size. It also assumes the gases behave as a perfect gas mixture.

SECTION 5

CONCLUSIONS

Various aspects and methods of measuring velocity, pressure and temperature in a high temperature, high pressure, dust laden environment were examined. These methods were examined on the basis of accuracy, utility, and state of development. In the dusty environments encountered in the present application some means need to be provided for keeping the sensing ports free of particulates, tars, etc. In the near term, the "S" type pitot/static probe offers the simplest solution to the problem of velocity measurement. Shielded thermocouples should provide adequate temperature determination in the near term.

To improve the accuracy of the next generation of sampling systems, flow sensing devices incorporating more refined means of cleaning pressure ports and thermocouples should be considered. The transient purging of a pitot/static tube offers a logical solution to this problem. More detailed analyses needs to be performed to determine the necessity for aspirating thermocouples.

Some of the newer developments in velocity, pressure, and temperature sensing were briefly examined. Under their current state of development, it is difficult to assess their utility. At present, some of these devices are being evaluated by Argonne Labs, Sandia Corporation and others to determine their application towards HTHP measurements.

APPENDIX A

BIBLIOGRAPHY

1. Hawksley, P. G., Badzioch, S., and Blackett, J. H., "Measurement of Solids in Flue Gases," The British Coal Utilization Research Association, 1971.

2. Parker, G. J., "Some Factors Governing the Design of Probe for Sampling in Particle and Drop Laden Streams," Atmospheric Environment, Volume 2, pp 477, 1968.

3. Sem, G. J., and Borgos, J. A., "Instrumentation for Measurement of Particulate Emissions from Combustion Sources," Environmental Protection Technology Series, September 1973.

4. Heflinger, L. O., Matthews, B. J., and Shelton, H., "Portable Laser Velocimeter for Stack Velocity Measurements," TRW report 20852-6002-RO-00, November 1972.

5. Cheremisinoff, P. N., "Industrial Pollution Control Measurement and Instrumentation," Technomic Publishing Company, 1976.

6. Lengelle, G., Verdier, C., "Gas Sampling and Analysis in Combustion Phenomena," AGARDOGRAPH No. 168, July 1973.

7. Pustinger, J. V., Shaw, D. A., Sherman, P. L., and Snyder, A. D., "Instrumentation for Monitoring Specific Particulate Substances in Stationary Source Emissions," Environmental Protection Technology Series, EPA-R2-73-252, September 1973.

8. Brooks, E. F., Beder, E. C., Flegal, C. A., Luciani, D. J., and Williams, R., "Continuous Measurement of Total Gas Flowrate from Stationary Sources," EPA-650-2-75-020, February 1975.

9. O'Fallon, N. M., Beyerlein, R.A., Managan, W. W., and Karplus, H. B., "Monitoring Coal Energy Processes," Industrial Research, June 1976.

10. Baas, P. B., and Mai, K., "Trends of Design in Gas Turbine Temperature Sensing Equipment," Temperature - Its Measurement and Control in Science and Industry, Reinhold Publishing Company, 1962.

11. Ladenburg, R. W., Lewis, B., Pease, R. N., and Taylor, H. S., "Physical Measurements in Gas Dynamics and Combustion, Volume IX, Princeton Series on High Speed Aerodynamics and Jet Propulsion, Princeton University Press, 1954.

12. Kesselring, J. C., Gorji, K. M., Young, W. S., Rodgers, W. E., and Knuth, E. L., "Flame Characterization Probes," EPA- 650/2-74-023, March 1974.

13. Ower, E., and Pankhurst, R. C., "The Measurement of Air Flow," Pergamon Press, 1969.

14. Gnyp, A. W., St. Pierre, C. C., Smith, D. S., Mozzon, D., and Steiner, J., "An Experimental Investigation of the Effect of Pitot Tube Sampling Probe Configurations on the Magnitude of the S-type Pitot Tube Coefficient for Commerically Available Source Sampling Probes," University of Windsor, February 1975.

15. Brooks, E. F., and Williams, R. L., "Technical Manual for Process Stream Volumetric Flow Measurement and Gas Sample Extraction Methodology," TRW 24915-6028-RU-00, November 1975.

16. Stoller, H. M., Schrider, L. A., and Northrop, D. A., "The Status of Instrumentation and Process Control Techniques for In-situ Coal Gasification," ISA-ASI 76224, pp 117-128, 1976.

17. Blann, D. R., "Measurement Methods at High Temperature and Pressure," Symposium on Particulate Control in Energy Processes, May 1974.

18. Beer, J. M., and Thring, M. W., "Measurements in Flames," Edward Arnold Publishers Ltd., 1972.

19. Mercer, T. T., "Aerosol Technology in Hazard Evaluation," Academic Press, Inc., 1973.

20. Vitols, V., "Theoretical Limits of Errors Due to Anisokinetic Sampling of Particulate Matter," Journal of the Air Pollution Control Association, p. 79, Feb. 1966.

APPENDIX B

COAL COMBUSTION PRODUCT ANALYSIS

series of combustion calculations typical of fluidized bed combustion (FBC) products was performed. The purpose of the combustion calculations presented here are twofold. First, it was desired to establish typical values of thermodynamic properties such as the ratio of specific heats and molecular weight for evaluation of quantities required to perform flow calculations. Once the molecular weight is determined, the gas constant, R, can be determined from R = 1545/molecular wt[ft-lb/lb-°F].

The second purpose of these calculations was to provide some insight into the effect of changes in pressure level and equivalence ratio upon the gaseous constituency. For instance, within the sampling system, changes in pressure will occur owing to internal flow pressure drops. As a result, the gas constituency will change as a result of these pressure changes. Physically, these changes will occur at a finite rate in accordance with the laws of chemical kinetics. While no attempt was made to model chemical kinetics, the equilibrium values shown, indicate the maximum change in gaseous constituency between two end states.

The calculations were performed using the Aerotherm Chemical Equilibruim (ACE) Code. A fuel typical of an eastern coal was used, while the equivalence ratio was varied from 0.5 to 2.0. Figure B-1 presents the mole fractions of some of the combustion products of interest. Other products have been ommited for clarity. Note that some species are fairly insensitive to changes in pressure ranging from 1 to 100 atmospheres. Figure B-2 presents the ratio of specific heats (necessary for compressible flow analysis) as a function of equivalence ratio and pressure level. At equivalence ratios exceeding unity there is little effect of pressure level upon specific heat ratio. Figure B-3 presents the corresponding values of molecular weight for the combustion products. Over the range of equivalence ratios and pressures shown, the molecular weight remains between 27 to 30 lb/lb-mole. Therefore, using an average value of about 28.5 would give reasonably accurate results over an extended range of conditions since the error in velocity would be proportional to the square root of the accepted error in molecular weight.

T(°K)	P(atm)	T(°K)	P(atm)	T(°K)	P(atm)	
1087 -	100	1829 -	100	1397 -	100	
1059 -	50	1828 -	50	1397 -	50	Adiabatic
1024 -	20	1827 -	20	1397 -	20	flame
997 -	10	1826 -	10	1397 -	10	temperature
914 -	1	1825 -	1	1397 -	1	

A-15807

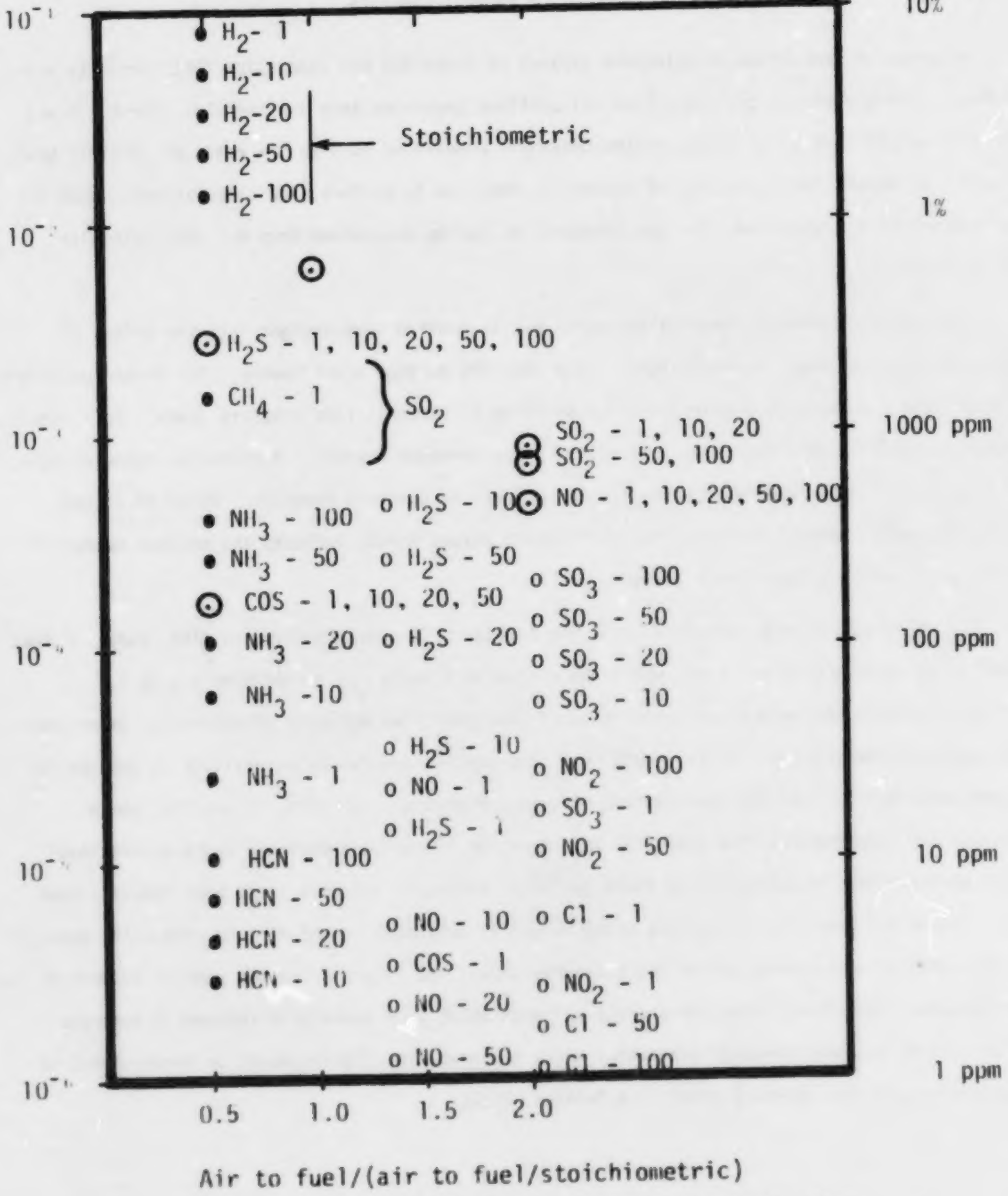

Figure B-1. Equilibrium combustion products from typical eastern coal.

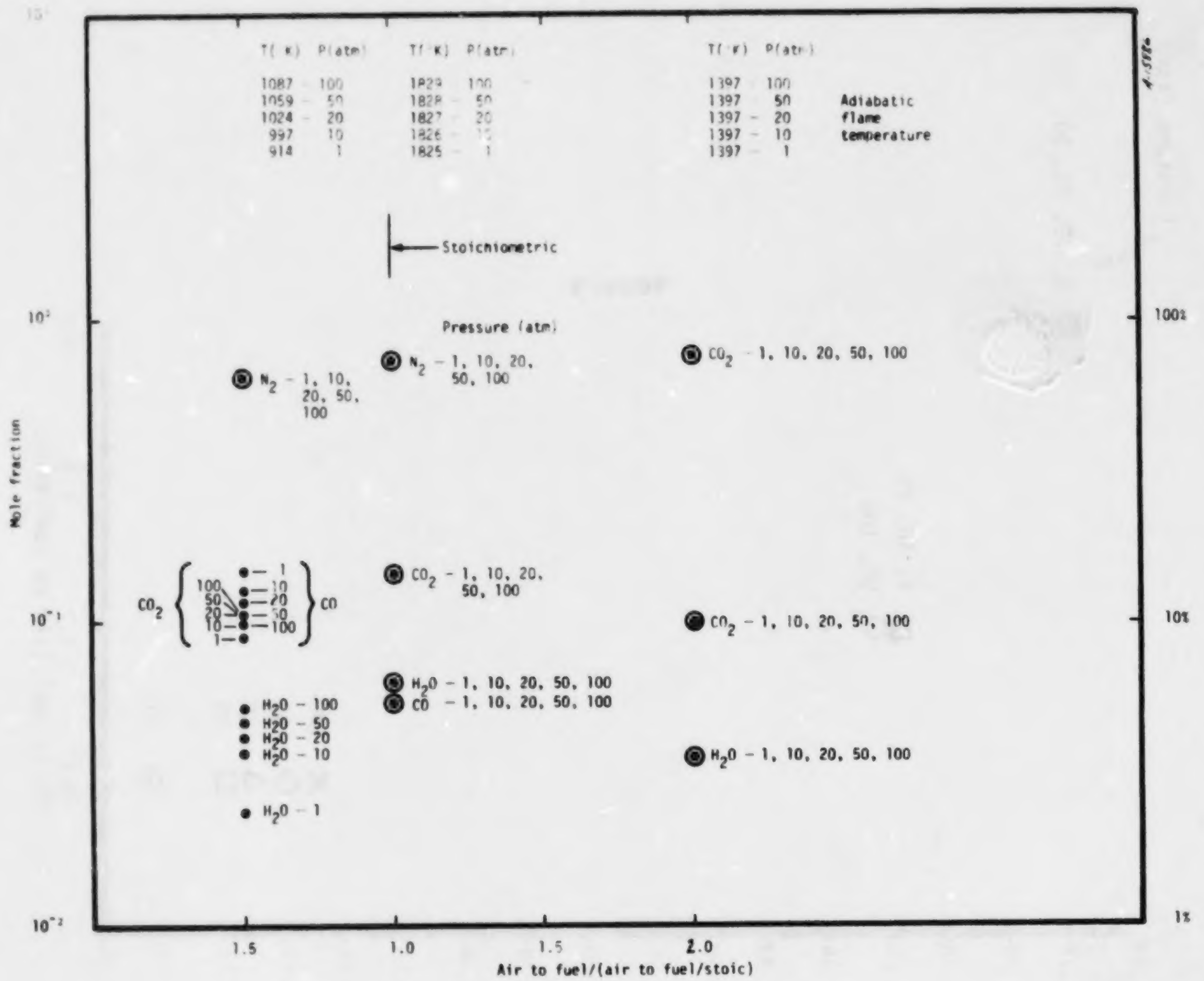

Figure B-1. Concluded

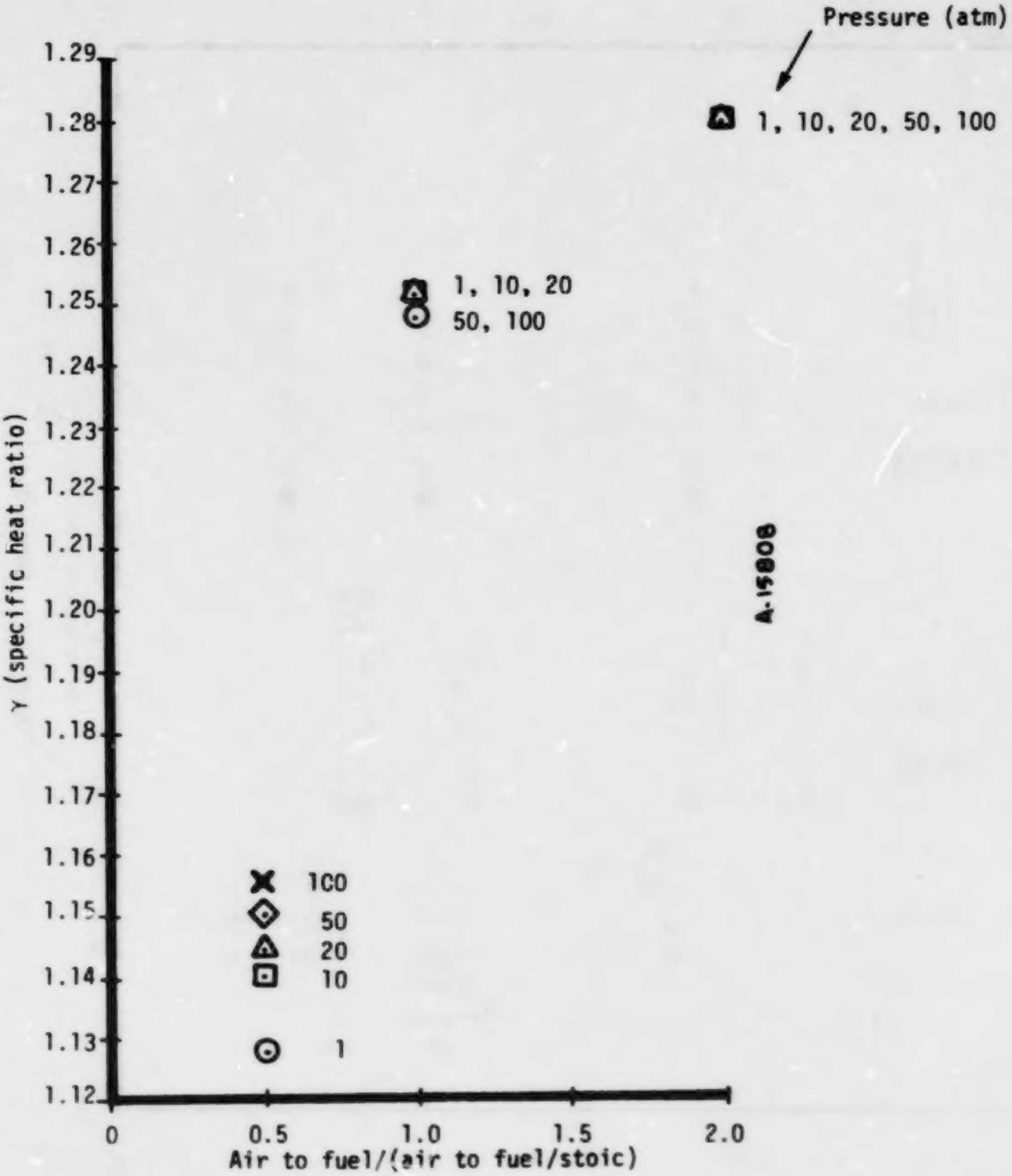

Figure B-2. Ratio of specific heats of combustion products from typical eastern coal.

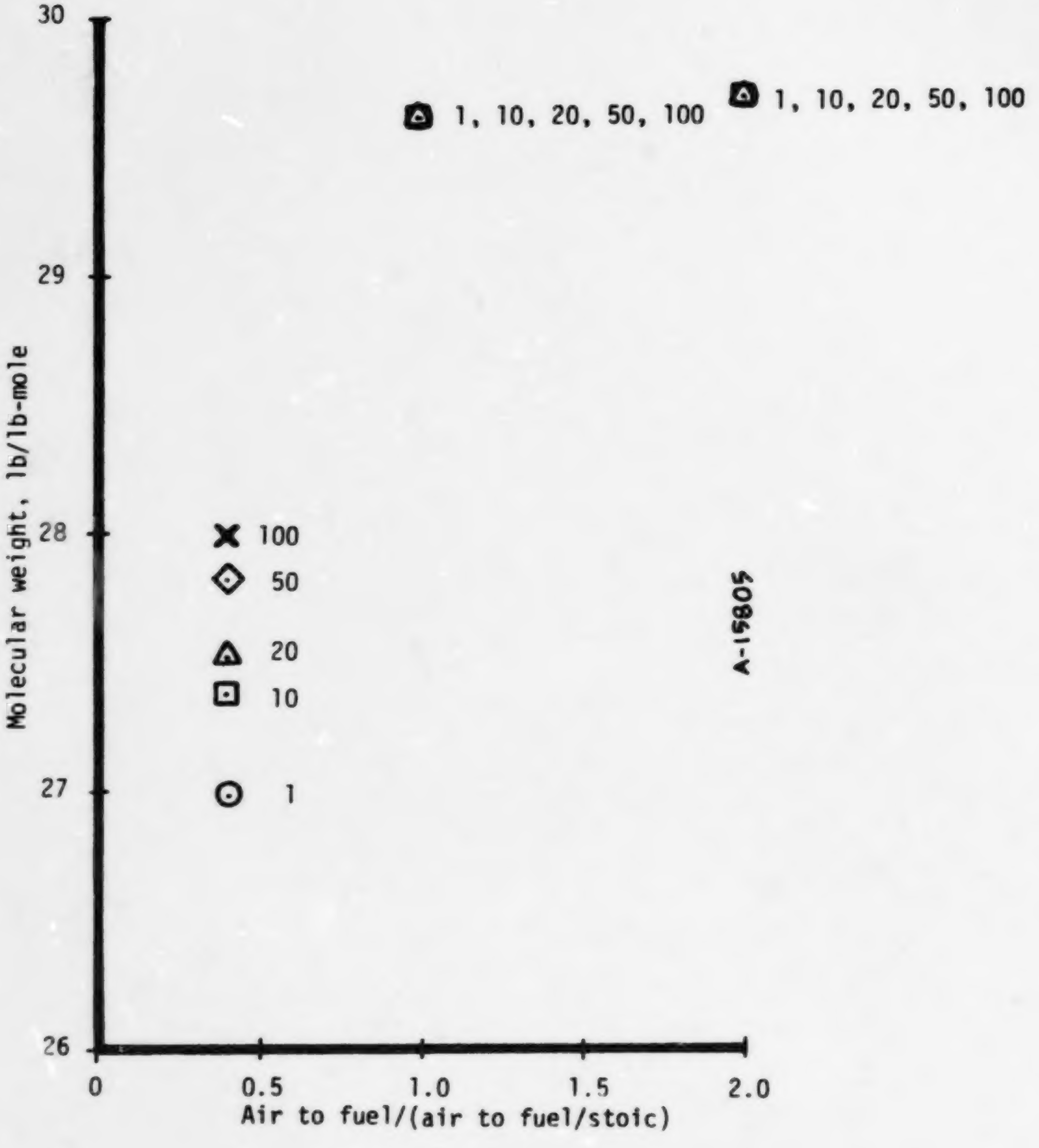

Figure B-3. Molecular weight of combustion products from typical eastern coal.

Appendix B

Aerotherm Project 7237

MATERIAL SELECTION FOR SAMPLING IN COAL CONVERSION SYSTEMS

Jacques Hull

Acurex Corporation/Aerotherm Division
485 Clyde Avenue
Mountain View, California 94042

June 1977

AEROTHERM REPORT TM-77-180

Prepared for
EPA Project Officer — William Kuykendal

Industrial Environmental Research Laboratories
U.S. Environmental Protection Agency
Research Triangle Park
North Carolina 27711

Contract No. 68-02-2153

TABLE OF CONTENTS

Section Page

1 INTRODUCTION B-1

2 BASIC METALLURGICAL TERMS B-3

3 GASIFIER CONDITIONS B-8

4 MECHANICAL PROPERTIES AT GASIFIER CONDITIONS B-21

5 CORROSION EFFECTS B-24

5.1 Basic Corrosion Mechanisms B-25
5.2 Gaseous Corrosion Reactions B-30

5.2.1 Hydrogen Embrittlement B-32
5.2.2 Oxidation B-32
5.2.3 Carburization B-34
5.2.4 Sulfidation B-35
5.2.5 Reactions With Other Gases B-38
5.2.6 Metal Surface Conditions (Fabrication Factors) B-38
5.2.7 Coal Gasification Gaseous Corrosion Data B-39
5.2.8 Refractories B-47

5.3 Liquid Corrosion Reactions B-48

5.3.1 Moderate Temperature Reactions B-48
5.3.2 Hot Corrosion B-50
5.3.3 Erosion-Corrosion B-50

6 EROSION B-52

7 GASIFIER FACILITIES PROBLEMS B-55

7.1 CO_2 Acceptor Problems B-55
7.2 Hygas Problems B-56
7.3 Synthane Problems B-58
7.4 Fluidized Bed Combustor Problems B-59
7.5 Miscellaneous Problems B-60

8 CONCLUSIONS -- SIGNIFICANCE TO SAMPLING PROBE MATERIALS B-62

BIBLIOGRAPHY B-65

LIST OF ILLUSTRATIONS

Figure — Page
1 Consol CO_2 Acceptor process (Reference 11) B-11
2 IGT Hygas process (Reference 11) B-12
3 Bureau of Mines Synthane process (Reference 11) B-13
4 Bituminous Coal Research - Bi-Gas process (Reference 11) B-14
5 Battelle-Union Carbide Agglomerated Ash process (Reference 11) B-15
6 Thermodynamic stability diagram for Cr-O-C (Reference 19) B-19
7 Thermodynamic stability diagram for metal-sulfur-oxygen (Reference 28) B-20
8a Magnification: 5000x B-33
8b Magnification: 1000x B-33
8c Magnification: 500x B-33

LIST OF TABLES

Figure — Page
1 Environmental Conditions in Various Coal Conversion Processes B-10
2 Inlet and Equilibrium Gas Composition of Phase I Corrosion Tests on ERDA/MPC IITRI Program[a] B-17
3 Basic Checical Composition of Selected Alloys[a] B-27
4 Specifications Known to Cause Stress Corrosion Cracking When Present at low Concentrations and as Impurities[a] B-31
5 Corrosion Rates in Stainless Steels and Superalloys in Simulated Reducing Coal Gas[a] at 1500°F and 1000 PSI. Loss of Sound Metal in Mils per year[b] (Based on 1000 hour data) B-41
6 Corrosion Rates in Stainless Steels and Superalloys in Simulated Reducing Coal Gas[a] at 1800°F and 1000 PSI. Loss of Sound Metal in Mils per year[b] (Based on 1000 hour data) B-42
7 Corrosion Rates in Stainless Steels and Superalloys in Simulated Mildly Oxidizing Coal Gas[a] at 1850°F and 150 PSI. Loss of Sound Metal in Mils per year (Based on 1000 hour data) B-43
8 Comparison of Corrosion of Selected Alloys in Laboratory and Pilot Plant Exposures at 1850°F[a] B-44
9 Comparison of Laboratory and Pilot Plant Corrosion Tests in Consol-Co_2 Acceptor Regenerator Environment[a] B-45
10 Acceptable Alloys for Service in Coal Gas Environments at 1800°F[a] B-46
11 Comparison of Corrosion Rates of Steels in Liquid and Gas Quench Phases[a] B-49
12 Failure Modes of Components in Coal Conversion Plants[a] B-57

SECTION 1
INTRODUCTION

The currently available stainless steels and superalloys have been designed to resist high temperature corrosion in highly oxidizing atmospheres. Basically, these materials are alloyed to counteract high temperature oxidation in air by relying on the selective oxidation of chromium to form protective oxide scales on external surfaces at the gas/metal interface.

The materials in coal conversion process equipment will be exposed at high temperature to environments in which the oxygen activity is generally secondary to the activity of other gaseous components, such as carbon and sulfur in the form of CO, CO_2, CH_4, SO_2, SO_3, H_2S etc. Existing alloys have not been designed to resist corrosion resulting from interaction of the metallic components with these gases. Consequently, these materials are susceptible to severe and sometimes catastrophic attack by sulfidation and/or carburization. Protective compounds are not formed at the gas/metal interface and unacceptable rates of corrosion can result.

The design of high temperature-high pressure (HTHP) probes for sampling in coal conversion systems must rely heavily on experience gained from the corrosion of materials in coal conversion pilot plants and in laboratory investigations simulating coal conversion conditions. Because of the existence of particulate matter such as char and flyash, erosive effects must also be considered as they tend to aggravate the corrosive attack.

In order to better understand the interrelation of the factors influencing the selection of materials for HTHP sampling probes, this discussion will deal with a series of topics in the following order: After defining metallurgical terms, the environmental conditions existing in various conversion systems are discussed. This leads to a discussion of the mechanical properties of materials in these environments, and is followed by a detailed discussion of the various corrosion modes, including gaseous corrosion, liquid phase corrosion, hot corrosion and erosion/corrosion. The direct effects of erosion are outlined, and this is followed by summaries of investigations relating to a number of component failures in coal conversion systems. Finally, the significance of this information to the selection of materials for sampling probes is discussed, and a bibliography is provided.

SECTION 2

BASIC METALLURGICAL TERMS

Alkali metals:	Principally sodium, potassium and lithium.
Aluminizing:	Forming an aluminum compound coating.
Annealing:	Heating to and holding at a suitable temperature and then cooling at a suitable rate to produce a desired microstructure.
Anodic corrosion:	The dissolution of a metal acting as an anode in contact with a dissimilar metal acting as a cathode, as a result of the formation of an electrolytic cell.
Austenite:	A solid solution of elements in face-centered cubic iron. The 300 series stainless steel are austenitic.
Brittleness:	The quality of a material that leads to crack propagation without appreciable plastic deformation.
Carbide:	A compound of carbon with one or more metallic elements.
Carburizing:	Introducing carbon into a solid ferrous alloy. In stainless steels, this can result in chrome carbide formation.
Caustic:	Strongly alkaline.
Cementite:	Iron carbide.

Char:	Coal combustion product containing unburned carbon.
Cold work:	Permanent strain produced by an external force.
Corrosion:	The deterioration of a metal by chemical or electrochemical reaction with its environment.
Crevice corrosion:	Corrosion caused by concentration of salts or gases in crevices resulting in differential cell build-up ultimately causing deep pitting.
Diffusion:	Movement of atoms or molecules to new sites within a material.
Ductility:	The ability of a material to deform plastically without fracturing.
Erosion:	Destruction of materials by the abrasive action of moving fluids usually accelerated by the presence of solid particles in suspension.
Eutectic:	An isothermally reversible reaction in which a liquid solution is converted into two or more intimately mixed solids on cooling.
Eutectic melting:	Melting of localized micro-regions whose composition corresponds to that of the eutectic.
Exfoliation:	A type of corrosion that progresses approximately parallel to the outer surface causing layers of the metal to be elevated by the formation of corrosion products.
Ferrite:	A solid solution of elements in body-centered cubic iron. The 400 series stainless steels are ferritic.
Finish:	Surface condition, quality or appearance of a metal.

Fluxing:	Removal of material from the surface by dissolving in a molten flux.
Flyash:	A finely divided siliceous material formed during the combustion of coal.
Grain size:	Average size of individual crystals in a polycrystalline metal or alloy.
Heat treatment:	Heating and cooling a solid metal or alloy to obtain a desired microstructure.
Hydrogen embrittlement:	A condition of low ductility in metals resulting from the absorption of hydrogen.
Impurities:	Elements or compounds whose presence in a material are undesirable.
Inclusions:	Nonmetallic materials in a solid metallic matrix.
Intergranular corrosion:	Corrosion occurring preferentially at grain boundaries.
Martensite:	A metastable phase of steel formed by transformation from austenite on cooling at a sufficiently rapid rate.
Microstructure	The structure of polished and etched metals as revealed by a microscope.
Modulus of elasticity:	A measure of the rigidity of the material.
Nitriding:	Introducing nitrogen into a solid ferrous alloy by using a nitrogenous material such as ammonia.
Oxidation:	A reaction in which there is an increase in valence resulting from a loss of electrons. Formation of an oxide scale on a metal surface.

Passivity:	A condition in which a metal, because of an impervious covering of oxide or other compound, has a potential much more positive than where the metal is in an active state.
Pearlite:	A lamellar aggregate of ferrite and cementite.
Phase:	A physically homogeneous and distinct portion of a material system.
Plastic deformation:	Deformation which remains permanent after removal of the load that caused it.
Polycrystalline:	Pertaining to a solid composed of many crystals.
Precipitation heat treating:	Artificial aging in which a constituent precipitates from a supersaturated solid solution.
Quenching:	Rapid cooling
Refractory:	A high melting point material.
Residual stress:	Stress present in a body that is free of external forces or thermal gradients.
Scaling:	Forming a thick layer of oxidation products on metals.
Sigma phase:	A hard brittle phase present in alloys containing sufficient chromium.
Slag:	A nonmetallic product resulting from the mutual dissolution of flux and nonmetallic impurities.
Solid solution:	A single solid homogeneous crystalline phase containing two or more chemical species.
Solution heat treatment:	Heating an alloy to a suitable temperature, holding that temperature long enough to allow constituents to enter into solid solution, and then cooling rapidly to hold the constituents in solution.

Spalling:	The cracking and flaking of particles on a surface.
Stabilizing treatment:	Heating austenite which contains stabilizing elements to tie down its carbon by forming carbides with these elements.
Stress-corrosion cracking:	Failure by cracking under combined action of corrosion and stress.
Stress-relieving:	Heating to a suitable temperature to reduce residual stresses, then cooling slowly to minimize development of new residual stresses.
Thermal fatigue:	Fracture resulting from the presence of temperature gradients which vary with time so as to produce cyclic stresses.
Thermal shock:	The development of a steep temperature gradient and accompanying high stresses.
Thermal stresses:	Stresses in a material resulting from nonuniform temperature distribution.
Toughness:	Ability of a material to absorb energy and deform plastically before fracturing.
Welding stress:	Residual stress caused by localized heating and cooling during welding.

SECTION 3

GASIFIER CONDITIONS

The term "gasifier" is used here to mean an assemblage of equipment for the purpose of converting coal to gas. The range of conditions present in gasifiers can vary widely (temperatures: room to beyond 3000°F, and pressures: atmospheric to in excess of 1000 psi). Raw gas produced can contain CO, CO_2, H_2, H_2O, CH_4, N_2, H_2S, can also contain NH_3, HCN, phenols, chlorides, organic acids, char, dolomite and flyash. The partial pressure of hydrogen present can be high, leading to possible hydrogen embrittlement. The dew point can be 300°F, leading to condensate attack, such as aqueous acid corrosion and chloride stress-corrosion cracking. Finally, the hydrogen sulfide content can be as much as 1.5 percent by volume, leading to sulfide corrosion failure.

Table 1 presents the environmental conditions present in a number of coal gasification processes. The moisture content can be as high as 50 percent* (Lurgi, Bi-gas), the hydrogen composition may reach 45 percent (Consol-CO_2 Acceptor), the methane content is generally under 20 percent, but may reach 73 percent (Hydrane), and carbon monoxide may be as high as 70 percent (Atgas).

---

*All percentages quoted herein are percent by volume unless otherwise stated.

Figures 1 through 5 represent schematics of five coal gasification pilot plants: Consol CO_2 Acceptor, IGT Hygas, Bureau of Mines Synthane, Bituminous Coal Research Bi-Gas, and the Battelle-Union Carbide Agglomerated Ash.

The CO_2 Acceptor process utilizes lignite and calcined dolomite. A slightly oxidizing condition is present in the regenerator, while reducing conditions exist in the gasifier unit. Hygas conditions are reducing, with a significant amount of H_2S present. Synthane's H_2S and moisture contents are both high. In Bi-Gas, the moisture content is even higher, and the temperature in the gasifier reaches 3000°F. The Agglomerated Ash pilot plant has both a gasifier and a burner unit, with reducing and oxidizing conditions, respectively. Two of these pilot plants have high dew points: 420°F in Hygas, and 492°F in Bi-Gas.
It is obvious that sampling conditions can vary widely from unit to unit, and within a unit.

The gas composition varies with temperature and pressure. An example of this is shown in Table 2. In the laboratory test program at the Illinois Institute of Technology Research Laboratories (IITRI), the equilibrium gas composition at 1000 psi varies considerably with temperature. For example, the hydrogen content is 4 percent at 900°F, 23 percent at 1500°F and 31 percent at 1800°F. Of course, this assumes equilibrium, which is not necessarily attained in practice. Rate kinetics can be important in certain instances. For instance, the CO/CO_2 equilibrium is rapidly attained in a matter of seconds, while the CH_4/H_2 equilibrium is slow and takes several minutes to achieve. Hot surfaces will accelerate reaction rates, and for

TABLE 1. ENVIRONMENTAL CONDITIONS IN VARIOUS COAL CONVERSION PROCESSES

Coal Gasification Process[a]	Raw Gas Analysis									Exit Cond.	
	(%) H_2O	(%) H_2	(%) CH_4	(%) H_2S	(%) CO	(%) CO_2	(%) N_2	(%) C_2H_6	Other	(°F) Temp.	(psi) Pres.
1 Atgas	---	9.6	20.0	---	69.7	---	0.7	---	---	2600	5
2 Bi-Gas	48.0	12.7	8.1	0.7	22.9	7.3	0.3	---	---	1700	1000-1500
3 CO_2 Acceptor	17.1	44.6	17.3	0.03	14.1	5.5	0.2	0.37	NH_3/0.8	1500	150-300
4 Hydrane	---	22.9	73.2	---	3.9	---	---	---	---	1800	1000
5 Hygas	24.4	22.8	14.1	0.9	18.0	18.5	---	0.5	---	600	1000
6 Koppers Totzek	9.6	33.1	---	0.3	50.4	5.6	1.0	---	---	2750	atm.
7 Lurgi	50.2	20.1	4.7	0.6	9.2	14.7	---	0.5	---	700-1100	450
8 Molten Salt Coal Gasification	22.6	34.8	5.8	0.2	26.0	10.3	0.3	---	---	1700	1200
9 Morgantown Producer	10.0	13.6	2.3	0.6	18.2	7.6	47.3	---	COS/0.1	1000	300
10 Synthane	37.1	17.5	15.4	0.3	10.5	18.2	0.5	0.5	---	1800	500-1000
11 U-Gas	12.0	11.6	4.1	0.6	17.0	8.8	45.4	---	---	1900	350
12 Winkler	23.1	32.2	2.4	2500 ppm	25.7	15.8	0.8	---	COS/400 ppm	1500-1850	atm.

T-356

[a] Reference 23

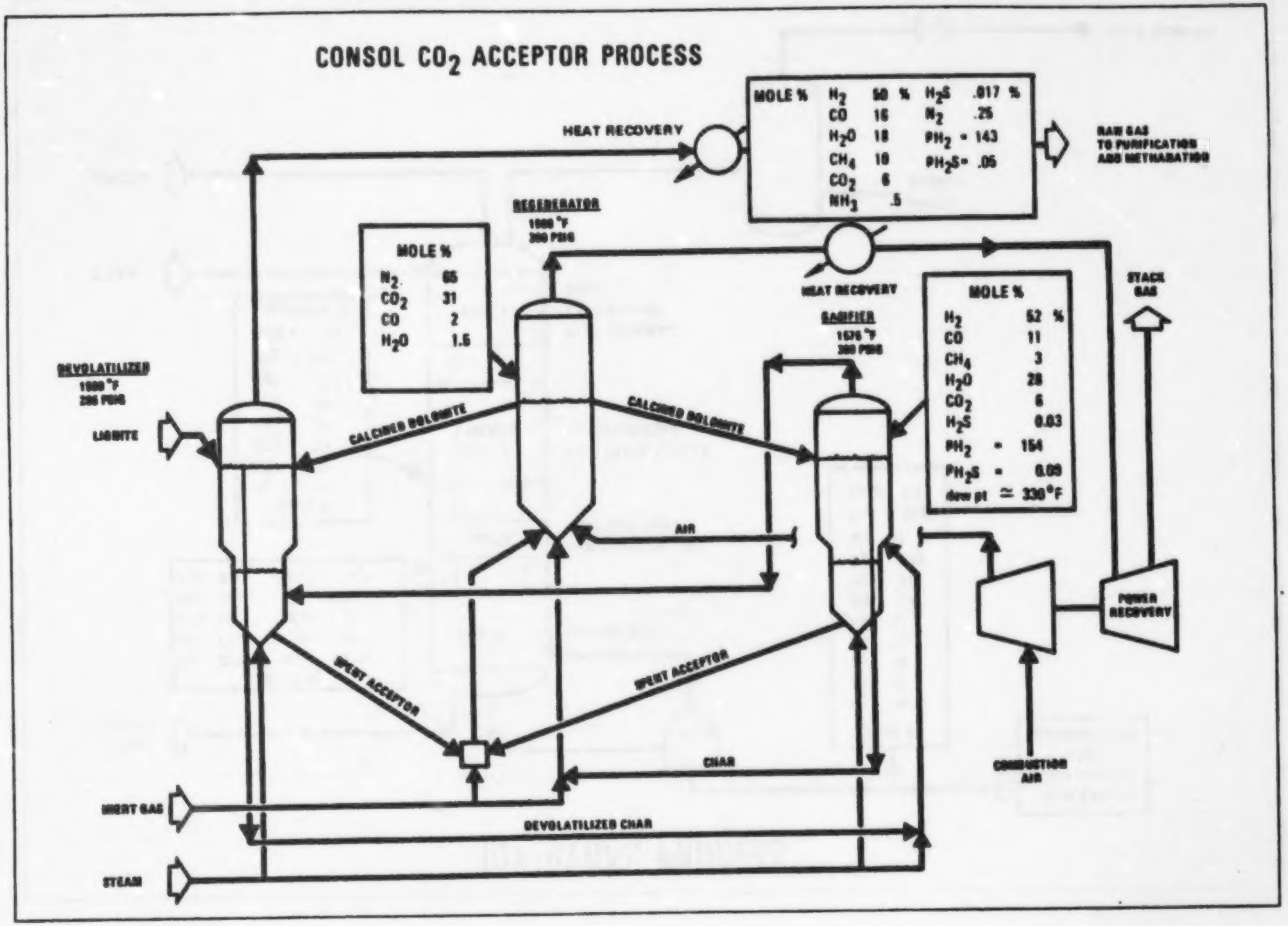
CONSOL CO_2 ACCEPTOR PROCESS
HEAT RECOVERY
MOLE % H_2 50 % CO 16 H_2O 18 CH_4 10 CO_2 6 NH_3 .5 H_2S .017 % N_2 .25 PH_2 = 143 PH_2S = .05
RAW GAS TO PURIFICATION AND METHANATION
REGENERATOR 1900 °F 300 PSIG
MOLE % N_2 65 CO_2 31 CO 2 H_2O 1.5
HEAT RECOVERY
MOLE % H_2 52 % CO 11 CH_4 3 H_2O 28 CO_2 6 H_2S 0.03 PH_2 = 154 PH_2S = 0.09 dew pt ≃ 330°F
STACK GAS
DEVOLATILIZER 1500 °F 295 PSIG
LIGNITE
GASIFIER 1575 °F 300 PSIG
CALCINED DOLOMITE
CALCINED DOLOMITE
AIR
POWER RECOVERY
SPENT ACCEPTOR
SPENT ACCEPTOR
CHAR
COMBUSTION AIR
INERT GAS
DEVOLATILIZED CHAR
STEAM

Figure 1. Consol CO_2 Acceptor process (Reference 11).

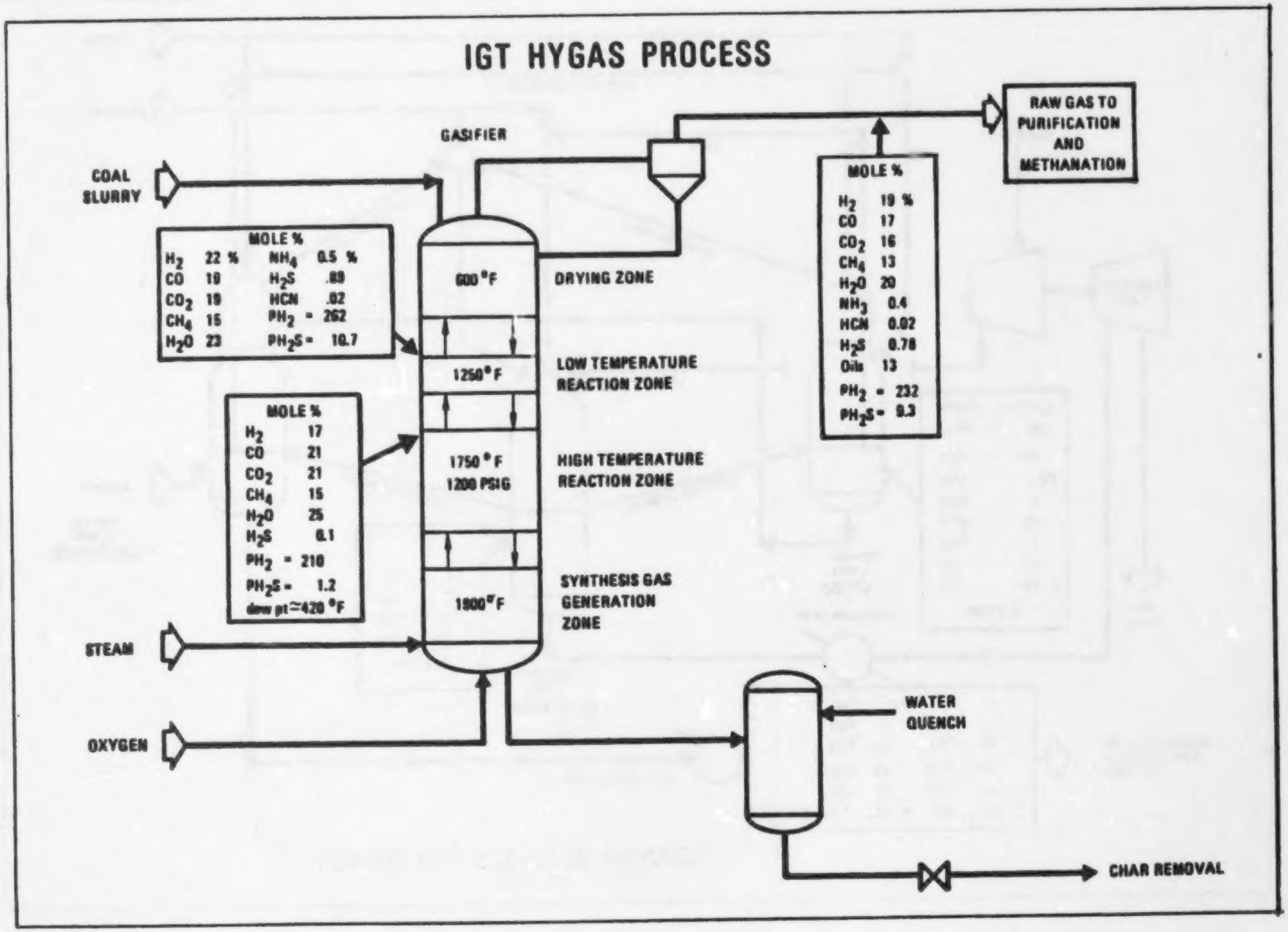
IGT HYGAS PROCESS
GASIFIER
COAL SLURRY
STEAM
OXYGEN
MOLE %
H2 22 %
CO 19
CO2 19
CH4 15
H2O 23
NH4 0.5 %
H2S .89
HCN .02
PH2 = 262
PH2S = 10.7
MOLE %
H2 17
CO 21
CO2 21
CH4 15
H2O 25
H2S 0.1
PH2 = 210
PH2S = 1.2
dew pt ≃ 420 °F
600 °F
1250 °F
1750 °F
1200 PSIG
1900 °F
DRYING ZONE
LOW TEMPERATURE REACTION ZONE
HIGH TEMPERATURE REACTION ZONE
SYNTHESIS GAS GENERATION ZONE
MOLE %
H2 19 %
CO 17
CO2 16
CH4 13
H2O 20
NH3 0.4
HCN 0.02
H2S 0.78
Oils 13
PH2 = 232
PH2S = 9.3
RAW GAS TO PURIFICATION AND METHANATION
WATER QUENCH
CHAR REMOVAL

Figure 2. IGT Hygas process (Reference 11).

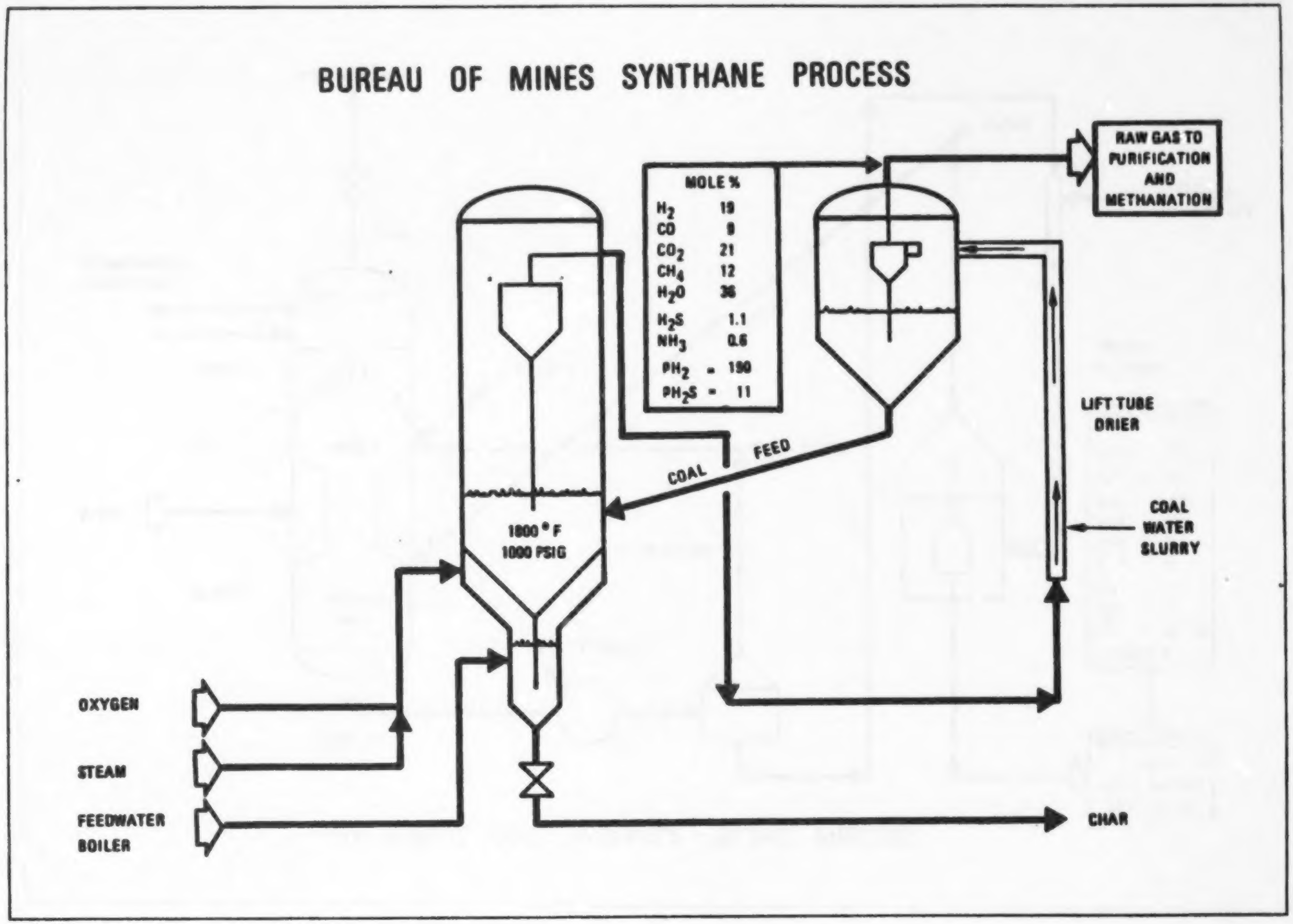
BUREAU OF MINES SYNTHANE PROCESS
RAW GAS TO PURIFICATION AND METHANATION
MOLE %
H_2 19
CO 9
CO_2 21
CH_4 12
H_2O 36
H_2S 1.1
NH_3 0.6
PH_2 = 190
PH_2S = 11
LIFT TUBE DRIER
COAL WATER SLURRY
COAL FEED
1800 °F
1000 PSIG
OXYGEN
STEAM
FEEDWATER BOILER
CHAR

Figure 3. Bureau of Mines Synthane process (Reference 11).

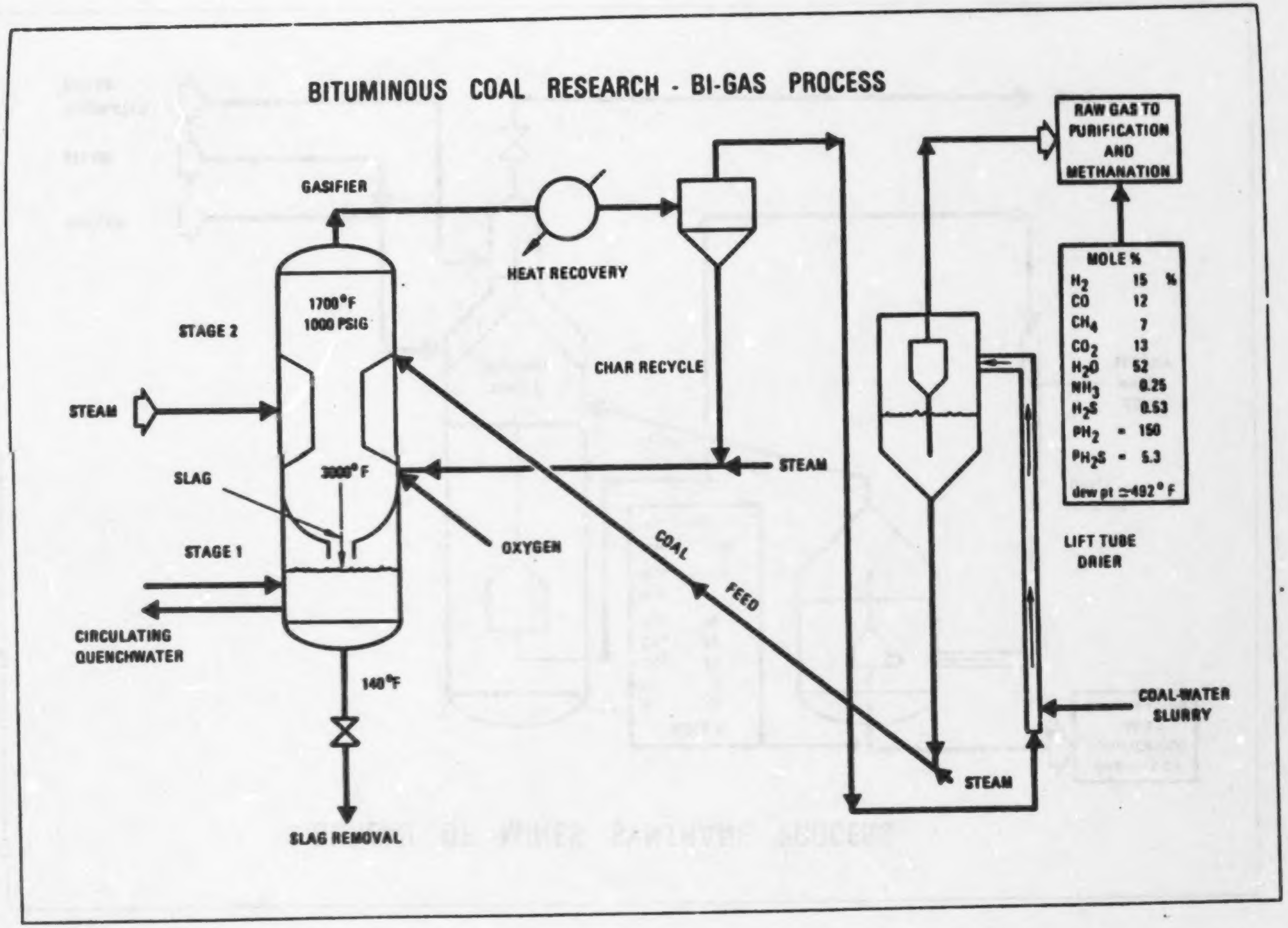
BITUMINOUS COAL RESEARCH - BI-GAS PROCESS
GASIFIER
HEAT RECOVERY
RAW GAS TO PURIFICATION AND METHANATION
1700°F
1000 PSIG
STAGE 2
STEAM
CHAR RECYCLE
MOLE %
H2 15 %
CO 12
CH4 7
CO2 13
H2O 52
NH3 0.25
H2S 0.53
PH2 = 150
PH2S = 5.3
dew pt ≃492° F
SLAG
3000° F
STEAM
STAGE 1
OXYGEN
COAL
FEED
LIFT TUBE DRIER
CIRCULATING QUENCHWATER
140°F
COAL-WATER SLURRY
STEAM
SLAG REMOVAL

Figure 4. Bituminous Coal Research - Bi-Gas process (Reference 11).

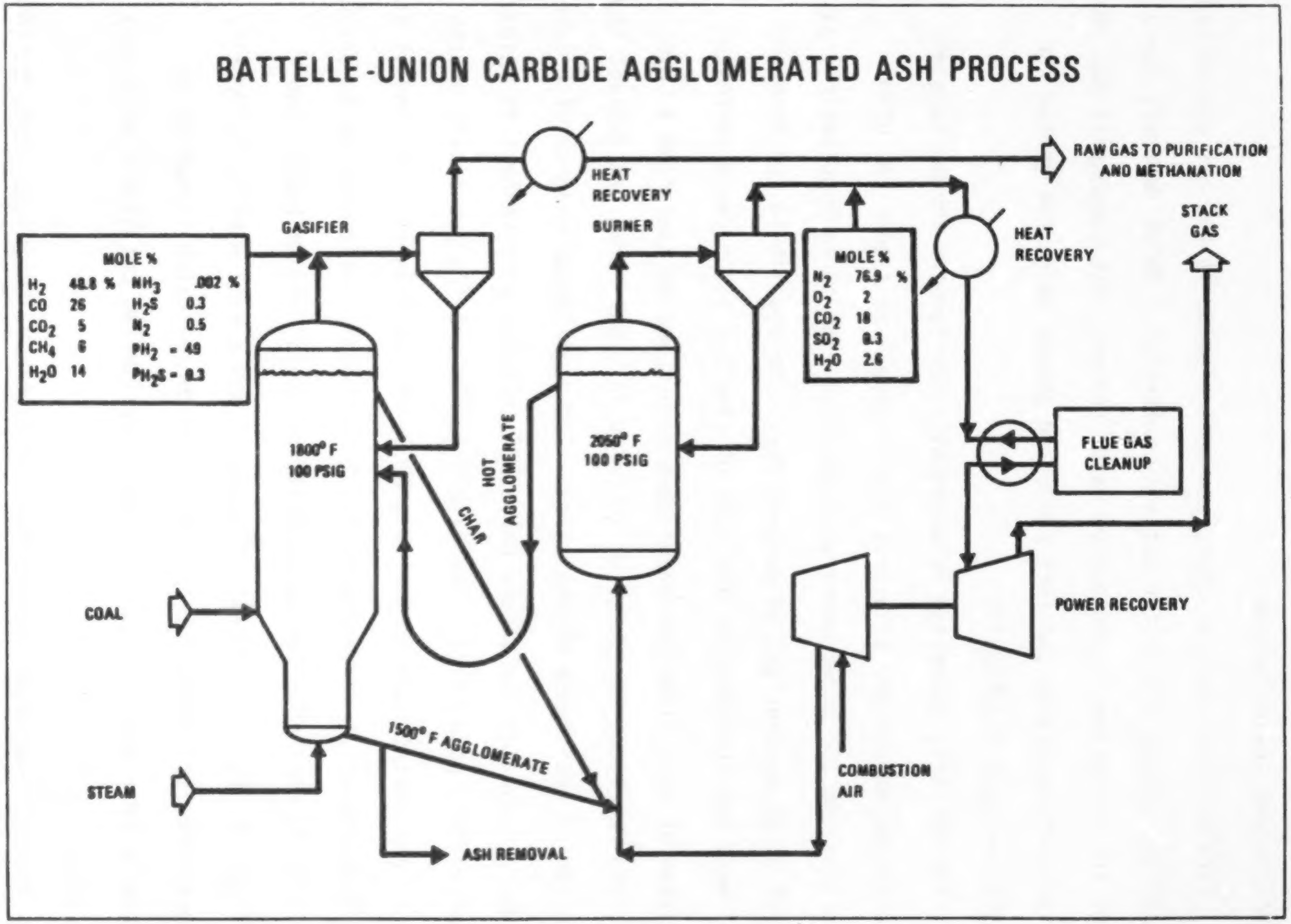
BATTELLE-UNION CARBIDE AGGLOMERATED ASH PROCESS
HEAT RECOVERY
RAW GAS TO PURIFICATION AND METHANATION
GASIFIER
BURNER
MOLE %
H_2 48.8 %
CO 26
CO_2 5
CH_4 6
H_2O 14
NH_3 .002 %
H_2S 0.3
N_2 0.5
PH_2 = 49
PH_2S = 0.3
1800° F 100 PSIG
HOT AGGLOMERATE
CHAR
2050° F 100 PSIG
MOLE %
N_2 76.9 %
O_2 2
CO_2 18
SO_2 0.3
H_2O 2.6
HEAT RECOVERY
STACK GAS
FLUE GAS CLEANUP
POWER RECOVERY
COAL
STEAM
1500° F AGGLOMERATE
ASH REMOVAL
COMBUSTION AIR

Figure 5. Battelle-Union Carbide Agglomerated Ash process (Reference 11).

this reason hot beds are often used to speed up the shift to equilibrium. Catalytic effects produced by the presence of such elements as nickel are currently under investigation.

Particulates, such as char, ash and dolomite in the gas stream can increase the carbon and sulfur activity potential. Thick deposits can also prevent the formation of protective oxide scales. Ash components can react with the surface scales and form condensed phases which can change the corrosion process drastically.

The activity potential relationships for forming chrome carbides versus chrome oxides are illustrated in Figure 6 at 1800^{o}F for both atmospheric and 102 atmospheres pressure involving three hypothetical gas mixtures at 10 percent and 30 percent CH_4. The equilibria for iron and nickel were not included for the sake of clarity, and because corrosion protection of iron-nickel-chromium base alloys are derived from a Cr_2O_3-rich scale, and reactions which tie up chromium in other forms can detract from the corrosion resistance of the alloy. The equilibrium diagram of Figure 6, therefore, indicates the stable phases of chromium with respect to oxidizing and carburizing potentials. The oxidizing/carburizing potentials of the gas mixtures are represented in the diagram by the various symbols, and it is clear that the third mixture will result in conditions conducive to carbon deposition (carburizing) at atmospheric pressure, and to borderline conditions at 102 atmospheres. Mixtures 1 and 2 will also be borderline at high pressure, but conducive to protective chrome oxide formation at atmospheric pressure. Of course, these equilibrium conditions will vary with temperature.

The sulfide/oxide equilibrium for aluminum, chromium, iron, nickel and cobalt are shown in Figure 7. It can be seen that in the presence of 0.1 to

1 percent H_2S in a hypothetical gas mixture, sulfides of iron and nickel will form if the H_2S content is above 0.1 percent and cobalt sulfide when the H_2S content exceeds 0.5 percent. (These gas compositions fall within the sulfide phase fields of these elements, as can be seen by continuing the horizontal lines delineating those phase fields.) Sulfides of chromium and aluminum do not form, since gases with these particular H_2S contents fall wicnin the oxide stability region of these metals. It must be noted that at this temperature the nickel and cobalt sulfide scales are liquid. This fact has significant implications which will be discussed in the section on erosion-corrosion.

TABLE 2. INLET AND EQUILIBRIUM GAS COMPOSITION OF PHASE I CORROSION TESTS ON ERDA/MPC IITRI PROGRAM[a]

	Gas Composition, Percent				
	Gasifier				
		Equilibrium[b]			
Component	Inlet[c]	900°F	1500°F	1800°F	Regenerator Inlet
H_2	24	4	23	31	1
CO	18	5	11	17	1
CO_2	12	25	19	15	30
CH_4	5	19	9	3	-
NH_3	1	1	1	1	-
H_2S	0-1.0	0-1.0	0-1.0	0-1.0	0.1(SO_2)
H_2O	39-40	45-46	36-37	32-33	0
N_2	-	-	-	-	68

[a] Reference 9

[b] At 1000 psi and indicated temperature

[c] Inlet gas composition constant for all tests in gasifier gas

In practice, several scale forming mechanisms compete with each other, and the complex processes lead to multilayer scale formation whose configuration is dependent on diffusion rates, nonequilibrium kinetics, etc. Often there is a race between the formation of a protective oxide scale and a damaging sulfide scale, and the outcome determines the corrosion resistance lifetime of the alloy. Preoxidizing the alloy preconditions it and improves the corrosion resistance lifetime of the alloy. The oxide scales act as diffusion barriers which provide a prolonged incubation period for such corrosion processes as the catastrophic formation of molten metal sulfides.

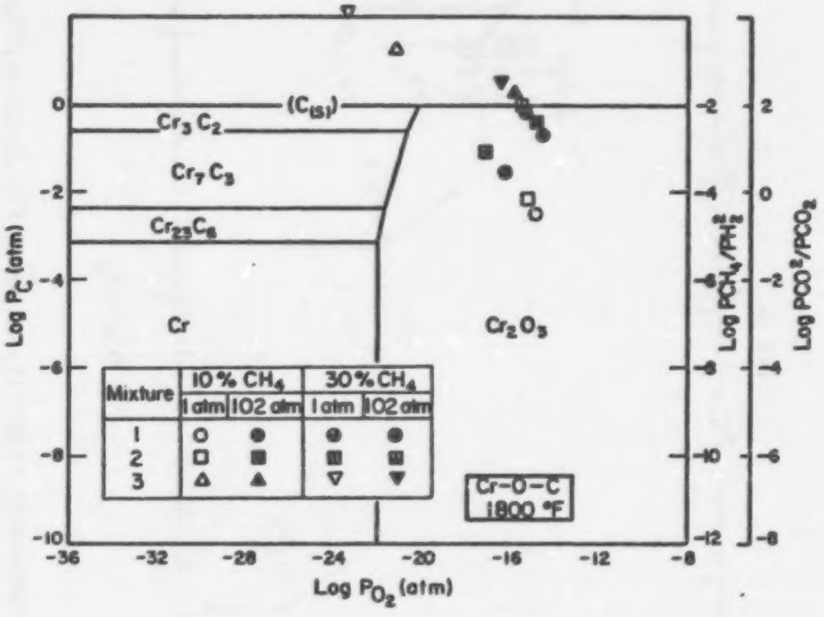

Figure 6. Thermodynamic stability diagram for Cr-O-C (Reference 19).

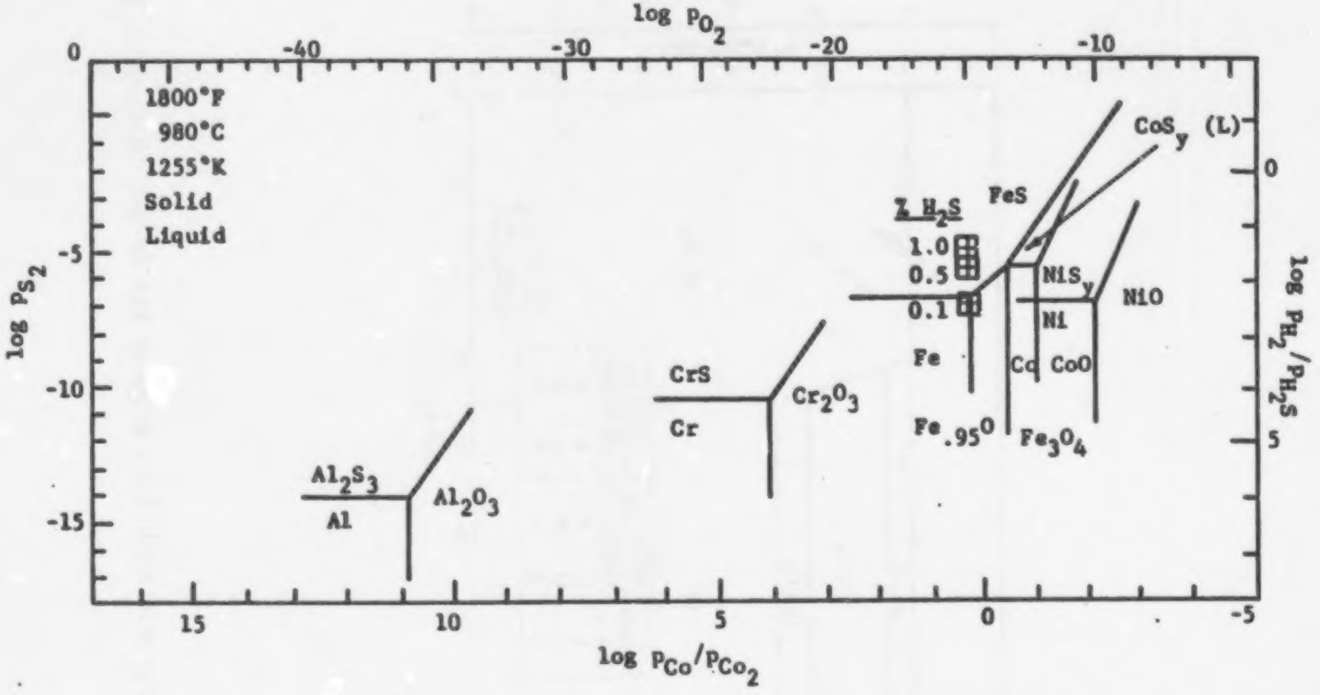

Figure 7. Thermodynamic stability diagram for metal-sulfur-oxygen (Reference 28).

SECTION 4

MECHANICAL PROPERTIES AT GASIFIER CONDITIONS

At elevated temperatures, the atomic mobility is enhanced, and the increased diffusion rates of the elements in the alloy lead to a loss in stiffness, strength and compositional stability. Creep (strength) rather than yield (strength) becomes the controlling mode of deformation, and fracture is governed by stress-rupture rather than by ultimate strength considerations. Thermal cycling can lead to fatigue failures, particularly in conjunction with corrosion, since this leads to corrosion-fatigue failures; the thermal cycling implies that a form of stress-cycling is present, that is to say, there is a thermal effect on an existing stress distribution. Of course, thermal cycling can also cause a change in the compositional stability, in the sense that different metallurgical phases are stable within given temperature ranges. Formation and dissolution of phases (such as precipitates) occur at various reaction rates and influence the mechanical properties since the alloy condition has changed. There can be a severe loss in ductility, resulting in embrittlement of the alloy and eventual failure. Low cycle fatigue is another form of failure which may occur at elevated temperatures under high stress-amplitude levels;

a stress of the same magnitude would result in nonsensitive amplitudes at room temperature.

Ceramic materials have outstanding elevated temperature stability and strength properties (tensile strength actually improves at elevated temperatures) but are notoriously poor in their thermal fatigue properties and crack very quickly when thermally cycled; their ductility is very low and their notch-sensitivity very high, as they do not significantly deform plastically at temperatures under 2000°F.

Superior mechanical properties at elevated temperatures are achieved in metals by liberal addition of nickel. Among the metals having significant elevated temperature resistance, ferritic alloys are generally limited to service temperatures of 1000°F, stainless steels to 1600°F, and high nickel alloys to 2000°F. Sigma-phase precipitate formation in high chromium alloys containing a ferritic phase can lead to catastrophic embrittlement in service in the temperature range 1000 to 1600°F. Chromium containing ferrite alloys (such as 446 stainless steel) are susceptible to what is commonly called 885°F precipitation embrittlement (actual range 750 to 950°F). Both sigma-phase and 885°F embrittlement can be avoided by redissolving the harmful precipitates by heating to above 1650°F.

Pressure translates itself into bi-axial tension on vessel wall components and into hydrostatic compression on internal parts. These stresses must be added to the existing stress components (such as thermal stress), resulting in pressure induced stress magnitudes which can approach the yield strength of the material at elevated temperatures, causing a significant amount of creep.

The effect of pressure on mechanical behavior appears to be minimal, for the range of pressures under consideration. Basically, increasing the pressure is equivalent to lowering the temperature in solid state kinetics. Reaction rates are slowed down somewhat, and hence, the alloy stabililty is improved. Metallurgical phenomena which are significant under atmospheric pressure may become unimportant at high pressures; the reverse may also be true. Consequently, corrosive reactions, and hence mechanical properties of partially corroded materials may be significantly different under high pressure.

SECTION 5

CORROSION EFFECTS

In order to understand the effects of corrosion on materials in coal conversion processes, the basic corrosion mechanisms must be reviewed in terms of the conditions existing in coal conversion equipment.

Many of the reactions involve gas/metal interactions which can lead to such corrosion phenomena as hydrogen embrittlement, oxidation, carburization, sulfidation, etc. In addition to the environmental factors, design and fabrication characteristics of the alloys may strongly influence the corrosion process.

Corrosion rates have been measured in laboratory tests and in pilot plants, and the results give a significant indication of the anticipated lifetime of various commercial alloys. The information is extended to include refractory ceramics as these have a significant place in coal conversion facilities, especially at the higher temperatures.

The liquid/metal interactions are also very significant. They may occur in components exposed to moderate temperatures at which many gases condense. They may also involve the highly significant hot corrosion phenomenon, which can be devastating even when the damaging alkali species is present only in minute quantities, such as parts per billion. And the interactions may involve slagging phenomena, such as the erosion-corrosion mechanism which takes place when low melting sulfides form on the metal surface.

Several of these phenomena can occur alternately, or even simultaneously. Sometimes the corrosion damage is slow, extending over a time frame of thousands of hours, and sometimes extremely rapid, occurring over a matter of minutes. It is not uncommon for a 1/4-inch thick plate to corrode through in less than 50 hours.

5.1 BASIC CORROSION MECHANISMS

Corrosion protection is imparted to stainless steels and superalloys by the presence of chromium in excess of 12 percent, above which the alloys resist attack by most mild corrodents, and do not rust in moist air. As the chromium level reaches 18 percent, the alloys become resistant to more aggresive corrodents, such as nitric acid. Pitting may occur in halide solutions, general corrosion in hydrochloric and sulfuric acids, and intergranular corrosion in sensitized stainless steels in contact with nitric acid. As a rule, superalloys are more corrosion resistant than stainless steels.

The chemical composition of a number of stainless steels and superalloys is tabulated in Table 3. These can be roughly classified as iron base, cobalt base or nickel base alloys.

Corrosion may involve an electrochemical cell mechanism of anodic attack. Consequently, the activity level of a surface can be reduced to a less anodic (more cathodic) condition by passivation with nitric acid (6 to 15 percent solution of 70 percent HNO_3 for 1/2-hour). This strongly oxidizing treatment builds up an oxide film on the surface. However, oxygenating agents must be present and replenished constantly to maintain passivity, otherwise, localized corrosion frequently occurs (as in crevices).

For instance, hydrogen reduces passivity drastically, and may even destroy it. It is also possible to overpassivate, which leads to increased susceptibility to pitting corrosion.

Pitting corrosion results from a localized breakdown of the oxide film, often under stagnant flow conditions, and even more often under unclean conditions. Impurities can form small local galvanic cells which may act as pit initiators.

Galvanic corrosion occurs when two dissimilar metals are joined. The more noble metal will be protected by the less noble one which gets consumed. This is a particularly severe problem when a massive noble metal is joined to a much smaller less noble metal. A high degree of localized corrosion will then ensue. One example of this occurs when a weld metal is less noble than the parent metal.

Crevice corrosion occurs in restricted areas where an occluded cell can develop, such as at a metallic joint, under scale deposits, etc. Oxygen becomes depleted inside the crevice creating an anode -- while outside, the presence of oxygen creates a cathode. Since oxygen cannot diffuse readily into the crevice, the site remains active, and rapid corrosion is promoted by the large cathode (i.e., the rest of the metal surface).

Environments containing moisture and halides can cause pitting and crevice corrosion. This can occur when chlorides are present even in ppm quantities. Such chlorides may be found in water and steam, in coal, and even in insulation. One such example occurs by the thermal decomposition of the phenolic resin binder in fiberglass insulation.

Severe general corrosion occurs when either hydrochloric or dilute sulfuric acid is present in the absence of an oxidizer.

TABLE 3. BASIC CHEMICAL COMPOSITION OF SELECTED ALLOYS[a]

Alloy	Composition, percent by weight Fe	Ni	Cr	Co	Al	Mo	Other
304	70	9	19				2 Mn
316	65	14	17				2 Mn
310	52	20	25				2 Mn, 1 Si
446	75		24				
In-600	7	76	16				
In-601	16	60	23		1		
In-800	47	31	21				1 Mn
In-793	43	32	21		2		1 Mn
In-671		49	50				
Stellite 6B	2	2	29	56		1	7 W, 1 C, 1 Mn
Haynes 188	1	23	23	36		1	15 W, 1 Mn
Multimet N155	29	20	22	20		3	4 W, 1 Cb, 1 Mn
RA-333	16	48	26	3		4	3 W, 2 Mn, 1 Si
HL-40	47	19	31				1 Si
Armco-21-6-9	63	7	21				8 Mn, 1 Si
Inconel 625	3	62	22			9	4 Cb
Incoloy 825	30	41	22			3	2 Cu, 1 Ti
Hastelloy X	19	46	22	3		9	1 W, 1 Mn, 1 Si
Armco 22-13-5	57	13	22			2	5 Mn
Co-Cr-W No. 1			30	55			12 W, 3 C
617		54	22	13	1	9	
AL29-4-2	63	4	29			4	
Thermalloy 63	38	35	26				
HK-40	47	20	28			1	2 Mn, 2 Si
FSK-414	2	11	30	48			7 W, 1 Mn, 1 Si

---

[a] Reference 9

Severe general intergranular attack can occur in noncorrosive environments if grain boundary diffusion of readily soluble elements such as sulfur has occured at high temperature during the fabrication process.

Sensitization in another problem encountered in alloys containing chromium: the intergranular precipitation of chromium carbide in austenitic stainless steels (such as 304 or 316) in the service temperature range 800 to 1500°F depletes the alloy of the chromium so necessary for protection from corrosive attack. Sensitization can be avoided by reducing the carbon content of the alloy (304L or 316L) or by stabilizing the alloy with strong carbide forming elements such as titanium, tantalum or columbium (321, 347 or 348 stainless steels). Desensitization can be achieved by heating above 1600°F to redisolve the carbides; it is generally done at 1900 to 2100°F, and must be followed by rapid cooling. It is important to remove residues of cleaning solutions used for degreasing, etc., as these can cause severe corrosion upon heating. It is also important that welding operations be rapid, otherwise the metal adjacent to the weld may become sensitized. For this reason, a desensitization post-weld treatment is recommended for critical components.

Knifeline attack is also associated with sensitization related corrosion. Here, a very thin layer of metal immediately adjacent to the fusion line of a weld is preferentially corroded in an intergranular manner. Crater corrosion may show up at the stopping point of weld beads. End-grain corrosion is similar to crater and knifeline attack. All three usually occur only in strongly oxidizing environments. Knifeline attack can be eliminated by reheating the weldments to 1950°F and then quenching. End grain attack can be avoided by not exposing the ends of bar stock or tubing, or the parting lines of forgings to corrodents. If this cannot be done, the exposed ends should either be fused or covered with weld metal deposit.

Chloride or caustic solution induced cracking can occur even when no stress is present, in which case nondirectional random cracking may occur intergranularly. However, chloride-corrosion cracking is usually considered to be one of the corrosion modes associated with stress-corrosion cracking (SCC). Intergranular failure, when it occurs, consists of characteristic branching normal to the stressed direction. The mechanism involves the depletion of chromium next to the grain-boundaries. (Chromium carbide precipitates in the grain boundary region enhance corrosion activity, but are not necessary to the mechanism, since grain boundaries, by their nature are more chemically active than the grains.) Failure occurs along the grain boundaries. Or, failure can occur transgranularly, again with the cracks forming normal to the stressed direction. The source of the stresses can be from such service conditions as thermal gradients, thermal cycling, etc. or from fabrication factors (such as bending and forming), surface finish (residual grinding stress, etc.), stress raisers (notches), thermal processing (welding), or fitting and assembly. Furthermore, prior cold working reduces resistance to corrosion.

Chloride stress cracking usually occurs transgranularly under stress at temperatures above 160°F with only a few ppm of chlorides. Austenitic stainless steels are particularly susceptible. Heat transfer intensifies stress corrosion problems, probably by increasing the concentration of chlorides at the metal surface. Nitrogen enhances stress-corrosion cracking in the presence of magnesium chloride. Increasing the nickel content of the alloy beyond 10 percent improves the resistance of the alloy to chloride cracking.

Caustic environments also contribute to stress corrosion cracking of austenitic stainless steels, but only at temperatures near or above the boiling point at ambient atmospheric pressure, and only with concentrated caustic solutions. Again, failure can be either transgranular or intergranular.

Intergranular stress corrosion cracking of austenitic stainless steels also occurs in polythionic acids ($H_2O_6S_2$-5), especially when the steels are sensitized, but transgranular cracking of nonsensitized steels has been observed. Proper care to prevent the entry of moisture during shutdown prevents formation of polythionic acid.

Stress relieving of tensile stresses is helpful in preventing stress corrosion cracking. The introduction of compressive residual stresses at surfaces (such as by shot-peening or cold reduction) is also helpful. In the case of chlorides, treating the water or steam helps prevent damaging chloride concentrations. Sensitized 304 stainless steel fails readily at 180°F when stressed in water containing 70 ppm chlorides, but only 2 ppm chlorides are required to crack desensitized stainless steel at 390°F. While 100 ppm chlorides can crack sensitized stainless steel at room temperature, only 2 ppm of fluorides are necessary to crack the same alloy at room temperature. Specific ions known to cause stress-corrosion cracking are listed in Table 4.

5.2 GASEOUS CORROSION REACTIONS

The gaseous equilibrium will determine the type of reaction which may occur with each element present in the alloy under set pressure and temperature conditions. The reaction may be oxidizing, carburizing or sulfidizing. Other gaseous elements (Cl, F) may also react, and hydrogen can react with stressed metal. Furthermore, the condition of the metal surface

TABLE 4. SPECIFICATIONS KNOWN TO CAUSE STRESS CORROSION CRACKING WHEN PRESENT AT LOW CONCENTRATIONS AND AS IMPURITIES[a]

Damaging Ion	Susceptible Alloy	Temperature
Fluoride	Sensitized austenitic stainless steels	room
Gaseous chlorine	Low alloy-high strength steels	room
Gaseous HCl and HBr	ibid	room
Halides in aqueous solutions	Austenitic stainless steels	hot
O_2 dissolved in liquid H_2O	Sensitized stainless steels	570°F
Gaseous hydrogen		
at ambient pressure	Low alloy-high strength steels	room
at high temperature and pressure	Low strength, medium strength steels	>390°F
Hydroxides (LiOH, NaOH, KOH)	Carbon steels, Fe-Ni-Cr alloys (caustic cracking)	>210°F
Gaseous H_2O	High strength aluminum alloys	room
Polythionic acids ($H_2O_6S_n$)	Sensitized stainless steels and Inco 600	room
H_2S gas	High strength-low alloy steels	room
MnS inclusions	High strength steels (crack site nucleation)	room
SO_2 gas with moisture	Copper alloys	room
Nitrogen oxides with moisture	Copper alloys	room
Ammonia in aqueous solutions	Copper alloys	room
Nitrates in aqueous solutions	Carbon steels	>210°F
N, P, As, Sb, Bi impurities in alloys	Stainless steels (with Cl^- present)	room
As, Sb, Bi in aqueous solutions	High strength steels (hydrogen cracking)	room
Carbonates in aqueous solutions	Carbon steels	210°F
CO-CO_2-H_2O gas	Carbon steels	---
Lead in aqueous solutions	High nickel alloys	---

---

[a] Reference 24

often controls the reaction with gases (or liquids), but refractories such as ceramics react quite differently from metals. All these reactions will be discussed in the following sections and corrosion data for alloys subjected to coal conversion gas environments will be presented.

5.2.1 Hydrogen Embrittlement

Stress is necessary for the occurence of hydrogen embrittlement. Atomic hydrogen enters high strength steels and forms bubbles at inclusions (Figures 8a and 8b). The higher the stress, the more hydrogen remains in the steel instead of diffusing through the steel. A decarburization process follows with the cementite (Fe_3C) in the steel decomposing to form methane (CH_4) by combining with the hydrogen. The resulting fissures crack the steel (Figure 8c). Austenitic steels are not generally subject to hydrogen embrittlement; the occurence is favored in ferritic steels, since carbides which can readily dissociate are present. The hazards of hydrogen embrittlement can be avoided by making use of the APL's Nelson Curves in selecting steels for service in hydrogen environments.

5.2.2 Oxidation

Superior oxidation resistance is found in alloys containing a significant amount of chromium, such as alloys In-601, In-617, Haynes 188, Multimet N155, 446 S.S., 310 S.S., RA-333, HL-40 and Thermalloy 63. These types of alloys are basically oxidation resistant to 2000°F. Above that temperature, some dispersion strengthened nickel base alloys are usable to 2300°F, but their room temperature ductility is poor. Coatings such as silicides, aluminides, etc. offer additional resistance to oxidation. Of course, cooling the alloys by water-jacketing, or by other means to the degree that chrome-moly steels and monel-clad or even plain carbon steels become usable, may present a viable alternative. Ceramic insulation

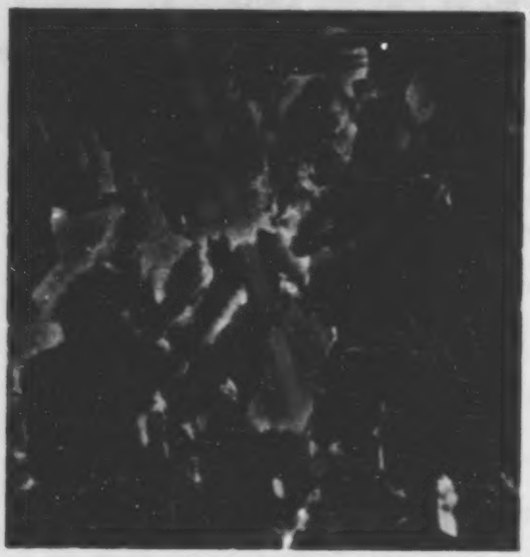

Figure 8a

Magnification: 5000x

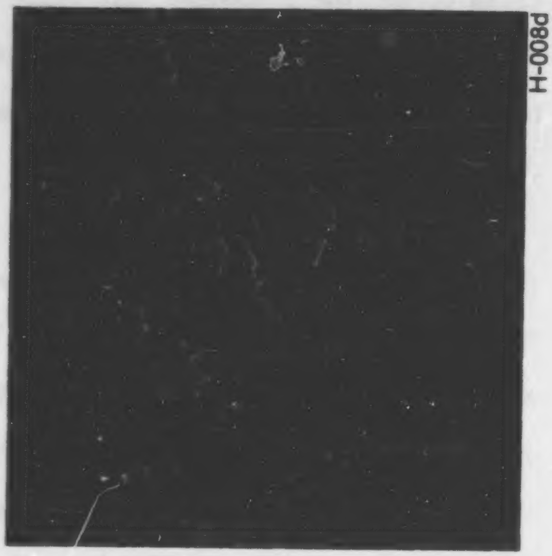

Figure 8b

Magnification: 1000x

Hydrogen bubbles at manganese sulfide inclusions in high strength steel.

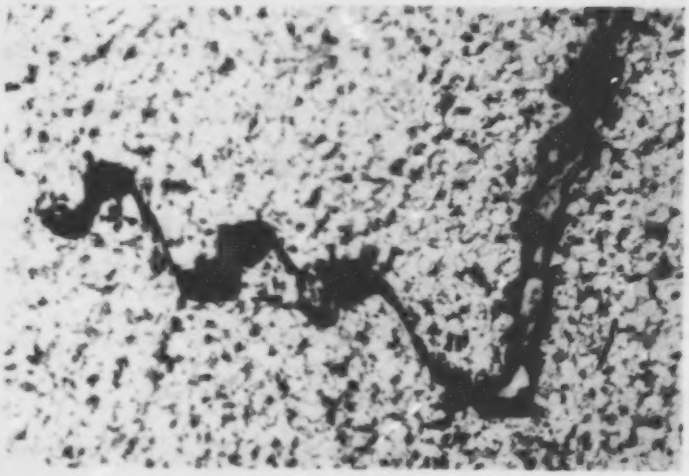

Figure 8c

Crack formation resulting from junction of the fissures formed in high strength steel. Magnification: 500x.

presents yet another choice. However, thermal cycling tends to crack the ceramic, and the component must be designed so that hot spots do not develop as a result of these fissures (flow paths must be periodically blocked). The best oxidation resistant materials are oxide ceramics such as alumina or zirconia.

Actually, most of the existing commercial alloys have been designed for oxidation resistance. Thin, adherent protective oxide coatings are formed (thick oxide films tend to spall off). However, there is a thermal expansion differential between the metal and the oxide, and the mismatch is greater for austenitic than ferritic steels, which can lead to cracking of the protective oxide barrier. The thermal expansion mismatch is low in superalloys: In-600, In-701, Hastelloy X and RA-333. Stainless steel service limits are 1650^{0}F for 304, 316, 321 and 347; 2000^{0}F for 446, and 2100^{0}F for 310.

5.2.3 Carburization

Hydrocarbon environments such as methane may cause carburization. It may be avoided if a strong chromium oxide film has formed on a smooth surface. Carburization occurs readily in low oxygen regions such as crevices, surface flaws, etc., or inside intergranular corrosion fissures in sensitized stainless steel, and in existing corrosion pits. It can be counteracted by the use of alloys of high chromium content, or by the addition of steam (oxidizing) or sulfur (sulfidizing).

Chromium carbides form during the carburization process, leading to a loss of ductility and eventual brittle fracture. This carbide formation depletes the chromium in the metal and leads to oxidation attack of the grain boundaries. Both CO and CO_2 can contribute to carburization.

Nickel can cause dissocation of methane at 1650°F, leading to carbon deposition. The carbon acts as a reducing agent, and can combine with the oxygen of the protective oxide, thereby permitting sulfides to form.

In atmospheres depleted of oxygen, pitting can result from graphitization of the chromium depleted matrix, with iron-nickel and graphite powders forming upon extended exposure.

Metal Dusting consists of catastrophic localized carburization in the temperature range 900 to 2000°F which may cause severe pitting corrosion. This can be avoided by adding sulfur or excess hydrogen or CO, or by reducing the presence of hydrocarbons and methane. It can be intensified by alternating reducing and oxidizing cycles.

5.2.4 Sulfidation

Sulfidation is a very significant problem in coal conversion. For example, a steel containing 9 percent chromium and 1 percent molybdenum subjected to a 6 percent H_2S content in H_2 gas at 900°F and 2000 psig will suffer a 128 mil loss of metal, while an In-800 alloy (20 percent chromium) under identical conditions will lose less than 6 mils. At 1800°F in an atmosphere containing 0.1 percent H_2S, 316 stainless steel suffered a 480 mil loss in 1000 hours, while an In-800 alloy lost only 35 mils under identical conditions. Aluminizing the In-800 alloy further reduced the loss to 14 mils. Alloys that are most resistant in a reducing environment such as H_2S are not necessarily equally resistant to oxidizing environments such as SO_2. Here, the 25 percent chromium containing alloys such as 310 stainless perform best. At 1850°F in an atmosphere containing 0.13 percent SO_2, 310 stainless lost only 13 mils in 1000 hours compared to In-800 alloy which lost 71 mils under identical conditions.

Chromium oxide scales are not generally protective in a reducing environment. They allow diffusion of the metal ions outward and sulfur inward. Sulfides form both above and below the oxide layer, and the sulfides below destroy the oxide scale, as it will no longer adhere to a metallic base. Thermal expansion differentials from thermal cycling speed up the destruction process.

High sulfur contents accelerate nickel sulfide formation. Because the nickel-nickel sulfide eutectic is molten at 1193°F, catastrophic attack will occur. To avoid nickel sulfidation at 1800°F, the H_2S/H_2 ratio must be very low (less than 1/300). This corresponds to no more than 0.1 percent H_2S at 1000 psi with a hydrogen content of 33 percent. Below this critical ratio, sulfidation can only occur by H_2S or SO_2 transport, and not by metal ion or sulfur transport. Consequently, nickel sulfidation does not then occur at a practical rate.

If enough oxygen is present in the gasification atmosphere, then a protective chrome oxide scale is stable, and nickel sulfide does not form.

A moderately protective oxide scale will also form when sufficient steam is present. With 310 stainless a 7.5 percent H_2O content is required with 1 percent H_2S; or a 20 percent H_2O content is required with 1.5 percent H_2S. In-800 has a higher nickel/chrome ratio and requires more water: 15 and 27.5 percent, respectively. Kanthal (Fe-Cr-Al) does not contain nickel and is not easily attacked by high H_2S, low H_2O combinations at 1500°F.

A high sulfur content (3 percent), such as is present in Illinois No. 3 coal, limited the operation of a FBC operated at the Coal Research Establishment in Great Britain to below 1600°F. This combustor operates with 10 to 20 percent air at low flow velocities of 3 ft/sec. While 16 alloys tested well at 1550°F for 2000 hours, all performed poorly at 1650°F. The best performer at 1650°F was 310 stainless steel.

Catalyzers are known to have a significant effect on sulfidation. In one experiment, the presence of calcium oxide in a sulfidizing atmosphere accelerated the corrosion attack very significantly.

Because liquid metal sulfide formation occurs at 1193°F with nickel, 1611°F with cobalt, and 1810°F with iron, there have been attempts to develop new sulfidation resistant alloys: Kanthal (78Fe-16Cr-5Al) does not form protective oxide scales, and molybdenum base alloys are effective only if protected from oxidizing atmospheres.

The evidence indicates that there is no foolproof means to avoid sulfidation in stainless steels and in superalloys at temperatures at which sulfide slags will form with basic elements of the alloy. This is because fully protective chome oxide scales do not develop. Of course, these scales are most protective in highly oxidizing atmospheres, and least protective in reducing atmospheres. However, cobalt sulfide and iron sulfide slags do not form at 1500°F, and the formation of nickel sulfide slag is relatively slow (if the H_2S content is below 0.5 percent) except in regions of high activity such as at crevices and adjacent to or under char deposits or where impurities acting as catalysts activate the reaction. This does not mean that sulfidation will not occur, but only that severe slag-type sulfidation may be avoided or delayed; the metal will gradually convert into corrosion products. But if the temperature is raised to around 1800°F, both cobalt sulfide slags and iron containing sulfide slags will form in reducing atmospheres, and sulfidation will rapidly become catastrophic. In contrast, sulfates rather than sulfides form in highly oxidizing atmospheres, and corrosion is not catastrophic. However, sulfidation can be rapid in moderately oxidizing atmospheres of high sulfur content.

Aluminizing (coating the surface of the alloy with an aluminum compound) will increase the incubation period for sulfidation to occur.

A pre-oxidation treatment helps form a protective oxide scale, and thereby increases the sulfidation resistance of chromium containing alloys; such pretreatment is practically mandatory.

5.2.5 Reactions With Other Gases

Little is known about the high temperature resistance of stainless steels and superalloys to other gaseous products. Except as noted, methane, ammonia, hydrogen, carbon dioxide and carbon monoxide do not produce corrosive reactions with these alloys, but have a secondary role in reactions involving sulfur, carbon and oxygen.

Gases such as chlorine and fluorine are highly damaging to metals at temperatures in excess of 1000°F, but the ppm content threshold is not known. It is suspected that even a few hundred ppm of these gases are strongly damaging at 1500°F. Alloys with a high nickel content tend to be more resistant to these gases. A high chromium content enhances surface reactions.

5.2.6 Metal Surface Conditions (Fabrication Factors)

The state of the metallic surface is of vital importance for developing corrosion resistance. This is clearly apparent when corrosion resistance is expressed in terms of the existence of a diffusion barrier consisting of a tough, adherent, protective oxide scale. It is necessary to avoid regions of high chemical activity, such as are present in the vicinity of char or bed materials, or at surfaces containing crevices, scratches, holes, etc., where protective oxides are hard to grow. Not only will the carbon and sulfur activity be changed at such sites, but the equilibrium gas composition can be affected locally.

Since cold work enhances diffusion, it is best to remove it by annealing. Even stencil marks can be corrosion sites. Therefore, only a full anneal is satisfactory, and further cold work (such as polishing, final machining, etc.) must not be performed. Such an alloy has been desensitized by the annealing treatment. Therefore, any welding must be performed prior to annealing, or the alloy may become sensitized. Pickling and passivating treatments are best avoided, otherwise grain boundary trenches can be opened up by excessive acid pickling. It may be best to leave the mill scale intact. If scale must be removed, only methods that do not create surface defects should be used.

5.2.7 Coal Gasification Gaseous Corrosion Data

Considerable data have been accumulated since 1973 in the ITTRI-MPC-ERDA program on screening alloys for coal gasification in the laboratory and in pilot plants.

Alloys such as In-800 and In-671 have successfully performed for 7000 hours in the laboratory at 1800°F and 1000 psi in a simulated coal gas containing 0.5 percent H_2S. But both these alloys did poorly in the Consol-CO_2 Acceptor Pilot Plant, and in erosion-corrosion tests; calcium oxide is present in these environments and may be responsible for this result. Coating the In-800 by aluminizing provided approximately 2000 hours protection, after which its behavior was considerably poorer than that of the uncoated alloy. The long term data indicate that extrapolation is unsafe in most cases, and that the computed annual rate is actually too conservative. (A sudden shift in the corrosion rate can occur at any time.) Only the uncoated In-800 alloy had a long term corrosion rate lower than the rate extrapolated from 1000 hour data.

Tables 5, 6 and 7 present laboratory corrosion data for 11 alloys at 1500, 1800 and 1850°F, respectively. Four alloys have a projected corrosion rate of less than 10 mils per year at 1500°F for up to 1 percent H_2S in the gas. These are 310 , 446, In-671 and In-800 aluminized. The situation is quite different at 1800°F: few alloys have a corrosion rate of less than 20 mils per year, even without H_2S present, in which only five alloys corrode at less than 20 mils per year. When 0.1 percent H_2S is present, the number of acceptable alloys is reduced to three (310 aluminized, In-800 aluminized, and In-671). The number drops to two with 0.5 percent H_2S (In-800 aluminized and In-671) and to only one with 1 percent H_2S (In-800 aluminized). However, when the atmosphere contains 0.13 percent SO_2, the situation changes somewhat. Although three alloys (310, 310 aluminized, and In-800 aluminized) again meet the acceptability test, alloy In-671 is replaced by 310 and the 310 alloy does better than the In-800 alloy. Consequently, 310 alloys are recommended for oxidizing conditions and either In-671 or In-800 for reducing conditions.

When comparison is made with pilot plant data, as in Tables 8 and 9, these conclusions remain basically unchanged, although the corrosion rates appear to be somewhat higher in a plant environment. Both In-671 and 310 stainless steel showed up well in the pilot plant oxidizing environment at 1500°F but not at 1700°F.

The corrosion-errosion data of Table 8 points out that a catastrophic corrosion rate occurs when slagging takes place. The corrosion rate increases by two orders of magnitude.

TABLE 5. CORROSION RATES IN STAINLESS STEELS AND SUPERALLOYS IN SIMULATED REDUCING COAL GAS[a] AT 1500°F AND 1000 PSI. LOSS OF SOUND METAL IN MILS PER YEAR[b] (BASED ON 1000 HOUR DATA)

	COMPOSITION		
Alloy	0.1% H_2S	0.5% H_2S	1.0% H_2S
304	16	46	39
316	21	36	41
310	4	3	4
310 aluminized	13	11	11
446	2	3	8
600	19	>1000	>>
601	25	>1000	657
671	4	2	6
793	13	21	15
800	24	17	15
800 aluminized	4	5	10

---

[a] Composition shown in Table 2.

[b] Reference 9.

TABLE 6. CORROSION RATES IN STAINLESS STEELS AND SUPERALLOYS IN SIMULATED REDUCING COAL GAS[a] AT 1800°F AND 1000 PSI. LOSS OF SOUND METAL IN MILS PER YEAR[b] (BASED ON 1000 HOUR DATA)

	COMPOSITION			
Alloy	0% H_2S	0.1% H_2S	0.5% H_2S	1.0% H_2S
304	219	549	584	>1000
316	115	480	365	>1000
310	17	159	34	164
310 aluminized	17	16	43	21
446	194	84	25	20-254
600	38	68	>1000	>1000
601	16	26	62	26-75
671	19	16	19	17-28
793	36	36	123	>1000
800	24	35	164	67-876
800 aluminized	13	14	20	12

[a] Composition shown in Table 2.

[b] Reference 9.

TABLE 7. CORROSION RATES IN STAINLESS STEELS AND SUPERALLOYS IN SIMULATED MILDLY OXIDIZING COAL GAS[a] AT 1850°F AND 150 PSI. LOSS OF SOUND METAL IN MILS PER YEAR[b]. (BASED ON 1000 HOUR DATA)

Alloy	Composition 0.13% SO_2
304	313
316	891
310	13
310 aluminized	13
446	>1000
600	885
601	51
671	25
793	79
800	71
800 aluminized	17

[a] Composition shown in Table 2.

[b] Reference 9.

TABLE 8. COMPARISON OF CORROSION OF SELECTED ALLOYS IN LABORATORY AND PILOT PLANT EXPOSURES AT 1850°F[a]

	Loss of Sound Metal in Mils Per Year		
Alloy	Laboratory Corrosion[b] Test	Laboratory Corrosion-Erosion[c] Test	Pilot Plant Consol-CO_2 Acceptor[d] Regenerator Test
310	13	3000	64
310 aluminized	13	3900	65
800	71	4700	218
800 aluminized	17	3700	65
671	25	1200	120
446	1100	1800	31

---

[a] Reference 9.

[b] 1850°F-1000 hrs-150 psi. Gas: 70% N_2, 27% CO_2, 3% CO, 0.13% SO_2

[c] 1850°F-50 hrs-14.6 psi. Gas: 33% H_2, 18% CO, 14% CO_2, 2.5% CH_4, 1% NH_3, 0.5% H_2S, 31% H_2O, 100 fps velocity (with char loading)

[d] >1700°F-1800 hrs-150 psi. Gas: 70% N_2, 27% CO, 3% CO, Trace H_2S

Additional data obtained on superalloys under the conditions of Table 6, indicated that only the superalloys shown in Table 10 may be acceptable in reducing environments at 1800°F.

TABLE 9. COMPARISON OF LABORATORY AND PILOT PLANT CORROSION TESTS IN CONSOL-CO_2 ACCEPTOR REGENERATOR ENVIRONMENT[a]

	Loss of Sound Metal in Mils Per Year				
Alloy	Laboratory Corrosion[b] Test	Pilot Plant[c] Test A	Pilot Plant[d] Test B	Pilot Plant[e] Test C	Pilot Plant[f] Test D
304	313	645	>1000	--	19
310	13	64	412	38	2
21-6-9	--	78	199	--	34
22-13-5	--	85	>1000	32	26
446	>1000	31	--	>364	--
800	71	218	>1000	145	14
793	79	149	317	177	16
825	--	753	>1000	--	30
Hastelloy X	--	438	>1000	--	8
671	25	>1000	>1000	--	2
310 aluminized	13	65	80	92	30
800 aluminized	17	65	79	121	31

[a] Reference 9

[b] 1850°F-150 psi-1000 hours Gas: 70% N_2, 27% CO_2, 3% CO, 0.13% SO_2

[c] >1700°F-150 psi-800 hours Gas: 70% N_2, 27% CO_2, 3% CO, Trace H_2S

[d] >1700°F-150 psi-1600 hours Gas: 70% N_2, 27% CO_2, 3% CO, Trace H_2S

[e] >1700°F-150 psi-1127 hours Gas: 70% N_2, 27% CO_2, 3% CO, Trace H_2S

[f] 1500°F-150 psi-2390 hours Gas: 48% H_2, 23% H_2O, 12% CH_4, 8.5% CO, 6% CO_2, 2.5% N_2

TABLE 10. ACCEPTABLE ALLOYS FOR SERVICE IN COAL GAS ENVIRONMENTS AT 1800°F[a]

0.1% H_2S	0.5% H_2S	1.0% H_2S
Haynes 188	Haynes 188	Haynes 188
Hastelloy X	Hastelloy X	Hastelloy X
Multimet N-155	Multimet N-155	Multimet N-155
Stellite 6B	Stellite 6B	Stellite 6B
Co-Cr-W No. 1	Co-Cr-W No. 1	
AL29-4-2	AL29-4-2	
800 aluminized	800 aluminized	800 aluminized
Inco 671	Inco 671	
310 aluminized		

[a] Reference 9

Recent data at 1.5 percent H_2S indicate that most alloys of Table 10 are unsatisfactory at high sulfur contents. Only Stellite 6B was fully satisfactory, while Inco 671 and 310 stainless were marginally acceptable at 1800°F.

The following conclusions can be drawn on the basis of laboratory tests and limited field data:

1. The addition of at least 25 percent chromium is necessary to obtain corrosion resistance in gasifier gas for 1000 hours at 1800°F.
2. A safe alloy for extended use in high sulfur coal gas at temperatures above 1600°F does not exist.
3. Only aluminized 800 or 310 alloys are usable for 1000 hours above 1700°F in an SO_2 environment. Alloy 310 may be used satisfactorily below 1600°F.
4. On the basis of limited data, it appears that Kanthal (Fe-Cr-Al) is an acceptable alloy below 1600°F.

5.2.8 Refractories

Refractories are used in diverse environments consisting of temperatures up to 2000°F in dry ash gasifiers, and in excess of 3000 °F in slagging reactors; pressures up to 1200 psi; gaseous environments which include H_2O, H_2, H_2S (or SO_2, SO_3), CO, CO_2, CH_4 and various hydrocarbons; and erosive velocities ranging between 5 and 100 ft/sec.

Potential problems include:

1. Gaseous corrosion - attack by steam, H_2, CO, CO_2, and alkali vapors in decreasing order
2. Slag erosion and corrosion
3. Erosion and abrasion by high velocity particles
4. Thermomenchanical failures leading to hot-spots
5. Attack by acids such as HCl and H_2SO_4
6. Attack of iron impurities in the ceramic by CO below 1850°F
7. Leaching out of silica by steam, and
8. Oxidation of the bond in silicon carbide bonded ceramics

Information to date indicates that high pressure steam is detrimental to the strength of dense, high alumina (95 percent) concretes at temperatures above 500°F. On the other hand, 50 percent alumina concretes do not appear to be affected. High temperature (1800°F) erosion of concrete is actually less than the erosion occuring at room temperature. Additionally, 90 percent phosphate bonded aluminas of high density have been found to be more stable in steam/CO atmospheres than cement (calcium aluminate) bonded aluminas of the same density. Superior slag erosion resistance is obtained with fused cast spinel type refractories ($MgO-Al_2O_3-Cr_2O_3$).

5.3 LIQUID CORROSION REACTIONS

Chlorides in ppm quantities can cause stress corrosion cracking only in aqueous solutions. It appears, therefore, that liquid phase corrosion can cause some alloys to fail even though they do not exhibit any corrosion problems in gases at high temperatures.

Thus, at temperatures below the dew point, (acid) liquid phase corrosion can be extremely serious. However, the gaseous environment may still be controlling: For instance, chloride stress cracking has not been observed in reducing environments.

Liquid phase corrosion in the form of slag occurs in both hot and slagging corrosion. A severe case of slagging corrosion occurs in combined erosion-corrosion phenomena. However, the most commonly observed liquid phase corrosion occurs at moderate temperatures.

5.3.1 Moderate Temperature Reactions

Corrosion studies have also been conducted at coal gasification quench phase conditions in the IITRI-MPC-ERDA program. It was found that at moderate temperatures in laboratory experiments, corrosion was more severe in liquid than in gas. The stress corrosion failure of 410 stainless at 462°F and 1200 psi occurs in 50 hours in liquid and 150 hours in gas (50 percent failures). Corrosion data also obtained at 462°F and 1200 psi in CO, CO_2, H_2S, NH_3, H_2, CH_4, N_2 gas and in HCN, phenol, chlorides, toluene and H_2O liquid derived from saturating water with the gas at the quench conditions, are described in Table 11.

TABLE 11. COMPARISON OF CORROSION RATES OF STEELS IN LIQUID AND GAS QUENCH PHASES[a]

Alloy	Aqueous Corrosion (Mils per Year)	Gaseous Corrosion (Mils per Year)
Carbon Steel (Ferritic)	160	85
410 Ferritic Stainless Steel	300	150
304 Stainless Steel	9	6
316 Stainless Steel	6	5

[a] Reference 9

It is evident that the austenitic stainless steels have a much lower corrosion rate than the ferrite alloys.

Other evidence obtained in these corrosion studies indicate that temperature is a key factor in these tests and that pitting occurs in the heat-affected weld zone in both 304 stainless and carbon steels.

Low temperature exposures were also carried out in the pilot plants. The annual aqueous corrosion rate in carbon steel is as high as 150 mils compared to about 8.5 mils in 304 stainless and 6 mils in 316 stainless.

The removal of residual stresses by stress relieving often helps reduce such corrosion problems as chloride stress cracking. Alloys containing in excess of 20 percent nickel combat most forms of liquid phase corrosion quite effectively. Specific acids such as sulfurous can be countered by adding molybdenum to the alloy, while boiling nitric acid is resisted by the addition of chromium. Gettering agents, such as columbium, tantalum and titanium are useful in neutralizing harmful alloying impurities. A number of specific corrosion problems in the liquid phase are listed in Table 4.

The problem of condensates in coal conversion facilities is often solved by a "wet wall" technique, such as cladding cabon steel or chrome-moly steel with monel (a copper-nickel alloy) which effectively resists corrosion at moderate temperatures.

5.3.2 Hot Corrosion

Chlorine acts as a carier for harmful low melting alkali metals such as sodium and potassium, or for transition metals such as vanadium. The result is slagging hot corrosion sulfate deposits at elevated temperatures, especially in the 1000-1800°F range. Sodium impurities can be a serious problem in quantities exceeding 40 parts per billion. Sulfates can be gettered by adding hafnium, binding the sulfur and thus avoiding this form of coal ash corrosion which can cause severe clogging of tubes, even in amounts below 50 ppm. While vanadium can be gettered by magnesium salts, the chlorine level can be reduced by preheating the coal.

Typical alkali contents of coal are of the order of several hundred ppm, and the sulfur content of coal can exceed 3 percent. Sodium sulfate forms a eutectic with potassium sulfate at 1526°F. Sodium chloride and potassium chloride react with SO_2 to form molten sulfates and free oxide ions, leading to a fluxing reaction on the metal surface, followed by spalling which removes the protective oxide scale, thus catastrophically destroying the metal. This is often called a "sticky ash" problem.

Cobalt-based alloys are less susceptible to hot corrosion than nickel-base alloys.

5.3.3 Erosion-Corrosion

Erosion-corrosion test results from the IITRI-MPC-ERDA program indicate that slagging erosion can virtually destroy 1/4 in. thick high temperature alloys in 50 hours. Aluminide coatings provide a significant degree of temporary protection, subject to an incubation period whose duration has not as yet been measured.

Sliding erosion-corrosion is caused by the impacting gas and char stream which is repeatedly peeling away the liquid phase from the metal surface, thereby intermittently exposing unoxidized metal to corrosion. Thus, the corrosion rate is increased even more than the slagging corrosion in which the slag is not peeled away. Normally, without erosion, a corrosion rate initially starts steeply linear with time, and rapidly levels off parabolically as a protective oxide scale builds up. But when the scale is prevented from building up by erosion, the rate remains steeply linear. Thus, when such a diffusion barrier is removed, the parabolic rate reverts to its former steep linear slope, and this causes catastrophic corrosion.

Another factor enhancing the corrosion rate is that of impacting erosion increasing the true metal surface, thereby increasing the metal reactivity.

One solution to erosion-corrosion is to hard face the metal with a castable ceramic. While this will not prevent corrosion, it will protect the oxide scale from erosive attack, and hence, the corrosion rate will be increased by erosion. Such a barrier is equally effective in reducing both hot corrosion and slagging corrosion, since small particle deposition (such as flyash) which interacts with protective oxide barriers can no longer take place on the metal surface. Of course, aluminizing a metal provides this type of barrier protection, although the thickness (and the lifetime) is significantly lower.

The erosion problem caused by char can be resolved either by adjusting the carbon reaction to burn additional carbon, or by char removal.

SECTION 6

EROSION

As stated previously, erosion itself increases the erosive wear by increasing the true surface area, and hence, the mechanical abrasion.

It is known that the angle of attack in particulate impact is perhaps the most important factor in erosive wear. The erosive rate is highest in brittle materials with a 90° impact angle, while in ductile metals, glancing angles of the order of 20° produce the higher erosion rates. This angle decreases to about 10° with very ductile metals, or with metals coated with thick soft corrosion products, or again with moderately ductile metals at high temperature (temperature softens metals and reduces their elastic moduli).

Other variables affecting erosive wear include particle velocity, particle flux, surface hardness, and particle size. Erosion is approximately proportional to the particle velocity to the two and one-half power for ductile metals, and to the four and one-half power for brittle materials for velocities up to 600 feet per second. Erosive wear appears to be proportional to grain loading, and inversely proportional to the impacted intrinsic hardness. (Hardening a steel does not improve the erosion characteristics.) Because of its spongy nature, char will not cause as much erosive damage as flyash, since it will tend to crush on impact.

Particle size has a significant effect on erosive wear. For a given gas velocity, particle velocity decreases with increasing particle size. Particles, greater than 3 microns impact and cause significant erosive damage. Smaller particles in the 0.3 to 1 micron range tend to deposit on surfaces and cause slagging corrosion damage. Sufficiently small particles tend to remain in the gas stream.

Erosive damage is essentially proportional to particle size in the 3 to 12 micron range. Particles of 20 micron size cause severe damage. The smaller particles tend not to deviate much from the gas stream lines, they most often contribute to low angle impact with long paths to impact, while the larger particles tend to deviate substantially from the flow direction, and consequently to impact at higher angles along a shorter path to impact. Because ductile metals erode more rapidly at low glancing angles (20o for flat surfaces, 40o for cylindrical surfaces), it is best to replace conventional elbows with T-connections, as a 90o impact is far less severe with metals. Furthermore, the char will cushion the impact by packing one wing of the T. An alternative is to line or coat with a ceramic, since while these materials are relatively sensitive to 90o impact, they are minimally sensitive to low angle impact. Thus, alumina ceramics can be slip cast over metals.

The most erosion resistant materials are (high density) ceramics, carbides, and then cobalt base alloys in that order.

Relative wear tests at Battelle, Columbus indicate that in 2.5 hours, Kennametal grade K703 with cobalt-chromium binder wore less than 7.6 microns and boron carbide wore 9.6 microns, compared to 25.4 microns for alumina and

31.7 microns for zirconium diboride. Silicon carbide erosion was in excess of 100 microns.

An EPRI program at Battelle has demonstrated that at low flow velocities of around 15 feet per second and with high char loadings, the particles tend to stick to the metal, promoting slagging corrosion. Hence, there should be no abrasive erosion at typical FBC velocities.

SECTION 7

GASIFIER FACILITIES PROBLEMS

A significant number of failures have occurred in gasifier facilities, including corrosive tube blockage, perforation, etc. A total of 374 failures recorded to date are listed in Table 12. The largest number of failures are attributed to erosion (73), then to design (46) or overheating (46) followed by sulfidation (39) and chloride stress corrosion cracking (38). The majority of failures occur in piping (170), then in valves (42), followed by bellows (36).

Some of these failures and their causes are described in the following sections.

7.1 CO_2 ACCEPTOR PROBLEMS

1. Preheater Coils

These coils consist of Inco 800 alloy tubing at 1600°F and 150 psi, exposed to the regenerator gas. The tubing failed by "metal dusting". This pitting resulted from carburization at low H_2O content and from both carburization and sulfidation at high H_2O content. It was initiated by local fracture of the protective scales, by stresses generated possibly by thermal cycling. Possible solutions include the development of more plastic protective scales and the addition to the alloy of gettering elements, such as titanium, zirconium, hafnium, columbium and tantalum, which combine strongly with the carbon and sulfur, thereby competing effectively with the carburization and sulfidation of critical elements of the alloy.

2. Gasifier Probe

A gasifier probe made of Type 310 stainless steel and sensor tubes made of Type 316 stainless steel failed as a result of "stress-enhanced sulfur corrosion" at a temperature of 1600°F.*

3. Expansion Joint Failure

A 1-inch long crack occured at a convolution of a Type 304 stainless steel bellows after 31 days in operation at 300°F and 200 psi in the recycle gas. Failure was the result of chloride stress cracking from chlorides in the steam used to purge the line.

4. Furnace Tube Pitting

Both Inco 800 and Type 321 stainless steel tubes pitted severely at temperatures above 850°F, presumably from reaction with the zinc oxide system used for sulfur removal. Up to 50 percent metal loss in the 321 steel resulted primarily from oxidation, and secondarily from sulfidation, carburization and nitridation.

7.2 HYGAS PROBLEMS

1. Slurry Dryer Grid

An oxidation-sulfidation failure occurred in an Inco 800 grid located in the fluidized bed at 600°F with the gas at 1200°F and 1000 psi pressure; the gas contained 1 percent H_2S, as well as CO, CO_2, H_2, N_2, CH_4 and H_2O.

---

*Conoco Tech Service Report 116-74-1301

TABLE 12. FAILURE MODES OF COMPONENTS IN COAL CONVERSION PLANTS[a]

Failure Mode	Pressure Vessels	Pumps	Piping	Valves	Bellows	Auxiliary Process Equip	Thermowells	Thermocouples	Totals
Corrosion									
Carburization	3		9			1	2	1	16
Metal Dusting	1	1	4			1			7
Oxidation	0		4	1		1		2	8
Pitting	2		9		4				15
Sulfidation	2		22	1	2		6	6	39
Creep	1		2			1			4
Design	2	10	15	5	4	10			46
Equipment Malfunction									
Overheating	4	3	19	1	8	7	2	2	46
Overstressing	0					1			1
Erosion	3	17	23	19	3	5	1	2	73
Fabrication			7	2	2			2	13
Fatigue			3	4		2			9
Quality Control			5	4	1	3		2	15
SCC	2		6		1			1	10
SCC-Cl	2	2	25	3	5			1	38
Unknown	1	1	17	2	6	3	1	3	34
TOTALS	23	34	170	42	36	35	12	22	374

T-355

[a] Reference 7

2. Thermocouple Sheath

Failure of a Type 316 stainless steel sheath required substitution by Type 310 stainless steel. Additionally, an inert nitrogen purge of the thermowell aided significantly in reducing this problem. Failure of the 316 steel had occurred by sulfidation; a low melting nickel sulfide eutectic had formed at temperatures below 1300°F. However, the 310 stainless steel sheath eventually failed as well.

3. Pressure Taps and Thermocouple Sheaths

Several Inco 800 alloy components failed by sulfidation. Replacement by 446 stainless steel proved superior to replacement by 310 stainless steel (see 2, above).

4. Cyclone Dip-Leg Pipe

An Inco 800 alloy internal cyclone pipe failed by hot corrosion combined with carburization and sulfidation. It was replaced by Type 310 stainless steel. It had been exposed to 1900°F at 20 psi for 2000 hours, of which 300 hours was with low steam gas, and 1700 hours in a gas of composition 30 percent CO_2, 15 percent H_2, 5 percent N_2, and 35 percent H_2O. The presence of molten slag (clinker) was detected on the dip-leg.

7.3 SYNTHANE PROBLEMS

1. Thermocouple Sheath

Two Inco 800 alloy sheaths failed by sulfide corrosion in the distribution cone of the gasifier. After approximately 50 hours service at 500°F in steam plus oxygen and some ash, failure resulted from the presence of 0.25 percent sulfur during start-up at 1000°F, thus sensitizing the Inco 800 alloy permitting sulfidation to occur in regions of residual stress (at bends). Type 310 stainless steel was substituted for the Inco alloy, and the start-up fuel was changed to sulfurless propane.

2. Stainless Steel Flange

A leaking crack was discovered in a Type 304 stainless steel weld neck flange in the preheat line to the gasifier. The flange was exposed for approximately 180 hours to 10 psi and 1100°F flue gas and for 700 hours to steam at 600 psi and 750°F (with 13 weight percent oxygen for 50 hours). While deionized water was used during operation, city water containing 28 ppm chlorides was used during checkout pretesting. Investigation revealed the presence of three long intergranular cracks in the flange material, plus a state of internal stress due to heavy cold working of the part during fabrication. It was deduced that the cracks initiated in the heat-affected weld zone where the flange joins the preheat piping, and that failure was due to intergranular stress corrosion.

7.4 FLUIDIZED BED COMBUSTOR PROBLEMS

Reactions occur on fired metallic surfaces beneath deposits which arise from condensation of components in the coal which are volatalized by the flame, and from impaction of flyash entrained in the flue gases. Salts responsible for accelerated corrosion are apparently molten at the indicated metal temperature, and are capable of reacting with and removing the protective scales. In the region of the flame, sulfur from the coal can deposit and react to form low melting sulfides, resulting in very rapid metal wastage. However, Inco 800 alloy tubes have been found to show only superficial damage at temperatures around 1400 to 1500°F.

7.5 MISCELLANEOUS PROBLEMS

1. Project Lignite Preheater Coil (U. of N. Dakota)

Three Type 316 stainless steel preheater coils used in a fluidized bed slurry heater ruptured rapidly as a result of chloride stress corrosion cracking; the make-up solvent provided the principal source of chlorides (~200 ppm). They were replaced by Inco 800 alloy. Even so, the failures occured in less than 30 hours each. A fourth coil was annealed after fabrication to remove all residual stresses, and its service life now exceeds 60 hours.

2. Project Gasoline Reactor Vessel (CONOCO)

A Type 316 stainless steel vessel was found to be subject to chloride stress corrosion cracking resulting from use of a molten zinc chloride catalyst.

3. MORGAS Butterfly Valve (ERDA-Morgantown)

Both solid Stellite 3 and Hastelloy-coated steel pressure valves eroded in less than 30 hours. Only tungsten carbide and Inconel 900 fixed orifices were able to withstand the 1300°F fine particulate environment.

4. Low Btu Gasifier Gas Generator (Westinghouse)

The generator operates on a mixture of propane, CO_2, steam and air at 1800 to 2400°F. The main burner components consisted of 304, 316 and 446 stainless steels and Inco 800 alloy. Carburization and oxidation failures occured. The burner was then provided with internal cooling to reduce temperatures to below 1000°F; a refractory flame shield was also provided. In addition, the burner material was changed to Inco 601, since it has superior resistance to cyclic carburization and oxidation.

SECTION 8

CONCLUSIONS -- SIGNIFICANCE TO SAMPLING PROBE MATERIALS

There is no simple solution to coal conversion material problems. The large number of documented material failures in gasifier facilities will attest to that. Many of these recorded failures, such as in piping components, have implications which are directly applicable to material selection for sampling probes.

The actual gas composition in contact with the material may vary a short distance away. The corrosion response of the material to a slight shift in composition can be quite dramatic. In fact, each individual sampling probe should be specifically designed for the actual gasifier location which is being sampled: temperature, pressure and anticipated gas composition are important considerations in the selection of sampling probe materials, as are the flyash characteristics, including the original coal composition. The alloys selected should, as far as possible, be chosen so that the thermodynamically stable phases are oxides and not sulfides or carbides.

The materials must of course be selected so that mechanical failure does not occur under operating conditions, and must take into account the effects of thermal cycling and of the phase stability of the alloying constituents (avoidance of phase changes, precipitation, etc.) at operating conditions and under transient heating and cooling as well.

Of course, temperature ranges, within which specific phenomena enhance corrosion for the particular alloys and operating conditions, must be avoided or traversed quickly. Furthermore, the component should be purged of condensable gases prior to cooling if possible, or at least flushed clean immediately after use.

The discussion of basic corrosion mechanisms emphasizes the importance of such factors as cleanliness, design considerations, fabrication parameters and heat treating, on avoidance or minimizing of corrosion. For example, designing to avoid char build-up, sharp edges, rough surfaces, etc.. Additionally, improper utilization or cleaning of the components can lead to severe corrosion problems. Therefore, it is important to devise procedures which will be applied from conceptual design to actual utilization. A pre-oxidation treatment of the components is recommended to improve the corrosion resistance.

Sufficient laboratory and pilot plant data have been obtained to permit the designer to select materials compatible with the environments in which they will be used, so that the equipment will survive for a reasonable length of time. It must be noted that intermittent use shortens the lifetime of the alloys compared to the life expectancy with uninterrupted use. Furthermore, the liftime of the material is predicted on the assumption that design, fabrication and utilization "flaws" will be avoided. A single scratch in a critical location can initiate catastrophic failure.

It appears that abrasion type erosion is not a problem for probes at most sampling locations. Generally, the flow velocity is such that the flyash will stick to the metal surface, which creates a severe problem of slagging corrosion. Therefore, it is important to design to avoid char (or flyash) entrapment, in-so-far-as possible. If this is not possible, a ceramic coating may be found to be a viable solution.

Of course, solutions to corrosion problems should not be left entirely to material selection. The component and system design can also contribute solutions: cooling to reduce temperatures, designing to reduce velocities (wherever possible) and to reduce stresses in critical parts, etc. The fuel may be modified by cleaning and treating it, and by removal or filtering of harmful material before it can reach critical parts.

In conclusion, it may be said that probes for sampling at high pressure and temperature can be built with existing commercial alloys, and, provided that the proper design, fabrication and utilization precautions have been taken, can provide several hundred hours of service prior to replacement of critical components.

BIBLIOGRAPHY

1. A. J. MacNab, "Design and Materials Requirement for Coal Gasification," Chem. Eng. Prog. 71 (11) 51-58 (Nov. 1975).

2. A. A. Foroulis and W. W. Smeltzer, Editors, "Metal-Slag-Gas Reactions and Processes," The Electrochemical Society Inc., Princeton, NJ (1975) Symposium Compilation of 78 papers.

3. J. P. Hirth and H. H. Johnson, "Hydrogen Problems in Energy Related Technology," Corrosion, 32 (1) 3-26 (Jan. 1976).

4. K. Natesan, "Corrosion-Erosion Behavior of Materials in a Coal-Gasification Environment," Corrosion, 32 (9) 364-370 (Sept. 1976).

5. F. C. Schora and G. Patel, "Design Considerations for Low Btu Coal Gasification," Industrial Heating, 43 (11) 15-21 (Nov. 1976).

6. M. S. Crowley: "Refractory Problems in Coal Gasification Reactors," Industrial Heating, 43 (11) 58-67 (Nov. 1976).

7. "Materials and Components in Fossil Energy Applications," ERDA Newsletters No. 1 to 9 (6/75 to 4/77), J. Richard Schorr, Editor, Battelle; Columbus, Ohio.

8. M. A. Howe, "Selection of Materials Used in Coal Gasification Plants," 7th Synthetic Pipeline Gas Symposium, AGA (Nov. 1975).

9. A. O. Schaefer, "A Program to Discover Materials Suitable For Service Under Hostile Conditions Obtained in Equipment For The Gasification of Coal and Other Solid Fuels," ERDA Reports FE-1784-12/15/18/21/24, IITRI Program, Materials Properties Council, NY, NY (Annual 1975; 1st, 2nd and 3rd quarters 1976; Annual 1976).

10. R. A. Perkins, W. C. Coons and F. J. Radd, "Metal Dusting in Coal Gasification Environments," Proc. Symp. Properties of High Temperature Alloys, Electrochem. Soc. (Jan. 1977).

11. A. J. MacNab, "The Material Design Interface in Coal Conversion Technology," Materials Problems and Research Opportunities in Coal Conversion Vol. II, Corrosion Center, Ohio State U. (Apr. 1974).

12. A. W. Huff, J. P. Young, and L. K. Ives, "High Temperature Erosion in Oxidizing and Reducing Atmospheres," NBS Reports ERDA E(49-18)1514 and 1536; OCR 14-32-0001-1514, EPA 65012-75-027-C.

13. "Materials for Coal Conversion Systems Design," ASM Conference, Pittsburg, PA (April, 1976).

14. R. A. Perkins, "Sulfidation Resistant Alloys for Coal Gasification Service," ERDA Quarterly Report FE-2299-6 (Dec. 1976).

15. H. D. Bastow and G. C. Wood, "Multilayer Scale Formation During Sulfidation of Nickel," Oxidation of Metals, 9 (6), 473-496 (Dec. 1975).

16. A. M. Hall, "Potential Materials Problems in Coal Gasification Systems," MFPG Coal Conversion Symposium, Battelle, Columbus, Ohio (April 1976).

17. "Materials for Coal Conversion Utilization," ERDA-EPRI-AGA Conference on Materials for Coal Conversion and Utililzation (Sept.-Oct. 1976).

18. W. R. Williams, "Lockhopper Valve Failures," ERDA-Morgantown, MFPG Coal Conversion Symposium, Battelle, Columbus, Ohio (April 1976).

19. I. G. Wright, "Correlations of High Temperature Corrosion of Alloys in Coal Conversion Environments," Battelle, Columbus Ohio, ERDA Contract W-7405-Eng-92 (Sept. 1976).

20. S. Bhattachryya, F. Bock, A. MacNab, and T. B,. Cox, "Alloy Selection for Coal Gasification Quench Systems," NACE Corrosion 77 Paper No. 51 (March 1977).

21. V. L. Hill and M. A. H. Howes, "Metallic Corrosion in Coal Gasification Pilot Plants," NACE Corrosion 77 Paper No. 50 (March 1977).

22. Charles Spengler et al., "Possible Materials Problem Areas in Power Generation Turbines Operating with Fuels or Gases Derived from Coal," NACE Corrosion 77 Paper No. 13 (March 1977).

23. "Clean Fuels from Coal Symposium II Papers," IGT, Chicago Ill., p. 904 (June 23-27, 1975).

24 Metals Handbook, Vol. X, Failure Analysis and Prevention, A.S.M., Metals Park, Ohio, p. 210 (1975).

25. R. A. Perkins, "High Temperature Corrosion of Stainless Steels in Coal Gasification Environments," NACE Corrosion 77 Paper No. 49 (March 1977).

26. L. H. Wolfe, "Laboratory Investigation of High Temperature Alloy Failure Mechanisms," NACE Corrosion 77 Paper No. 12 (March 1977).

27. H. F. Wigton, "Corrosion of Superalloys, Inconels and Stainless Steels by the Products from Fluidized-Bed Coal Combustion," NACE Corrosion 77 Paper No. 52 (March 1977).

28. N. Parikh et al., "Corrosion of Materials at Temperatures and Environments Expected in Proposed Processes for the Gasification of Solid Fuels," IITRI-B8149-27, Summary Report for Metals Properties Council (Jan. 1975).

29. J. Hull et al., "Hydrogen Induced Delayed Failure of X60 High Strength Steel Pipe," Summary Report No. 8679, SRI, Menlo Park, CA (Nov. 30, 1970).

Appendix C

Acurex Corporation/Aerotherm Division

May 1977

Aerotherm Project 7237

TAR SAMPLING IN COAL GASIFICATION PROCESSES

W. V. Krill

AEROTHERM REPORT TM-77-173

Prepared for
Industrial Environmental Research Laboratory
Environmental Protection Agency
Research Triangle Park
North Carolina 27711

Contract 68-02-2153

INTRODUCTION

With the advent of diminishing petroleum fuels as a natural resource (i.e., natural gas and fuel oil), interest in coal as an alternate fuel source is growing. Over 40 coal gasification processes from bench to full scale are currently under development in this country. Other coal processes producing solid and liquid fuels are also being developed. As a result, new technologies in process stream handling and measurement are required if these processes are to be demonstrated on a commercial scale.

High molecular weight hydrocarbons (tars) are a byproduct of many coal gasifiers. These hydrocarbons which are entrained in the gas stream as either vapors or mists are important to process development for several reasons:

1. Entrained tars are difficult to transport over long distances (for units producing pipeline gas), having a tendency to deposit on pipe walls as stream temperature decreases or flow irregularities are encountered

2. Tars may not be compatible with gas turbine fuel systems and combustion chambers (for units producing electrical power), causing tar buildup and flow restriction within these components

3. Some tars have been identified as being highly carcinogenic and cannot be released to the environment

In addition, tars hamper sampling system operation which is normally required for gas stream measurements by process developers.

Since coal gasification is largely in the developmental stage in the United States, little attention has yet been paid to tar production. Similarly, only limited tar quantity and physical property data is available. Interest in tar production is increasing, however, as developers continue to solve process operational problems and turn their attention toward producer gas quality.

In response to the need for an understanding of the tar production problem, the Aerotherm Division of Acurex Corporation has conducted a survey of tar collection technology under its current contract "Measurements for High-Temperature, High-Pressure Processes" for the Environmental Protection Agency. Under this contract, a variety of measurement techniques and equipment for use in high-temperature, high-pressure process streams have been investigated. The investigation of tar collection methods for sampling systems is a natural extension of studies related to gasification sampling problems.

This tar survey has focused on:

- Development of a thorough understanding of tar problems
- Compilation of a comprehensive list of tar physical properties
- Evaluation of existing detarring hardware for possible application to sampling systems
- Formulation of tar collection design specifications and recommendations for collector concepts for process sampling systems

Each of the above survey elements will be discussed in the following sections of this document.

TABLE OF CONTENTS

Section | Page

1 TAR PRODUCTION VARIABLES C-1

2 TAR PROPERTIES C-3

2.1 Chemical Composition C-3
2.2 Condensation Temperature C-5
2.3 Chemical Stability C-5
2.4 Other Properties C-7

3 TAR COLLECTION CONCEPTS C-8

3.1 Electrostatic Precipitator C-9
3.2 Scrubber C-11
3.3 Condenser C-11
3.4 Cyclone C-14
3.5 Filter C-14

4 TAR COLLECTORS FOR SAMPLE SYSTEM APPLICATION C-17

REFERENCES C-22

LIST OF ILLUSTRATIONS

Figure | | Page
1 Tar yield as a function of distillation temperature C-6

2 Typical electrostatic precipitator C-10

3 Typical water-jet scrubber C-12

4 Typical quench chamber scrubber C-13

5 Typical shell-and-tube condenser C-15

6 Typical cyclone separator C-16

7 ESP collector for sampling system adaptation C-19

8 Gasification process sampling scheme C-21

LIST OF TABLES

Figure | | Page
1 Grand Forks Slagging Lurgi Tar Analysis[a] C-4

2 Typical Elemental Analysis of Gasifier Tars C-5

SECTION 1

TAR PRODUCTION VARIABLES

An understanding of the severity of tar problems associated with coal gasification processes has been gained by conducting a survey of process developers. This survey has identified specific process problem areas related to tar, summarized past experience with tar handling, and evaluated present and future requirements for tar sampling.

Operational problems related to tars are quite diverse among process developers. Tar properties, quantities produced, and the physical state are largely dependent upon:

- Gasifier type and supporting cleanup devices
- The type of coal used in the process
- Gasifier temperature levels and temperature histories of the coal and producer gas
- Other physical characteristics of the gasifier and support equipment

As a result, each process developer is dealing with different tar production parameters and tars of different physical properties. A given process may produce a wide range of tar and oil types entrained within its producer gas stream which will vary significantly with coal type, temperature, pressure, gasification rate, etc.

There are nearly as many variations in gasifier types as there are facilities in this country (40 or more). The units are largely distinguished by such features as:

- Gasifier bed geometry and coal transport technique
- Oxygen or air firing
- Steam introduction

Since gasifier design features are usually quite unique to a given unit, tar production is similarly a unique function of a given process. In general, developers have not investigated the phenomena of tar production as related to the above process variables to any significant extent. The uniqueness of gasifier units also makes it difficult to correlate information among processes to further the understanding of tar problems. Some preliminary work has been performed to demonstrate the effect of coal type on tar production. Lowry (Reference 1) has stressed that composition is strongly dependent upon coal type. More recently, Riley-Stoker Corporation has suggested a 100-percent or more increase in tar production with bituminous coals as compared to lignite (Reference 2). It also appears from this study that tar yield may be a direct function of the percent of volatile matter contained within a given type of coal.

The effects of coal type on tar production may be overshadowed by the effects of reactor temperature and temperature history which have a strong influence on the tar produced. Offtake temperature varies widely among gasifier types and even among sizes of a given type. In general, commercial-size plants will have higher offtake temperatures than their developmental bench and pilot scale versions.

It has been suggested by several sources (Reference 2 for example) that formation of heavy tars is favored by high temperatures and long residence times of the gasifier products at those temperatures. Survey information compiled by Aerotherm supports this hypothesis. Gasifiers with low offtake temperatures, 300°F to 500°F (e.g., the slagging Lurgi at Grand Forks Energy Research Center and the Riley-Morgan demonstration unit) reportedly produce relatively small amounts of tar. Most of the heavy hydrocarbon output is present as light oils. Many gasifiers operate with an offtake temperature in the 800°F to 1400°F range and report severe tar problems related to cleanup equipment use and sampling systems operation. Examples of these facilities are: (1) CO_2 Acceptor, Rapid City, South Dakota; (2) G.E., Schenectedy, New York (Lurgi); (3) Morgantown Energy Research Center, Morgantown, West Virginia; and (4) Westinghouse Process Development Unit, Waltz Mill, Pennsylvania.

Again, the quantity of tar production data related to process temperature is very limited. For many processes, in fact, potential tar problems may exist that have yet to be identified. As the scale of gasification units increases (and hence the offtake temperature increases in many instances), greater attention will be paid to the related tar problems.

SECTION 2

TAR PROPERTIES

A gasifier process survey in conjunction with a literature review was conducted to identify current data available on the physical properties of coal tars. This data is important to a fundamental understanding of tar problems and to the evaluation and selection of tar collection equipment. The properties that are discussed below include:

- Chemical composition
- Condensation temperature
- Chemical stability
- Other physical properties
- Health hazards

2.1 CHEMICAL COMPOSITION

The chemical composition of coal process tars is the one property which makes all other properties difficult to quantify. Several thousand molecular species have been estimated to be present in some isolated tar samples which indicates that a wide range of associated physical properties exist as well. Therefore, in most cases, only hydrocarbon groups and average physical property data can be reported for a given sample.

An example of the hydrocarbon groups that have been reported are shown in the data for the Grand Forks Energy Research Center slagging Lurgi gasifier (Reference 3). A list of 24 groups is shown in Table 1. Note the diversity of the identifed compounds. Typical analytical techniques for tars have included gas chromatography and gas chromatography coupled with mass spectrometry. Ultimate analyses have also been performed in several instances (References 2 and 3), providing the typical results shown in Table 2.

TABLE 1. GRAND FORKS SLAGGING LURGI TAR ANALYSIS[a]

Constituents	Pct
Saturated hydrocarbon	10.3
Nonvolatile residue	7.7
Phenol/cresol/xylenol	22.4
Indanol	1.0
Dibenzofuran	3.78
Hydroxyanthracene	1.01
Indanes	0.22
Naphthol	3.93
Indenes	0.96
Pyridines	1.81
Quinolines	1.35
Naphthalene	4.76
Acenaphthene/biphenyl	0.37
Fluorene/acenaphthalene	1.76
Phenanthrene/anthracene	0.85
Dihydropyrene	0.81
Pyrene/fluoranthene	0.49
Chrysene	0.49
Benzenes	1.78
Indole	0.23
Carbazole	0.21
Benzocarbazole	0
Benzofuran	5.16
Benzonapthofuran	2.30

[a] Performed by mass spectrometry

TABLE 2. TYPICAL ELEMENTAL ANALYSIS OF GASIFIER TARS

Element	Amount (by Mass)
C	85 %
H	8 %
N	1 %
O	5 %
S	0.5%
Ash	0.5%

2.2 CONDENSATION TEMPERATURE

Condensation temperature (or equivalently, distillation temperature) of tars is probably the most important physical property to process developers. It determines whether tars are entrained in the gas stream as vapors or as liquid mist and thus their propensity for depositing internally on process ducts and in cleanup equipment. Since condensation temperatures vary widely among hydrocarbon groups (from room temperature for light oils to over 1500°F for tars) and even among species of a given group, tar samples typically have a wide range of condensation temperature. Note that condensation temperature is a function of pressure as well (Reference 4). Some of the more common pure hydrocarbons (e.g., naphthalene) have been shown to have condensation temperatures which are strongly pressure-dependent above 10 atmospheres. This is expected to be true for other hydrocarbon species as well. Since a wide range of gasifier operating pressures has been identified (atmospheric to 2500 psig), process pressure will play an important role in tar collection. In general, higher process pressures will result in fewer species condensing at a given temperature.

Condensation temperature data is normally obtained by fractional distillation of the tar sample. As an example of several techniques for vapor pressure and distillation temperature measurements, see References 5 through 8. Reference 2 (see Figure 1) reports distillation temperatures from approximately 300°F to 1600°F, illustrating the wide range usually obtained. This data is taken from laboratory tests of References 9 and 10. The quantity of tar which will condense at any given temperature is dependent upon the distillation distribution. Distributions of the shape of Figure 1 are typical.

The total tar sample typically represents as much as 10 percent by weight of the coal feed. Process developers currently burn these tars as product gas is flared or collect them by scrubbing (or other techniques) for eventual dumping as landfill.

2.3 CHEMICAL STABILITY

Little fundamental work has been performed to indicate the chemical stability of coal tars. Some experience does exist, however, to indicate chemical changes which a tar sample can undergo during a period of time after it is extracted from the process. Some samples have been reported to have a large undistillable fraction, indicating that samples are subject to

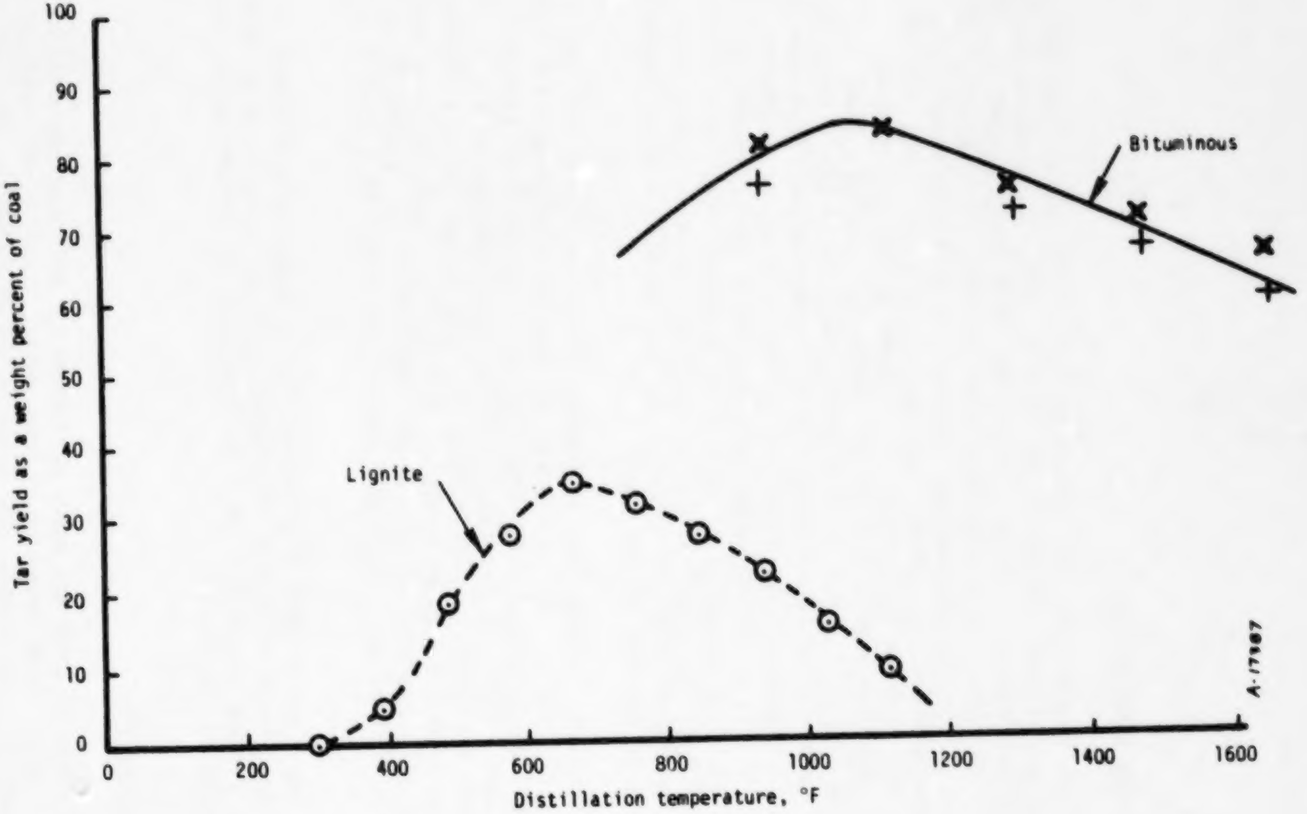

Figure 1. Tar yield as a function of distillation temperature.

polymerization and oxidation reactions. Even light oil samples that are initially collected floating upon a water surface seem to become inseparable from the water or completely polymerized to the solid phase after a period of time.

The importance of tar stability is twofold. First, the process developer does not want to contend with a substance that is difficult to remove from cyclones, scrubbers, etc. Second, the integrity of tar samples taken for analysis may be difficult to maintain, providing data of only limited accuracy. Chemical stability also influences tar collection techniques, and further problem definition is required for full development of sampling systems capable of separating tars.

2.4 OTHER PROPERTIES

A number of other tar properties of interest have been investigated. However, data is extremely limited. Lowry (Reference 1) lists data sources and some data for:

- Specific gravity
- Temperature coefficient of specific gravity
- Heat capacity and heating value
- Heat of vaporization
- Thermal conductivity
- Surface tension
- Viscosity
- Dielectric properties

Much of this data is for coal tar products (e.g., from coke ovens) which are known to have significantly different properties from gasification tars. More recent gasifier studies (Reference 2) have reported some of the fundamental properties (specific gravity, viscosity), but data is generally sparse.

One final property of gasifier tars should be emphasized. Many of the hydrocarbon compounds that can exist in tars are known carcinogens, particularly the aromatics and other benzene ring compounds (Reference 11). It is especially important that all persons dealing with tar wastes and samples avoid skin contact and breathing vapors. Also, safe procedures in all aspects of tar handling require further study and definition.

SECTION 3

TAR COLLECTION CONCEPTS

A variety of equipment has been used for extraction of tars from process gas streams on the process level. Each of these concepts have been reviewed in consideration of adapting the most appropriate technique to a sampling system for collection of tar samples.

Very few of the tar collectors identified have been shown to perform satisfactorily on the process level. The unit must be capable of performing several difficult functions in an efficient manner:

- Condensation of tar vapors to the mist phase (when required)
- Collection of all mist droplets in the stream regardless of drop size and total mass loading
- Operation without internal fouling by the collected material
- Provision for simple access of collected material

Nearly all classical dust and mist collection techniques have been applied to tar removal. These include:

- Electrostatic precipitators
- Scrubbers
- Condensers
- Cyclones
- Filters

The success or failure of each relates directly to the properties of the tars themselves. An evaluation of each collection technique is given below.

3.1 ELECTROSTATIC PRECIPITATOR

The electrostatic precipitator (ESP) has historically been the most widely applied technique for tar removal. Reference 9 shows application to gas detarring as early as 1915 in the United States. Possibly as many as 600 unit installations exist throughout the country, making the detarring of fuel gases the second largest application of the ESP.

The basic ESP concept is illustrated in Figure 2. A high voltage potential (typically 10 to 30 kV) exists at the discharge electrode providing a potential difference between the electrode and precipitator shell. The particles entering in the gas stream pick up charge from the field and then migrate toward the shell as a result of Coulombic forces. Variation of the unit's geometry, field potential, and field configuration provide different design variables for specific applications.

The success of electrostatic precipitation for gas detarring has been reported (see References 2 and 12 through 15 for example). The discussions are generally qualitative in nature rather than quantitative, but the general level of success is demonstrated. Only Reference 2 has attempted to provide quantitative data in terms of both mass collected and ESP efficiency at various tar mist particle size ranges.

In general, the wide range of tar particle size range and total mass loading make collection difficult. Tars often exist in the gas stream as both fog (particle diameters as small as 0.1μ) and mist (particle diameters from 1μ to 60μ or greater). The ESP is one device which can be designed to efficiently collect particles over this entire size range. The ability to collect small particles is particularly significant as other collection methods lack this ability. Very small particles tend to follow gas streamlines and, therefore, devices which depend on condensation by impingement are ineffective for fine mists. The unique ability of the ESP to collect fine particles has been demonstrated in Reference 2. Other references cited demonstrate the efficiency of electrostatic precipitation for both tar and light oil collection.

In addition, the ESP can easily accommodate a large collected mass over a long time interval. The collected tar mixture is usually of a low enough viscosity that the collected material can be continually withdrawn from the bottom of the unit (see Figure 2).

The possible explosion hazard associated with an electrical spark in a combustible gas mixture caused initial apprehension in the gas industry when electrostatic precipitation was introduced. Successful demonstrations in the early 1900's, however, had shown that flammability limits for most process gases were so low that the explosion risk was minimal. Therefore, due to high efficiency and generally low maintenance, the ESP has become the most popular means of gas tar removal on the process level.

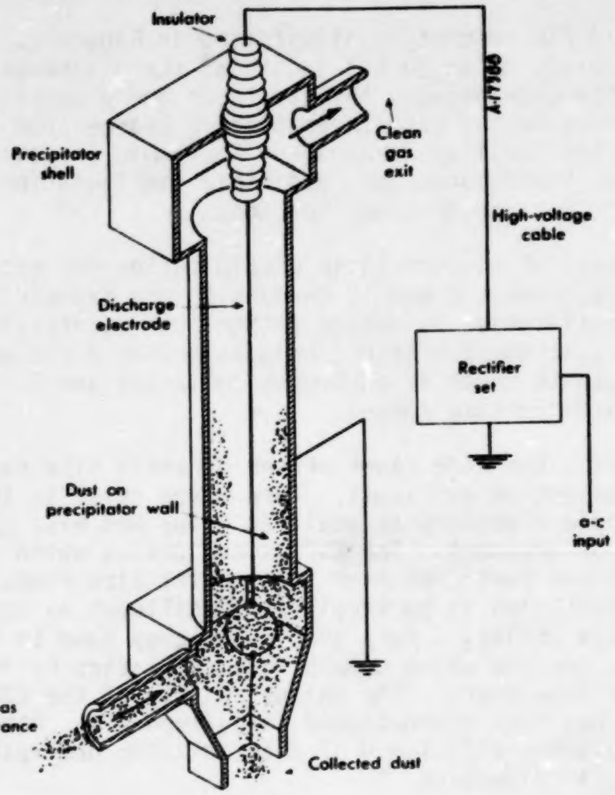
Insulator
A-11988
Clean gas exit
Precipitator shell
High-voltage cable
Discharge electrode
Rectifier set
Dust on precipitator wall
a-c input
Gas entrance
Collected dust

Figure 2. Typical electrostatic precipitator.

3.2 SCRUBBER

A number of coal gasification facilities utilize scrubber units for gas cleanup, usually intended for water, oil, and tar removal. A number of scrubber types exist, but only the spray and water chamber scrubbers will be discussed here.

A typical spray scrubber is shown in Figure 3. A high velocity, atomized water stream is sprayed either axially or radially into the throat of a venturi section. The tar laden gas stream also enters the venturi. Particle collection is accomplished by impingement of the water droplets upon the smaller tar particles, causing them to be entrained in the water stream and removed at the bottom of the unit. Support equipment includes the pump, a water supply, and waste water handling equipment.

The success of the venturi scrubber is related to tar particle size. The impaction collection mechanism (of the water droplet on the tar particle) is most efficient and can scrub smaller particles from the gas stream when water droplets are very finely atomized and moving at high velocity. This requires a large pressure drop at the atomizing nozzle and large pumping requirements. The result is a very substantial increase in scrubber energy input for particle removal down to 1μ in diameter. In general, collection of submicron particulate by the spray scrubber is prohibited by the impaction mechanism of collection. Since submicron tar particles (fog) exist in many coal gasification processes, the venturi will allow some entrained tar to remain in the process stream.

Quench chamber scrubbers force the gas to bubble through a contained liquid water bath. The quench chamber is illustrated in Figure 4. Efficient scrubbing of tars and oils from the gas stream relies on obtaining good contact between the tar mist and the quench water. This is achieved by breaking gas bubbles down to the smallest possible sizes.

Reference 2 has reported collection capabilities of the quench chamber and compared them to those of an ESP unit. The quench chamber was found to be less efficient in total collection, again limited by the submicron tar particles existing in the producer gas. The chamber appears to be most effective in removing lower temperature condensate fractions (light oils) and water, possibly due to the existence of larger particle sizes among these fractions. In the study of Reference 2, it was concluded that scrubbing techniques are significantly less effective then electrostatic precipitation for tar removal.

In conclusion, scrubbing has been found to be effective in some tar collection applications. However, the technique is ineffective for submicron particulate collection which may result in significant tar carryover in some process applications.

3.3 CONDENSER

Condensers differ from other tar collection devices (i.e., the ESP) in that they are capable of condensing tar vapors to the liquid phase as well as

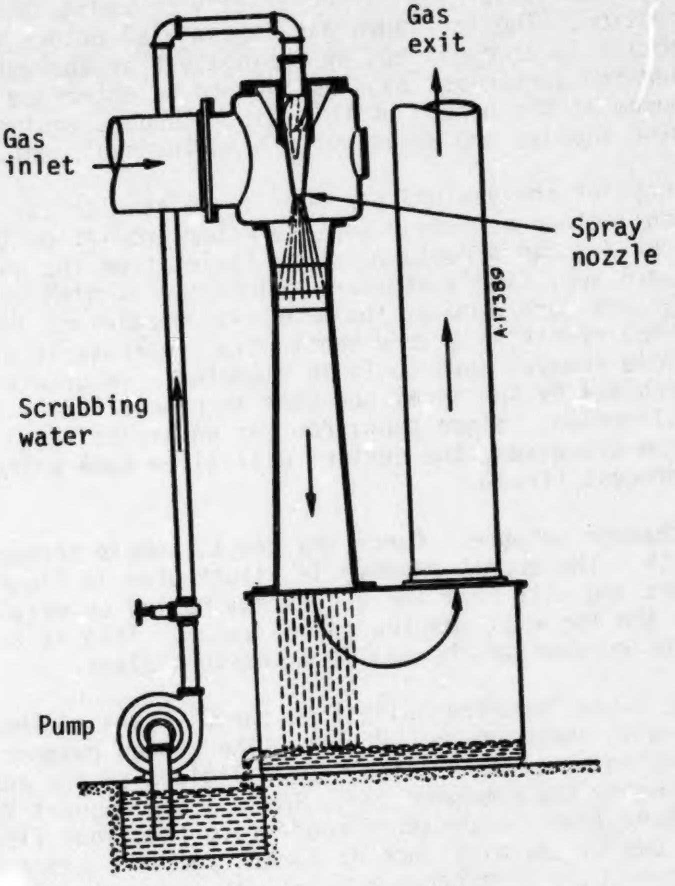
Gas exit
Gas inlet
Spray nozzle
A-17389
Scrubbing water
Pump

Figure 3. Typical water-jet scrubber.

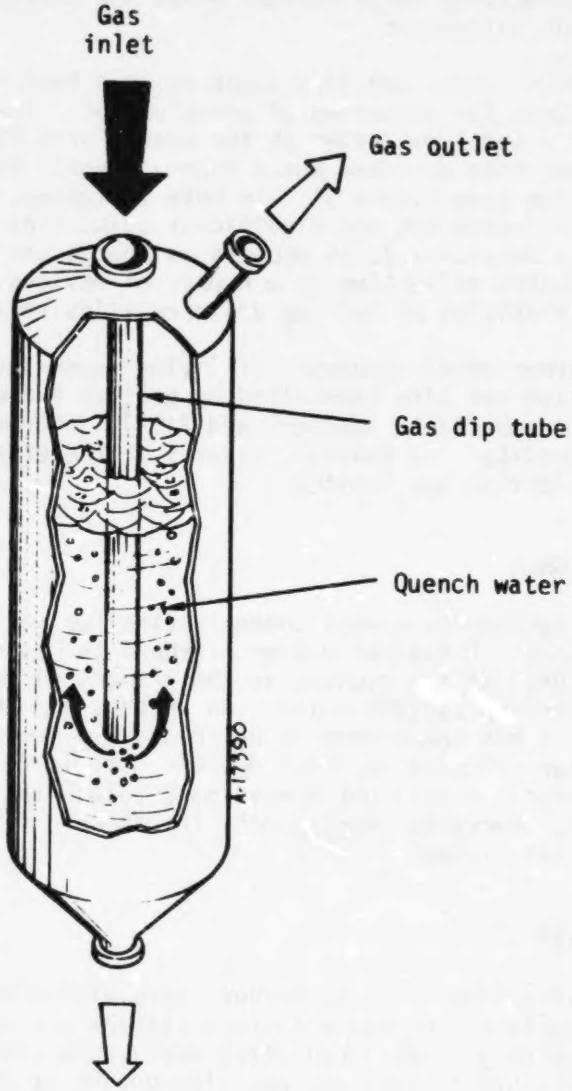
Gas inlet
Gas outlet
Gas dip tube
Quench water
A-17390
Condensate drain

Figure 4. Typical quench chamber scrubber.

collect the tar mist. Other collector types operate effectively only if tars are condensed to mist prior to entering the unit. In the condenser, the mist collection is performed by exposing the gas stream to large, cooled surfaces, allowing tar droplets to attach to the walls. Particle migration to the wall is essentially unaided (contrasted to the Coulomb forces existing in the ESP), and relatively large surface areas and small flow passages are required for efficient collection.

Process survey and literature reviews have revealed several types of condensers used for detarring of producer gas. The Riley-Stoker gasifier process and a sampling system at the Grand Forks slagging Lurgi (References 2 and 3) have both utilized basic tube-and-shell heat exchange condensers for tar collection (see Figure 5). In both instances, it was reported that light oils were collected but not significant quantities of tar. As was noted for scrubbers in Section 3.2, it appears as though the large drop size of light oils facilitates collection by a number of devices. The smaller (often submicron) particles of tar fog are more illusive and difficult to collect.

A rather novel condenser utilizing centrifugal impellers to aid the tar collection was also identified by process survey. This unit has since gone out of production, however, and little information is available as to its functionality. In general, reports of the effectiveness of condensers for tar collection are limited.

3.4 CYCLONE

The cyclone is a most common device for solid particulate removal in many processes. A typical design is shown in Figure 6. Most gasification facilities utilize the cyclone as the primary cleanup device. Hence, several reports regarding cyclone collection of tars are in existence. Riley-Stoker (Reference 2) has shown them to be relatively ineffective in collecting entrained tar relative to other devices. It is interesting to note that cyclones generally will not remove particulate that is smaller than 1 micron in diameter. Carryover may result, therefore, if many fine particles exist in the process stream.

3.5 FILTER

Various filtration techniques were also investigated for application to tar collection. Ordinary fibrous filters are not a useful tar collection technique as only a small collected mass would clog the filter and restrict flow. Packed bed filters are one alternative as they are usually mounted within a large chamber (to provide laminar gas flow) and can collect a large volume of tar and other condensibles. Unfortunately, packed beds are generally ineffective for particles of a few microns diameter or smaller. A packed bed/solvent bath combination filter would increase small particle collection efficiency but would require some additional development. Therefore, filtration may be a viable technique for some process tar measurements.

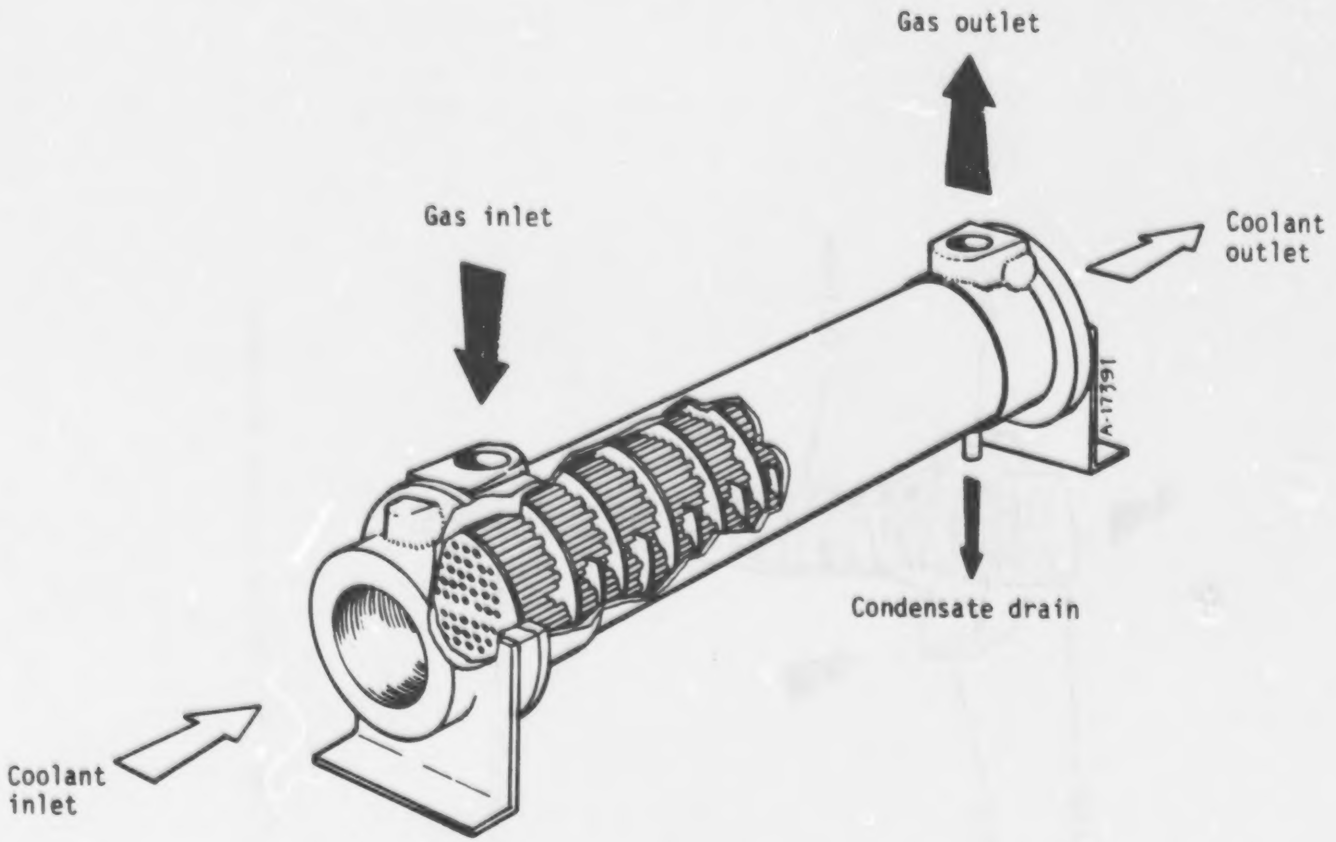
Gas outlet
Gas inlet
Coolant outlet
A-17391
Condensate drain
Coolant inlet

Figure 5. Typical shell-and-tube condenser.

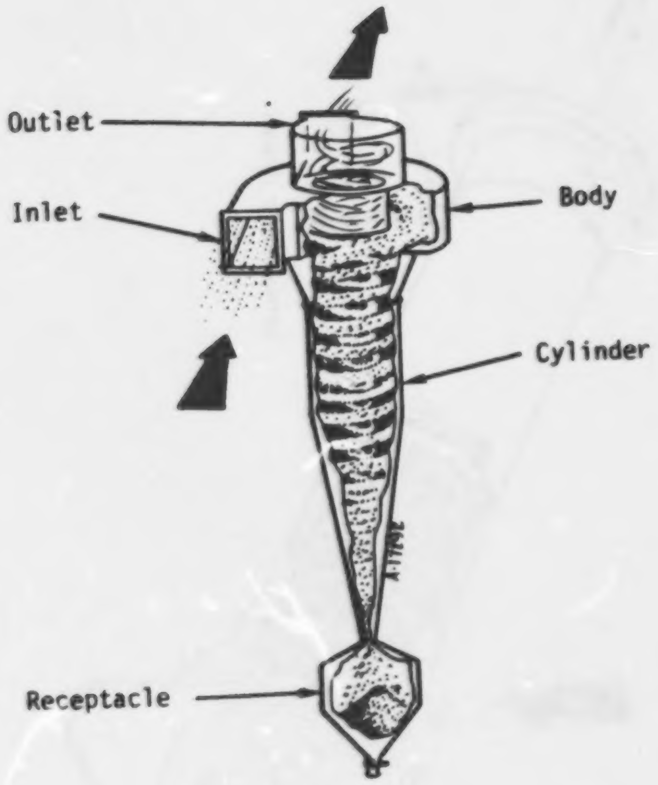
Outlet
Inlet
Body
Cylinder
Receptacle

Figure 6. Typical cyclone separator.

SECTION 4

TAR COLLECTORS FOR SAMPLING SYSTEM APPLICATION

The survey of the physical properties of coal gasifier tars and of existing and potential tar collector techniques has led to recommendations for tar collection in process sampling systems. Since sampling system experience in tar collection is currently in its infancy, hardware development is required. This development may be either a simple scaledown of existing full scale process equipment or the development of new designs for specific application to sampling systems.

To summarize the previously discussed survey findings, a list of design specifications and hardware requirements can be formulated. All specifications fall into two basic categories:

1. Collector efficiency
2. Collector applicability to the high temperature and pressure environment of a gasification system

Collection efficiency is a key requirement of sampling system hardware as the objective of sampling is usually to obtain a quantitative measurement of the process stream constituents. Any tar material which passes through the collector, then, provides inaccuracies in the measurements obtained. It is also important that the device be capable of interfacing with the severe environment of the process stream. This requirement includes safe and reliable operation over its lifetime.

The efficiency of the developed collector depends upon its ability to collect tar mist particles over the entire size range present in the gas stream. As has been noted, process experience suggests that fine particulate (below 1 diameter) does exist in most gas streams and is particularly hard to capture. The percentage of the total tar mass that is submicron in size is largely unknown; thus, the collector should be required to have reasonably high collection efficiency for small particles. Of the techniques discussed in Section 3, only electrostatic precipitation and filtration have this potential.

There are a number of other factors which will have an impact on collection efficiency. In general, the longer the tar particles are exposed to the collecting surfaces, the greater the number that will ultimately be removed from the gas. Therefore, collector residence time may be an important design parameter. The designer must also consider the total mass to be collected (in relationship to sampling time and tar loading). This mass must be contained so as to not interfere with collector operation. All collectors discussed can be designed to meet these requirements with the exception of some filter units which will clog under limited operation and thus be unsuitable for sampling system application.

It almost goes without saying that a sampler component must be compatible with the environment in which it will be used. It is pointed out here, however, to illustrate requirements of the collector design. One must as a minimum consider:

- Material requirements to withstand stream temperature and possible corrosive and erosive properties
- Structural design to withstand pressure loadings at temperature
- Ease of sample extraction such that samples will not be contaminated
- Safety requirement of containing hot gases and possibly toxic tar substances
- Geometry and size that are compatible with other system components

Probably all of the collector concepts of Section 3 could be designed to incorporate these features. Collector selection, therefore, is mainly dictated by collection efficiency requirements.

In consideration of tar properties, collection concepts, and collector requirements, the electrostatic precipitator appears to be the most appropriate for sampling system adaptation. Its general high efficiency, compatibility with design requirements, and wealth of practical experience on the process scale make it the optimum choice for further development. There are applications where filters and/or condensers may also give adequate performance. Cyclones and scrubbers do not appear adequate for tar collection in any application. One should be fully aware of the limitations and design problems associated with these units before development is begun.

Aerotherm has demonstrated the applicability of the electrostatic precipitator by preliminary design calculations. A typical gasifier test condition of 5000 lbm of producer gas per hour with a density of 0.31 lbm/ft^3 and 0.03 lbm of entrained tar per lbm of gas was assumed for the design specification. In addition, a sampling system operating at a rate of 1 acfm was assumed. These assumptions result in 0.6 lbm of tar that must be collected by the sampling system every hour.

It was desirable to have the resulting ESP of compact design such that it would be compatible with sampling systems. The result was a two-stage collector based on a Southern Research Institute (SoRI) concept, shown in Figure 7. The cylindrical design fits into a space of 7 inches in diameter and 6 inches in length. A disc-shaped electrode charged to 10,000 volts

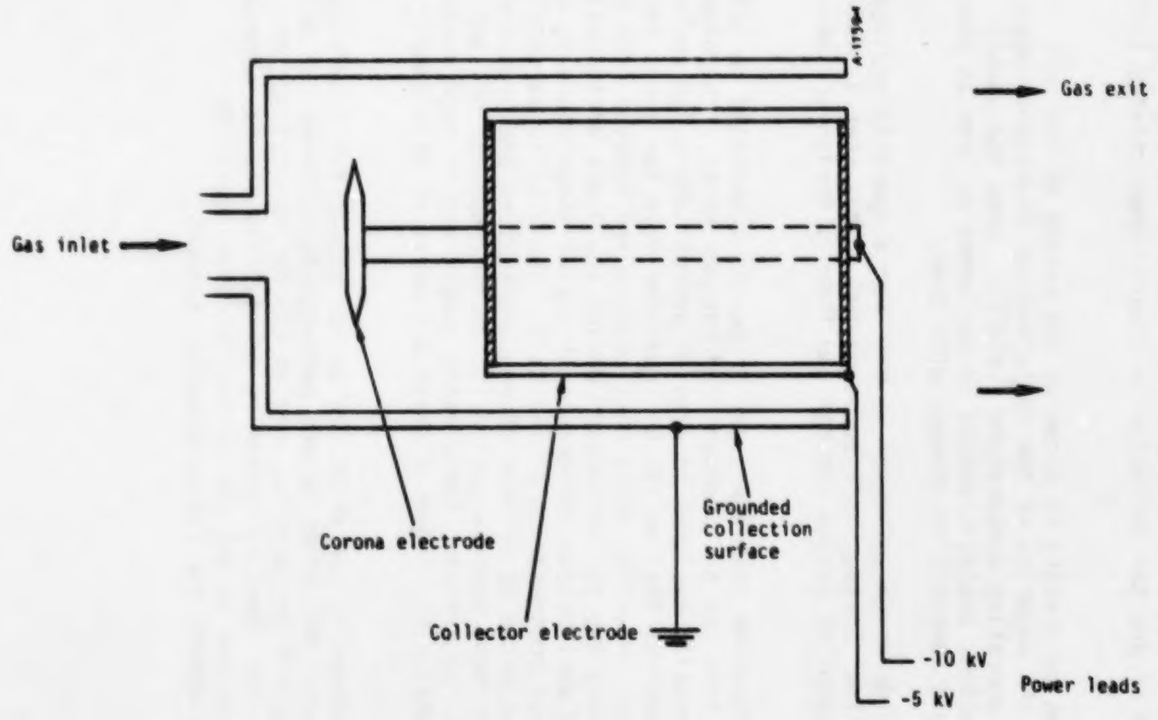
A-11594
Gas inlet
Gas exit
Corona electrode
Collector electrode
Grounded collection surface
-10 kV
-5 kV
Power leads

Figure 7. ESP collector for sampling system adaptation.

promotes primary charging of incoming tar droplets. An annular secondary field at 5000 volts provides a large surface area for particle collection.

The acceptability of the design is further demonstrated by its computed collection efficiency. For all particle sizes above 1 micron, the efficiency is virtually 100 percent. At 1 micron, efficiency falls to 99.6 percent and at 0.3 micron falls to 99.2 percent. Hence, the high collection efficiency requirement of any tar collector is clearly demonstrated by the ESP approach.

The sample flows by gravity to a cup at the bottom of the unit for eventual removal: the majority of the collected tar fractions remain fluid at the elevated operating temperature (~450°F). Once the sample is condensed and collected, analysis should be performed as soon as possible in order to avoid sample composition changes with time.

In order to decide which collector is best for a specific application, an overall sampling strategy must be developed. This step is followed by design of a sampling system concept and finally design of individual components.

Most coal gasification developers are primarily interested in solid particulate carryover from the gas producer and cleanup units. Therefore, sampling systems are usually designed to provide appropriate solid collection capabilities. This requires that solids be separated from tar mists and collected independently. Usually, solid particulates are removed from the sample stream first since any tar collection device would act efficiently on solids as well. Solid particulate collection at stream temperature is desirable to avoid additional condensation of the tars. Thus, solid particulates should be removed first while at or near stream temperature and pressure. For tar removal, the stream must then be cooled (to allow condensation) and passed into the collection device. The cleaned sample gas is then vented or retained for further analysis. Figure 8 shows a diagram of this sampling scheme.

This sampling scheme is one which can be envisioned for a multicomponent producer gas stream. One might select particulate cyclones for solids collection, a condenser for gas cooling, and an ESP for tar collection. The exact configuration of the sampling system is necessarily process dependent. The tar collection technique is but one system function requiring consideration and development for future sampling systems.

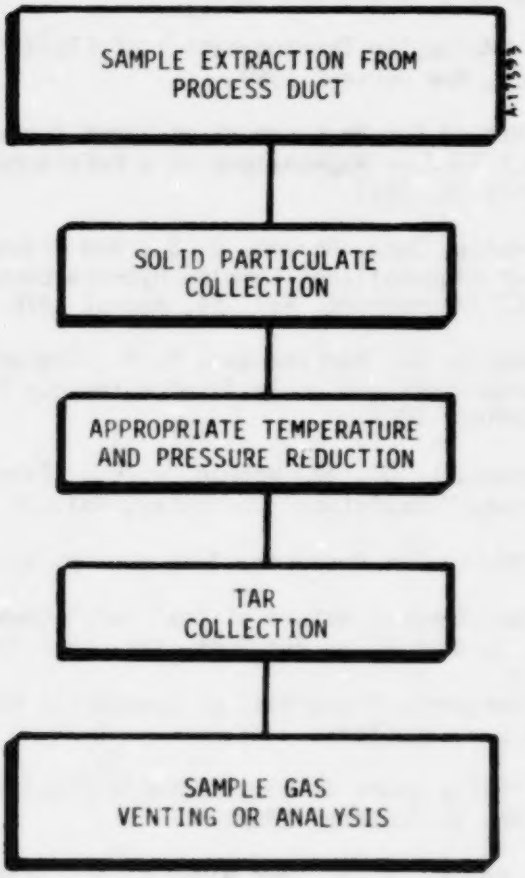
SAMPLE EXTRACTION FROM PROCESS DUCT
A-17593
SOLID PARTICULATE COLLECTION
APPROPRIATE TEMPERATURE AND PRESSURE REDUCTION
TAR COLLECTION
SAMPLE GAS VENTING OR ANALYSIS

Figure 8. Gasification process sampling scheme.

REFERENCES

1. Lowry, H. H. (editor), "Chemistry of Coal Utilization -- Supplementary Volume," John Wiley and Sons, Inc., 1963.

2. Lisaukas, Robert A., Johnson, Stephen A., and Earley, William P., "Control of Condensible Tar Vapors from a Fixed Bed Coal Gasification Process," 4th Energy Resource Conference, Paper No. IMMR11-PD14-76, June 1976.

3. "Quarterly Technical Process Report, July-September 1976, Grand Forks Energy Research Center," GFERC/QTR-76/5.

4. Prausnitz, J. M., "Molecular Thermodynamics of Fluid-Phase Equilibria," Prentice-Hall, Inc., New Jersey, 1969.

5. Sinke, G. C., "A Method for Measurement of Vapor Pressures of Organic Compounds Below 0.1 Torr -- Naphthalene as a Reference Substance," J. Chem. Thermodynamics, 6, 1974.

6. Smith, George, Winnick, Jack, Abrams, D. S., and Prausnitz, J. M., "Vapor Pressures of High-Boiling, Complex Hydrocarbons," The Canadian Journal of Chemical Engineering, Vol. 54, August 1976.

7. McKay, J. F., Amend, P. J., Harnsberger, P. M., Cogswell, T. E., and Latham, D. R., "Separation and Analysis of Petroleum Residues," Laramie Energy Research Center, ERDA.

8. Green, J. E., Schmach, L. J., and Worman, J. C., "Simulated Distillation by Gas Chromatography," Analytical Chemistry, Vol. 36, No. 8, 1964.

9. Rambush, N. E., "Modern Gas Producers," London, p. 102, 1923.

10. Rhodes, E. O., "The Chemical Nature of Coal Tar," Chemistry of Coal Utilization, Vol. 2, John Wiley and Sons, Inc., New York, p. 1290, 1945.

11. Sax, N. Irving, "Dangerous Properties of Industrial Materials," Van Nostrand Reinhold Co., New York.

12. White, Harry J., "Fifty Years of Electrostatic Precipitation," Journal of APCA, Vol. 7, No. 3, November 1957.

13. White, Alfred H., Rowley, R. B., and Wirth C. K., "Electrical Separation of Tar from Coal Gas," Journal of Gas Lighting and Water Supply, September 1914.

14. Cree, K. H., "Cottrell Electrical Precipitation as Applied to the Manufactured Gas Industry," American Gas Journal, Vol. 162, March 1945.

15. Thompson, R. J. S. and Cosby, N. T., "Notes on the Removal of Particulate Matter and Vapour Phase Sulphur Compounds from Gases," The Gas World -- Coking, Vol. 148, August 2, 1958.

Appendix D

Aerotherm Project 7237

FIELD TESTING OF A SAMPLING SYSTEM FOR HIGH TEMPERATURE/HIGH PRESSURE PROCESSES

William Masters
Acurex Corporation/Aerotherm Division
485 Clyde Avenue
Mountain View, California 94042

June 1977

AEROTHERM REPORT TM-77-177

Prepared for
EPA Project Officer — William Kuykendal

Industrial Environmental Research Laboratories
U.S. Environmental Protection Agency
Research Triangle Park
North Carolina 27711

Contract 68-02-2153

TABLE OF CONTENTS

Section		Page
1	INTRODUCTION	D-1
2	SUMMARY OF RESULTS	D-2
3	EQUIPMENT DESCRIPTION	D-4
	3.1 Sampling System	D-4
	3.2 Exxon Miniplant Test Facility	D-15
4	TEST DESCRIPTION	D-20
5	DATA	D-23

LIST OF ILLUSTRATIONS

Figure		Page
3-1	High-temperature, high-pressure sampling system	D-7
3-2	System schematic	D-8
3-3	Exploded view of HTHP probe	D-9
3-4	Probe housing and duct interface valve	D-10
3-5	Access valves	D-11
3-6	Dowtherm console	D-13
3-7	Flow control oven and gas train	D-14
3-8	Control consoles	D-16
3-9	Pressurized fluidized bed coal combustor system	D-17
3-10	HTHP probe assembly installed at Exxon miniplant	D-19
5-1	Particle size distribution	D-32
5-2	Impactor substrates	D-34
5-3	Impactor substrates	D-34
5-4	Impactor substrates	D-35
5-5	Impactor substrates	D-35
5-6	Impactor substrate Run 3, Stage 5	D-36
5-7	Impactor substrate Run 2, Stage 5	D-37
5-8	Particle photomicrographs Stage 1	D-38
5-9	Particle photomicrographs Stage 2	D-39
5-10	Particle photomicrographs Stage 4	D-40
5-11	Particle photomicrographs Stage 6	D-41
5-12	Particle chemical composition	D-42

LIST OF TABLES

Table		Page
3-1	Sampling System Capabilities	D-5
3-2	Utility Requirements	D-18
5-1	Test Conditions	D-24
5-2	Probe Instrumentation Readings	D-25
5-3	Gas Train Instrument Readings	D-26
5-4	Anisokinetic Correction Factors	D-27
5-5	Structure Temperatures	D-29
5-6	Particulate Content	D-30
5-7	Particle Size Distribution	D-33

SECTION 1

INTRODUCTION

This report describes field testing of an advanced sampling system which can measure the particulate concentration and trace element content of high-temperature, high-pressure (HTHP) processes. Tests were held at a pilot-scale coal combustion plant where pressurized fluidized bed combustion is being developed. The field tests were successful in demonstrating sampling system capabilities and producing sample data.

Acurex/Aerotherm has developed the HTHP sampling system for the Industrial Environmental Research Laboratory of the U.S. Environmental Protection Agency. This work is part of a program Measurements of High-Temperature, High-Pressure Processes (Contract 68-02-2153), intended to produce the new sampling technology needed for advanced coal conversion processes. Fluidized bed combustion and coal gasification processes emit gases containing large quantities of fine particles. These particles must be removed to prevent damage to process equipment (mainly turbines) and to eliminate potential environmental pollution. Development of particulate removal equipment is an important step toward making advanced coal conversion processes practical. The sampling system described in this report is one of the first tools available for measuring the collection efficiency of fine particle removal devices operating in high-pressure, high-temperature environments.

SECTION 2

SUMMARY OF RESULTS

The field demonstration of the high-temperature, high-pressure sampling system was successfully completed. Three sampling runs were made: one using a filter to collect particulate, and two using a cascade impactor. Trace metals and trace organics sampling equipment was operated during the filter run. The test produced the following data:

- Particulate concentration
- Particulate size distribution
- Moisture content
- Particulate chemical composition
- Particulate shape
- Duct gas temperature and pressure
- Access port and valve temperatures

The test also produced samples of trace organics collected on XAD-2 sorbent, and trace elements collected in oxidizing impinger solutions. These samples have not yet been analyzed.

For a more detailed description of the test data, see Section 5 of this report.

The test series demonstrated the capability of the sampling system to operate in the severe PFBC environment. Sample data was obtained from the 1360°F, 9-atmosphere gas stream. Generally, the system operated as designed: obtaining access to the pressurized duct while the process was operating, inserting the sampling probe, sampling the gas stream, and withdrawing the sample. However, as might be expected in a first field test, a few hardware problems were found. Most of these were corrected before the sampling tests, but one uncorrected problem, a malfunctioning impactor heater, gave sample collection temperatures which were lower than desired. The heater will be replaced before future use of the system.

During the test sequence, the sampling operations proceeded very smoothly. The three sampling runs were completed within a 30-hour period (20 working hours). The tests showed the versatility of the system, operating with two different types of particle collectors, with and without trace element sampling equipment.

SECTION 3

EQUIPMENT DESCRIPTION

The following discussion is divided into two parts: first, a description of the advanced sampling system itself; and second, a description of the Exxon Miniplant PFBC facility where the sampler demonstration took place.

3.1 SAMPLING SYSTEM

The sampling system described in this report samples particulate, trace organics and trace metal contaminants in high-pressure, high temperature gas streams. The system represents an advancement in the state of the art designed to sample new coal conversion processes. System capabilities are summarized in Table 3-1.

The basic functions of the sampling system are to:

- Safely contain facility pressure
- Insert the sample probe into the process duct while the process is operating
- Extract a representative sample
- Cool the sample to a temperature which is compatible with developed particle collectors yet prevents condensation (~450°F)
- Collect and aerodynamically size particulates
- Collect trace organics and trace metals
- Monitor duct conditions and control sample flowrate to give accurate isokinetic capture conditions
- Remove the sample probe and close off duct access so that collected samples may be removed while the process remains pressurized

TABLE 3-1. SAMPLING SYSTEM CAPABILITIES

Sample Environment	
• Temperature	1200°F – 1800°F 650°C – 1000°F
• Pressure	3-20 atmospheres
• Gas Constituency CO CO_2 NO SO_2 H_2O NO_x H_2S COS CS_2 HCN NH_3 Organics	Concentrations subject to further investigation, dependent on process sampled
• Stream Velocity	8-150 fps
• Particulate Grain Loadings	0-15 gr/ft^3 (subject to further consideration and actual process characteristics)
• Particulate Size Range (for classification)	0.2 – 10 microns (Notes: Larger particulates may be acceptable in most cases of total mass determination or if classify, they may be amenable to "scalping" ahead of classification device)
• Duct Size	Variable depending on probe; std. is 8 inches I.D. minimum
Sampling System Configuration	Modular, so as to allow in-situ or extractive sampling by cooled probe
Traverse Capability or Penetration of Nozzle into Duct or Vessel	Approximately 18" either in-situ or extractive configuration (some dependence on internal configuration of duct or vessel). Can be extended by relatively minor hardware modification (longer probe, chamber extension, spool piece, etc.)
Access Process Port Requirements	Standard: 4" IPS minimum, 300 lb flange access through 4" IPS alloy gate value (Note: Smaller ports may be acceptable if special probe assembly is used)
Gas Constituency Analysis	Depends on specific process requirements; will be better identified during program based on state-of-the-art review

To perform these functions, the sampling system includes the following subsystems:

- Sample probe assembly
- Dowtherm coolant system
- Hydraulics for probe traverse actuation
- Flow control oven
- Trace organics module
- Trace metal impinger train
- Control consoles

The sampling system is shown in Figures 3-1 and 3-2.

Probe Assembly

The probe assembly includes the sampling probe, probe housings and duct access valves. The probe itself consists of the sample inlet nozzle, cooler section, particulate collector and heated transport tube, as shown in Figure 3-3. Two types of particulate collectors were used in the demonstration tests: one was a University of Washington Mark III cascade impactor, with seven stages of particulate sizing; the other was a glass fiber thimble filter with large total mass capacity, but no sizing capability. The inlet nozzle diameter was 0.75 inch for all tests. The front portion of the probe includes a sample conditioning cooler which reduces sample temperature from process temperature to about 450°F. Electric heaters along the rear portion of the probe maintain the sample temperature.

The sampling probe is mounted within a housing which contains process pressure. The housing is a tube-within-a-tube assembly which telescopes to traverse the probe into and across the process duct. Hydraulic cylinders connecting the two housing tubes actuate probe motion. The housing assembly is shown in Figure 3-4.

For the demonstration test series, the probe housing was connected to the process duct by two 4-inch diameter gate valves in series. The 4-inch valve bore provides sufficient clearance for the probe to be inserted through the valves into the process stream. Two valves were used to give redundant shut-off capability. The installed access valves are shown in Figure 3-5.

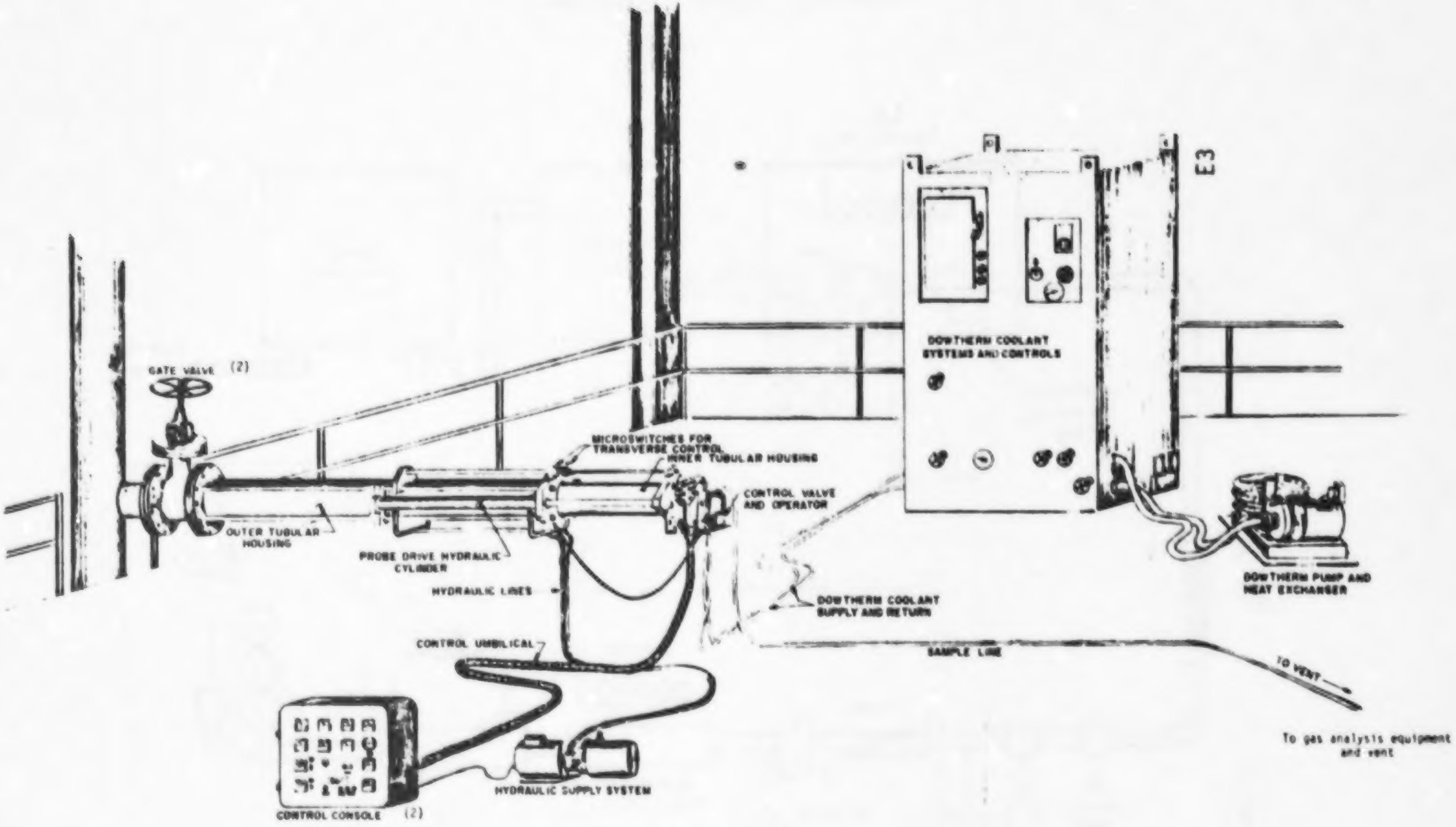
GATE VALVE (2)
OUTER TUBULAR HOUSING
PROBE DRIVE HYDRAULIC CYLINDER
MICROSWITCHES FOR TRANSVERSE CONTROL
INNER TUBULAR HOUSING
CONTROL VALVE AND OPERATOR
HYDRAULIC LINES
CONTROL UMBILICAL
CONTROL CONSOLE (2)
HYDRAULIC SUPPLY SYSTEM
DOWTHERM COOLANT SUPPLY AND RETURN
SAMPLE LINE
TO VENT
To gas analysis equipment and vent
DOWTHERM COOLANT SYSTEMS AND CONTROLS
DOWTHERM PUMP AND HEAT EXCHANGER
E3

Figure 3-1. High-temperature, high-pressure sampling system.

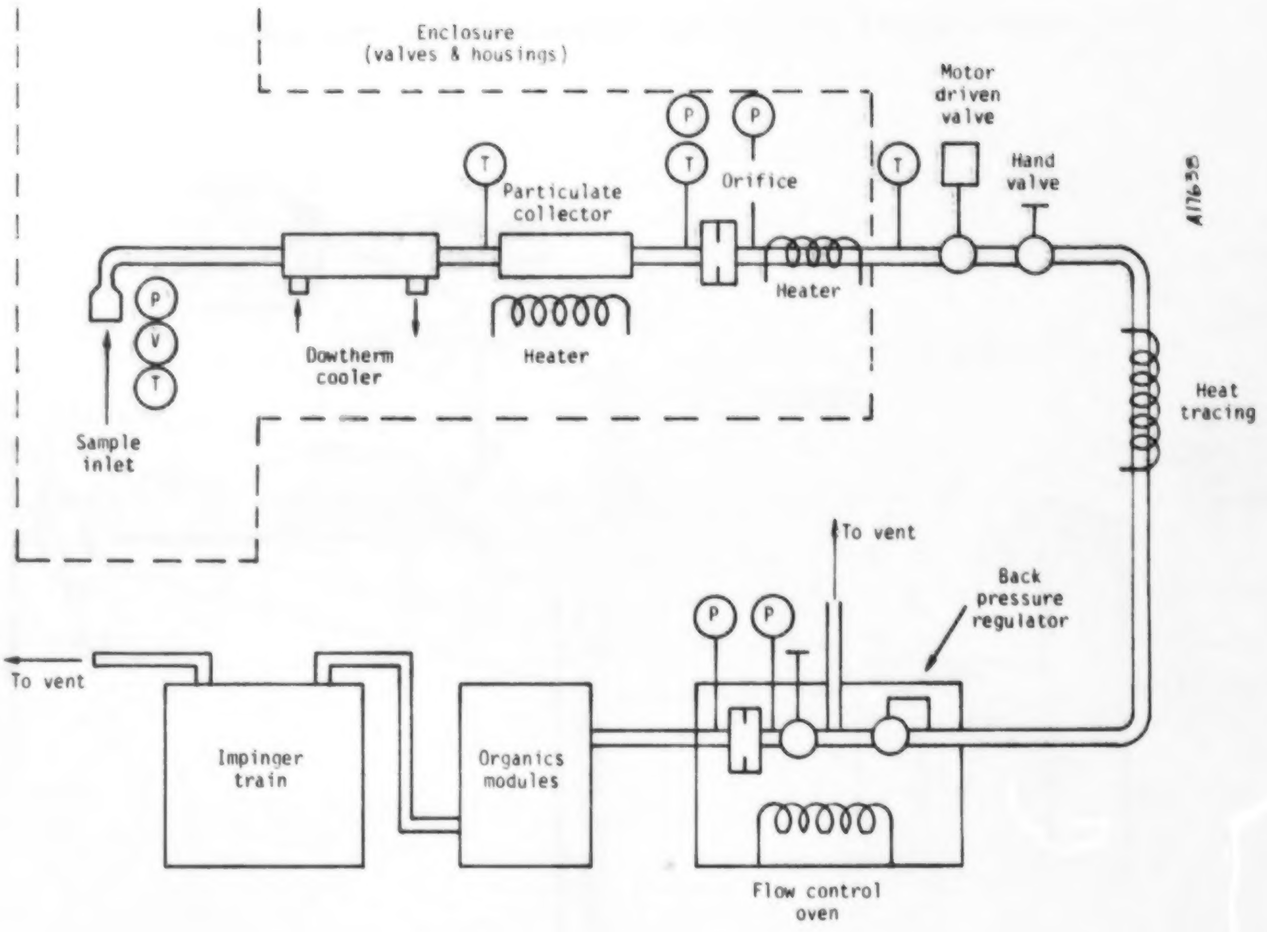
Enclosure
(valves & housings)
Motor driven valve
Hand valve
A17638
P
P
T
T
Orifice
T
Particulate collector
Heater
Heater
P
V
T
Dowtherm cooler
Sample inlet
Heat tracing
To vent
Back pressure regulator
P
P
To vent
Impinger train
Organics modules
Flow control oven

Figure 3-2. System schematic.

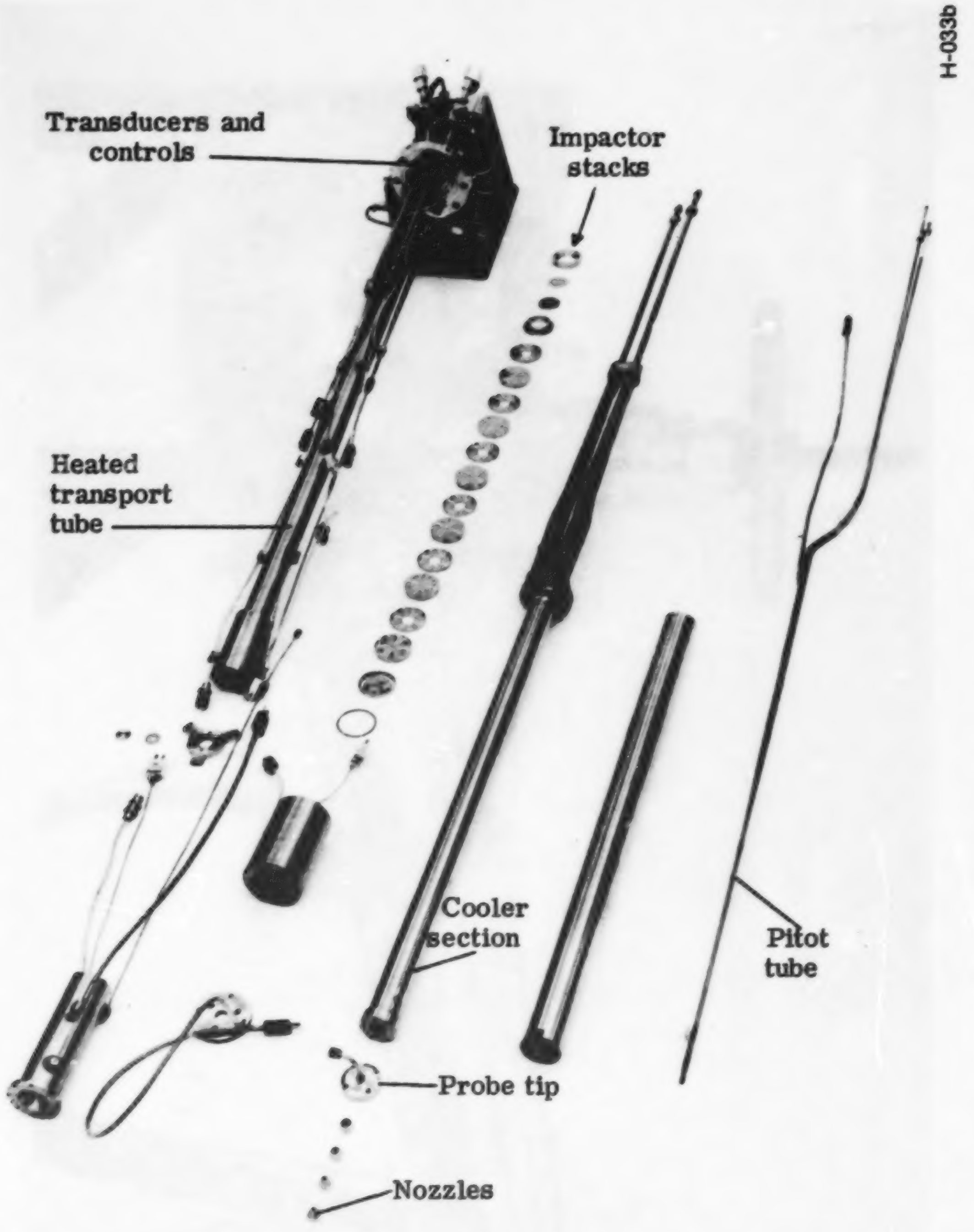
H-033b
Transducers and controls
Impactor stacks
Heated transport tube
Cooler section
Pitot tube
Probe tip
Nozzles

Figure 3-3.

Exploded view of HTHP probe.

H-035b

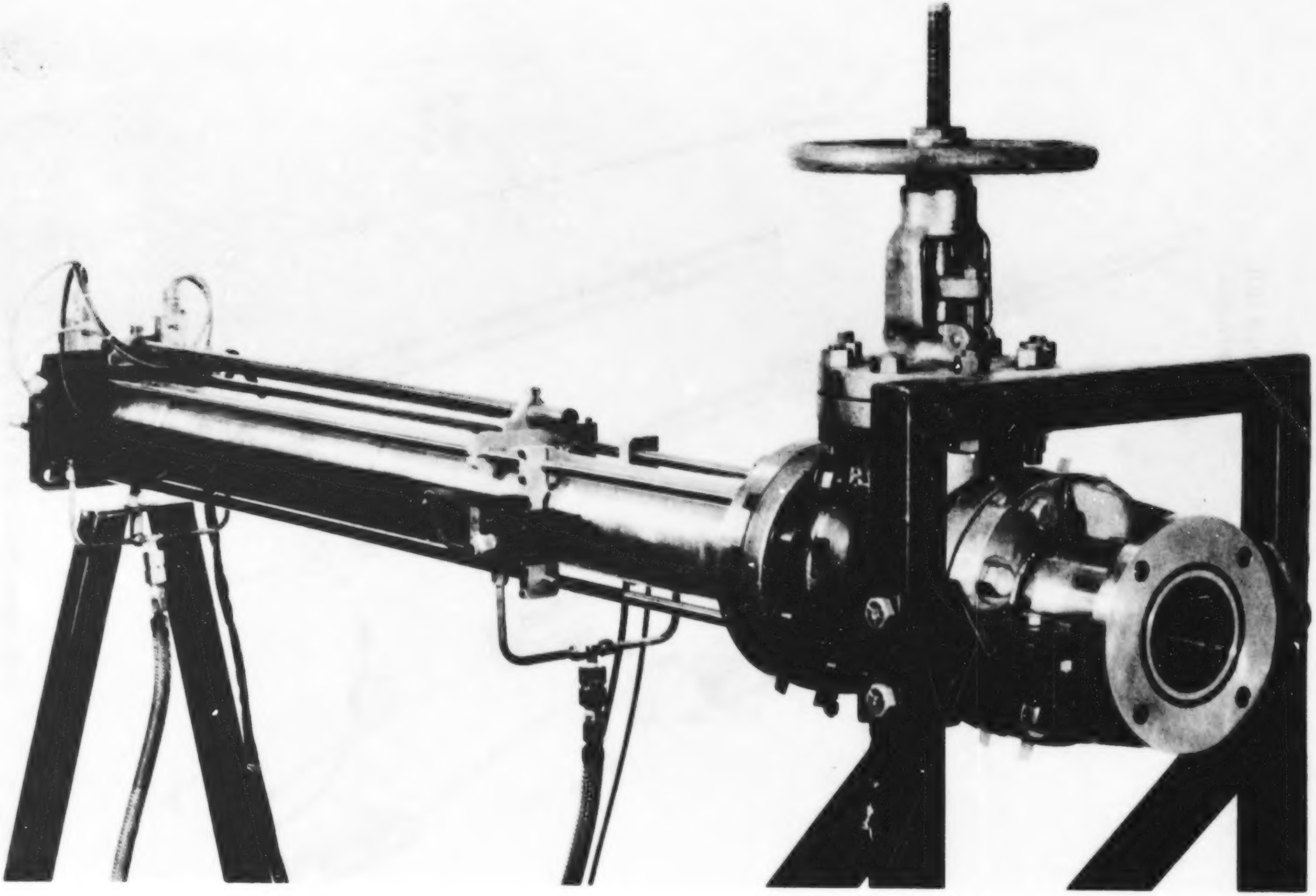

Figure 3-4. Aerotherm HTHP sampling probe and duct interface valve.

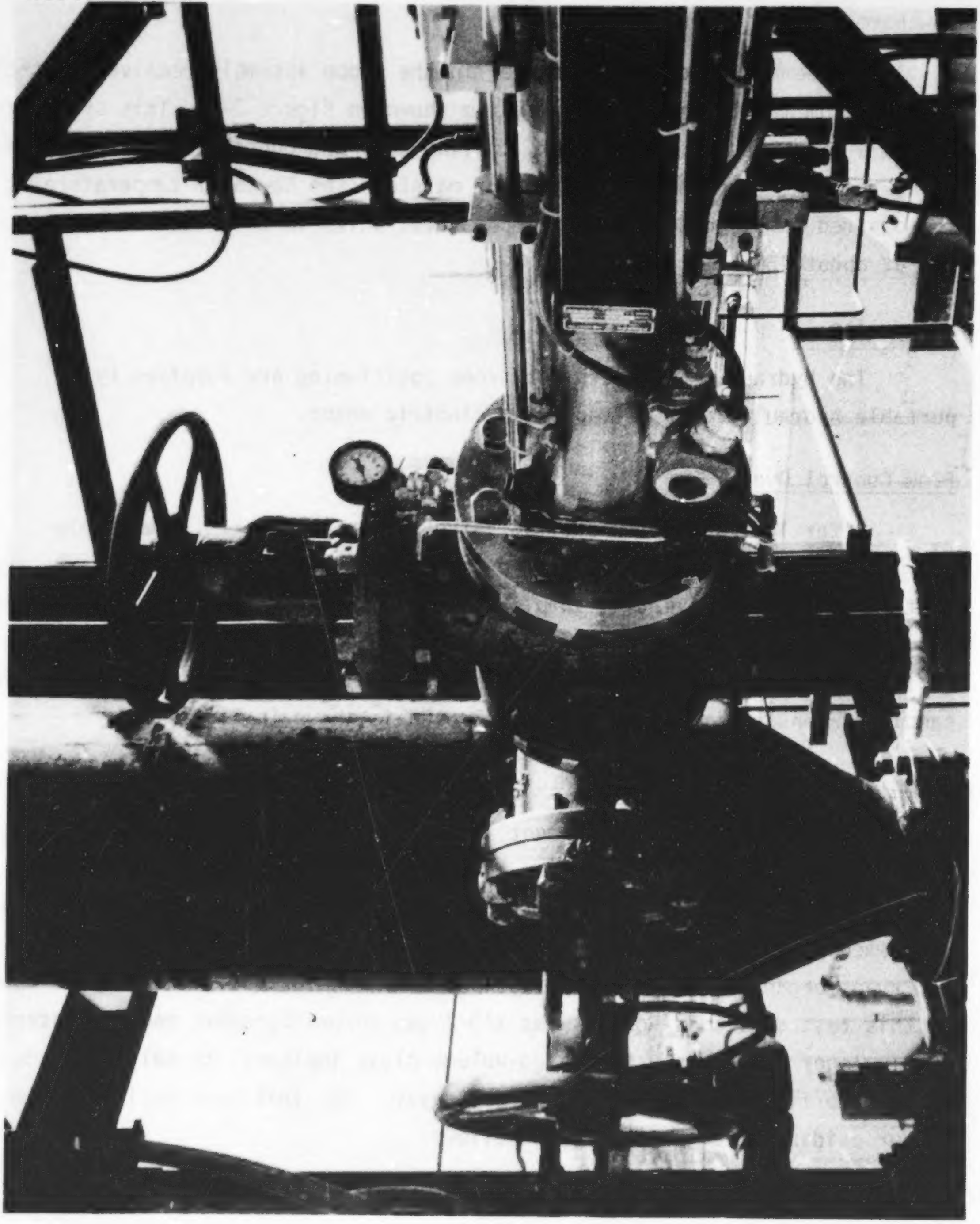

Figure 3-5. Access valves.

Dowtherm Coolant System

The sample conditioning cooler in the probe assembly receives Dowtherm coolant from the Dowtherm supply system shown in Figure 3-6. This system includes a pump, heater, surge tank, cooling coil and controls. During operation, the heater and heater controller maintain the Dowtherm temperature at the desired sample conditioning temperature, which in this test series was set at about 450°F.

Hydraulics

The hydraulic cylinders for probe positioning are supplied by a portable hydraulic pump driven by an electric motor.

Flow Control Oven

After leaving the throttling valve at the probe exit, the sample gas is brought to the flow control oven which contains the back pressure regulator, valves for diverting sample flow from the vent to the organic module and impingers, and the orifice controlling the flowrate through these components. The oven enclosure maintains all of the controls at 450°F, preventing sample condensation. The flow control oven is shown in Figure 3-7.

Organics and Trace Metal Collectors

The gas collection equipment included in the sampling system consists of an organics module and impinger train (see Figure 3-7). Both units are identical to those used in Acurex/Aerotherm's commercially available Source Assessment Stack Sampler. The organic module cools the sample gas to 70°F and traps organic vapors in a porous polymer granular bed. The polymer used in this test series is Rohm & Haas XAD-2 gas chromatographic packing material. The impinger train uses three high-volume glass impingers to collect trace metal vapors, followed by a silica gel dryer. For this test series the impinger oxidizing reagents were as follows:

Impinger	Solution
#1	6M H_2O_2
#2	0.2M $(NH_4)_2S_2O_8$ + 0.02M A_gNO_3
#3	0.2M $(NH_4)_2S_2O_8$ + 0.02M $AgNO_3$
#4	Silica Gel

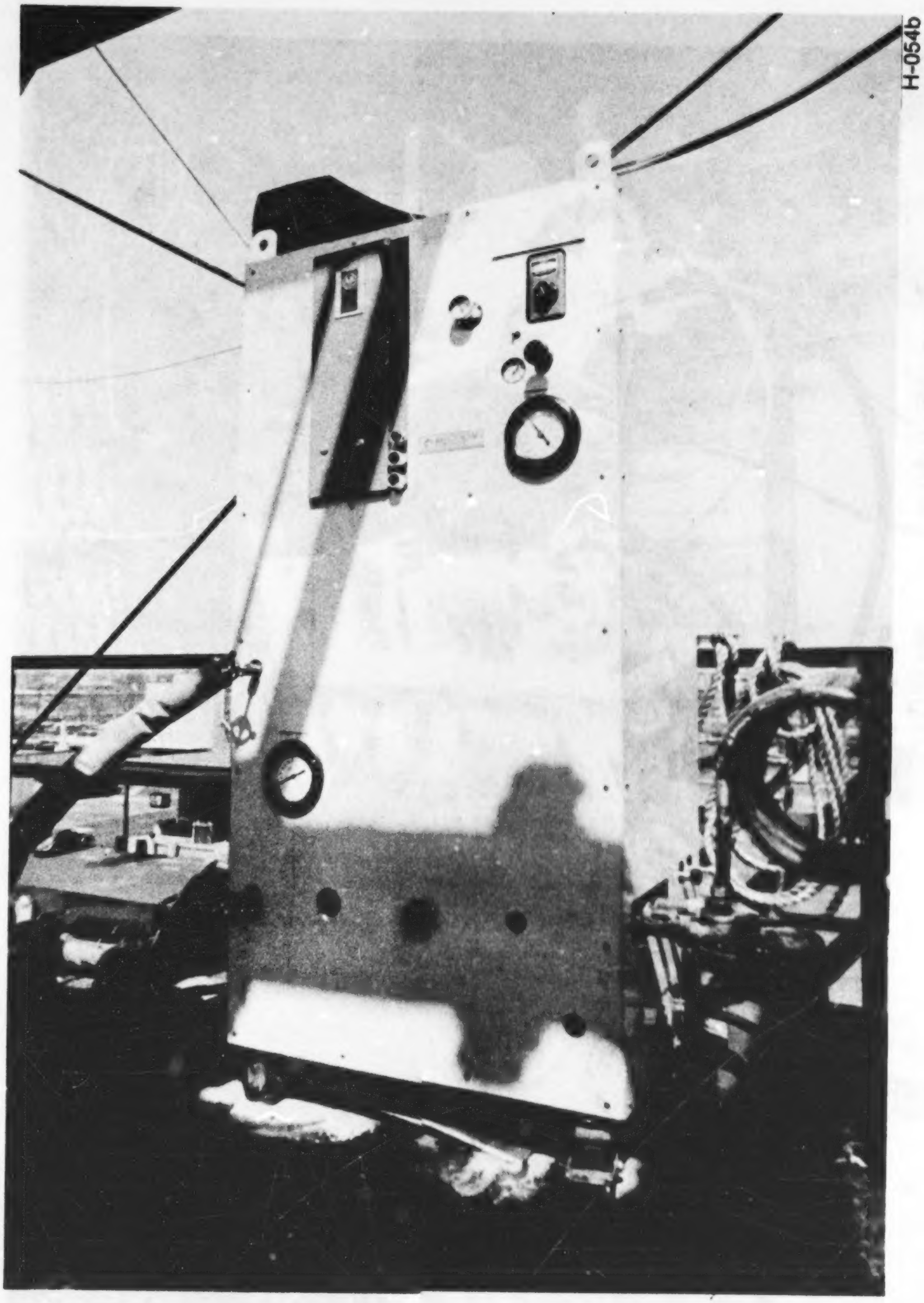

Figure 3-6. Dowtherm console.

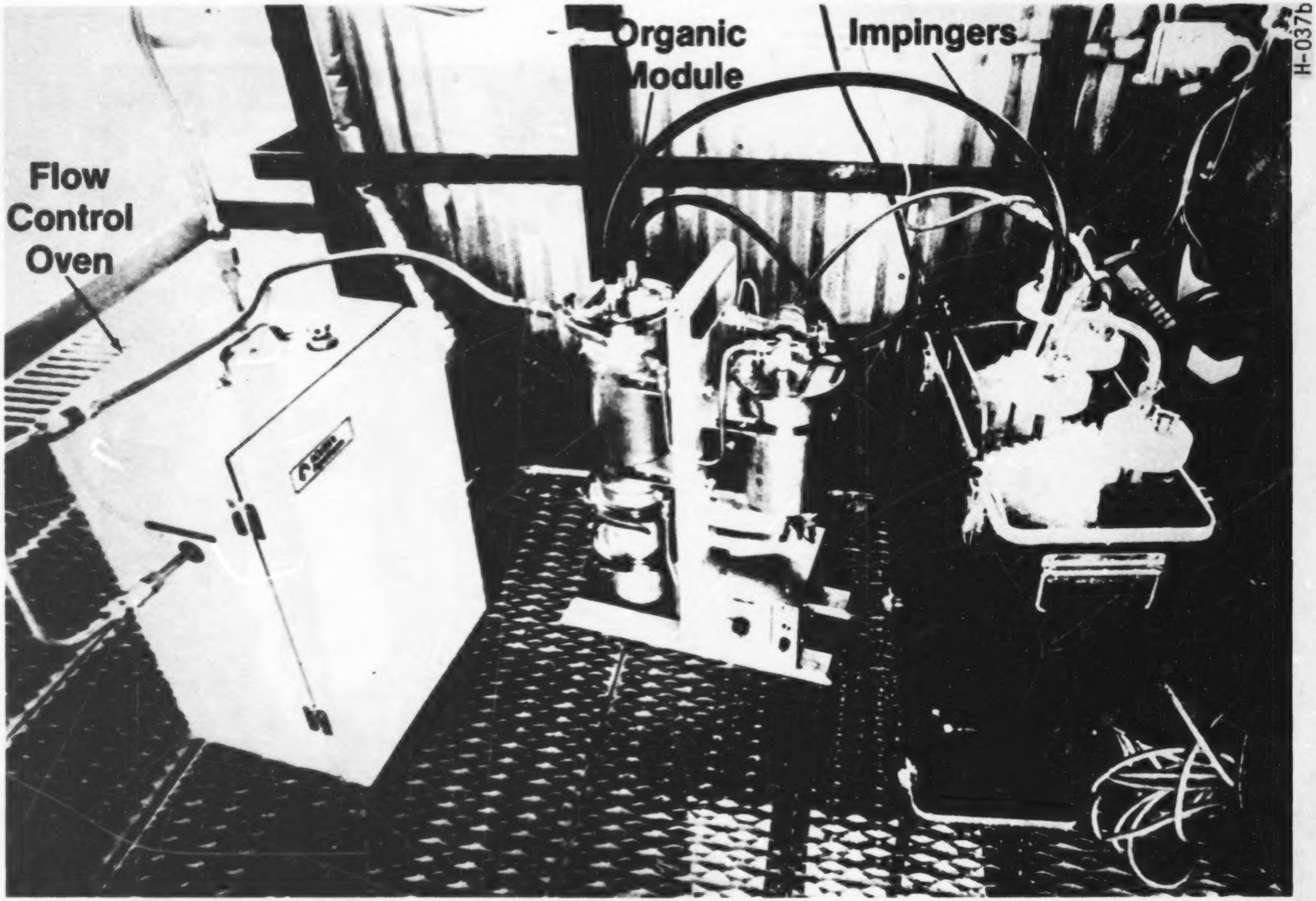
Flow Control Oven
Organic Module
Impingers
H-037b

Figure 3-7. Flow control oven and gas train.

Controls

The sampling system includes instruments for measuring conditions in the duct, gas sample, system heaters and coolant. The system also has controls for the sample flowrate, traverse drive, heaters, coolant pump, and purge gas. Most of the instrument readouts and controls are housed in the two portable control consoles, shown in Figure 3-8.

3.2 EXXON MINIPLANT TEST FACILITY

This section describes the Exxon Miniplant facility itself, and the deployment of the sampling system in the facility during the demonstration tests.

The Miniplant is a pilot scale pressurized fluidized bed combustor operated by the Exxon Research and Engineering Company in Linden, New Jersey. The PFBC process is being developed as a more efficient and cleaner method of burning coal. A sketch of the PFBC system is shown in Figure 3-9. Coal, along with limestone or dolomite which act as SO_2 sorbents, is injected into the bottom of the pressurized boiler. Coal is burned in the limestone bed which is fluidized by the incoming combustion air. Sulphur dioxide formed in the combustion process is removed by the limestone bed. Steam coils immersed in the fluidized bed remove some of the heat of combustion and maintain the bed temperature in the range of 1500°F to 1700°F. Steam thus generated operates a steam turbine. The desulphurized flue gas passes through a particulate removal system and is then expanded across a gas turbine. The particulate removal system must reduce the particulate loading down to levels sufficiently low to protect the gas turbine and meet current pollutant emission standards. The Miniplant facility does not presently include a final gas cleanup device or turbines.

The Miniplant facility consists of the combustor tower and control building. The combustor is a four-story structure, with platforms at each level. Stairways connect the platforms. A crane on the top level is available for moving large equipment. The control building includes a laboratory area.

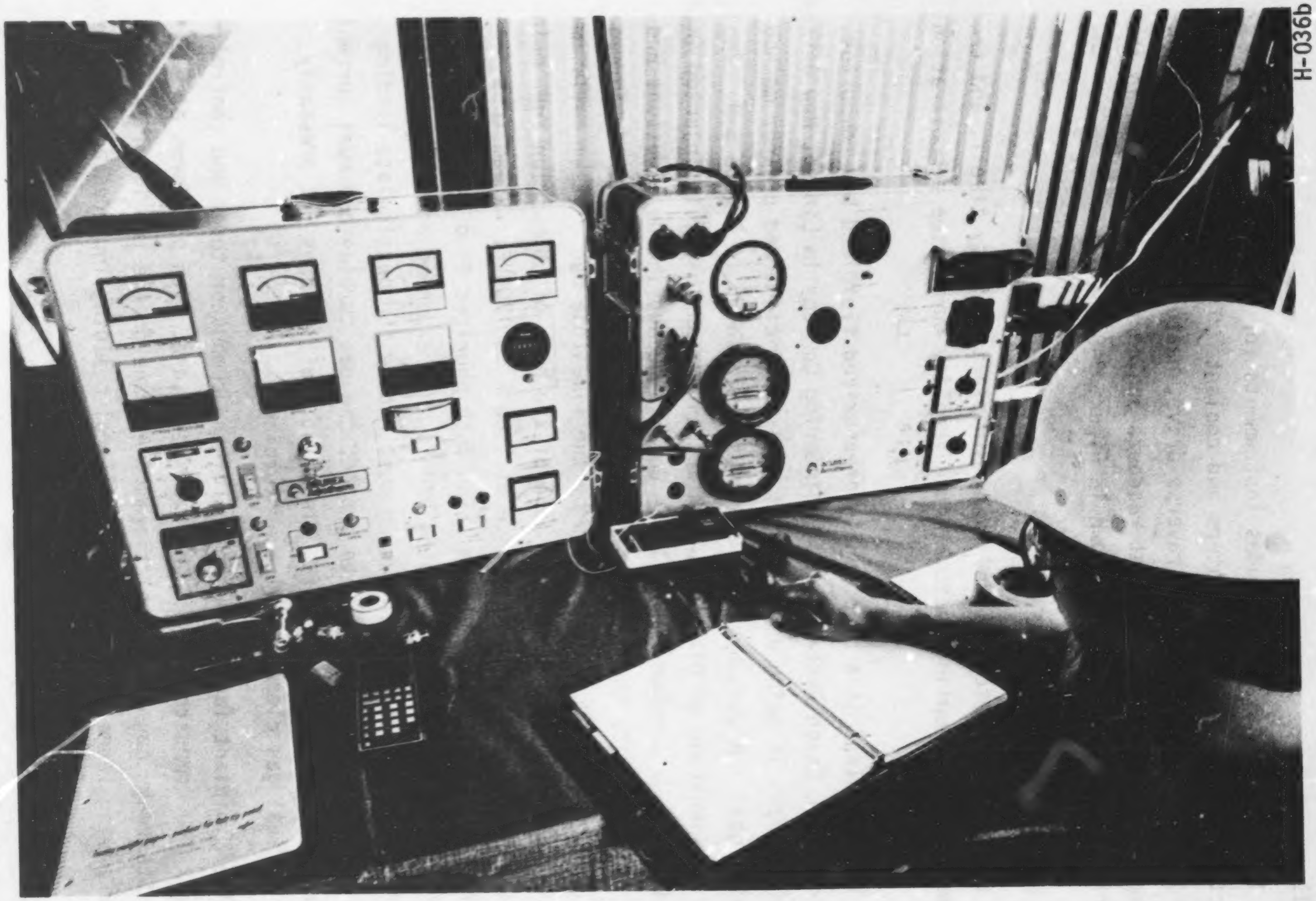

Figure 3-8. Control consoles.

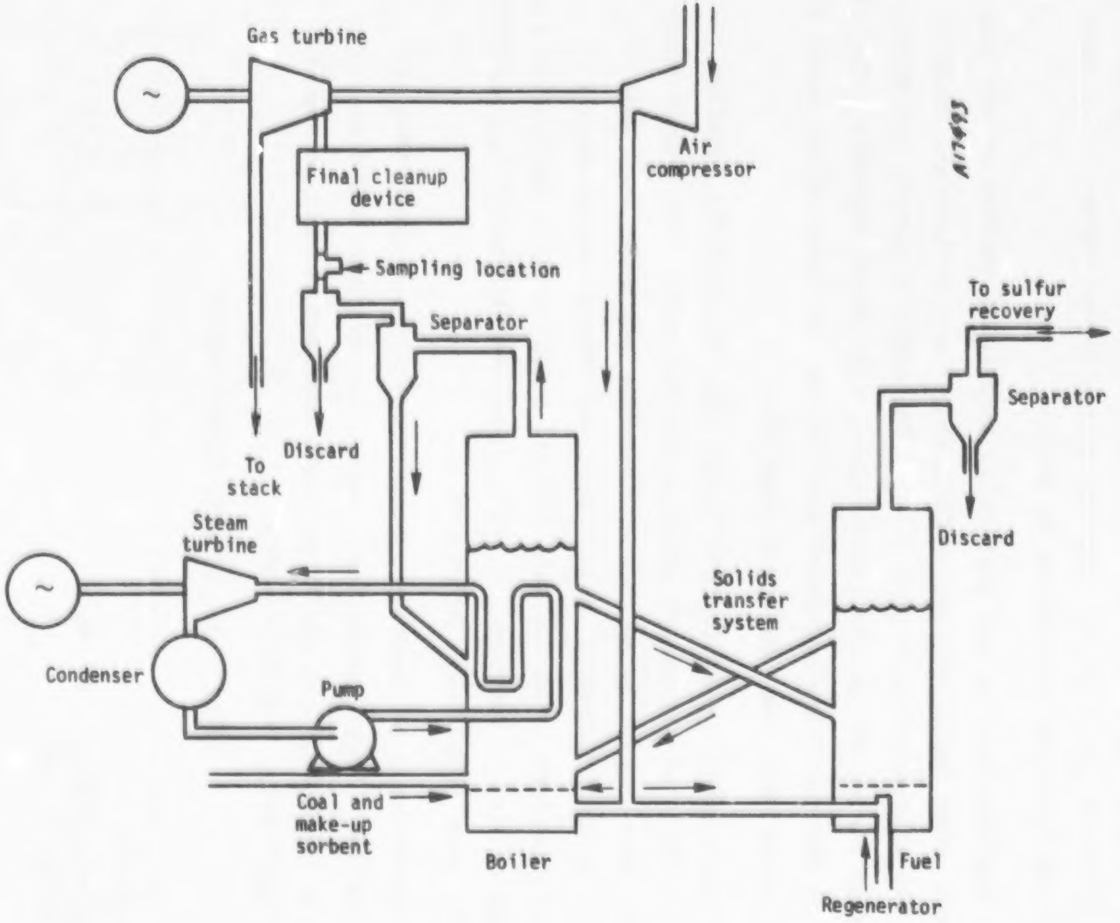
Gas turbine
Air compressor
A17495
Final cleanup device
Sampling location
Separator
To sulfur recovery
Separator
Discard
To stack
Discard
Steam turbine
Solids transfer system
Condenser
Pump
Coal and make-up sorbent
Boiler
Fuel
Regenerator

Figure 3-9. Pressurized fluidized bed coal combustor system.

For the sampler demonstration tests, the sampling location was downstream of the secondary cyclone (particulate removal device), as indicated in Figure 3-9. At this location, there is a specially constructed duct section with a sampling port. The sampling port has a 4-inch 300-pound pipe flange which interfaces with the sampling system access valves. The duct diameter at the sampling location is 10 inches.

The sampling location was physically located at the top of the combustor tower. When installed, the probe assembly was horizontal, about 4 feet above the platform (see Figure 3-10). The coolant console and hydraulic pump were also placed on the top platform, near the probe assembly. The control consoles and gas train equipment were set up one floor below, where a partial enclosure gave some weather protection.

The route between the laboratory area and the sampling location included four flights of stairs and about a 100-foot walk. The sample probe assembly was hand-carried along this route before and after each sampling run. Probe cleaning, assembly, disassembly and sample removal were all done in the laboratory. The lab facility had a scale, oven, desiccator and other equipment used in sampler preparation and sample processing. Labware and materials were supplied by Aerotherm.

The Exxon facility provided a number of utilities supporting the sampler operation. Power connections, water, and nitrogen supplies are summarized in Table 3-2. In addition, Exxon supplied technician support during equipment setup and disassembly.

TABLE 3-2. UTILITY REQUIREMENTS

Electrical:	
480 VAC, 3 phase, 40 amp	1 line
115 VAC, 15 amp	6 lines
Water:	
5 gpm, 50 psi	1 line
Purge Nitrogen:	
(flow and pressure required depending on stream conditions)	1 line
● For this test, about 2 scfm at 125 psi	

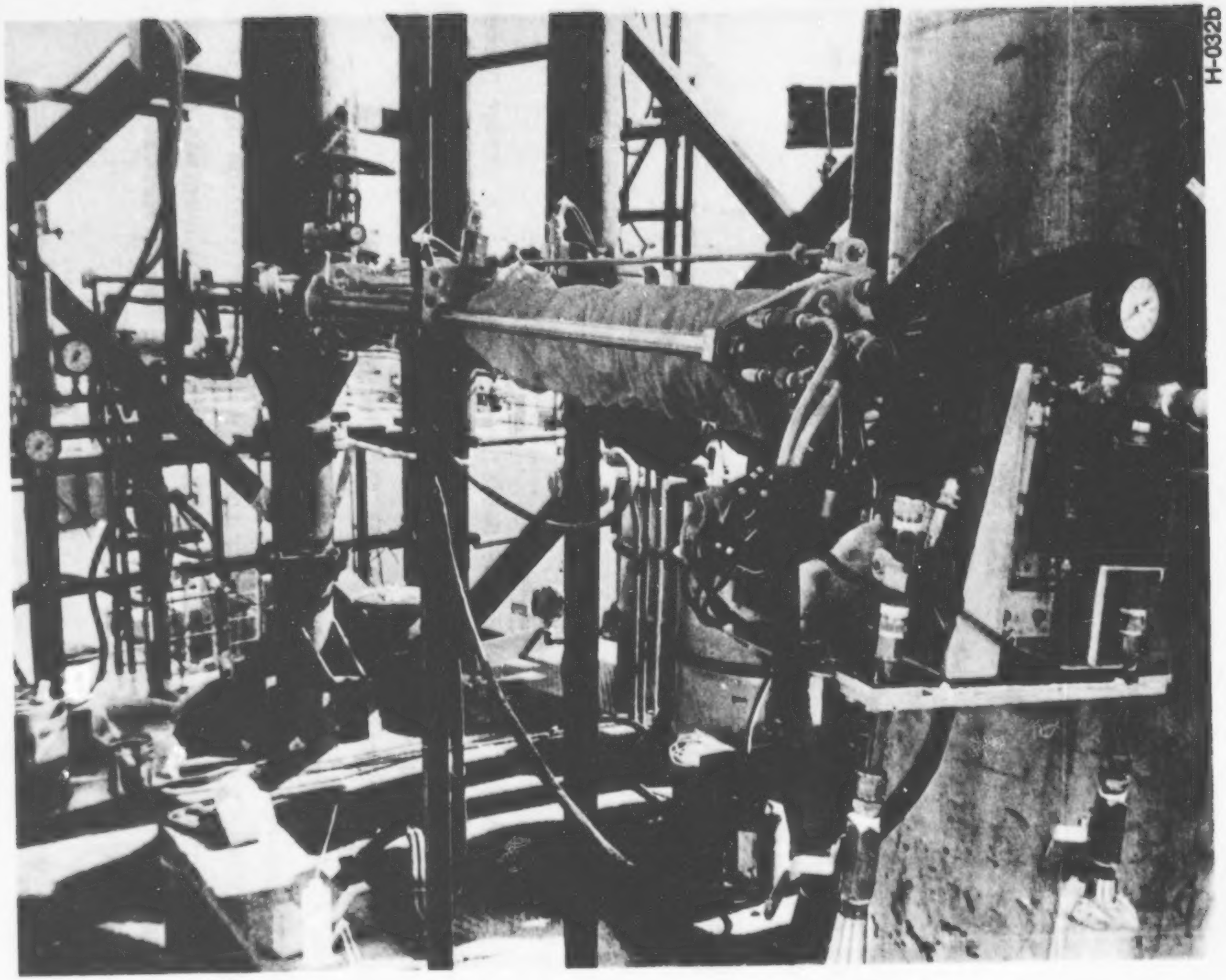

Figure 3-10. HTHP probe assembly installed at Exxon miniplant.

SECTION 4

TEST DESCRIPTION

This section describes assembly and operating procedures for the sampling equipment and some of the significant events which occurred during the test series. The narrative of events is divided into sections on: pretest activities, sampling runs, and post-test activities.

Procedures

Equipment setup and operation was done according to a formal procedure which defined proper installation of access valves and probe housing, probe setup and assembly, system preparations for testing, test sequence, shutdown and sample removal.

In several cases, we made decisions in the field to change predefined procedures. For example, the exposure and limited space on the sampling platform made impactor removal at the sampling location impractical. The entire probe was carried to the lab for disassembly.

In precleaning the sampling equipment, the procedures in the IERL-RTP Procedures Manual for Level 1 Environmental Assessment (EPA-600/2-76-160a) were followed with one exception; the nitric acid passivation of some internal surfaces of the probe, organic module and flow control oven was omitted because large acid containers were not available. Sample removal and post-test cleaning also followed Level 1 procedures.

Pretest Activities

Pretest activities included planned unpacking, setup and checkout, plus fixing several problems with the facility and sampling system. The test preparations were completed between March 22 and March 30.

Heavy equipment was installed with the help of Exxon personnel. For the nitrogen purge gas, Exxon provided a connection to the facility nitrogen supply. Exxon also assisted in making a support for the cantilevered probe housing.

First Sampling Run

For the first test run, the sampling system was set up using the thimble filter particulate collector and gas train equipment. Following preheating, the duct access valves were opened and the sampling probe inserted into the duct stream. The sample flow control valve was opened until the flow indicating orifice indicated a sample flow of 0.75 acfm at nominal particulate collector conditions. When flow conditions were established, the gas train flow control valve was opened, diverting total sample flow through the organic module and impinger train. Sampling continued for 30 minutes. Instrument readings during the test run are listed in Table 5-1. At the end of the test run, the motor driven sample flow valve was left open and the sample flow was shut off using the manual ball valve. The probe was then withdrawn and gate valves were closed. After cooldown, the probe assembly was removed. The probe and gas train were taken to the lab area for sample recovery and cleaning.

Second Test Run

For the second test run, the cascade impactor was used for particulate collection. Since this was to be a very short test with a small amount of gas sample collected, gas train equipment was not used. Based on estimated particle concentration and impactor capacity, the maximum sampling duration was estimated to be between 30 seconds and 1 minute. For this test run, 30 seconds was chosen. To achieve proper sample flow as soon as possible, the motor driven control valve was left at the same setting as the earlier filter run, and on-off control accomplished with the manual ball valve. As soon as the probe reached the in-stream position, the sample flow was started. No attempt was made to adjust flow while sampling. After 30 seconds, sample flow was stopped with the ball valve, the probe was withdrawn and access valves closed. After cooldown and probe removal, the probe assembly was carried as carefully as possible down the combustor tower stairs to the lab. There, the impactor assembly was removed, disassembled and inspected. The amount and patterns of the catch seemed to indicate normal operation of the device (see Figures 5-2 through 5-5). However, on one stage (Stage 4) the substrate shifted slightly, and on another (Stage 7) some of the jets were plugged. After sample removal and cleaning, the probe was ready to be set up for the third and final test run.

Third Test Run

The third test run also used the impactor for particulate collection and omitted the gas train equipment. Based on the lightly loaded appearance of the 30-second impactor catch from Run No. 2, we increased the duration of this run to 1 minute. The flow control method for this run was identical to Run No. 2. The manual valve was again used to start and stop sample flow, with no attempt to adjust flowrate during sampling. Again the probe was taken to the lab for disassembly and sample removal. The impactor substrates were noticeably more heavily loaded than for the 30-second impactor run (see Figures 5-6 and 5-7). With the completion of sample removal and cleaning of the sampling equipment, the testing phase was finished.

Post-Test Activities

Following test completion, sampling system hardware was packed and stored onsite at Exxon in preparation for a follow-on sampling program. Test samples were brought back to Aerotherm, where some initial analysis has been performed. The results of this evaluation are described in the following section.

SECTION 5

DATA

This section presents the detailed information collected during the test series. The section is divided into descriptions of test conditions, instrument readings, and sample properties.

Test Conditions

Plant generating conditions are listed in Table 5-1. The nominal conditions were identical for all three sampling runs. The facility ran steadily without interruption during the tests.

Instrument Readings

The sampling system includes a number of instruments which measure duct, sample and equipment operating conditions. Readings from these instruments are presented in Tables 5-2, 5-3 and 5-4.

Table 5-2 gives readings from probe assembly instruments. Duct temperature and pressure were somewhat lower than expected, at about 1360°F and 110 psig. Sample conditioning data showed that the sample gas was cooled below the desired 450°F in passing through the unheated particle collection device. In Run No. 1, with the filter collector, minimum temperature after the impactor was 225°F. Temperatures remained above the dewpoint, however (207°F for 120 psig, 6-percent water), so no water condensation occurred in these tests. Correcting the impactor heater malfunction will eliminate the low collection temperatures for future sampling.

The sample flowrate was maintained within the impactor operating range throughout the test series (0.8 to 0.9 acfm at orifice inlet conditions). This flowrate gave nozzle velocities which were considerably above duct velocity (anisokinetic). However, for the high gas temperature and

TABLE 5-1. TEST CONDITIONS

Run:	50.4 #1	50.5 #2	50.5 #3
Date	3-31-77	4-1-77	4-1-77
Time	3:30 p.m.	10:30 a.m.	2:40 p.m.
Ambient temperature	64°F	70°F	67°F
Bed Conditions			
Temperature	1650°F	1650°F	1650°F
Pressure	9 atm	9 atm	9 atm
Ca/Sulphur Ratio	1.25	1.25	1.25
Excess Air	30%	30%	30%
Coal	Champion	Champion	Champion
Dolomite	Pfzizer	Pfzizer	Pfzizer
Flowrate — scfm	544	546	546
Average Duct Velocity — ft/sec	6.7	6.3	6.7

TABLE 5-2. PROBE INSTRUMENTATION READINGS

	Time	Elapsed Time (minutes)	Stack Pressure (psig)	Stack Gas Temp. (°F)	Dowtherm Inlet Temp. (°F)	Dowtherm Exit Temp. (°F)	Sample Temp. Impactor Inlet (°F)	Sample Temp. Orifice Inlet (°F)	Sample Temp. Transport Tube Exit (°F)	Sample Flow-rate (acfm)^b	Impactor Heater Temp. (°F)	Transport Tube Heater Temp. (°F)
Run No. 1												
	3:10 p.m.	0	(125)^a	(170)	431	420	-	322	-	0	-	450
Insertion	3:22 p.m.	0	(125)^a	(190)	425	407	-	332	-	0	-	452
Sample Flow	3:32 p.m.	0	110	1360	437	435	-	332	-	0	-	450
	3:35 p.m.	0.1	109	1350	437	435	-	352	-	0.73	-	450
		5.0	110	1350	437	435	-	373	-	0.64	-	450
		10.0	110	1340	437	435	-	395	-	0.82	-	450
		15.0	109	1320	437	435	-	410	-	0.83	-	445
		20.0	110	1320	425	407	-	421	-	0.85	-	460
		25.0	110	1320	437	435	-	441	-	0.87	-	460
		30.0	110	1320	437	435	-	459	-	0.88	-	460
Shut-off		-										
Run No. 2												
Before Insert	10:30 a.m.	0	(121)^a	(195)	431	420	-	332	-	0	-	445
Sample Flow		0.5	120	1360	431	420	-	225	-	0.90	-	445
Run No. 3												
	2:58 p.m.	0	(125)^a	190	431	420	-	327	-	0	-	445
Insertion		0	111	1360			-	327	-	0	-	
Sample Flow		0		1360			-		-	0	-	
		0.33		1360			-		-	0.91	-	
		0.67		1360			-		-	0.39	-	
		0.83		1360			-		-	0.88	-	
Shut-off		1.0										

T-395

TABLE 5-3. GAS TRAIN INSTRUMENT READINGS

T-396

	Time	Elapsed Time	Flow-rate (acfm)	Transport Line Temp. (°F)	Flow Control Oven Temp. (°F)	Organic Module Temp. (°F)	Impinger Train Temp. (°F)	Ambient Temp. (°F)
Run No. 1			1[a]					
	3:10 p.m.	0	0	444	449	58	70	65
	3:22 p.m.	0	0	453	-	-	-	
	3:32 p.m.	0	0	-	-	-	-	
Start Flow		0	0.73	-	-	-	-	
		5.0	0.64	449	396	70	69	64
		10.0	0.82	449	425	72	69	65
		15.0	0.83	447	458	74	70	67
		20.0	0.85	447	454	75	71	67
		25.0	0.87	456	446	76	73	65
Stop Flow		27.65	0.88	450	444	75	73	66

[a] At orifice conditions — see Table 4-2.

TABLE 5-4. ANISOKINETIC CORRECTION FACTORS

Run	Sample Flowrate (acfm)	Nozzle Velocity (ft/sec)	Estimated Duct Velocity (ft/sec)	Velocity Ratio	Particle Concentration[a] Correction Factor $\frac{C_{measured}}{C_{true}}$
1	0.85	9.3	6.7	0.72	0.99
2	0.90	13.0	6.3	0.48	0.98
3	0.90	11.3	6.7	0.59	0.99

[a] Calculation per method in Handbook of Aerosols, TID-26608, 1976, Section 5.1-1 and Figure 5-2.

pressure, fine particles and low velocities involved, the variance from isokinetic conditions has an insignificant effect on measured particulate concentration. A comparison of duct and sampling velocities and the calculated correction factors for anisokinetic conditions is presented in Table 5-4. As shown, the measured particulate concentrations are within 1 or 2 percent of isokinetic measurements.

Table 5-3 lists the instrument readings from the gas sampling equipment used during Run No. 1. Gas sample flow was started shortly after particulate sampling began, so the total elapsed time is less than shown in Table 5-2. During gas sampling, all sample flow was diverted to the gas train, so the flowrates given for the gas train are the same as those through the particulate collector. The temperature readings show that all gas train components were operating correctly.

During the test series, we measured the surface temperatures of the access port, valves and probe housing. These readings are presented in Table 4-5. The valve surface temperature remained below 258°F at all times. Accessible surfaces of the probe housing also remained cool, below 167°F.

Sample Properties

The tests produced data on particulate concentration, size distribution, appearance and chemical composition, and on moisture content. The organic and trace metals samples have not yet been analyzed, so this report contains no data on these constituents.

The measured particle concentrations are listed in Table 5-6. The values of 0.43 to 0.64 grain/scf are reasonable compared to other measurements made in unpressurized portions of the Exxon process. These have ranged from 0.2 to 1.2 grain/scf. The 0.64 grain/scf value from the 30-minute sample is the most accurate measurement from our tests. It comes from the largest sample and best defined conditions.

The moisture content measured in Run 1 was 6.2 percent by volume. This compares well with Exxon's preliminary estimate of 5.8 percent.

TABLE 5-5. STRUCTURE TEMPERATURES

Pretest (11:00 a.m., 3-30-77)

Duct Wall	349°F
Nozzle Cylinder	
Top	294°F
Side	280°F
Bottom	189°F
Valve — Duct Side	
Top	258°F
Side	220°F
Bottom	195°F

Run No. 1 (3:30 p.m., 3-31-77)

Time	Valve — Probe Side	Inner Probe Housing	Outer Probe Housing
0	147	133	133
10 min	159	131	154
20 min	157	133	167
60 min	190		

TABLE 5-6. PARTICULATE CONTENT

	Run #1	Run #2	Run #3
Date:	3-31-77	4-1-77	4-1-77
Time:	3:30 p.m.	10:30 a.m.	3:00 p.m.
Particle Catch: (grams)			
Filter	3.2515	—	—
Impactor	—	0.0554	0.0892
Residue	1.8565	0.0334	0.0595
Total	5.108	0.0884	0.1497
Sample Volume: (scf)	122.5	3.13	5.03
Particle Content: (grain/scf)	0.64	0.43	0.46
Particle Content: (gr/scf) (Anisokinetic Correction Applied)	0.65	0.44	0.47

Particle size distribution information is presented in Figure 5-1 and Table 5-7. As shown, there is some difference in the results from the two impactor runs. However, both show that most of the particulate falls within the 1 to 10 micrometer range.

The impactor substrates are shown in Figures 5-2 through 5-7. Generally, the patterns are typical of normal impactor operation. Stage 7, however, shows evidence of several plugged jets. A comparison of Figures 5-6 and 5-7 show the differences in particulate loading for substrates from Run 2 and Run 3. Run 2 substrates were lightly loaded, while those from the longer duration Run 3 showed heavy, three-dimensional deposits.

The particulate sample from Run 2 were photographed using a scanning electron microscope (see Figures 5-8 through 5-11). The particulate is irregular in appearance, suggesting that it may be calcium sulphate crystals from the dolomite bed and ash from low-temperature combustion. Some of the photos show congealed masses of particles. The cause of this phenomena could be any of the following: a property of the collected particulate, condensation on the particulate or the conductive spray applied to the sample for SEM photography.

The chemical composition of collected particulate was analyzed by dispersive X-ray fluorescence analyzer. Spectra of X-ray emissions are shown in Figure 5-12. The analysis shows detectable amounts of aluminum, silicon, calcium, sulphur, iron, potassium, titanium and copper.

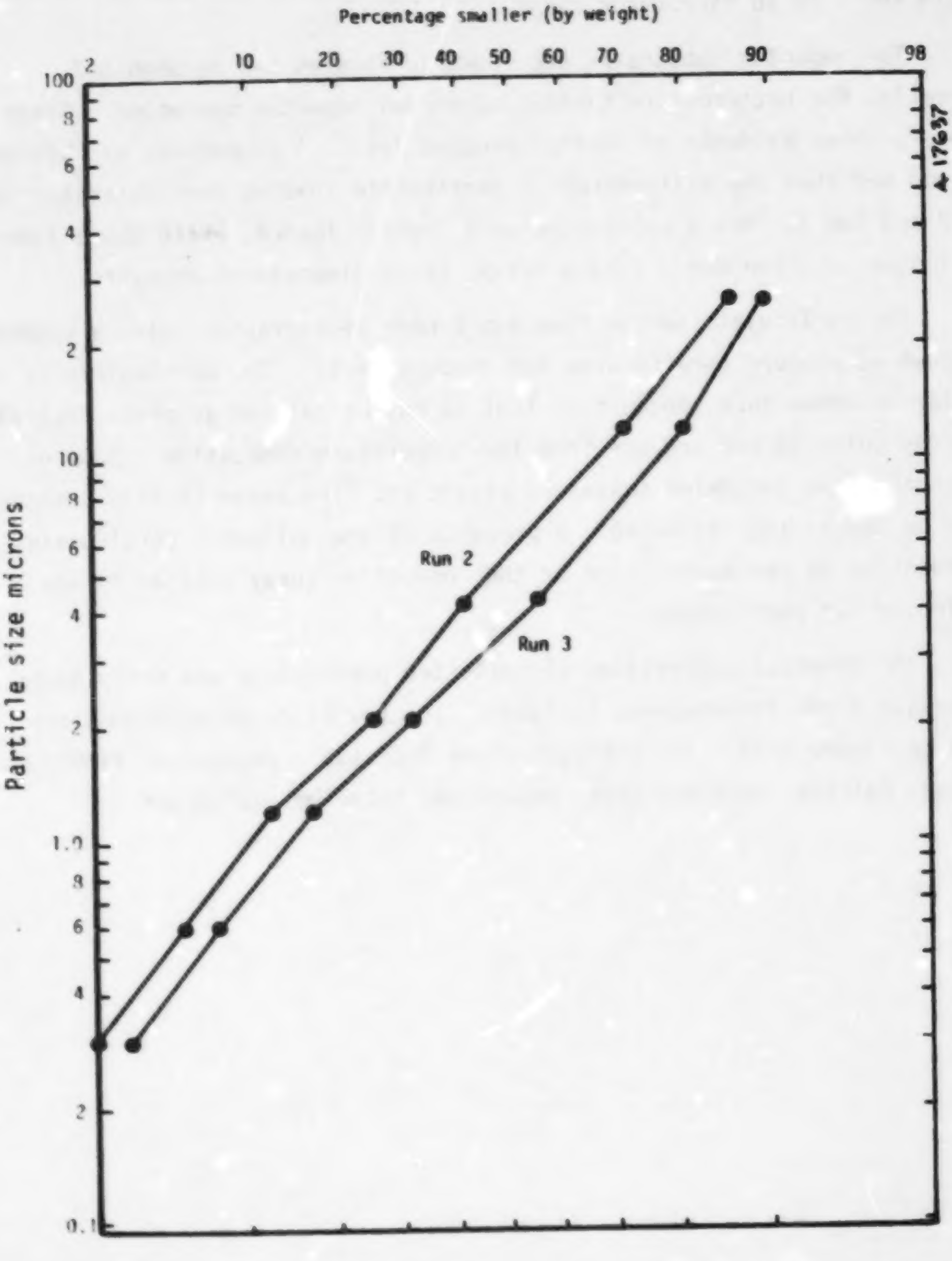

Figure 5-1. Particle size distribution.

TABLE 5-7. PARTICLE SIZE DISTRIBUTION

Stage	D_{50} Microns	Run #2			Run #3		
		Weight Collected	% Total Weight	% Smaller	Weight Collected	% Total Weight	% Smaller
1	26.0	0.0076	13.7	86.3	0.0093	10.4	89.6
2	12.0	0.0080	14.4	71.8	0.008	9.0	80.6
3	4.3	0.0171	30.9	41.0	0.0221	24.8	55.0
4	2.1	0.0139	25.1	15.9	0.0215	24.1	31.7
5	1.2	0.0022	4.0	12.0	0.0135	15.1	16.6
6	0.6	0.0036	6.5	5.4	0.0081	9.1	7.5
7	0.3	0.0020	3.6	1.8	0.0039	4.4	3.1
Filter		0.0010	1.8		0.0028	3.1	
		0.0554 grams			0.0892 grams		

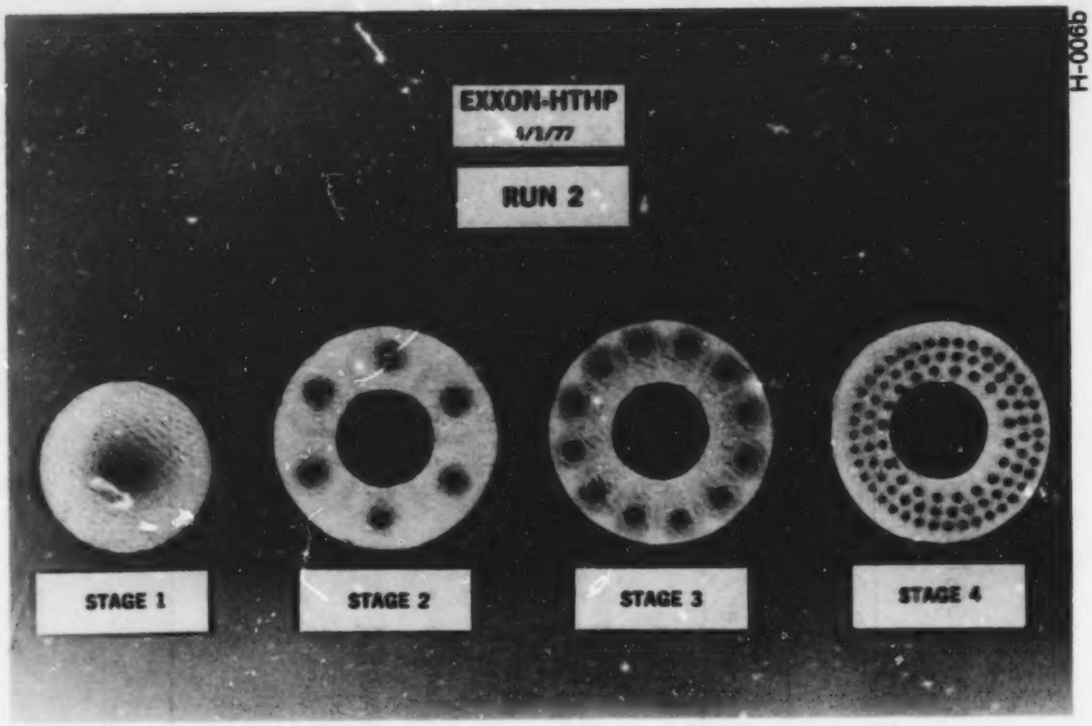
H-006b
EXXON-HTHP
4/1/77
RUN 2
STAGE 1
STAGE 2
STAGE 3
STAGE 4

Figure 5-2. Impactor substrates.

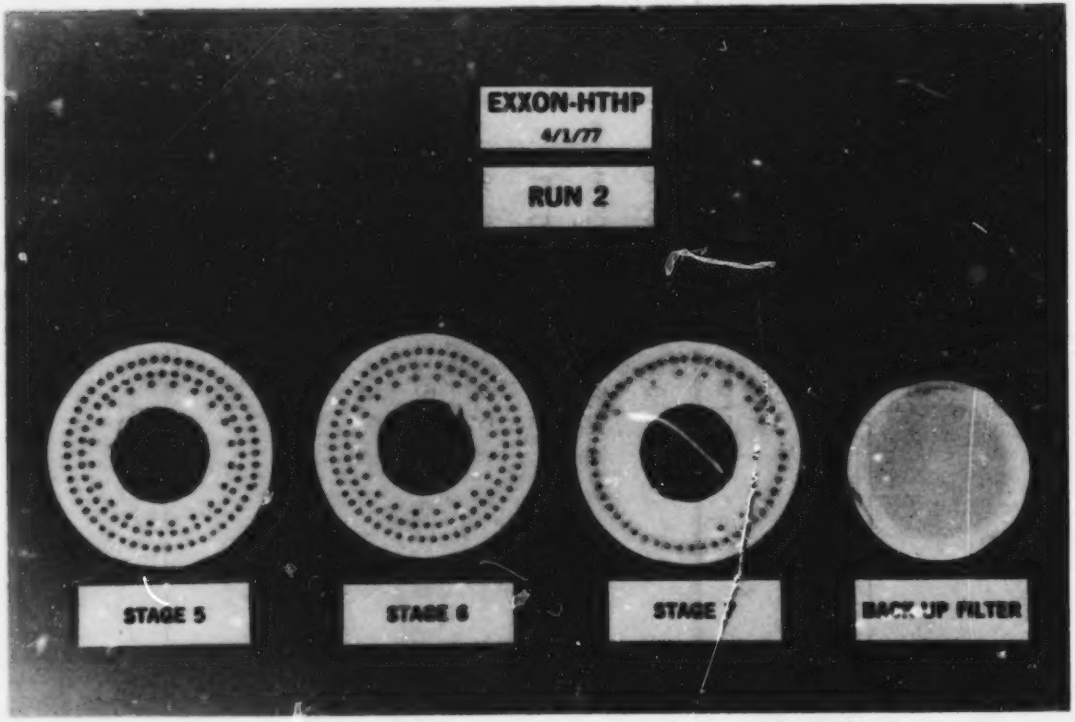
EXXON-HTHP
4/1/77
RUN 2
STAGE 5
STAGE 6
STAGE 7
BACK UP FILTER

Figure 5-3. Impactor substrates.

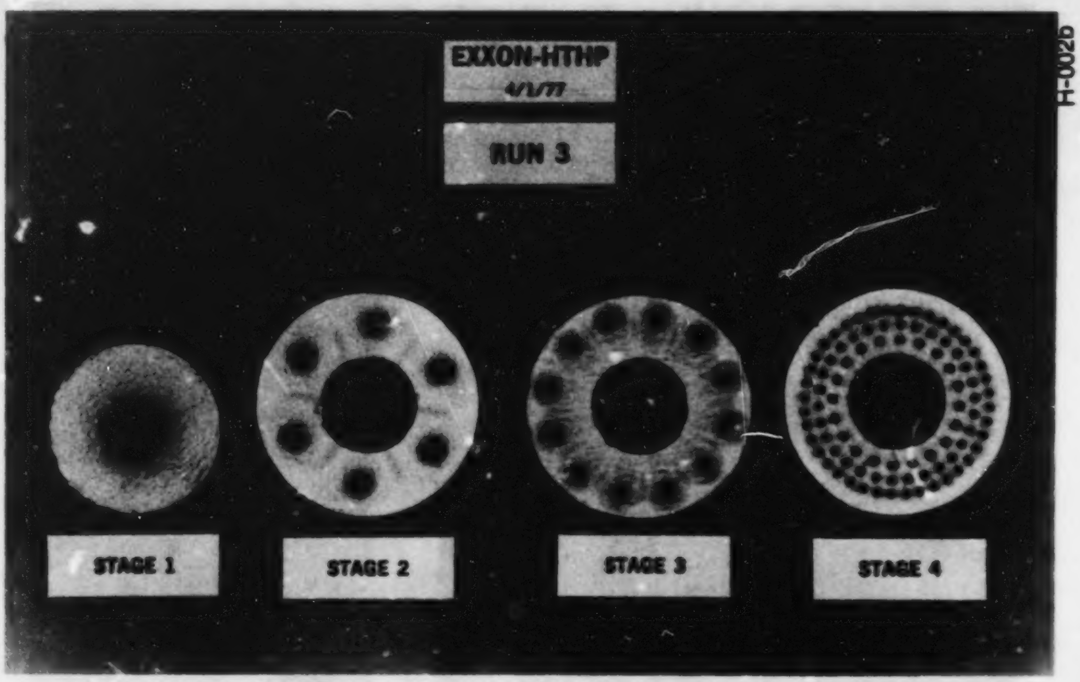
EXXON-HTHP
4/1/77
RUN 3
H-0026
STAGE 1
STAGE 2
STAGE 3
STAGE 4

Figure 5-4. Impactor substrates.

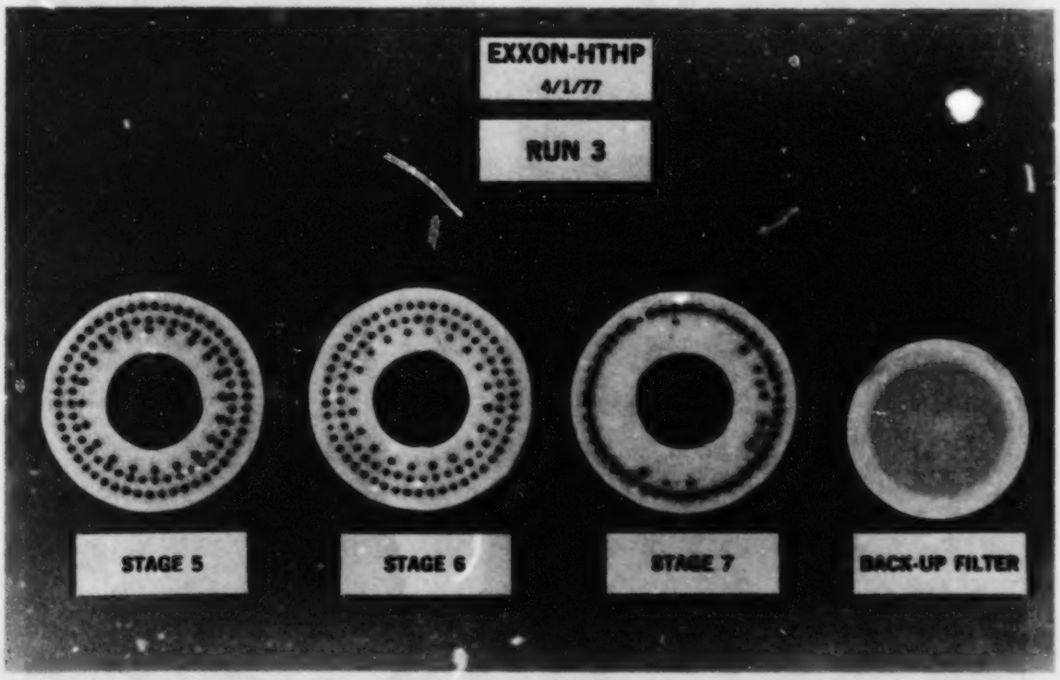
EXXON-HTHP
4/1/77
RUN 3
STAGE 5
STAGE 6
STAGE 7
BACK-UP FILTER

Figure 5-5. Impactor substrates.

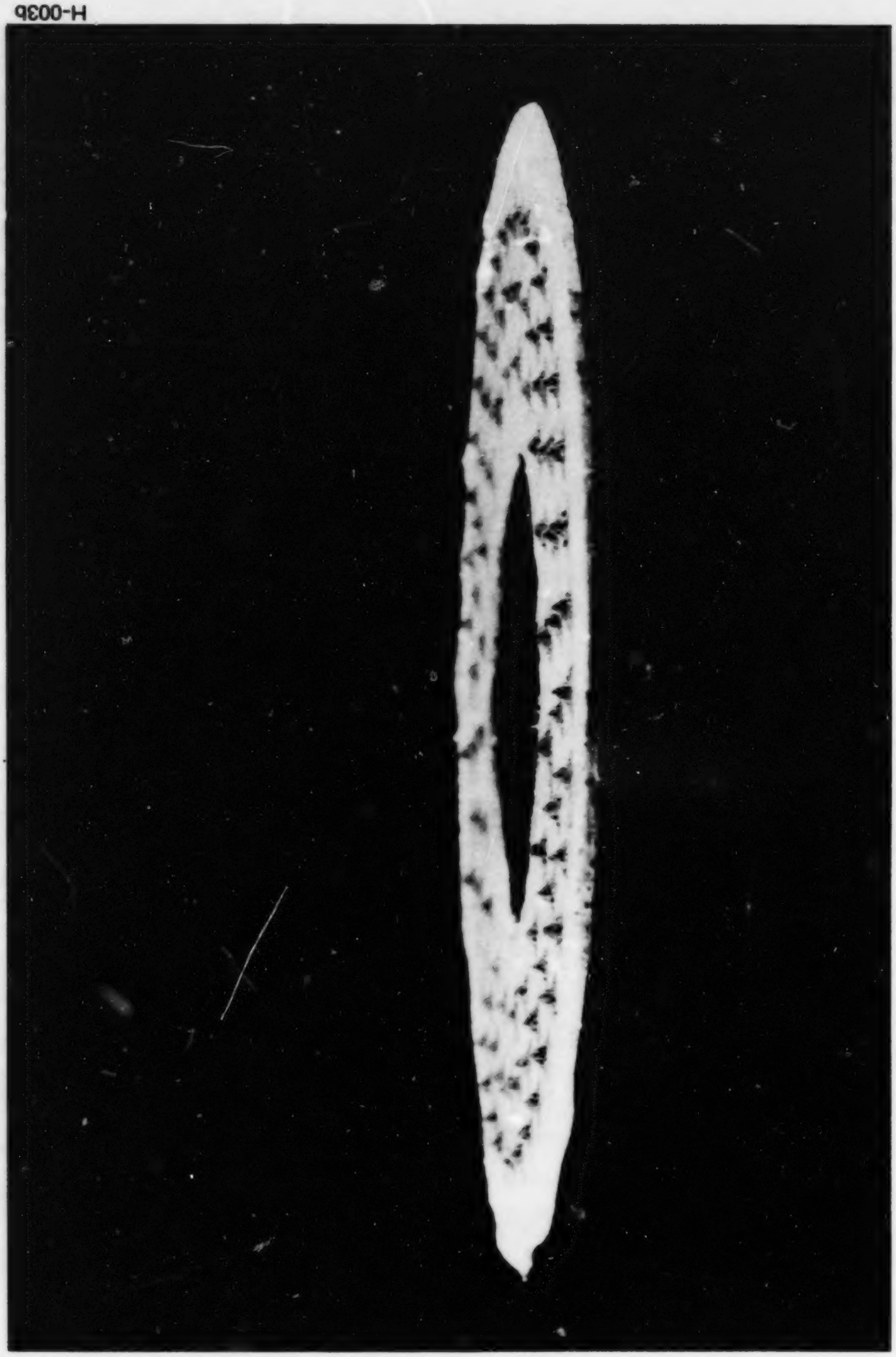

Figure 5-6. Impactor substrate Run 3, Stage 5.

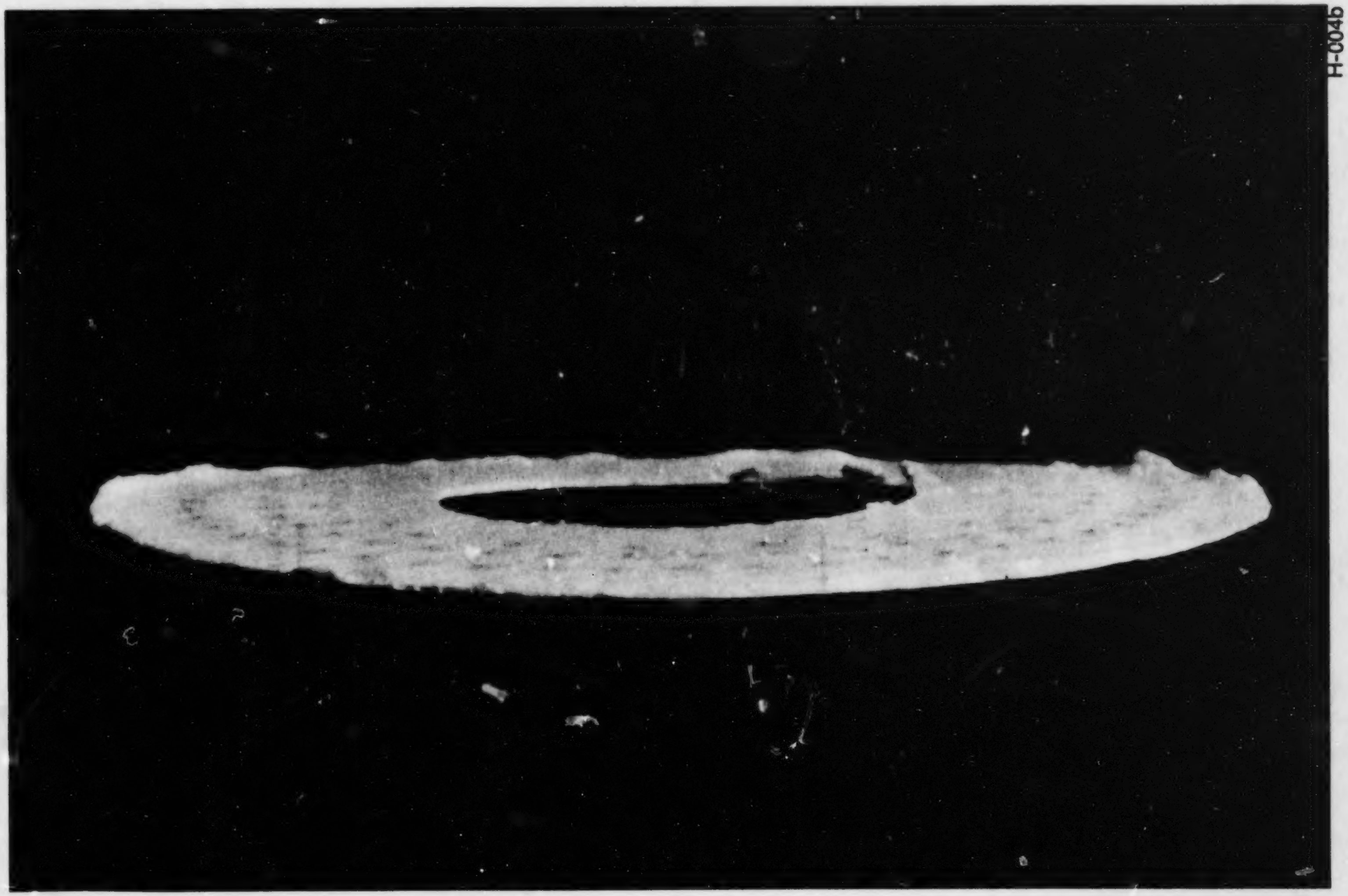

Figure 5-7. Impactor substrate Rune 2, Stage 5.

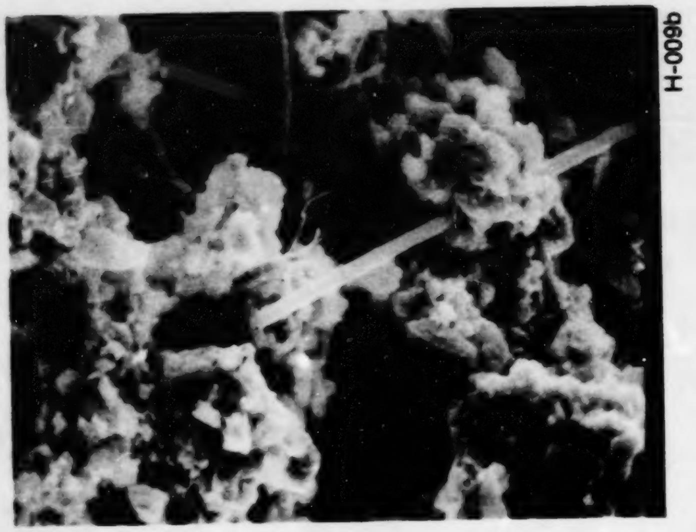

1000X
10 Microns

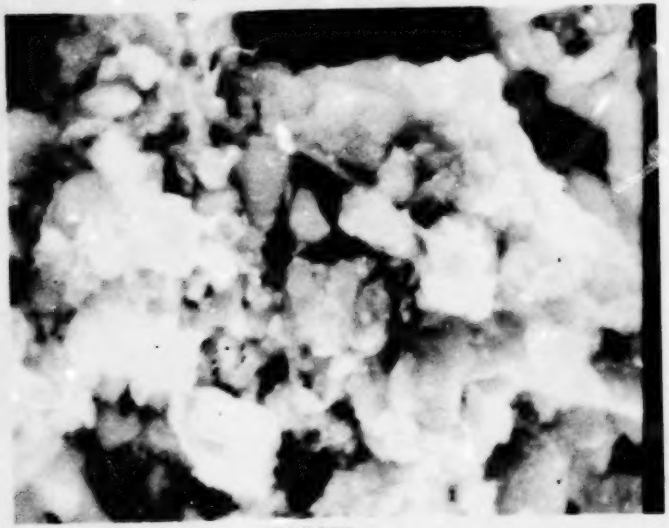

3000X
3 Microns

Figure 5-8. Particle photomicrographs Stage 1.

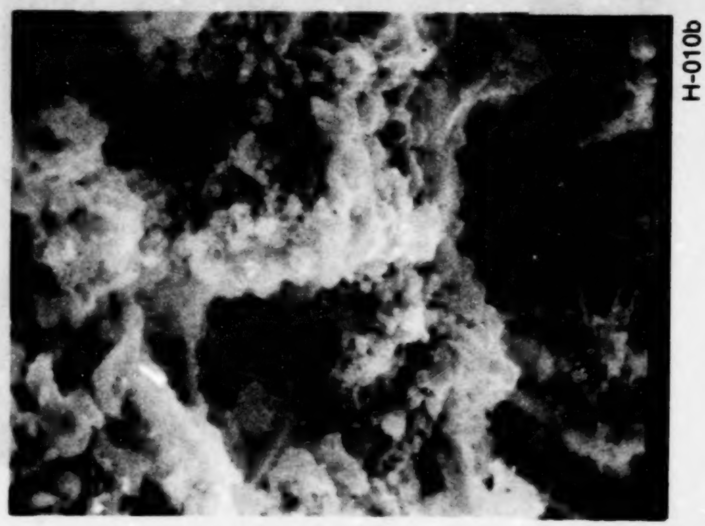

1000X

⊢—⊣ 10 Microns

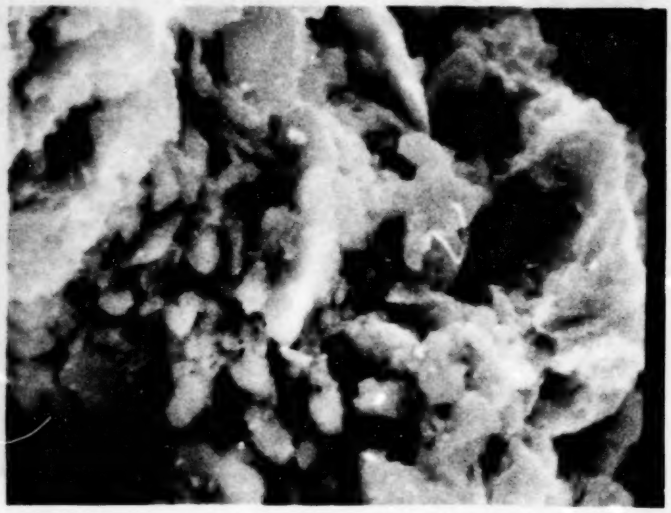

3000X

⊢—⊣ 3 Microns

Figure 5-9. Particle photomicrographs Stage 2.

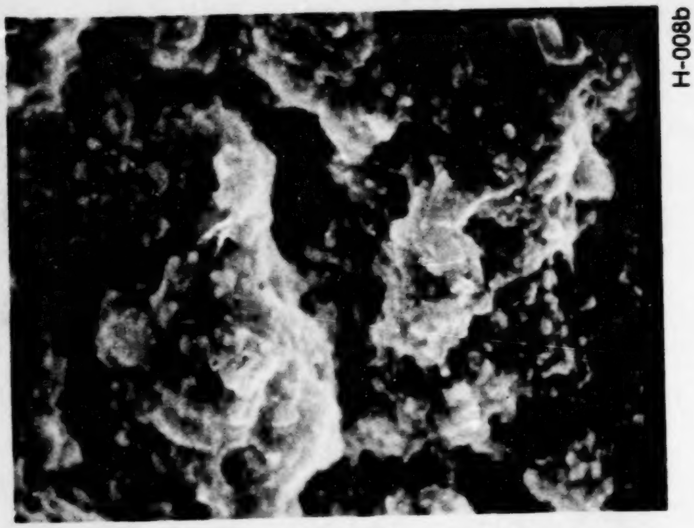

1000X

⊢—⊣ 10 microns

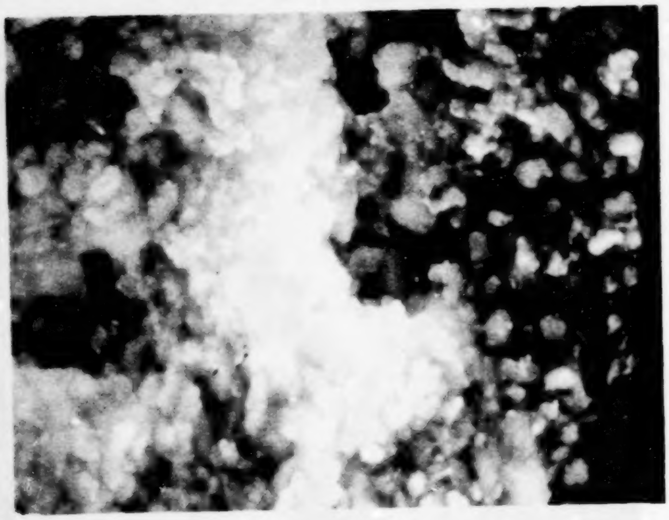

3000X

⊢—⊣ 3 microns

Figure 5-10. Particle photomicrographs Stage 4.

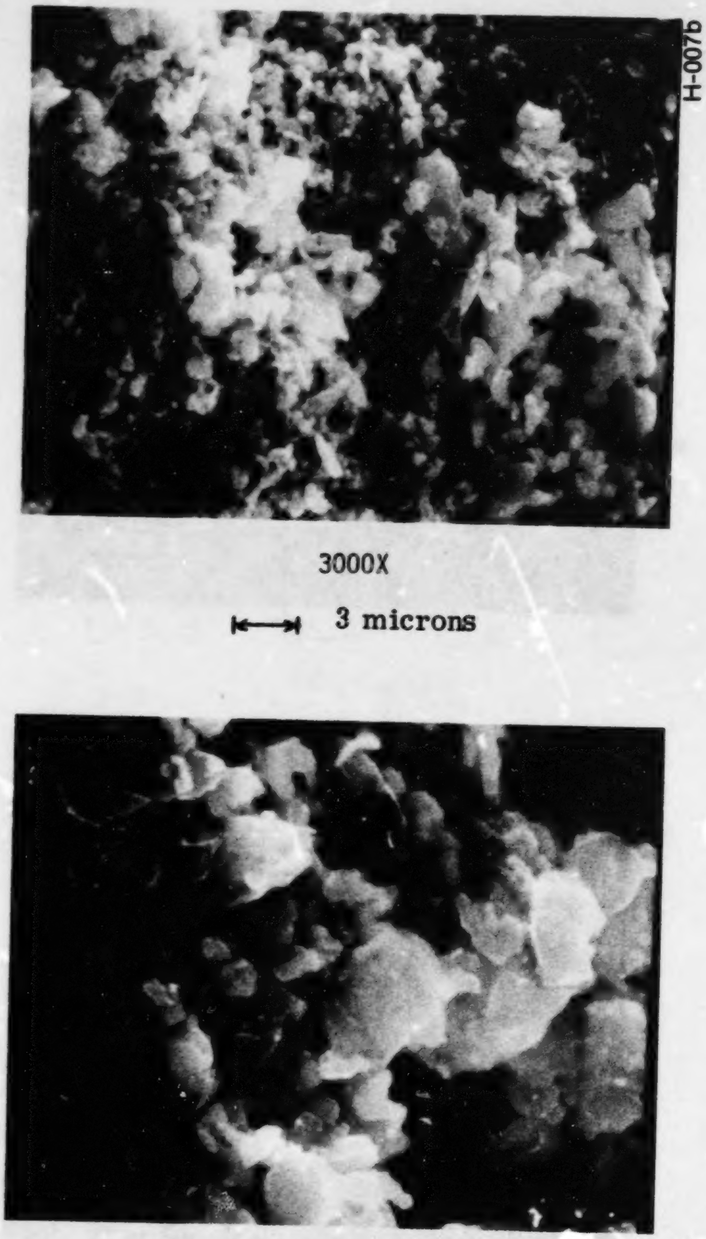

3000X

3 microns

10000X

1 micron

Figure 5-11. Particle photomicrographs Stage 6.

H-005b

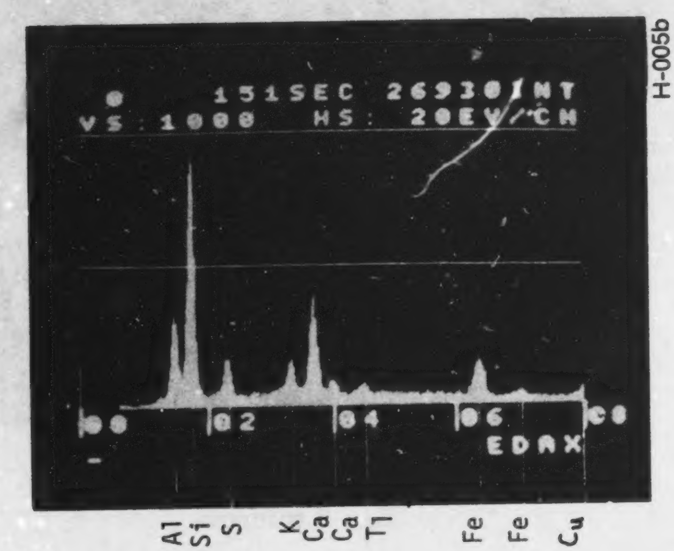

Stage 1, Run 2

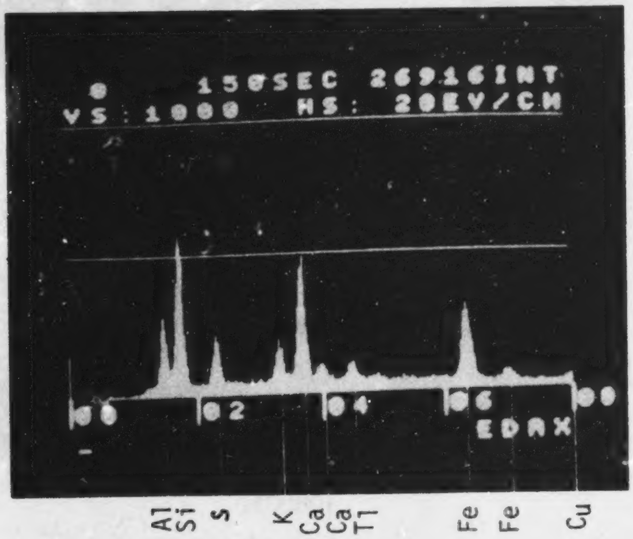

Stage 6, Run 2

Figure 5-12. Particle chemical composition.

Appendix E

Acurex Corporation/Aerotherm Division

March 1977

Aerotherm Project 7237

IERL-CRB SAMPLING MANUAL FOR LEVEL 1 ENVIRONMENTAL ASSESSMENT

AEROTHERM REPORT TM-77-160

Prepared for

EPA Project Officer: William B. Kuykendal

Industrial Environmental Research Laboratory
U.S. Environmental Protection Agency
Research Triangle Park, North Carolina 27711

Contract 68-02-2153
Task 03

INTRODUCTION

This sampling procedures manual has been prepared for the Process Measurements Branch of the Industrial Environmental Research Laboratory, EPA. The procedures that are described apply to Level 1 environmental assessment of combustion facilities located at Research Triangle Park, North Carolina.

Under the present assessment program, only combustion facilities are considered. It is anticipated, however, that future needs will arise for extension of sampling equipment and analysis techniques to noncombustion facilities as well. This manual deals with flue gas and influent fuel stream sampling for specific combustion facilities. Sampling includes stack gases and vapors, stack gases that contain particulate, and liquid fuels. Other Level 1 sampling requirements (fugitive emissions, slurries, and solids) are not of concern here.

The approach to Level 1 environmental assessment sampling consists of five functions:

1. Test planning
2. Preparation of sampling systems
3. Obtaining the samples
4. Recovery of the samples from sampling equipment
5. Data reduction

Each of these functions is described in a separate section of this manual. At the end of Sections 1 to 4, an outline of the procedures to be used during that phase of the assessment is provided for the operator's use.

Completion of the sampling procedures provides contained samples ready for analytical evaluation. Analysis procedures to be performed in the IERL Level 1 EA laboratory are provided under a separate manual prepared by A. D. Little, Inc. (Reference 1).

For reference, a list of the IERL-CRB combustion research facilities is given below.

- Aerotherm experimental furnace

- Residential furnaces (two)
- Avco and North American firetube boilers
- Caterpillar diesel engine
- Dynamic Science Unit — model package boiler
- Solar gas turbine

Table 1 briefly describes each facility and its sampling conditions.

TABLE 1. IERL-CRB COMBUSTION RESEARCH FACILITIES

Facility	Description	Stack/Port Characteristics	Stack Gas Properties
1. Aerotherm Experimental Furnace	280,000 Btu/hr capacity Fuels: oil, natural gas, methanol Primary and secondary air systems Exhaust gas recirculation system Tube heat exchanger for cooling of exhaust gases	8" stack — has an elbow above mezzanine level and runs horizontally into a blower. Sample ports located in insulated horizontal section	400°F to 500°F Slight positive or negative pressure Velocity: 80 to 260 fpm
2. Residential Furnaces (2)	Oil- or gas-fired home heaters. Furnaces change periodically, attaching to permanent stacks	6" galvanized stacks, uninsulated, sampled 3' above mezzanine level A damper is provided above the sample location in each stack for draft	250°F to 600°F Slight negative pressure Velocity: 100 to 325 fpm
3. Avco and North American firetube boilers	2 to 2.5 million Btu/hr Fuels: #2 oil, natural gas Steam recycled by tube heat exchangers	14" stacks, insulated Avco unit has sample port ~3' above mezzanine level. North American unit has offset in stack above mezzanine — sample port located near mezzanine level downstream of offset	250°F to 600°F Slight positive pressure Small fluctuations may occur due to flame instabilities Velocity: 450 to 850 fpm
4. Caterpillar Diesel Engine (D334)	Precombustion chamber design with supercharge Speed: 1,800 rpm Used for power generation Electrical power converted to heat Located exterior to Wing G with full weather housing	12" stack, straight pipe attached to horizontal engine muffler Sample location ~3' above mezzanine	300°F to 900°F Slight positive pressure Velocity: 500 to 3,000 fpm
5. Dynamic Science Unit Model Package Boiler	4 million Btu/hr with #2 or #6 oil or natural gas, Dowtherm heat exchange system Exhaust gas recirculation system	15" SST stack with surrounding protection cage Sample locations are above EGR entrance into stack	900°F to 1,500°F Slight positive pressure with some flame-induced pulsations Velocity: 650 to 1,000 fpm
6. Solar Gas Turbine	Dual impeller design for power generation Electric power converted to heat for discharge Located exterior to Wing G with full weather housing	16" stack, lower half included in unit housing Contains muffler Sample locations are ~3' above mezzanine	500°F to 1,000°F Slight positive pressure Velocity: 6,000 to 14,000 fpm

TABLE OF CONTENTS

Section Page

1 SAMPLE PLANNING E-1

1.1 Personnel Training E-1
1.2 Identification of Safety Requirements E-2
1.3 Identification of Test Conditions and Data Requirements E-3
1.4 Sample Schedule and Manpower Requirements E-4

2 SAMPLE SYSTEM PREPARATION E-6

2.1 Source Assessment Sampling System E-6
2.2 Gas Grab Sampler E-12
2.3 Continuous Gas Analysis E-14
2.4 Liquid Fuel Sampling E-15

3 SAMPLING E-17

3.1 Sampling with the SASS Train E-17
3.2 Gaseous Grab Sampling E-24
3.3 Liquid Fuel Sampling E-27

4 SAMPLE RECOVERY E-30

4.1 SASS Train Breakdown E-30
4.2 Sample Extraction E-30
4.3 System Cleanup and Reassembly E-31

5 DATA REDUCTION E-33

REFERENCES E-34

APPENDIX A – SAMPLE DATA SHEETS E-35

APPENDIX B – LIST OF SAMPLING EQUIPMENT E-42

LIST OF ILLUSTRATIONS

Figure Page

1 Sample Planning Procedures E-5

2 Source Assessment Sampling System (SASS) E-7

3 Liquid Cooled Sampling Probe E-9

4 Probe Coolant System Schematic E-10

5 Grab Sample Probe E-13

6 System Preparation Procedures E-16

7 SASS Sample Port with Gate Valve E-20

8 Residential Furnace SASS Sample Port E-21

9 CRB Combustion Facility Stack Velocities E-22

10 Gas Grab Sample Port with Ball Value E-25

11 Residential Furnace Gas Grab Sample Port E-26

12 Sampling Procedures E-28

13 Sample Recovery E-32

SECTION 1

SAMPLE PLANNING

Planning an environmental assessment must assure that a representative sample is extracted from the process stream and provided to the EA laboratory for analysis. It is the intent of sample planning to identify the procedures that are to be followed in obtaining specific emission data, provide familiarity with sampling equipment and process operating conditions, and to identify potential sampling problems that may be encountered during the test. Coordination with laboratory personnel to identify sample container and analysis time requirements during the planning stage will facilitate procedures during the sampling period.

1.1 PERSONNEL TRAINING

An important step in planning an environmental assessment is to familiarize all involved personnel with Level 1 sampling and analysis procedures. These procedures are documented in Reference 2. For specific application of sampling procedures to combustion facilities at RTP, particular attention should be directed to Chapters 1, 2, 3, and 5 which address overall Level 1 sampling strategy for gaseous, particulate, and liquid phase sampling.

The Level 1 EA Procedures Manual also describes sampling equipment with which personnel must be thoroughly familiarized prior to testing. Hardware of specific interest includes: (1) the Source Assessment Sampling System (SASS) for collection of particulate, trace elements, and organic compounds, (2) a grab sampler system which collects gaseous phase emissions for subsequent analysis by gas chromatography, and (3) equipment required for collection of liquid fuel samples. Conceptual descriptions of each type of sample hardware are presented. In addition, continuous gas analyzers may be used for environmental assessment of specific gas species that are not routinely analyzed by gas chromatography in the Level 1 laboratory.

Specific hardware description for the SASS is presented in Reference 3. Assembly, setup, disassembly, transport, and operation of the SASS must be totally familiar to all sampling personnel.

Since details of the gas grab and liquid fuel sample systems are not provided in other documents, a brief description of each is presented in Section 2 of this manual.

1.2 IDENTIFICATION OF SAFETY REQUIREMENTS

Safety precautions to be exercised in the use of the Level 1 sampling systems are stated in Section 3 of this manual. Potential hazards exist due to the high temperatures within and surrounding the combustion facility effluent stacks. Proper use of all sampling equipment at each of the sampling sites will provide safe working conditions. Procedures for working in the high-bay area should be followed explicitly.

NOTE

If the sampling operator feels that all safety requirements have not been satisfied for all personnel involved, it is his obligation to discontinue all sampling procedures until the unsafe condition is corrected.

1.3 IDENTIFICATION OF TEST CONDITIONS AND DATA REQUIREMENTS

The identification of test conditions can facilitate sampling procedures by providing the operator with knowledge of probable stack conditions. The variables that should be identified by the combustion facility operator for the sampling crew include:

- Fuel type and consumption rate
- Stoichiometry
- Changes in test configuration that may affect sampling operations
- Changes in operating conditions that may affect sampling results
- Period of operation

In many instances, stack conditions can be calculated or approximated from past test experience. Pretest knowledge of stack temperature and velocity are of particular value to the sampling crew. Moisture content, gas composition, and particulate content of the combustion gases are also of interest prior to testing as considerable preliminary sampling effort can be saved when these variables do not have to be specifically measured.

Specific data requirements for a Level 1 environmental assessment are subject to EPA objectives and formulated during the test planning stage. In general, data pertinent to the CRB combustion facilities will include analyses for:

- Collected SASS samples
    - Particulate
    - Trace elements
    - Organic compounds

- Stack gases
    - General inorganic combustion species (CO, CO_2, O_2, NO_x, H_2O, etc.)
    - Sulfur compounds
    - Light hydrocarbon species (C_1 to C_6 hydrocarbons)
- Influent liquid fuel streams

The sampling operator should formulate test objectives and requirements with the facility manager during test planning. He must also be familiar with the analysis techniques applicable to each sample type, such that valid samples can be provided to the laboratory. Refer to Chapters 7 to 10 of Reference 2 for details of analysis techniques.

Sampling system data must be taken by the crew during operation of the systems. SASS data requirements include periodic recording of the control module readouts:

- Pitot tube pressure differential
- Orifice flow pressure differential
- Initial and final gas meter readings
- Sample elapsed time
- Stack temperature
- Gas cooler temperature
- Impinger outlet temperature
- Oven temperature
- Inlet and outlet gas meter temperatures
- Probe coolant temperatures
- Pump vacuum

Continuous and grab gas and liquid fuel sampling require records of:

- Sample time
- Gas concentrations from continuous analyzers

Sample data sheets are provided in Appendix A of this document for:

- Velocity and temperature traverse
- Stack gas moisture measurement

- Stack gas composition (molecular weight) measurement
- Particulate sampling data
- Gas grab and liquid fuel data
- Continuous gas analysis

Similar sheets should be prepared for each of the functions required by the test plan. Final copies (post-test) are provided to the facility manager, sampling operator, and laboratory personnel.

1.4 SAMPLE SCHEDULE AND MANPOWER REQUIREMENTS

Early identification of facility test periods allows planning of the environmental assessment schedule. Since the SASS is the most time consuming of the sampling systems (~4 hours operation per test point), its start time should be as early in the test period as possible to ensure adequate sample time. Taking supplemental gas grab samples, liquid fuel samples, and operation of continuous gas analyzers can then be performed periodically between SASS adjustments.

Two men are required for SASS setup. During operation, at least one person (and periodically both) can be made available for gas and fuel sampling operations.

All steps identified above for sample planning are shown schematically in Figure 1.

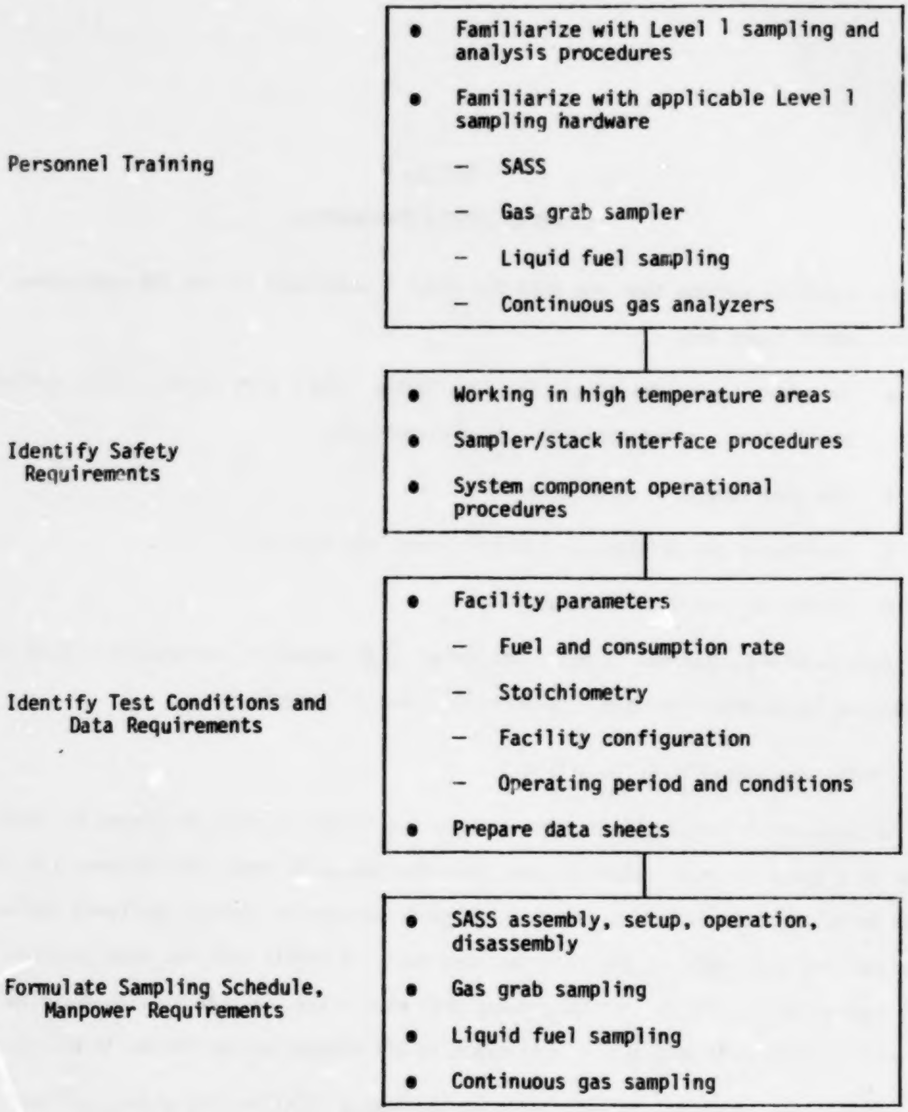
Personnel Training
• Familiarize with Level 1 sampling and analysis procedures
• Familiarize with applicable Level 1 sampling hardware
– SASS
– Gas grab sampler
– Liquid fuel sampling
– Continuous gas analyzers
Identify Safety Requirements
• Working in high temperature areas
• Sampler/stack interface procedures
• System component operational procedures
Identify Test Conditions and Data Requirements
• Facility parameters
– Fuel and consumption rate
– Stoichiometry
– Facility configuration
– Operating period and conditions
• Prepare data sheets
Formulate Sampling Schedule, Manpower Requirements
• SASS assembly, setup, operation, disassembly
• Gas grab sampling
• Liquid fuel sampling
• Continuous gas sampling

Figure 1. Sample planning procedures.

SECTION 2

SAMPLE SYSTEM PREPARATION

The sampling systems that are used for Level 1 assessment of the CRB combustion facilities and their sample types are:

- Aerotherm Source Assessment Sampling System (SASS) with special liquid cooled probe — particulates, trace elements, organic compounds
- Gas grab sampler — stack gases
- Continuous gas analyzers — specific stack gas species
- Liquid containers — fuel sampling

Each sampling apparatus is described below. For reference, a complete list of all sampling equipment to be assembled for the assessment is given in Appendix B.

2.1 SOURCE ASSESSMENT SAMPLING SYSTEM

A schematic of the Source Assessment Sampling System is shown in Figure 2. Main components consist of a probe for extraction of gases from the stack, an oven with cyclones and filter for collection of particulate matter, a gas cooler/organic adsorption module, impingers for trace element collection, and gas transport and metering equipment. A single SASS has been provided for all Wing G combustion facilities that interfaces with each stack. A special liquid-cooled probe interfaces with the standard SASS and is applicable to all combustion facilities in Wing G.

Before full setup of the SASS train at the sample location, the probe, cyclone and filter holder, gas cooler, and impinger components should be prepared and partially assembled in the laboratory. Two persons are required for these functions. Procedures for precleaning SASS components are presented in Section 3.3 of Reference 2. Assembly of the cyclones, filter, probe, oven, and impingers is outlined in Reference 3. Final assembly of the system at the sample location can be completed after transport of assembled components from the laboratory.

A sampling cart to be used to transport sampling equipment to the sampling site is provided. The cart can also be used during operation of the SASS, supporting the control module, gas cooler,

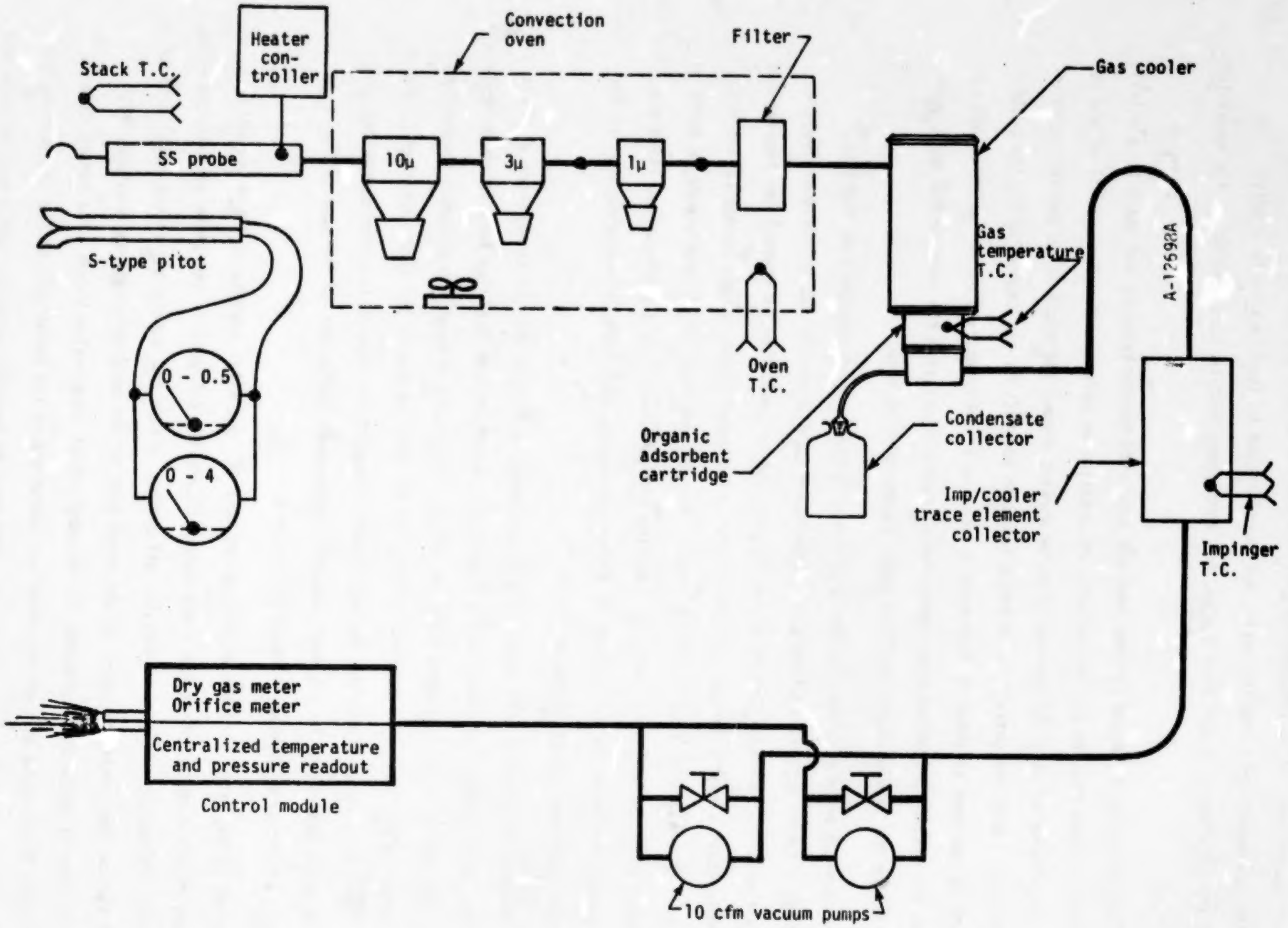
Stack T.C.
Heater con- troller
Convection oven
Filter
Gas cooler
SS probe
10μ
3μ
1μ
S-type pitot
Gas temperature T.C.
A-1269BA
0 - 0.5
0 - 4
Oven T.C.
Organic adsorbent cartridge
Condensate collector
Imp/cooler trace element collector
Impinger T.C.
Dry gas meter
Orifice meter
Centralized temperature and pressure readout
Control module
10 cfm vacuum pumps

Figure 2. Source Assessment Sampling System (SASS).

and impinger components. It is recommended that the control module and vacuum pumps not be transported to the laboratory on a routine basis, but hand-carried to the stack to be sampled. The sample cart can be wheeled to the Wing G area, but components must be hand-carried to the mezzanine level.

The gas sampling probe and cyclone oven are supported horizontally at the stack by a unirail support system. Setup details for the unirail are detailed in Reference 3. The unirail should be setup well in advance of facility startup to allow working around the stack in an ambient temperature environment. Once the unirail is in place (clamped securely to the sample port), the probe is connected to the oven as shown in Reference 3, and the assembly mounted on the unirail support. Assembly of the system is completed by connection of sample lines from the oven to the gas cooler, the impingers to the sample pumps, and from pumps to the control module.

The sampling probe provided for the SASS train (a nonstandard component of the SASS, shown in Figure 3 with support equipment) is temperature-conditioned by two independent cooling fluids. A closed-loop oil circulation system is provided to condition and control the temperature of the sample gases flowing through the probe liner. The outer fluid (water) maintains the probe outer sheath temperature at a safe working level. The gas sample is to be conditioned to 400°F at the entrance to the cyclone oven under all sampling circumstances. As a consequence, there are sampling conditions where the oil system is either extracting heat from or providing heat to the sample gases (dependent on stack temperature).

A temperature control unit supplied with the probe maintains the oil temperature at a set value. This unit contains an electrically heated oil reservoir that supplies heat to the circulating oil. Heat may also be extracted from the oil by circulating through the adjacent finned tube heat exchanger rather than the reservoir. A fan is provided on top of the heat exchanger to aid in cooling. Switching between the heating and cooling loops of the unit is provided automatically by a solenoid valve controlled by the dual setpoint temperature controller at the base of the unit. A schematic of the probe system is shown in Figure 4.

Setup of the probe includes connection of both oil and water systems to their respective supply and return connections on the probe body. Locate the oil pump in the probe vicinity to allow traversing. To connect the probe hydraulic oil system, attach the supply and return metal braided hoses to the two most-rearward tubes on the probe body by the quick-disconnects provided. The oil supply line is permanently attached to the pump outlet (hand-valve side). The return line is provided with disconnects at each end which are connected to the probe body at one end and the top of the oil reservoir tank at the other end. This hose is provided with one female and one male end

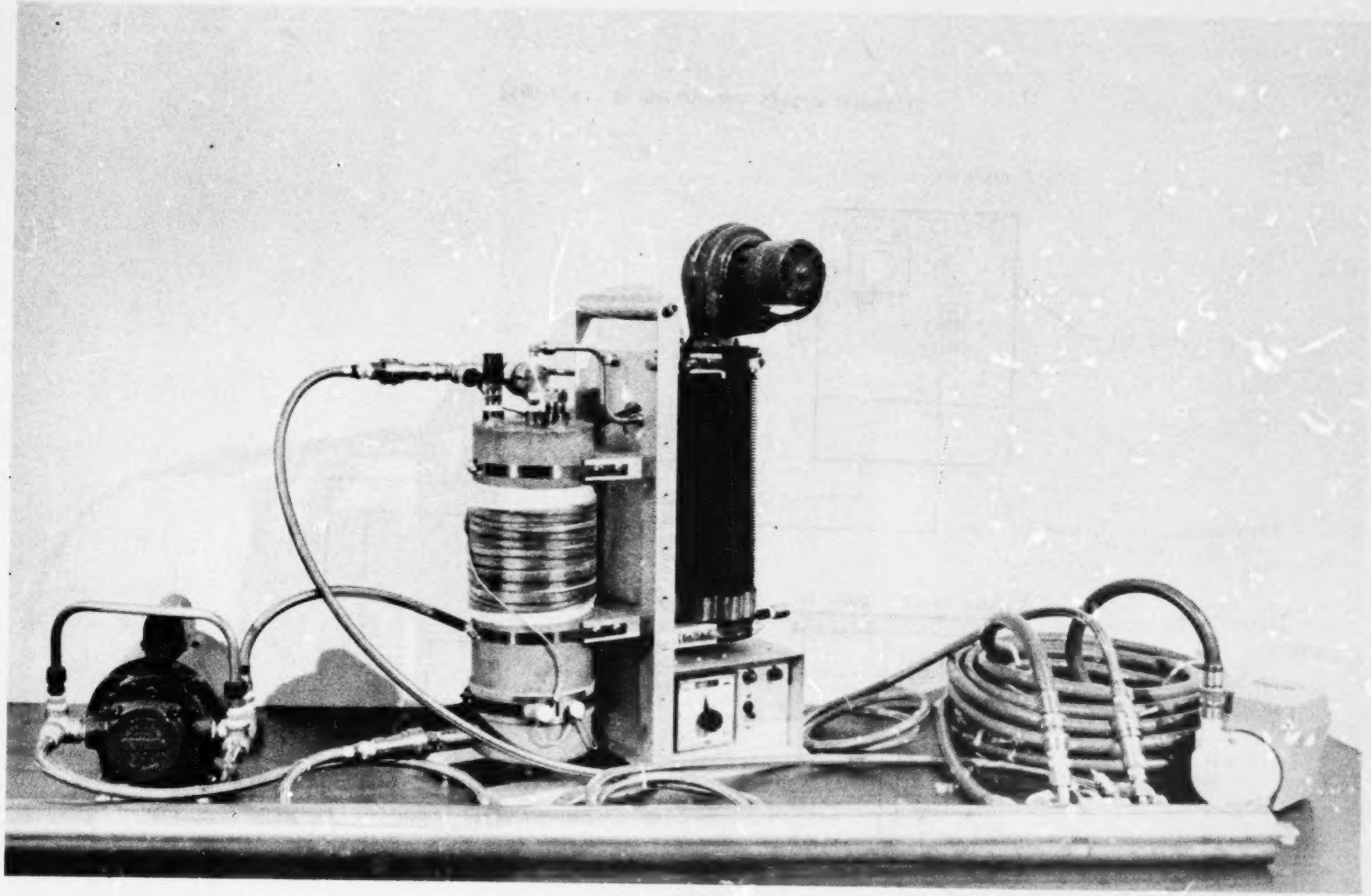

Figure 3. Liquid cooled simpling probe.

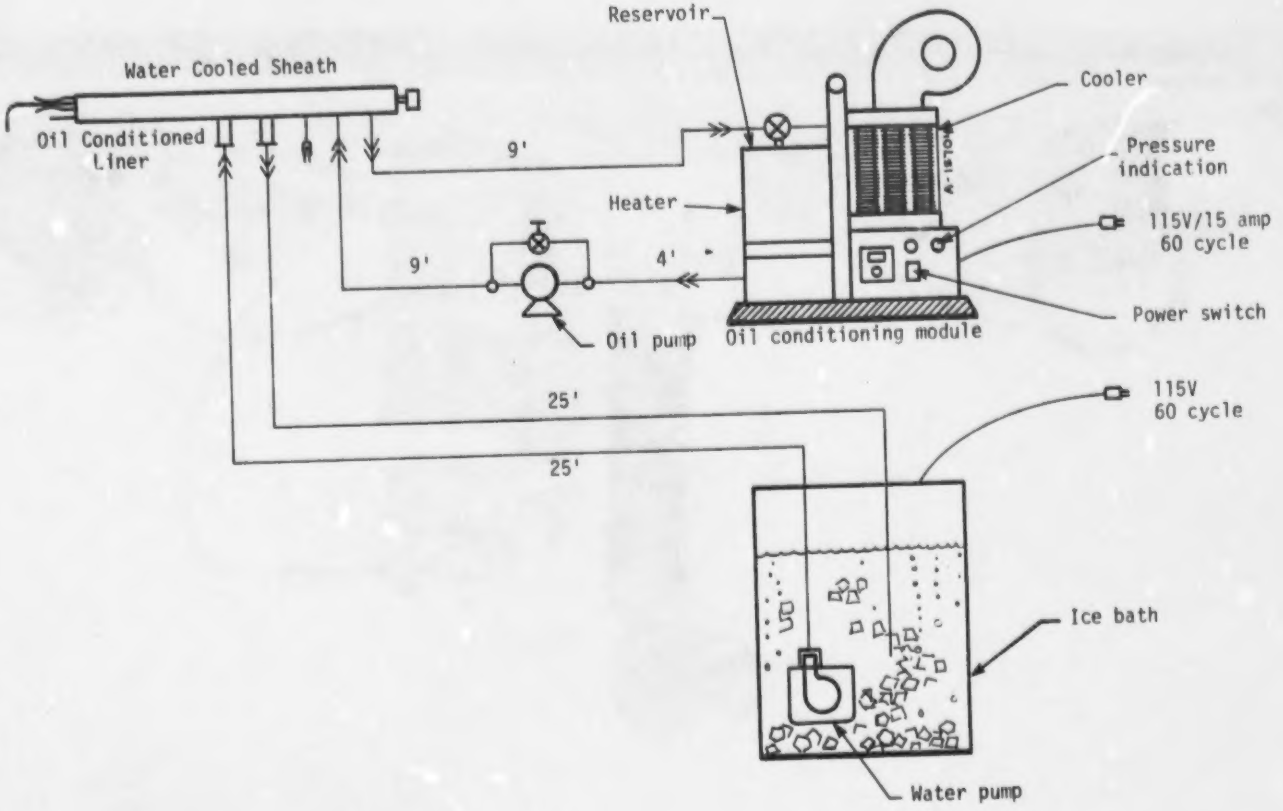
Reservoir
Water Cooled Sheath
Cooler
Oil Conditioned Liner
9'
Pressure indication
Heater
115V/15 amp 60 cycle
9'
4'
Power switch
Oil pump
Oil conditioning module
25'
115V 60 cycle
25'
Ice bath
Water pump

Figure 4. Probe coolant system schematic.

and can only be connected in one direction. Completion of the oil system is accomplished by connection of the pump supply line to the bottom of the oil reservoir with the appropriate disconnect.

The water coolant system is connected by two garden hoses at the front-most fittings on the probe body. Water circulation can be provided by either the water pump provided with the probe system and an ice bath (see Figure 4) or a pressurized water system (city water or closed-loop). If the ice bath option is employed for the water system, between 25 and 100 pounds of ice per hour will be required, dependent upon the heat load.

CAUTION

Both water and oil should be supplied to the system prior to startup of circulation pumps. Startup details are provided in Section 3.

The probe umbilical connection is somewhat simplified over that of the standard SASS probe. As the umbilical provided with the system was constructed for the standard probe, it will contain power connections that are not required for the liquid probe. The connections required are:

- Pitot tube pneumatic lines (color-coded)
- Stack gas thermocouple

The umbilical connection is completed to the impinger, oven, and gas cooler thermocouples as described in Reference 3.

Both electrical power and cooling water are required for operation of the SASS and probe. Power requirements are one 115V, 15A circuit for each of the following units:

- Sample probe temperature control unit
- Oil pump
- Control module
- Gas cooler
- Sample vacuum pumps

In addition, a cube or crushed ice supply (~15 lb/hr) is required for the impinger bath. Filling of the water circulation system for the impinger ice bath requires several gallons and operates as a closed-loop system after filling.

The final function to be performed prior to sampling with the SASS is to leak-check the assembled train. The probe nozzle inlet is blocked off (a plug fitting is provided with the probe) while 15 inches Hg vacuum is pulled on the system by the sample pumps as per the SASS operating manual. If the noted flowrate is less than 0.05 cfm, the system is then ready for sampling. If the leak rate is greater than 0.05 cfm, the source of the leak must be found and corrected.

Periodic calibration of the pitot tube, orifice meter, and dry gas meter SASS components is required to maintain sampling accuracy. The following calibration program should be followed for Level 1 environmental assessment. All calibration should be performed on schedule and logged in a convenient location.

The accuracy of the stack flow velocity measurement is dependent upon knowing the coefficient C_p of the S-type pitot tube. Calibrations are performed as follows:

- Prior to the first field test and at 1-year intervals — calibrate pitot tube by EPA Method 2 as described in Reference 4
- Prior to and after each system use — visually inspect pitot tubes for signs of damage, recalibrate if damage is noted

The orifice meter and dry gas meter provide accurate measurement of the sample gas flowrate and total volume. Calibration procedures are detailed by EPA Method 2 and in Reference 3. The Level 1 calibration schedule is as follows:

- Prior to the first field test and at 1-year intervals — calibrate as per EPA Method 2
- Prior to and after each system use — perform calibration check by comparing the volumes measured by the dry gas meter and the orifice meter (flowrate multiplied by the run time). Recalibrate both components if the measured volumes do not agree within ± 5 percent.

The above calibration check should be performed for at least two system flowrates. Those recommended are 4.0 cfm and 8.0 cfm. An example of the check is as follows. The system flowrate is adjusted to a steady-state condition at the approximate recommended flowrate. A timed interval is established during which the orifice meter is read successively and the total gas meter volume is recorded. The volume of gas passing through the orifice meter is the product of the run time and the flowrate (corrected to calibration temperature conditions) and is compared to the gas meter volume (also corrected to calibration conditions).

2.2 GAS GRAB SAMPLER

Stack gases are to be grab-sampled from the stack periodically according to the test plan. These samples are simply extracted from the stack into an evacuated flask and transported to the laboratory for analysis.

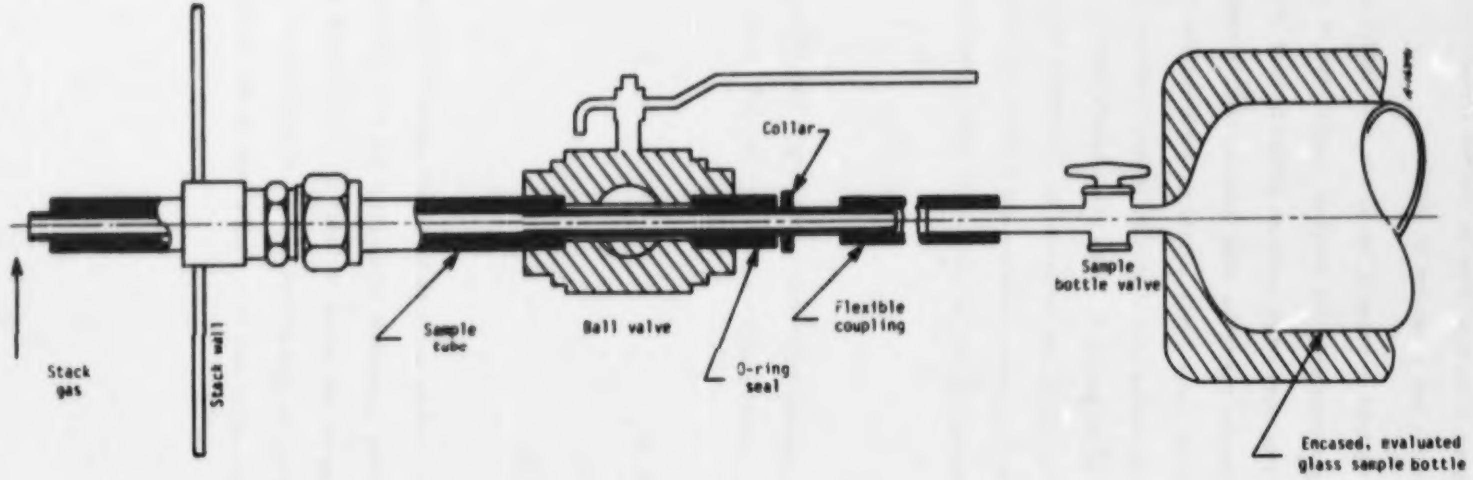
Collar
Sample bottle valve
Flexible coupling
Sample tube
Ball valve
O-ring seal
Stack gas
Stack wall
Encased, evaluated glass sample bottle

Figure 5. Grab sample probe.

The grab sample system is shown in Figure 5. A stainless steel tube and ball valve are fixed permanently to each facility stack. The sampling probe (stainless steel with a ceramic liner) slides in through the fixed-tube port and is connected to the sample bottle by a flexible line. The flexible line contains a pyrex glass wool plug to prevent particulate influx to the sample bottle. Complete operating details are presented in Section 3.

Several functions are required in preparation of the grab sample system. Since the quality of the sample is dependent upon maintaining the original composition of the gas from stack to analyzer, the probe and connecting tube inner surfaces should be made inert prior to use. This function is accomplished by allowing the probe inner tube surface to remain in contact with a 1:1 (v/v) aqueous nitric acid solution for a 1-hour period as performed for SASS train components. Three successive cleaning stages follow with distilled water, isopropyl alcohol, and methylene chloride (see Section 3.3.3.1 of Reference 2). The glass sample bottle, encased in its protective cover and having been similarly cleaned and evacuated by laboratory personnel, is connected to the flexible tubing and probe. The evacuation pressure and temperature should be labeled on each sample bottle. The probe/bottle assembly, as well as additional sample bottles, are then transported to the sample location.

2.3 CONTINUOUS GAS ANALYSIS

Certain combustion gas species generated in the Wing G facilities cannot be routinely analyzed by the grab sample/gas chromatography technique of the IERL Level 1 laboratory. These species, which may include:

- Nitric oxides — NO, NO_x
- Carbon dioxide — CO_2
- Carbon monoxide — CO
- Oxygen — O_2

as well as others of interest, can be analyzed by a continuous gas analysis system. The analyzers require initial calibration with a standard calibration gas prior to providing continuous monitoring of the stack gases. Setup of the system includes this calibration and provision of a sample line from the analyzer bench to the appropriate stack. Alternatively, gases can be injected into the analyzers from grab sample containers if a sample line to the stack is not available.

2.4 LIQUID FUEL SAMPLING

The method of sampling liquid fuels in the Wing G facilities is extraction by tap and collection directly in a glass laboratory container. The container should be prepared according to Level 1 procedures (cleaning, etc.) by laboratory personnel such that it is ready for transport to the sample location.

Figure 6 shows the sample system preparation procedures described above.

Source Assessment Sampling System

- Collect all system components
- Perform periodic component calibrations (if required)
- Prepassivate and clean all sample contact surfaces for 1 hour with 1:1 (v/v) nitric acid
  - Probe liner and nozzles
  - Cyclones and filter holder
  - Heated sample line
  - Gas cooler components
  - Impinger bottles
- Subassemble cleaned components
- Transport components from laboratory to sample location
- Setup components at stack
  - Unirail support
  - Suspend oven and probe on unirail
  - Place control module, sample pumps, probe heater, probe pump, and probe ice bath (if used) at sample site
- Connect SASS component sample hoses
- Connect probe coolants
  - Oil system
  - Water system
- Connect probe umbilical
  - Pitot tubes
  - Thermocouples
- Provide power, water connections
- Leak check assembled system

Gas Grab Sampler

- Collect sample probe, tubing, sample bottles
- Prepassivate and clean probe and tubing
- Assemble probe and tubing
- Transport components to sample location

Continuous Gas Analysis

- Provide sample line, filters, and water removal device from sample gases
- Calibrate analyzers with standard calibration gases

Liquid Fuel Sampling

- Secure cleaned sample bottles from laboratory
- Transport to sample location

Figure 6. System preparation procedures.

SECTION 3

SAMPLING

The sampling procedures for the SASS, grab sampler, and liquid tap sampling are discussed in this section. Procedures for continuous gas analysis are specific to each analyzer and sampling personnel are referred to the appropriate operator's manuals. Each Level 1 assessment will begin and end with attention to the SASS train — its operation being the most time consuming of the sampling procedures. Gas and liquid fuel samples can easily be taken after the SASS has achieved steady operation.

The two persons that are required for SASS setup will also be required to perform the sampling operations. One person can perform startup, operation, and shutdown procedures for the SASS. The second person is then available to perform grab sampling and monitoring of continuous gas analyzers.

3.1 SAMPLING WITH THE SASS TRAIN

In order to reach a steady sampling operation with the SASS train, several functions are required:

- Attachment of the probe nozzle or pitot tubes (or both) to the probe
- Calculation of sampling points for velocity and temperature traverse by EPA Method 1 (Reference 4)
- Warmup of the probe coolant fluid to achieve proper sample conditioning
- Insertion of the probe body into the stack
- Measurement of stack velocity and temperature by traversing
- Measurement of static pressure, ambient pressure, moisture content, and gas composition
- Selection of the average velocity sampling point
- Selection of the proper nozzle size to achieve isokinetic sampling conditions
- Initiation of sample flow

In general, stack velocity measurements will be required before actual sampling can begin. The usual measurement method involves attachment of the pitot tubes to the SASS probe. The probe is then inserted into the stack and a stack traverse made from which a velocity profile can be generated (one-dimensional). After calculation of the sample point of average stack velocity, the proper nozzle size for isokinetic sampling can be selected.

Connection details for pitot and nozzle are given in Reference 3. Nozzle selection procedures are also detailed.

The assessment test plan will require that a velocity traverse be performed when

- The average velocity sample point is not adequately known from previous testing
- Test conditions are significantly different from those of past assessments

The appropriate sample points across the duct are then calculated by EPA Method 1. The calculation procedure for circular ducts is described in Reference 4.

Before insertion of the probe into the stack, probe cooling systems must be allowed to reach steady state. Turn the probe power switch on and set the temperature controller to approximately 250°F. Allow the fluid to heat (~30 minutes). Similarly, the SASS oven must be heated to 400°F in order to maintain a constant gas flowrate through the cyclone train.

Following heatup, turn the probe oil circulation pump on. The pump will begin laboring hard due to the low temperature fluid in the lines and the probe. Soon after the pump has been started, the motor should start to speed up and the pressure light on the module should extinguish (1 minute). Allow the probe liner to warm up (2 minutes).

Should the pump stall before warm fluid is passing through its line, adjust the relief valve on the pump by turning the handle on the valve counter-clockwise until the motor can handle the load. Once the pump is turning easily readjust the valve until the pressure light goes out. Now allow some warm fluid to enter the cooler by turning the temperature control 50°F lower for approximately 1 minute. The solenoid valve will chatter for a few seconds, and after the exchange of fluid has taken place, settle down. Submerge the water pump in the ice bath (if used) and place the ice bath in a convenient location. The water pump is rated at 24-foot 6-inch pressure shutoff and 810 gph. Do not place the pump more than 12 inches above or below the probe before the lines are filled with water.

Insure that the oil bath has reached the desired temperature, the pressure light is out, the fan is running, the water is circulating, and the probe is ready for insertion.

With the pitot tube and/or nozzle securely attached to the sample probe, and the probe fully heated by the steps above, the probe can be inserted into the stack. Two sample port types are provided on the Wing G facility stacks. The first, used on all facilities except the residential furnaces, contains a gate valve for sealing of the combustion gases from the high-bay area. The second, used only on the residential furnace stacks contains no valve but is a simple T section through which the probe can be passed. Figures 7 and 8 show the two sample port configurations, respectively.

Before inserting the probe into the gate valve port, the port cap shown in Figure 7 is slipped over the end and onto the body of the probe. Verify that the port seal is in place on the outlet edge of the port. The probe is first inserted through the seal and into the port to Position 1 in Figure 7. The port cap is then screwed firmly to the port to hold the seal in place. The port is now effectively sealed such that the gate valve can be opened without escape of stack gases. With the gate valve in the full-open position, the probe is slid further into port Position 2. The probe is generally left in this position (out of the gas stream) until sampling is to begin. For sampling, the probe is slid further to the appropriate location (Position 3, Figure 7). The above procedure is simply reversed for extraction of the probe.

CAUTION

The probe outside diameter must fit securely through the port seal before opening of the gate valve. Care must be taken to avoid contact with hot stack and port surfaces.

Each residential stack port is covered with a cap which is removed just prior to probe insertion. Since negative stack pressures are present, no gas will be emitted to the high bay. A special port seal for the residential stack is supplied that is slipped over the probe (Figure 8) before removal of the port cap. With the cap removed, the probe is inserted to a point where the nozzle is just out of the gas stream. The seal can then be slid toward the front of the probe and wedged between probe and port with moderate hand pressure. To insert the probe into the stream for sampling, it is necessary to first loosen the seal (pull back along the probe body). The probe can then be moved into the stack and the seal again wedged into the port.

Stack velocity and temperature measurements are performed as the first step in the sampling procedure. Reference 3 provides details for calculation of stack velocity from SASS data. Figure 9 shows the approximate range of velocities to be encountered in each of the Wing G facilities.

In addition to stack velocity and temperature traverse data, selection of the proper sampling nozzle is dependent upon the gas composition (molecular weight) and moisture content. The techniques

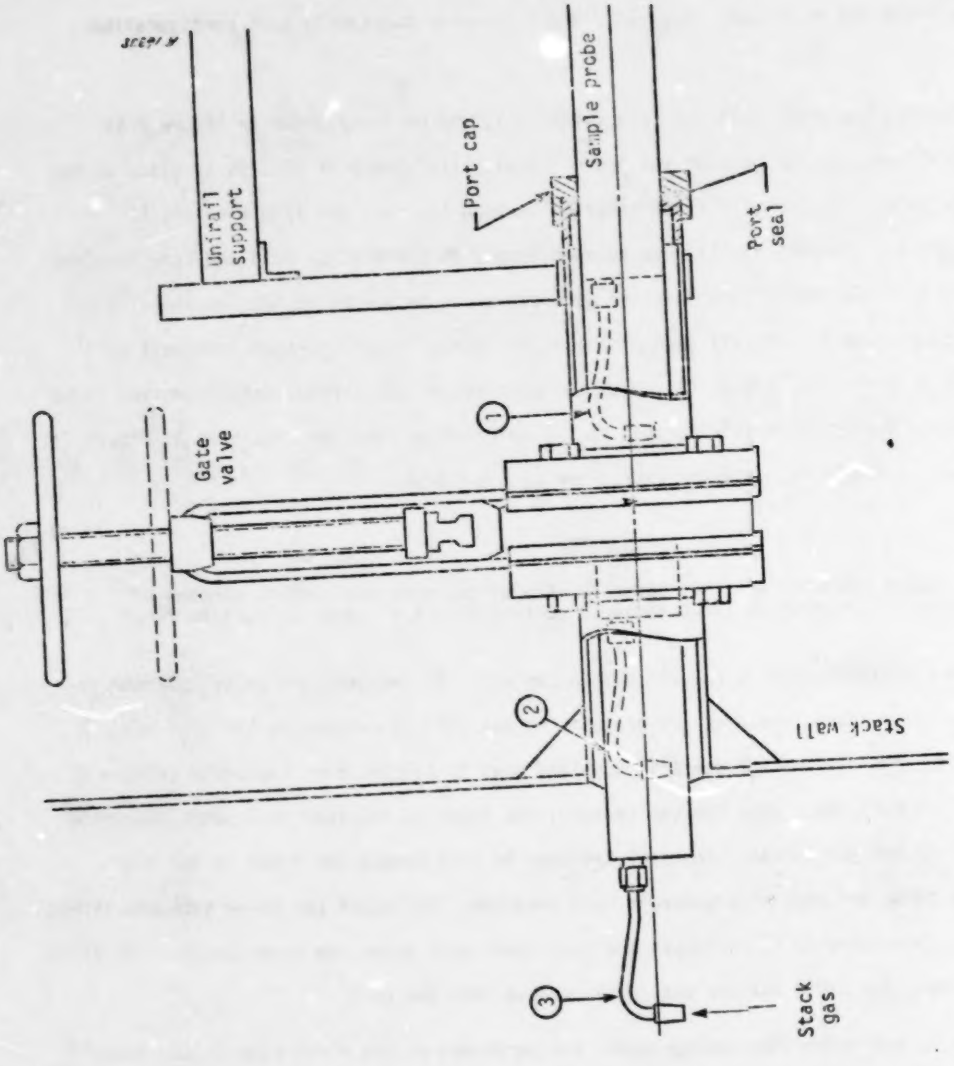
Unirail support
Port cap
Sample probe
Port seal
①
Gate valve
②
Stack wall
③
Stack gas

Figure 7. SASS sample port with gate valve.

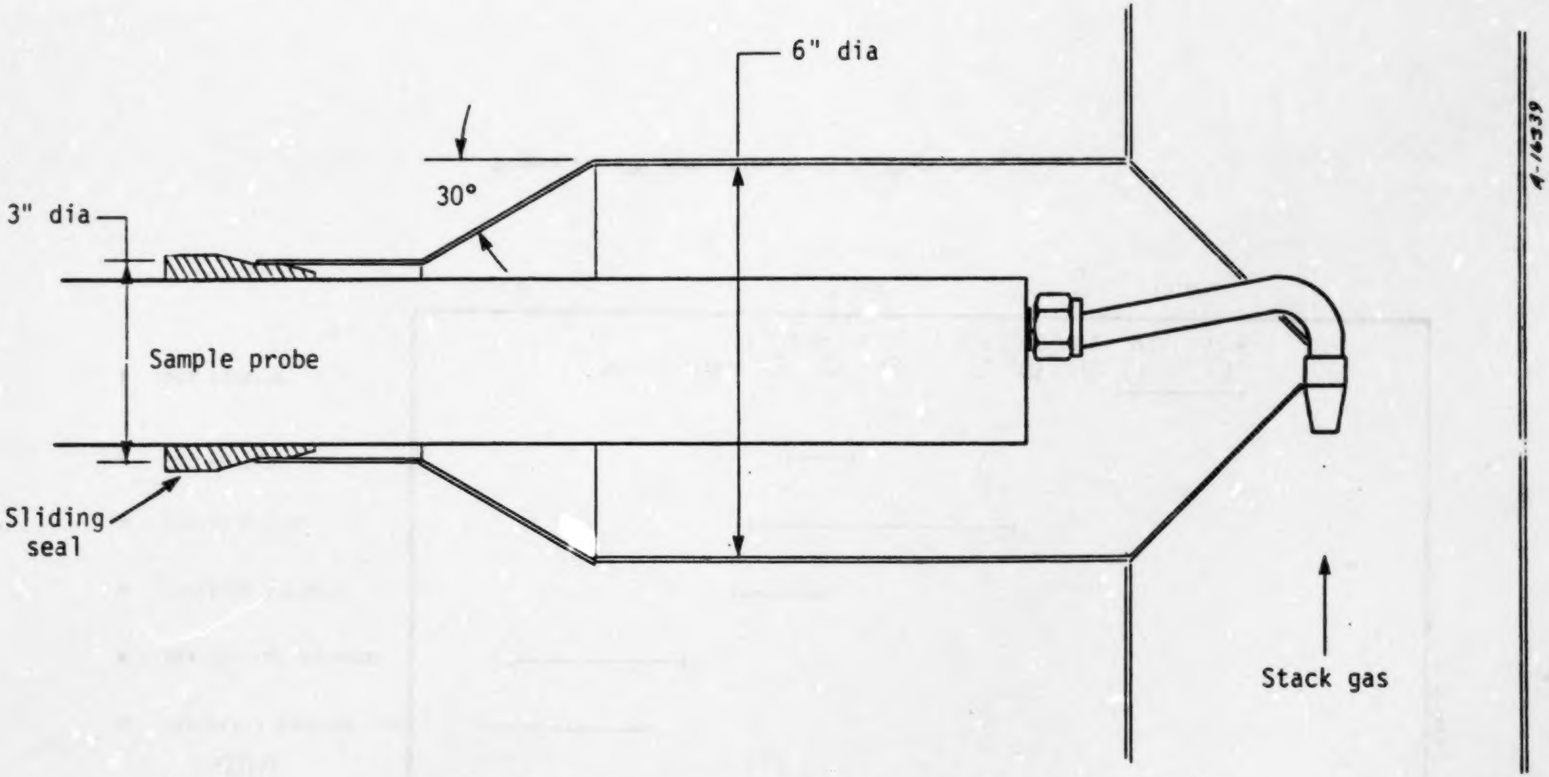
6" dia
30°
3" dia
Sample probe
Sliding seal
Stack gas
A-16339

Figure 8. Residential furnace SASS sample port.

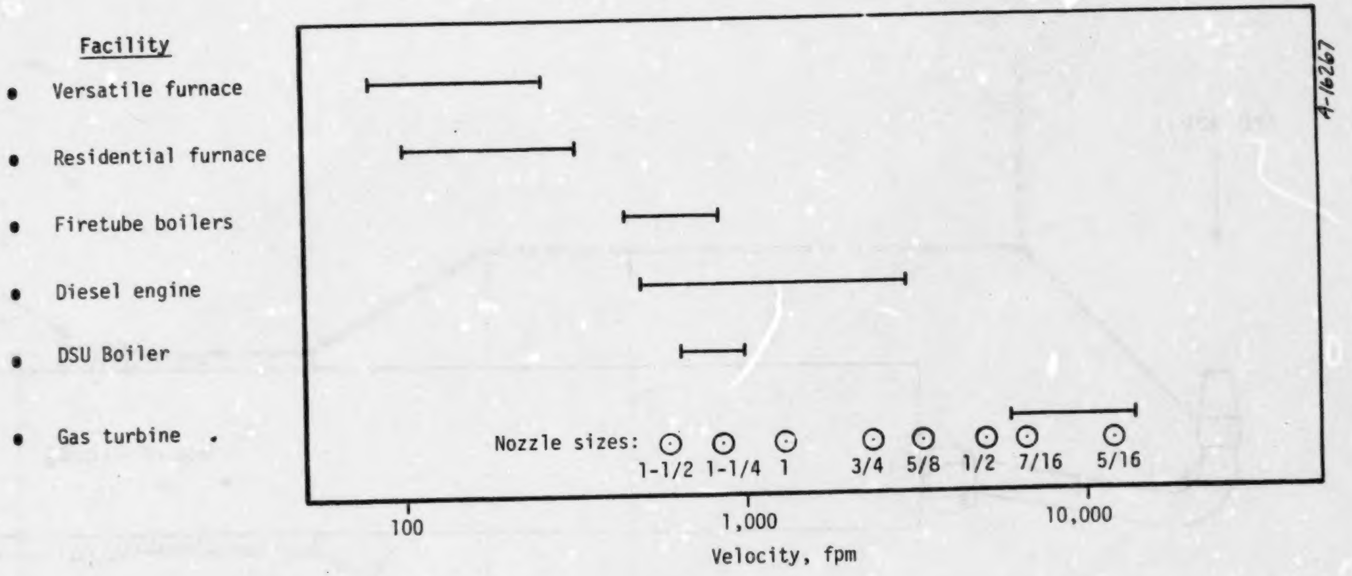

Figure 9. CRB combustion facility stack velocities.

employed are EPA Methods 3 and 4, respectively, described in Reference 4. The equipment for performing each of the EPA sampling methods is incorporated into the SASS, and the calculation procedures are outlined in Reference 3.

The measurements of moisture content and gas composition can be omitted from an assessment if the process operating point is being duplicated and composition data is available from past testing. When gas composition measurement is required, continuous gas analysis for CO, CO_2, and O_2 is the recommended technique over the EPA standard Orsat analyzer.

Isokinetic sampling conditions are achieved by variation of the nozzle inlet area rather than by changes in the SASS sample flowrate. Figure 9 indicates the nozzle sizes supplied with the SASS plotted at their approximate isokinetic sampling velocities for the fixed system flowrate. Therefore, a preliminary nozzle may be selected by use of the figure. Wherever multiple nozzles are shown for a given facility, higher stack velocities dictate that the smaller of the listed nozzles will be required. Note that only two of the Wing G facilities (the diesel engine and gas turbine) require sample nozzles of 0.75 inch or smaller diameter. Since nozzles larger than 0.75-inch diameter cannot be mounted on the probe simultaneously with the pitot tubes, all other facilities will require separate velocity measurements with use of the pitot tubes only.

NOTE

Figure 9 is provided only as a guide to nozzle selection. The proper nozzle size for isokinetic sampling must be selected by the calculations of stack velocity shown in Reference 3.

The nozzles that are provided for the Wing G combustion facilities have the following diameters: 5/16, 7/16, 1/2, 5/8, 3/4, 1, 1-1/4, and 1-1/2 inches. Two of the facilities, the versatile and residential furnaces, require nozzles larger than 1-1/2 inches and hence, cannot be sampled isokinetically with the nozzles provided. Larger nozzles are not compatible with the SASS probe and these two facilities will always be sampled nonisokinetically using the 1-1/2-inch nozzle.

Following nozzle selection and mounting on the probe, the probe is reinserted through the stack port and allowed to reach a steady-state temperature that provides the proper sample temperature (400°F). The probe nozzle should remain within the port until the probe body is fully heated. When the operator is satisfied that the probe has reached steady state, the probe can be inserted into the gas stream and sampling begun by steps listed in the SASS operating manual.

Level 1 environmental assessment specifies 30 m^3 of sample by the SASS train which will require a 3- to 4-hour period. Periodic adjustments of the SASS are required during the sample period, including:

- Probe coolant temperature and flowrate adjustments to maintain cyclone collection temperature (the objective is to maintain a sample temperature of 400°F at the entrance to the cyclone oven)
- Possible filter change, should fine particulate cause clogging
- Maintenance of proper sample flowrate
- Monitoring of changes in stack temperature
- Recording of data at periodic intervals

See Reference 3 for more specific details regarding SASS train operation. Following completion of the sampling, the system is shutdown and extracted from the stack by pulling probe and oven back to clear the valve, closing the gate valve, and final withdrawal from the port.

CAUTION

Avoid escape of hot gases through the port due to over-extraction of the probe prior to closing of the gate valve.

3.2 GASEOUS GRAB SAMPLING

Gas grab samples are to be taken periodically as required by the test plan. As with the SASS sampling system, grab sample port configuration is common to all Wing G facilities except the residential furnaces. All other facilities are provided with a permanent sample probe tube and valve.

The more common port with hand valve is constructed with an O-ring seal at the port outlet. Silicon grease should be applied to the probe's outer wall to lubricate this seal, taking care that the grease does not come in contact with the probe inner surfaces. The probe is partially inserted to seal the port, the hand valve opened, and the probe inserted until its stainless steel collar butts up against the port opening.

The residential furnace ports contain no valve and simply require removal of the port cap and insertion of the sample probe. The sample probe is of different construction than that used on the other facilities. The two port and probe types are shown respectively in Figures 10 and 11.

The glass bottle (previously evacuated and attached to the sample probe) has a sample volume of 3 liters. The sample is taken by opening of the bottle valve and allowing the stack gases to be drawn into the sample bottle. Bottle and stack pressure equalize within a few minutes at which time the bottle valve is placed in the closed position and the probe is removed from the stack.

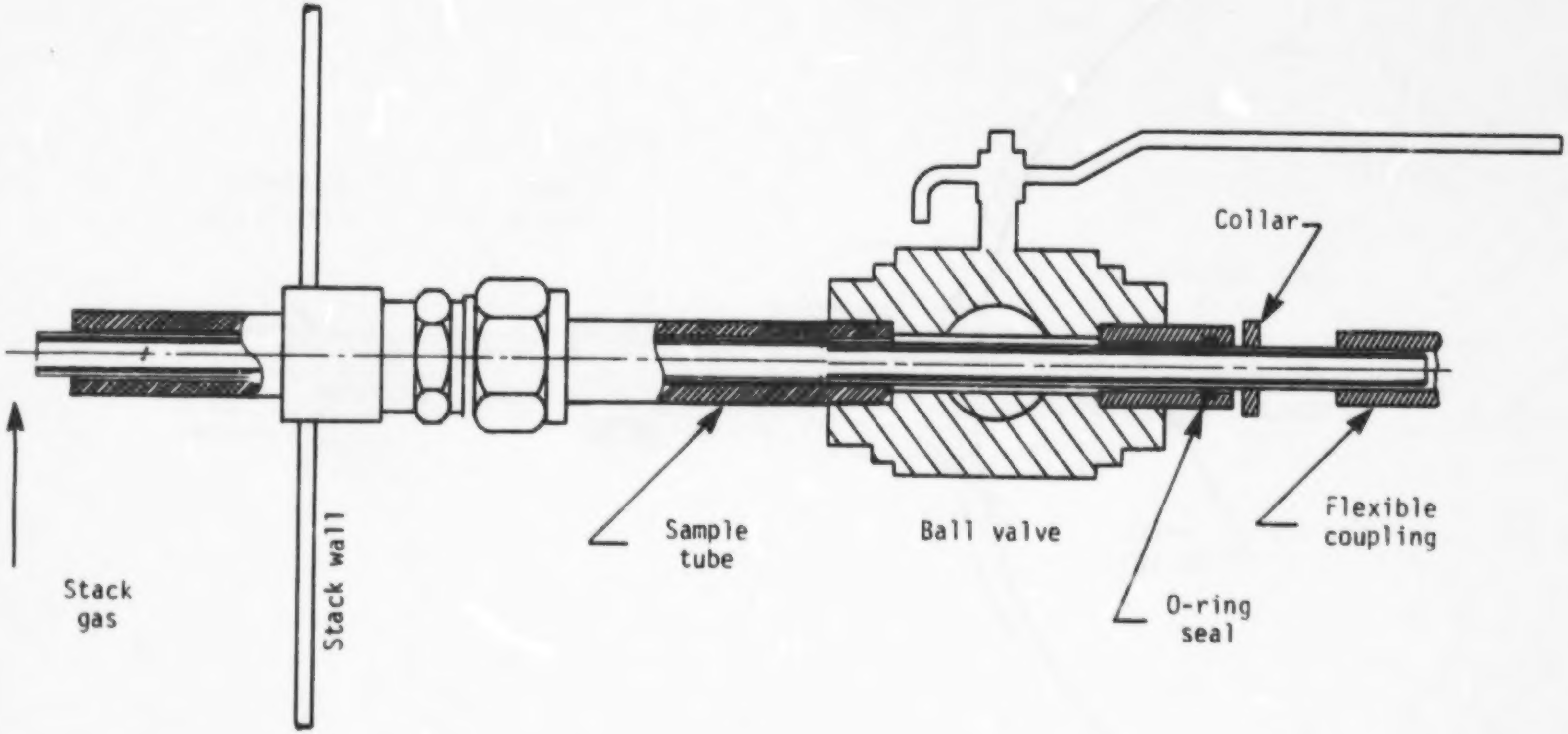
Collar
Stack gas
Stack wall
Sample tube
Ball valve
O-ring seal
Flexible coupling

Figure 10. Gas grab sample port with ball valve.

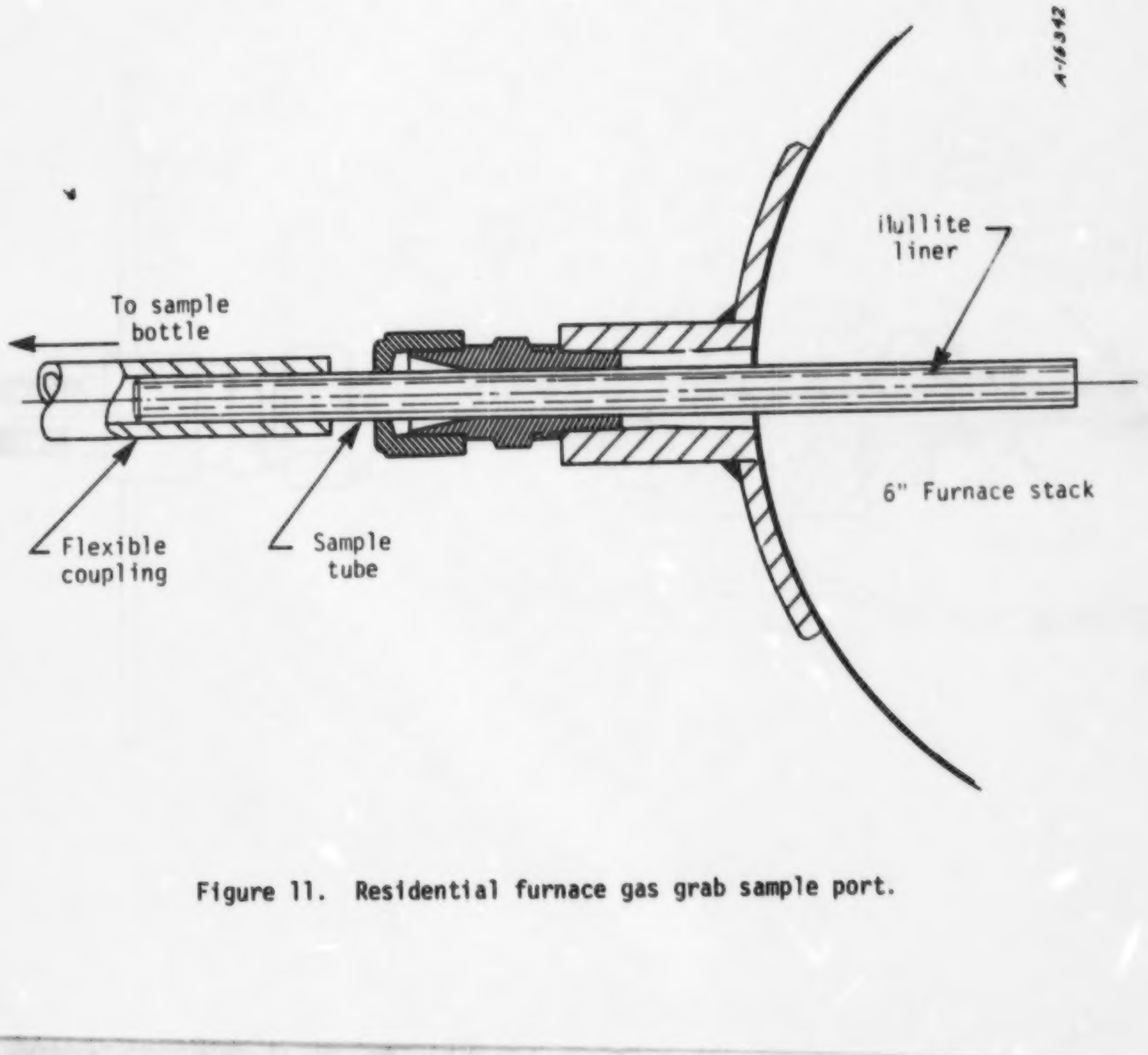
A-16342
Mullite
liner
To sample
bottle
6" Furnace stack
Flexible
coupling
Sample
tube

Figure 11. Residential furnace gas grab sample port.

CAUTION

The sample probe must remain in the outer housing during opening and closing of the port valve to avoid escape of hot stack gases.

In order to take additional samples during the test period, the grab sample probe can be detached from the evacuated bottle at the flexible line and a new bottle attached. The above sampling procedure is then repeated. In order to maintain sample integrity, sample bottles should be taken to the laboratory for analysis as soon as possible rather than waiting until completion of the entire day's sampling.

3.3 LIQUID FUEL SAMPLING

The RTP Wing G facility area contains a fuel-oil system with taps at specific locations. In order to sample the liquid fuel, these taps are opened as the fuel is flowing in the line, filling a glass laboratory bottle. The tap is then closed off, completing the sampling procedure.

A schematic of all sampling procedures is shown in Figure 12.

SASS Train

- Attach probe nozzle and/or pitot tubes
- Calculate stack traverse points
- Warmup probe coolant fluids
  - Turn power switch on
  - Set temperature controller and allow oil to heat
  - Start oil pump
  - Allow fluid to flow through cooling loop
  - Start water flow circuit
  - Verify proper operation
- Insert probe into stack
- Perform velocity and temperature traverse
- Measure appropriate stack variables
  - Stack static pressure
  - Ambient pressure
  - Exhaust gas moisture content
  - Gas composition
- Withdraw probe from gas stream
- Calculate average velocity sampling point
- Select proper nozzle for isokinetic sampling
- Reinsert probe into stack
- Initiate sample flow
- Record data at periodic intervals
- Perform periodic SASS adjustments
  - Probe coolant temperature and flowrate
  - Filter change if required
  - Maintain sample flowrate
- Shutdown sample gas flow at sample completion
- Withdraw probe from stack
- Shutdown probe coolant system
  - Turn off temperature controller
  - Turn off coolant pumps
  - Turn power switch off

Gaseous Grab Sampling

- Attach probe tubing to evacuated flask
- Insert probe into stack by appropriate procedure
- Open bottle valve to initiate sample flow
- Allow stack and bottle pressures to equalize
- Close bottle valve
- Withdraw probe from port and insure the port seal
- Detach probe tubing from sample bottle
- Label sample bottle for time taken
- Transport contained sample to laboratory as soon as possible to avoid changes in sample composition

Figure 12. Sampling procedures.

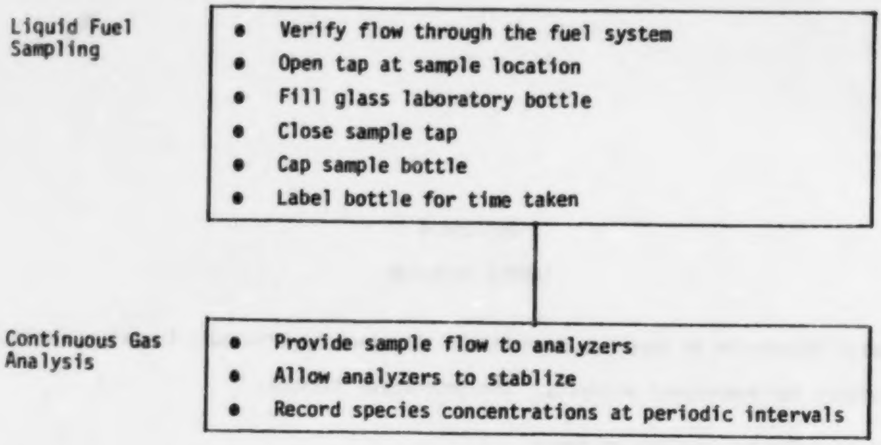
Liquid Fuel Sampling
Verify flow through the fuel system
Open tap at sample location
Fill glass laboratory bottle
Close sample tap
Cap sample bottle
Label bottle for time taken
Continuous Gas Analysis
Provide sample flow to analyzers
Allow analyzers to stablize
Record species concentrations at periodic intervals

Figure 12. Concluded

SECTION 4

SAMPLE RECOVERY

Following completion of sampling operations, the sampling crew must transfer samples to laboratory containers for subsequent analysis. The procedures include:

- Disassembly of sampling hardware
- Transport of equipment to the analysis laboratory
- Extraction of samples from the SASS train
- Equipment cleanup and reassembly

The most time-consuming sample recovery involves the SASS samples. The pertinent procedures are discussed below.

4.1 SASS TRAIN BREAKDOWN

Following cooldown of probe and oven, the SASS is partially disassembled at the sample location. Cap off the nozzle at the probe inlet and disconnect power, water, and probe coolant supplies such that the probe and oven can be removed from the unirail support. Disconnect the sample hoses from impingers and gas cooler and separate each component in the system. The probe, cyclones and filter holder, impingers and case, gas cooler, and liquid fuel samples are then ready for return to the laboratory. The SASS control module and pumps can be left in place. The mechanics of SASS breakdown are more fully explained in the SASS operator's manual. The cart can be used to facilitate moving of the SASS components to the laboratory.

4.2 SAMPLE EXTRACTION

Sample material held within the SASS must be properly extracted and put into laboratory containers. The complex procedures, designed to avoid sample contamination, are outlined in Reference 2, Figures 12 to 14. All containers should be prepared by laboratory personnel. The particulate catch includes not only that of the cyclone cups and filter, but also particles deposited within the probe liner, nozzle, and cyclone interconnecting tubes. All particulate is to be washed from contacted surfaces and placed in individual, weighed laboratory containers.

The condensed water from the gas cooler is collected and bottled for future measurement and analysis. The gas cooler unit also contains the organic adsorbent module that is emptied into a laboratory container. Finally the four impinger bottles contain solutions that must be washed into laboratory containers by the procedures of Reference 2.

Gas and liquid grab samples are collected directly into their storage containers. No additional preparation is required. All sample bottles should be labeled as to test numbers, sample time, and contents as they are taken or prepared. The sample crew then stores all samples in the area provided in the analysis laboratory.

4.3 SYSTEM CLEANUP AND REASSEMBLY

All SASS train components contacted by the sample gas require passivation by acid treatment and cleaning to inert the surfaces prior to the next system use. The grab sample probe should be similarly treated. If the sampling systems are to be used soon after the just-completed test, this function may be performed before reassembly of the SASS. The final step in sample preparation is reassembly of the cyclones/filter/oven and impingers and storage until the next Level 1 assessment. Sample recovery procedures are outlined in Figure 13.

Sampling System Disassembly

- Partially disassemble SASS train at sample site. Isolate
  - Probe
  - Cyclone oven
  - Gas cooler module
  - Impinger bottles
- Transport above SASS components to laboratory
- Transport remaining gas and fuel sample bottles to laboratory

Sample Extraction

- Disassemble SASS components as required
- Transfer particulate samples to individual containers
  - Probe and nozzle catch
  - Cyclones
  - Filter and holder
  - Tube connections
- Collect gas cooler condensate in provided container
- Transfer polymeric adsorbent material to provided container
- Wash reagents from impinger bottles to laboratory containers
- Label all containers for content, sample time, and test number
- Store sample containers in laboratory
  - Gas grab bottles
  - Liquid fuel bottles
  - SASS collection containers

Sample System Storage

- Passivate and clean SASS and grab sample equipment
- Reassemble SASS components
  - Cyclones, filter holder, and oven
  - Gas cooler module
  - Impinger bottles
- Store above components in analysis laboratory

Figure 13. Sample recovery.

SECTION 5

DATA REDUCTION

The responsibility for data reduction for the environmental assessment lies jointly with sampling and analysis personnel. The sampling crew provides copies of all data sheets to the laboratory, complete with final calculations of average stack velocity, moisture content, gas composition, particulate sample volume, and grab sample conditions. Following sample analysis, the laboratory should provide concentration data for all sample components pertinent to the Level 1 requirements (Reference 2). The final step, converting sample data into process mass emission rates, can be performed by either sampling or analysis personnel.

The calculated emission rates are the main objective of the environmental assessment. EPA methods (Reference 4) are a good source of calculation details for total particulate weight and gaseous species concentrations. These calculations as well as other specie and elemental mass data are then easily converted to emission rates with the stack and sample system gas flowrates. All emission rate data are finally reported to program, facility, sampling, and analysis personnel.

REFERENCES

1. "IERL-CRB Analysis Manual for Level 1 Environmental Assessment," A. D. Little, Inc., February 1977.

2. Hamersma, J. W., Reynolds, S. L., and Maddalone, R. F., "IERL-RTP Procedures Manual: Level 1 Environmental Assessment," EPA-600/2-76-160a, June 1976.

3. "Operating and Service Manual — Aerotherm Source Assessment Sampling System," Acurex Corporation, Aerotherm Division, April 1977.

4. U.S. Environmental Protection Agency, "Standards of Performance for New Stationary Sources," Federal Register, Vol. 36, No. 247, Part II, December 1971.

APPENDIX A

SAMPLE DATA SHEETS

Facility
Stack Diameter (in.)

Date
Time
Run

Operators

Static Pressure (in. WG)
Ambient Pressure (in. Hg)
Type S Pitot Coefficient

Stack Pressure (in. Hg)
Molecular Weight (lb/lb-mole)
B_{wo}

VELOCITY TRAVERSE DATA

Sampling Point Number	Velocity Head (in. WG)	$\sqrt{\Delta P}$	Stack Gas Temp (°F)	Sampling Point Velocity (fps)
		Average	Average	

Facility

Stack Diameter (in.)

Date

Time

Run

Operators

Static Pressure (in. WG)

Ambient Pressure (in. Hg)

Type S Pitot Coefficient

Wet Bulb Temp (°F)

Dry Bulb Temp (°F)

Moisture (% vol.)

B_{wo}

STACK GAS MOISTURE (CONDENSATION)

	Condensate Collection Bottle Weight (gm)
Final	
Initial	
Liquid Collected	
	Total, $V_{\ell c}$

Clock Time	Dry Gas Meter (ft^3)	Gas Flowrate (cfh)	Gas Meter Temp (°F)	Velocity Head (in. WG)	Stack Gas Temp (°F)	Gas Cooler Temp (°F)
	Total, V_m	Average	Average, T_m			

Facility

Stack Diameter (in.)

Date

Time

Run

Operators

Static Pressure (in. WG)

Ambient Pressure (in. Hg)

Type S Pitot Coefficient

STACK GAS MOLECULAR WEIGHT

Clock Time	Gas Flowrate (cfh)	Velocity Head (in. WG)	Stack Gas Temp (°F)

CO_2 (% by Volume)	O_2 (% by Volume)	CO (% by Volume)
Average	Average	Average

Facility
Stack Diameter (in.)

Date
Time
Run

Operators
Static Pressure (in. WG)
Ambient Pressure (in. Hg)
Type S Pitot Coefficient

Stack Pressure (in. Hg)
Molecular Weight (lb/lb-mole)
B_{wo}
Meter Box Number
Orifice Meter Coefficient
Probe Length (ft)
Nozzle Diameter (in.)

PARTICULATE SAMPLING DATA

Sampling Point Number	Clock Time	Stack Gas Temp (°F)	Probe Coolant Temp (°F)	Gas Cooler Temp (°F)	Impinger Outlet Temp (°F)	Oven Temp (°F)	Dry Gas Meter Temp		Velocity Head (in. WG)	Orifice Meter (in. WG)	Gas Meter Volume (ft³)	Pump Vacuum (in. Hg)
							Inlet (°F)	Outlet (°F)				
							Average	Average				
		Average								Average	Total	
							Average					

Facility

Stack Diameter (in.)

Date

Time

Run

Operators

Stack Pressure

Ambient Pressure

GAS GRAB AND LIQUID FUEL SAMPLES

Clock Time	Stack Gas Temp (°F)	Gas Grab Sample No.	Liquid Fuel Sample No.

Facility
Date
Time
Run
Operators
Stack Pressure
Ambient Pressure

Analyzer Calibrations

O_2: %
CO: ppm
CO_2: %
NO: ppm
NO_x: ppm

CONTINUOUS GAS ANALYSIS

Clock Time	Stack Temp (°F)	Analyzer Gas Temp (°F)	Gas Concentrations				
			O_2 (%)	CO (ppm)	CO_2 (%)	NO (ppm)	NO_x (ppm)

APPENDIX B

LIST OF SAMPLING EQUIPMENT

I Source Assessment Sampling System*

1. Unirail support
2. Control module
3. Sample gas pumps
4. 25-foot sample hose (1/2 inch)
5. 4-foot pump-to-control module hoses
6. 25-foot umbilical
7. 3-cyclone assembly
8. 6-inch filter assembly
9. Cyclone oven
10. Organic module/gas cooler unit
11. 42-inch oven-to-gas cooler sample line
12. Impinger assembly and case
13. Water circulation pump
14. Sample probe
15. Probe temperature-control unit
16. Probe hydraulic oil pump assembly
17. Metal braided hydraulic hoses (3)
18. Garden hoses (2)
19. Water circulation pump
20. 8 probe nozzles, sizes 5/16 inch to 1-1/2 inches
21. S-type pitot tubes
22. 142 mm glass fiber filters
23. Organic adsorbent material
24. Hydraulic fluid — Therminol "66" (Monsanto)
25. Crushed ice supply (impingers)
26. Sample containers
27. Vacuum grease

II Gas Grab Sampler

1. Sample probe and connecting tubing
2. Evacuated, encased sample bottles (3ℓ)
3. Glass wool plugs
4. Silicon grease

III Liquid Fuel Sampling

1. Glass sample containers

---

*See Reference 2 for component descriptions and part numbers.

Appendix F

Aerotherm Project 7237

A PROGRESS REVIEW OF SOURCE ASSESSMENT SAMPLING SYSTEM PROGRAMS

David Blake

Acurex Corporation/Aerotherm Division
485 Clyde Avenue
Mountain View, California 94042

June 15, 1977

AEROTHERM REPORT TM-77-176

Prepared for
Environmental Protection Agency
Research Triangle Park
North Carolina 27711

Contract 68-02-2153

TABLE OF CONTENTS

Section Page

1 INTRODUCTION F-1

2 SASS TEST OBSERVATIONS F-1

3 TRAINING SESSIONS F-2

4 CYCLONE CALIBRATION F-3

5 COORDINATION WITH OTHER TLE CONTRACTORS F-6

6 SASS SUPPORT OPERATIONS F-11

LIST OF ILLUSTRATIONS

Figure Page

1 Cyclone test apparatus F-4

2a SiO_2 test dust F-7

2b SiO_2 dust — small cyclone cup catch F-7

2c SiO_2 test dust — small cyclone filter catch F-8

3a Aluminum test dust F-9

3b Aluminum dust — small cyclone cup catch F-9

3c Aluminum dust — large cyclone cup catch F-10

1. INTRODUCTION

During the past year the TLE contract has supported several tasks pertaining to the development, use, and improvement of the Source Assessment Sampling System (SASS). The specific tasks involved were Task 07 (Cyclone Calibration), Task 08 (SASS Support), and several Support Service Tasks of less than 100 hours duration. Activities related to the SASS have been conducted in five general areas:

- SASS test observations
- SASS training sessions
- Cyclone calibration
- SASS support operations
- Coordination with other TLE contractors.

Each of these activities will be discussed individually.

2. SASS TEST OBSERVATIONS

Two observations* of SASS tests were made by Aerotherm personnel in the past year. In each case, the purpose of the observation was two-fold: to advise the test crew on use of the train and to observe the train under actual field conditions so that problems could be noted and corrected.

The first observation was of a SASS test of an experimental coal fired boiler at KVB, Inc. The observation was very valuable in helping to identify several problems associated with the use of the SASS train as it was then configured. Changes subsequently made as a result of this observation included:

- Elimination of Swageloc connectors in the cyclone assembly, as they are easily damaged and are inoperative when hot. Modified pipe union fittings now provide good performance
- Provision for a Marmon clamp to secure the two parts of the large cyclone, eliminating the screw fasteners

---

*The Plant Mitchell observation occurred in May 1977, which is after the close of the reporting period (April 1976 – April 1977). It will be covered in the next annual report.

- Modification of the shape of the middle cyclone to make after-test cleaning easier
- Increasing the size of the small cyclone cup
- Modification of the impinger bottles to reduce the possibility of breakage

The other observation was of a SASS test of the Comanche Power Plant of the Colorado Public Service Comapny, performed by Radian Corporation. This test was the first one conducted at the increased flowrate of 4.0 scfm. The results of this test indicated that a single vacuum pump was inadequate for maintaining that flowrate. The SASS train's design was therefore modified to incorporate two pumps.

3. TRAINING SESSIONS

Twice during the past year training sessions were conducted for SASS users by Aerotherm personnel. The first session was held at Battelle Columbus Laboratories. The purpose was to train Battelle sampling crew members in the setup, checkout, operation, and cleanup of the SASS train for Battelle's upcoming test at the Exxon pressurized FBC. A secondary objective was to explain the design and use of the SASS to interested members of the Battelle technical staff. Approximately eight field crew members were given 2 full days of hands-on practice in the use of the trains. During the 2 days, the SASS train was disassembled, reassembled, and leak-checked three times. About 15 members of the Battelle technical staff attended a presentation on the SASS design.

The other training session was conducted at EPA/RTP. The goals were the same as at Battelle — to provide general information on the SASS design to interested EPA staff members, and to allow EPA technicians to practice assembling the SASS train under the direction of an Aerotherm engineer familiar with its use. A representative from Southern Research Institute was also present. A 1-day session was held with about 15 people attending the discussion of SASS design, and 5 people completing the practice sessions in assembly, operation, and leak checking. A satisfactory leak check was routinely achieved using inexperienced technicians under Aerotherm direction.

4. CYCLONE CALIBRATION

The cyclone calibration task is intended to experimentally evaluate the performance of the three SASS cyclones using "real" solid particles. At the time the calibration task was begun, other calibration tests were underway at Southern Research Institute. The SoRI method involves the use of a vibrating orifice particle generator which produced precisely sized particles of a dye solution. When dried by the carrying gas stream, a monodisperse aerosol is produced. Collection efficiency versus particle size curves that characterize the cyclone performance can be obtained by feeding several different sizes of monodisperse dye particles into the cyclone to be tested.

Several problems that existed with the SoRI method led to the decision to try a completely different approach to cyclone calibration. These problems were: unavailability of a dye material useable at 205°C, and the extremely low particle mass concentrations used in the SoRI method. It was felt that these low concentrations (several orders of magnitude lower than field concentrations) might not adequately simulate wall-sticking and particle-particle interaction effects.

The following describes the calibration method used by Aerotherm: A dust cloud was generated from a test dust of known properties, then the dust was fed into the cyclone and the cyclone efficiency measured from the quantity and size distribution of the dust collected (in the cup) and passed by the cyclone (in the filter). Figure 1 shows the experimental setup.

In the first series of experiments, a highly classified silica dust material was used. The dust was classified by the Donaldson Company into nine size fractions, starting with AC Fine test dust. This particular material was chosen because of its availability, its wide use as a test dust in the HVAC industry, and the familiarity of Donaldson Company with the behavior of the material in their classifiers.

The approximate performance of each of the SASS cyclones was known from previous SoRI tests. Accordingly, three to six of the classified dusts were chosen for calibrating each cyclone, depending on the mean particle size of the dust. The size distribution of the test dust and the dust collected in the cyclone cup was measured using the x-ray sedograph at EPA/RTP.

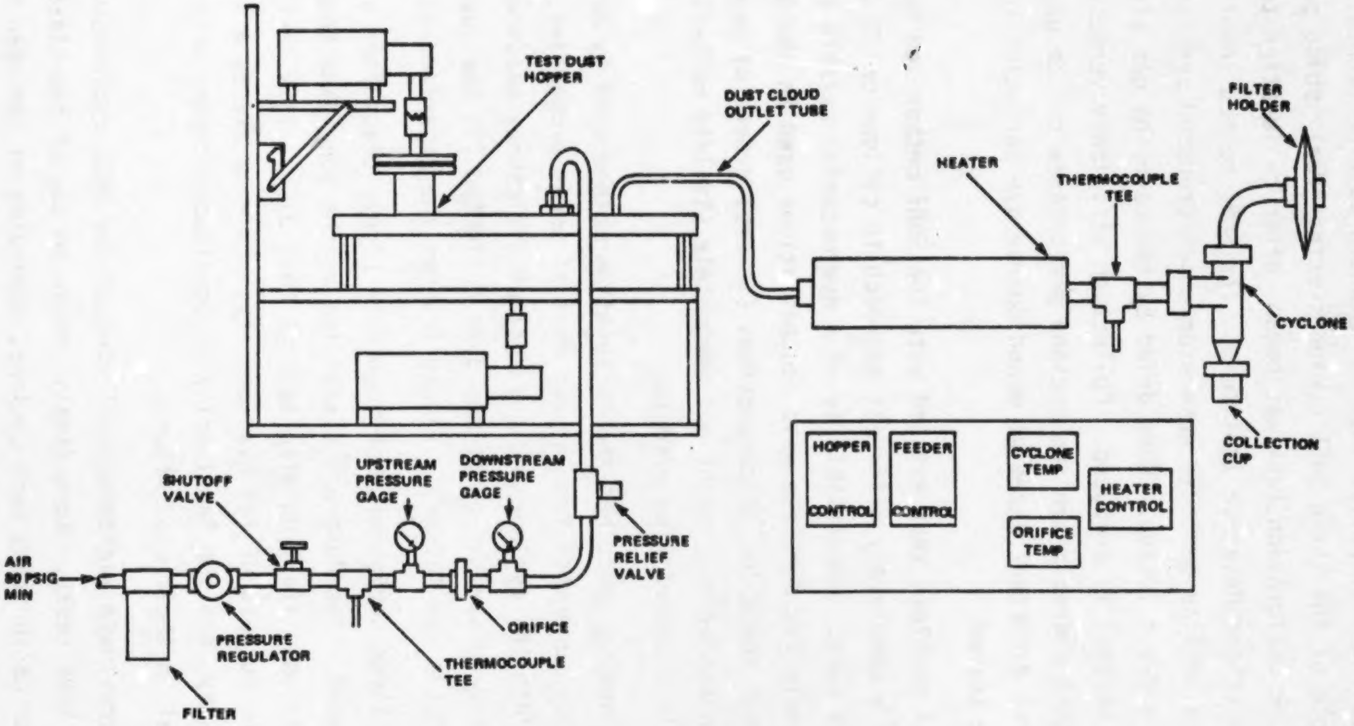
TEST DUST HOPPER
DUST CLOUD OUTLET TUBE
HEATER
THERMOCOUPLE TEE
FILTER HOLDER
CYCLONE
COLLECTION CUP
HOPPER CONTROL
FEEDER CONTROL
CYCLONE TEMP
HEATER CONTROL
ORIFICE TEMP
SHUTOFF VALVE
UPSTREAM PRESSURE GAGE
DOWNSTREAM PRESSURE GAGE
AIR 80 PSIG MIN
PRESSURE RELIEF VALVE
PRESSURE REGULATOR
ORIFICE
THERMOCOUPLE TEE
FILTER

Figure 1. Cyclone test apparatus.

From the size distribution data, it should be possible to construct a cyclone efficiency versus particle size curve for the particle size range of the test dust. When this was attempted, it became apparent that the experimental results were inconsistent and in some cases contradictory. For several experiments, for example, the mass median size of the cyclone cup catch was smaller than the feed material; the filter catch mass median diameter was even smaller. This result is clearly impossible unless the size distribution measurement method is faulty or unless the test dust is changing its characteristics during the test.

There is some evidence that the latter explanation is the cause of the unexpected test results. Figures 2a, 2b, and 2c are scanning electron micrographs of the feed, cyclone cup, and filter fractions, respectively, from a calibration run with the small cyclone. The magnification is 3000X. It is qualitatively apparent that the cyclone cup fraction is smaller than the feed fraction, as indicated by the x-ray sedograph measurements. The most interesting point, however, is the appearance of the particles. The test dust particles (Figure 2a) are generally smooth and evidence cleavage planes. The particles collected by the cyclone (Figure 2b), however, are very rough and pitted, and seem to be rounded off. The filter fraction largely consists of very small particles that are not evident in the test dust. All of this seems to indicate that the test dust has been eroded and reduced in average size somewhere in the calibration apparatus. As velocities in the dust cloud outlet tube and heater are deliberately kept high (near sonic) to avoid reagglomeration of the dust, it is suspected that particle-particle contact in this region is causing the erosion. The hardness and frangibility of the test dust undoubtedly is also a major factor.

In order to overcome the problem of test dust degradation, either the apparatus or the test dust will have to be changed. The easiest solution appears to be to obtain a test dust that is not subject to erosion. After a search for such a dust, a spherical aluminum powder material was discovered. Being malleable, no particle erosion is anticipated. Also, the fact that the particles are spherical should make measurement of the size distribution and subsequent data analysis easier. One possible problem is the low melting point of aluminum and associated possibility of sticking to the hot wall in the heater sections of the test apparatus. If necessary the heater can be lengthened to reduce wall temperature below the melting point.

Some calibration tests have been completed using the aluminum test dust. Size distribution analysis has not been completed; however, photomicrographs indicate reasonable results. Figures 3a, 3b and 3c show the test dust, the small cyclone cup catch, and the large cyclone cup catch. The test dust is primarily spherical with a relatively narrow distribution of particulate sizes. Since the small cyclone is collecting almost all of the test dust, the small cyclone cup catches (Figure 3b) look very much like the test dust (Figure 3a). The large cyclone cup catch, however, clearly shows preferential collection of the larger particles, as it should. Completion of the size distribution analysis will allow calculation of cyclone efficiency curves.

5. COORDINATION WITH OTHER TLE CONTRACTORS

Two trips to EPA/RTP were made during the past year to attend the TLE contractor's meetings. The purpose of these meetings was a general review of programs and progress. In addition, numerous contacts with the other contractors occurred on a less formal basis. Some of these contracts were with

- Southern Research Institute — numerous discussions regarding cyclone calibration tasks at SoRI and Aerotherm. Also, discussions and planning for the SoRI solvent-refined coal SASS test
- Arthur D. Little, Inc. — many discussions about the performance of various organic sorbents and the applicability of Viton seals to the SASS trains
- Research Triangle Institute — the main contact was a meeting at Aerotherm where the field performance of the SASS train was discussed
- TRW, Inc. — numerous conversations about use of the SASS train on the incinerator ship Vulcanus, performance of the KVB boiler test, and corrosion problems in the SASS trains.

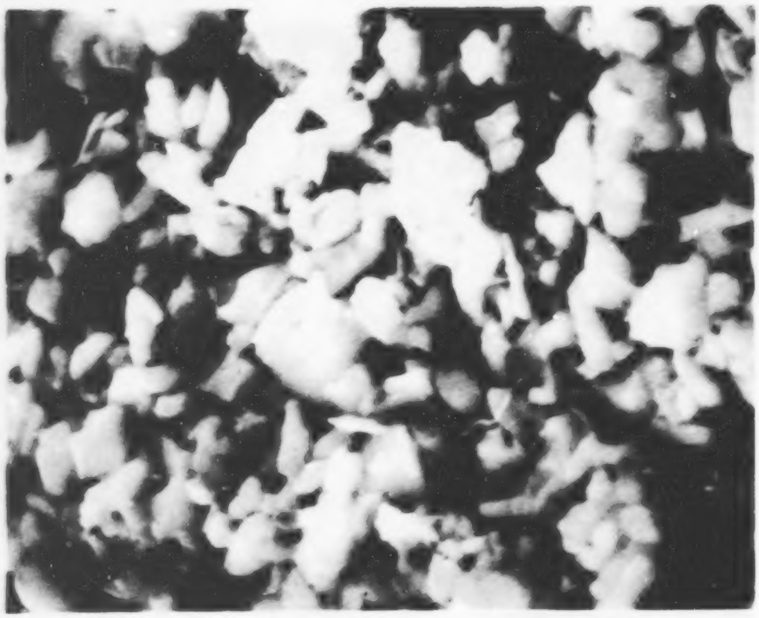

SiO_2 test dust
Figure 2(a).

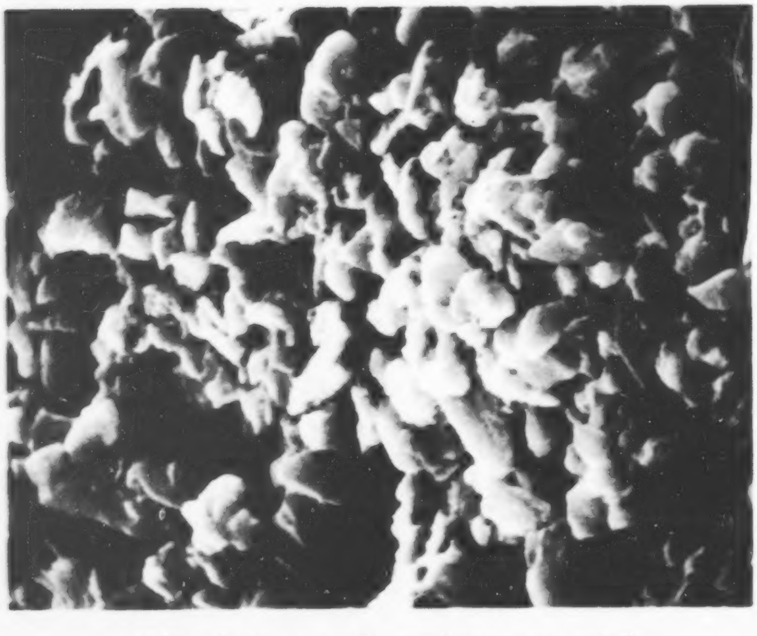

SiO_2 dust - small cyclone cup catch.
Figure 2(b).

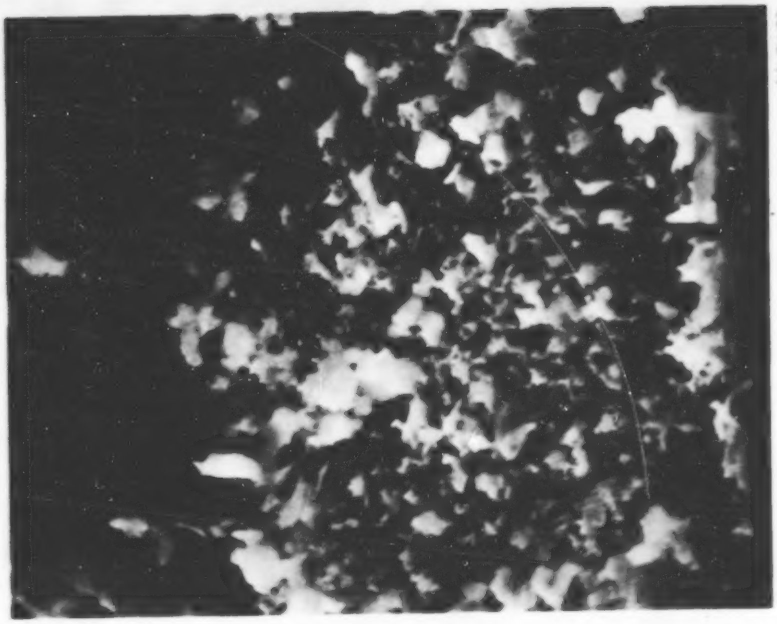

SiO_2 test dust - small cyclone filter catch

Figure 2(c).

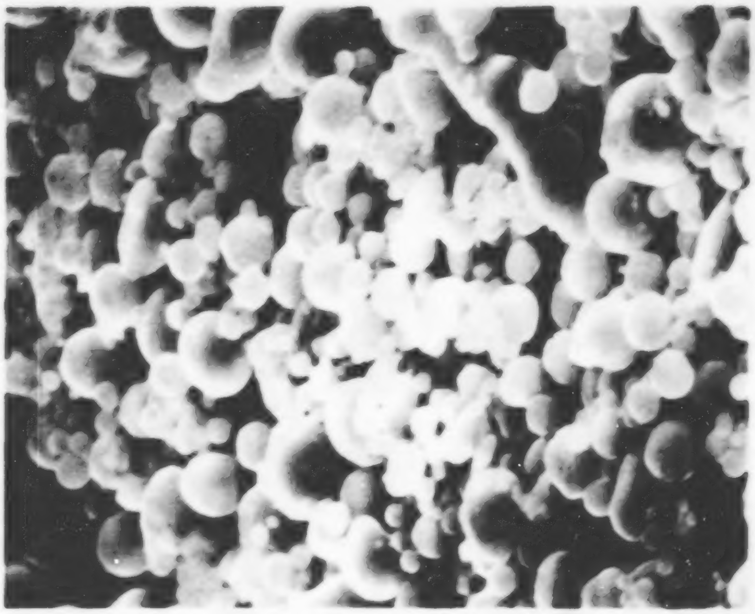

Aluminum test dust
Figure 3(a).

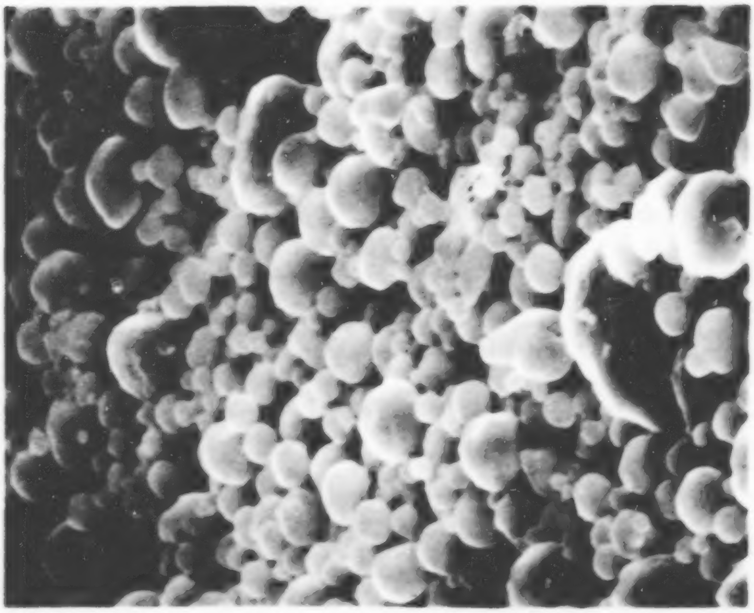

Aluminum dust - small cyclone cup catch
Figure 3(b).

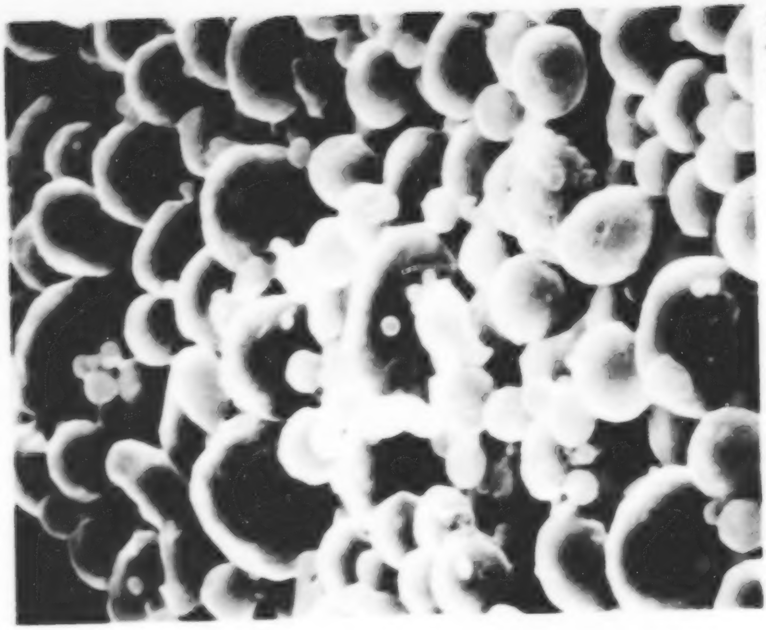

Aluminum dust - large cyclone cup catch

Figure 3(c).

6. SASS SUPPORT OPERATIONS

Task 08 of the TLE contract is intended to support a number of activities concerning development of the SASS train. The major activities are listed here

- An operating manual for the SASS train was prepared. The manual provides complete, detailed instructions for setting up, checking-out, running, and trouble shooting the train.
- An oversize filter holder was designed and constructed to reduce the number of filter changes during a SASS test. The oversized filter has 2.3 times the area of a standard filter. For most sources, one filter should last an entire 5-hour run even when testing ahead of the control device (1-3 gr/scf).
- A spare parts inventory has been provided for government owned SASS trains.
- A list of desirable SASS train modifications has been assembled, in response to comments by field crews. Some 22 system modifications are now under consideration.
- The two partial SASS trains used for sampling the incinerator ship, Vulcanus, have been upgraded to full SASS status.
- Six complete sets of SASS train blueprints have been submitted to the Project Officer.
- A comprehensive final report, detailing the SASS development project, is now underway.
- A corrosion/welding consultant has been retained to examine and report on ways of minimizing corrosion in the SASS train by proper choice of materials and construction techniques.

APPENDIX G

CONVERSION TO INTERNATIONAL SYSTEM OF UNITS

To convert	to	multiply by
acfm	meter^3/minute, m^3/min	2.8317×10^{-2}
atmospheres	newton/meter^2, newt/m^2	1.0133×10^{5}
°F	Celsius, °C	°C = 5/9(°F − 32)
°R	Kelvin, °K	°K = 5/9 °R
ft^3	meter^3, m^3	2.8317×10^{-2}
ft/sec, fps	meter/second, m/s	3.048×10^{-1}
gpm	meter^3/minute, m^3/min	4.5461×10^{-1}
grain	kilogram, kg	6.4780×10^{-5}
grain/scf	kilograms/meter^3, kg/m^3	2.2877×10^{-3}
inches, in	meter, m	2.54×10^{-2}
lbm	kilogram, kg	4.5359×10^{-1}
microns, μm, μ	meter, m	1.00×10^{-6}
pound	newton, newt.	4.4482
psia	newton/meter^2, newt/m^2	6.8948×10^{3}